AN INVESTIGATION OF THE DESTRUCTION OF ION EXCHANGE RESINS

PAUL ANTHONY HACKNEY

Doctor of Philosophy

University of Aston in Birmingham

August 1992

1

SUMMARY

THE UNIVERSITY OF ASTON IN BIRMINGHAM

AN INVESTIGATION OF THE DESTRUCTION OF ION EXCHANGE RESINS

PAUL ANTHONY HACKNEY

A thesis submitted for the degree of Doctor of Philosophy 1992

Ion exchange resins are used for many purposes in various areas of science and commerce. One example is the use of cation exchange resins in the nuclear industry for the clean up of radioactively contaminated water (for example the removal of ^{137}Cs). However, during removal of radionuclides, the resin itself becomes radioactively contaminated, and must be treated as Intermediate Level Waste. This radioactive contamination of the resin creates a disposal problem.

Conventionally, there are two main avenues of disposal for industrial wastes, landfill burial or incineration. However, these are regarded as inappropriate for the disposal of the cation exchange resin involved in this project. Thus, a method involving the use of Fenton's Reagent (Hydrogen Peroxide / soluble Iron catalyst) to destroy the resin by wet oxidation has been developed. This process converts 95% of the solid resin to gaseous CO_2, thus greatly reducing the volume of radioactive waste that has to be disposed of. However, hydrogen peroxide is an expensive reagent, and is a major component of the cost of any potential plant for the destruction of ion exchange resin. The aim of my project has been to discover a way of improving the efficiency of the destruction of the resin thus reducing the costs involved in the use of hydrogen peroxide.

The work on this problem has been concentrated in two main areas:-
1) Use of analytical techniques such as NMR and IR to follow the process of the hydrogen peroxide destruction of both resin beads and model systems such as water soluble calixarenes.
2) Use of various physical and chemical techniques in an attempt to improve the overall efficiency of hydrogen peroxide utilization. Examples of these techniques include UV irradiation, both with and without a photocatalyst, oxygen carrying molecules, and various stirring regimes.

KEY WORDS

Ion exchange resin	Waste disposal	Cerium
Ultraviolet	Fenton's reagent	

ACKNOWLEDGEMENTS

LIST OF CONTENTS

List of Contents

7

18

19

21

CHAPTER ONE

INTRODUCTION

1.0 INTRODUCTION

This thesis represents an account of work carried out on methods of treatment prior to disposal for spent, radioactive ion exchange resins, which are produced during nuclear power station operation.

Ion exchange resins are used by the British nuclear reactor operators (Nuclear Electric, Scottish Nuclear, Atomic Energy Authority) for water and effluent treatment, forming one of several types of intermediate level radioactive waste arising from nuclear power station operation. One type of resin, the strong acid cation exchange resin, 'Lewatit DN', was chosen for special study because it is used by Nuclear Electric and Scottish Nuclear at several power generation sites. Lewatit DN is primarily used by these companies to remove selectively ^{137}Cs from aqueous streams that also contain large quantities of other alkali ions such as sodium.

As radioactive ions are trapped in the resin structure, the resin becomes increasingly radioactive, and at the end of its life the resin is classed as Intermediate Level Waste (ILW) i.e., it has an activity greater than 12 $GBq.t^{-1}$ of β and γ radioactivity. This radioactive contamination necessitates careful consideration about the eventual fate of the resin.

1.1 Historical Perspective on Radioactive Resin Management

When the first nuclear stations in Britain were constructed in the 1950s and 1960s the waste management policy of the time was accumulation of the ILW at the site of production. It was envisaged that this would be followed by eventual retrieval, encapsulation and disposal of the waste when a technically and economically viable disposal route became available. This policy had the advantage of not foreclosing any disposal options, and by the early 1980s it had been decided that sea dumping was the appropriate disposal method. A special waste packaging plant was constructed at Trawsfynydd Power Station in Wales to encapsulate the waste in Dow vinyl ester polymer, and then place it in special sea dump drums made of 'iron shot concrete' (encased in a mild steel liner). 394 drums of waste had been processed in this manner before a British Government moratorium on sea dumping was announced, closing off this disposal option [1]. This decision necessitated the development of an alternative waste management strategy.

1.2 The Current Approach to Radioactive Resin Disposal

The current approach to resin disposal is that resins should be stored only temporarily at the power stations, until they can be processed at the power station site. This resin processing involves either direct encapsulation of the resin or use of a method to reducing its bulk, prior to encapsulation. A consequence of this policy is that resin stores in recently constructed power stations are much smaller than those in older stations. For example there are 25 to 30 years storage capacity at the Magnox stations (constructed in the 1950s), but only about 1 year's storage capacity at Sizewell B (constructed in the late 1980s).

Processing the resin at the power station, rather than at a central location, is currently the preffered option because of the difficulties and expense of transporting untreated resin to the central processing plant. It would be possible to build a processing plant at each resin storage site but this would also be expensive. It will instead probably be cheapest to build a mobile processing plant which would visit each of the resin production sites in turn, carrying out a treatment campaign at each location.

After processing the resin would be moved to a deep, underground repository operated by UK N.I.R.E.X Ltd. (UK Nuclear Industry Radioactive Waste Executive).

1.3 Two Options for the Disposal of Radioactive Ion Exchange Resins

Although it is not currently the nuclear industry policy, it might be technically feasible to store the radioactive resin permanently at the site of production. The other technical option available is burial of the resin at a central location after initial on-site processing, which is the current Nuclear Electric policy. Each of these options are discussed in the next section.

1.3.1 Permanent Storage of Radioactive Resin at Site of Production

1.3.1.1 Description of the Technique

At present, due to the moratorium on sea dumping of ILW, the radioactive resin is still being accumulated at the sites where it is being produced. It would be technically feasible to convert the temporary store at each of these locations to a permanent storage location either as part of the decommissioning programme, or alternatively by building a storage facility at each plant. In any store the resin would be stored until the level of radioactivity had fallen to an

environmentally harmless level, over a period of several hundred years. The resin could then be disposed of cheaply in a shallow burial site.

1.3.1.2 Calculation of Necessary Storage Time

The main contaminant of Lewatit ion exchange resin is ^{137}Cs, which has a half life of 30.17 years. ILW has a radioactivity level of at least 12 G.Bq. t^{-1} of β and γ, whereas the level of radiation that is generally regarded as acceptable for release into the environment is 4×10^5 Bq. t^{-1} of β and γ [1]. Assuming that the resin had a radioactivity level of 12 G.Bq. t^{-1} of β and γ, and ^{137}Cs were the only radioactive ion present, it would take 540 years for the radioactivity level to fall to a 'safe' level.

In practice however, the resin will be contaminated by low levels of radionuclides with longer half lives than ^{137}Cs, meaning that the resin would have to be treated as LLW for an indefinite period of time.

1.3.1.3 Problems with the Technique

Regular monitoring of the storage area for leaks and defects in containment equipment would be required for the whole storage period, at each storage location which could be very expensive in the long term. There may also be a moral consideration to this technique: "Should we try to minimise the financial and technical burden we leave to our descendants?".

1.3.2 Processing the Resin, Followed by Underground Storage

There are currently two options for treatment of the resin prior to storage of ion exchange resins underground. The first option is direct encapsulation of the resin in cement, while the second option involves processing the resin to reduce its volume before it is added to the cement. In both cases the cement is then generally enclosed in steel or iron drums, which are transported to a central, permanent storage location.

1.3.2.1 Direct Encapsulation of the Resin in Cement

This storage technique is a very quick and uncomplicated way of producing a solid wasteform, for disposal underground. It cuts out the extra processing step required if a volume reduction

technique is used, with a consequent reduction in plant cost. Other advantages of the absence of an extra processing step are a reduction in the radiation dose to staff and public, and a reduced possibility of problems with equipment during the processing of the resin.

1.3.2.1.1 Problems with the Technique

1) Mixing ion-exchange resin with cement substantially increases the volume that must be stored underground, relative to the non-cemented resin. It is likely that the cement : unprocessed resin ratio will be not greater than 0.6 : 1 (0.6 m^3 cement for every 1 m^3 resin) [2]. If the volume of the radioactive resin could be reduced prior to cementation, there would be considerable cost savings. This is because the cost of storage of radioactive waste in an underground repository is a function of the volume stored (the radioactive content of the waste is the other major cost determining factor).

2) There may be problems involved with the long term storage of certain types of organic materials underground.

TABLE 1.0

POSSIBLE FATES OF ORGANIC MATERIAL IN AN UNDERGROUND NUCLEAR WASTE STORAGE FACILITY [1]

Type of Organic Material	Likely fate in an underground repository
Cellulosics	Will degrade to form radionuclide chelating agents under anaerobic, but not aerobic conditions. Conditions in the repository will be reducing after the first hundred years.
Condensation Polymers (e.g. Lewatit DN)	This type of material is not currently thought to pose a problem under reducing conditions, but it is believed that organic chelating agents will be formed under aerobic conditions. Aerobic conditions will predominate for the first hundred years after the repository is closed.
Addition Polymers, and other non-oxygen containing organics	It is believed that these will not produce chelating agents under either anaerobic or aerobic conditions.

It is believed that chemical, radiolytic, thermal, and microbial attack of organic materials would be the main processes by which organic chelates would be released [3,4,5]. Chelating agents might then increase the solubility of radioactive ions such as plutonium in water, thus increasing the

risk of contaminated water reaching the biosphere. Another effect of chelating agents may be to block metal absorption sites in the repository backfill and host rocks, again potentially enhancing the mobility of radionuclides through these barriers. Microbial action and radiolytic generation processes may result in the production of gases such as CO_2 and H_2 resulting in a pressure build-up in the storage vessel. This would encourage rupture of the vessel, particularly if it had become corroded, in turn releasing radioactive materials into the repository earlier than otherwise would have been the case. Finally, it is possible that there will be future regulatory action to ban completely materials that could produce organic chelating agents from nuclear waste stores (because of the problems described above).

1.3.2.2 Using Resin Volume Reduction Techniques Before Cementation and Burial

These techniques have the advantages of giving significant volume reduction and removing organics from the permanent burial site, (these issues are discussed in the previous section) but have the disadvantages of adding extra processing stages. Extra processing stages increase capital costs, and increase exposure of operational personnel to radiation.

1.3.3 The Decision on Direct Encapsulation .vs. Resin Volume Reduction Techniques

At the time of writing of this PhD no final decision has been made whether the resin should be reduced in volume before incorporation into cement. However, some years ago, Nuclear Electric, one of the main producers of radioactive ion exchange resins in Britain, decided to instigate a research project to investigate potential resin volume reduction techniques.

1.4 Possible Resin Volume Reduction Strategies

All the treatment methods described in this section have the potential for meeting the aims of Nuclear Electric's research project. The benefits and problems of each technique are described, and the decision made by Nuclear Electric as to which resin treatment method to investigate is detailed at the end of the section.

1.4.1 Incineration of the Resin

1.4.1.1 Description of the Technique

The resin would be burned at high temperature, producing CO_2, H_2O and sulphur oxides and leaving behind a radioactive ash. This process has the advantage of producing a large reduction in waste volume. For example, an average volume reduction ratio of 75 is claimed by Studsvik of Sweden for incinerated Low Level Waste (LLW) [6]. This figure is arrived at by comparing the volume of the ash-containing cement product with untreated, uncompacted waste. The incineration process is also very swift, with the resin being destroyed within seconds of addition to the incinerator.

1.4.1.2 Problems with the Technique

There are several serious problems with the incineration of radioactive ILW.

a) The treatment of the off-gases. When LLW is incinerated, there is often no requirement for extensive off-gas treatment, due to the low level of radioactivity involved. When ILW is incinerated, the off-gases need to be carefully filtered or wet scrubbed to stop gaseous radioactive contaminants reaching the atmosphere. The gaseous radioactive contaminants are a problem because the high temperatures involved in incineration cause vaporisation of volatile radioisotopes. Examples of these radioisotopes would be tritium in the form of water or ^{14}C in the form of CO_2. Other, non-volatile radioactive isotopes may also be carried over as solids in smoke particles.

The requirement to scrub the off-gases adds significantly to the complexity, and therefore cost, of the incineration plant. The filters or contaminated water used to remove radioactive materials would then themselves have to be disposed of safely, reducing the overall volume reduction factor i.e. a secondary waste problem has been created

b) The activity of the residue. With high volume reduction factors very radioactive ashes are produced, which cause further disposal and handling problems.

c) Transportability. It would be difficult to construct a mobile incineration plant to process ion exchange resins at each power generation site, as incinerators tend to be large and complex.

d) Poor public image. Incineration has a poor public image, due partially to well publisised accidents at conventional (non-radioactive material) incinerators. There is also extensive

36

lobbying against incinerators by many environmental protection groups, who claim that the technique is unsafe. This public opposition would cause problems in obtaining planning permission for any proposed incinerator.

All these problems suggest that incineration is unlikely to be the best method for treatment of ion-exchange resin.

1.4.2 Acid Digestion of the Resin

1.4.2.1 Description of the Technique

It has been shown that it is possible to digest ion-exchange resins at high temperatures (between 200-260°C), using mixtures of concentrated acids such as H_2SO_4 and HNO_3 [7]. The resin is placed in concentrated H_2SO_4, the mixture heated up and the HNO_3 is then added slowly, oxidising the resin as it is added. After all the resin has been oxidised, more resin can be added to the H_2SO_4 and HNO_3 added to oxidise the new batch of resin.

1.4.2.2 Problems with the Technique

A complex off-gas treatment plant is required to treat gaseous products such as NOx and SOx, which substantially adds to the costs of the design. Additionally, the severe operating conditions require that expensive acid and heat resistant materials such as tantalum be used to construct the reaction vessel [8]. Finally, treatment of the end reaction liquor is difficult due to its acidity, requiring large quantities of neutralising agents that add appreciably to the bulk of the final product. There are also difficulties in encapsulating the sulphates produced in the neutralisation of the acids into cement [1]. No precise volume reduction factor for this process has yet been found, due to the absence of research data indicating how often the H_2SO_4 can be reused before neutralisation of the reaction solution was necessary.

1.4.3 Biological Digestion of the Resin

1.4.3.1 Description of the Technique

The resin would be used as the feedstock for the growth of a cocktail of microbes, which would ultimately convert the resin to CO_2 and water. This is potentially a simple and cheap process, relative to other volume reduction techniques, due to the absence of complex equipment or

expensive chemicals in this process.

1.4.3.2 Problems with the Technique

Very little research has been carried out on this approach to radioactive waste destruction and many technical details of the process are unclear. Perhaps the major problem is that it is not known which (if any) microbes could be used to degrade the resin [1]. Plant sizes are likely to be large and the whole resin degradation process would be a lengthy one. This would add significantly to the cost of the process. It is also not known what level of volume reduction that would be achievable, nor how the secondary waste arisings would be treated.

1.4.4 Electrochemical Digestion of the Resin

1.4.4.1 Description of the Technique

In this process Ag^{2+} ions in nitric acid oxidise organic matter at a temperature of between 55 and 95°C. The Ag^{2+} ions are generated by passing a large electrical current through the nitric acid, which converts reduced Ag^+ ions back to Ag^{2+} ions. This process has been successfully applied to the destruction of several types of organic materials, including rubber, polyurethane, epoxy resins, lubrication oil and solvents [9]. Very good volume reduction ratios of up to 75 are claimed for waste destroyed by this method.

1.4.4.2 Problems with the Technique

The plant required is bigger and more complex than the equivalent chemical oxidation plant. This extra size is largely due to the production of nitrogen oxides, which have to be removed from the off gas, which requires a large, expensive off-gas treatment system. The high electrical currents used (around 10000 Amps) require that costly equipment is used, and the high energy consumption of this technique makes the apparatus very expensive to run. Finally, due to the high cost of Ag, the soluble Ag ions have to be recovered from the reaction solution, adding another processing step to this already complex processing technique.

1.4.5 Hydrogen Peroxide Digestion of the Resin

1.4.5.1 Description of the Technique

The resin is destroyed by the addition of Fenton's reagent (hydrogen peroxide / iron catalyst), which first solubilises the resin and then converts the dissolved organic material to CO_2 and H_2O. Since the reaction is carried out at comparatively low temperatures (95 to 100°C), and at atmospheric pressure, equipment costs are kept reasonably low. The end reaction liquor can then be neutralised, evaporated and incorporated into cement for long term storage.

1.4.5.2 Problems with the Technique

One problem with this process is the cost of the H_2O_2 used to oxidise the resin, as H_2O_2 is a comparatively expensive reagent. This problem is made worse by a tendency for the H_2O_2 to decompose to form H_2O and O_2 towards the end of the resin digestion reaction. This decomposition is wasteful, as the preferred reaction in solution is the formation of hydroxyl radicals. The oxygen thus formed is a fire risk and must be removed safely from the resin destruction equipment. Finally, the H_2O_2 itself requires careful storage and handling prior to use as it is a powerful oxidising agent.

1.4.6 The Decision on Resin Volume Reduction Method

The factors that must be considered when deciding the best treatment method are summarised in Table 1.1 (see overleaf) [10].

TABLE 1.1

SELECTION OF RESIN TREATMENT METHOD

FACTOR TO BE CONSIDERED	PREFERRED SITUATION
Safety	Benign reagents (if applicable) Readily controlled process design Simple design
Ease of Engineering	Low temperature Low pressure Non-aggressive solvents (if applicable)
Compatibility with existing disposal facilities	Minimal secondary waste arisings
Economic	Low energy usage and/or cheap reagents Compact plant size Favourable kinetic and thermodynamic factors Low labour costs
Robustness	Plant simplicity Availability and reliability Absence of novel critical items Tolerant to variations in waste
Proven technology	Plant scale trials, active testing
Transportability	Small and compact plant

After considering all technological, economic, and social factors, the Central Electricity Generating Board made a decision to develop further the hydrogen peroxide digestion process. (The CEGB's nuclear generating and laboratory facilities were placed under the control of the company 'Nuclear Electric PLC' in 1989. All references to my sponsoring body from this point onwards will be to Nuclear Electric)

1.5 The Hydrogen Peroxide Digestion of Spent Ion Exchange Resins

1.5.1 The Chemistry of Fenton's Reagent

This reagent was discovered in 1894 by Fenton, who used it to oxidise α-hydroxyacids and α-glycols[11]. Some 40 years later, Evans showed that oxidations of this type involved the hydroxyl

40

radical $\cdot$OH [12]. Two years later Merz and Waters proposed a mechanism for the action of Fenton's reagent and showed that it could be used to oxidise a wide range of organic compounds [13].

1.5.1.1 Dissociation of the 0-0 bond in Hydrogen Peroxide

The bond dissociation energy of the O-O bond in hydrogen peroxide is around 200 kJ/mole [14]. This is a weak bond compared with an average C-H bond (400 kJ/mole) or saturated C-C bond (300 kJ/mole). The bond may be dissociated by UV light, ionising radiation or thermal vibration [15]. However, in the presence of a catalyst, such as Fe^{2+} or Fe^{3+}, these uncatalysed decomposition routes have only secondary importance.

The decomposition of H_2O_2 has a favourable enthalpy of reaction and there is also an increase in ΔS during O_2 formation. This drives the reaction in favour of the products.

$$2H_2O_2 \longrightarrow 2H_2O + O_2 \quad \Delta H^0 = -150 \text{ kJ/mole}$$
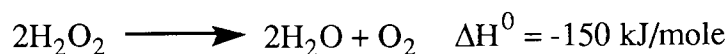
1.5.1.2 The Catalysed Decomposition of Fenton's Reagent

Two mechanisms have been proposed to explain data from kinetics experiments on the decomposition of H_2O_2. These mechanisms are known as the "free radical" scheme and the "complex" scheme.

1.5.1.2.1 The Free Radical Scheme

The following simplified reaction scheme, seen in Table 1.2 (see overleaf), has been developed by various workers, mainly over the last 30 years [16,17].

41

TABLE 1.2

THE FREE RADICAL SCHEME

Reactants		Products	Rate Constant (where known)
$H_2O_2 + e^-$	$\xrightarrow{k_1}$	$\cdot OH + OH^-$	$k_1 = 1.2 \times 10^{10}$ dm^3 mol^{-1} s^{-1}
$Fe^{3+} + HO\text{-}OH$	$\longrightarrow$	$[Fe^{(III)} O_2H]^{2+} + H^+$	
$[Fe^{(III)} O_2H]^{2+}$	$\longrightarrow$	$Fe^{2+} + HO_2\cdot$	
$Fe^{2+} + HO\text{-}OH$	$\xrightarrow{k_2}$	$Fe^{3+} + OH^- + \cdot OH$	$k_2 = 7.6 \times 10^1$ dm^3 mol^{-1} s^{-1}
$Fe^{2+} + \cdot OH$	$\xrightarrow{k_3}$	$Fe^{3+} + OH^-$	$k_3 = 3.0 \times 10^8$ dm^3 mol^{-1} s^{-1}
$\cdot OH + HO\text{-}OH$	$\xrightarrow{k_4}$	$H_2O + HO_2\cdot$	$k_4 = 1.2 \times 10^7$ dm^3 mol^{-1} s^{-1}
$HO_2\cdot$	$\longrightarrow$	$H^+ + O_2^-$	
$O_2^- + Fe^{3+}$	$\longrightarrow$	$O_2 + Fe^{2+}$	

This set of reactions may also be represented by a single electron transfer cycle for H_2O_2 decomposition, as shown in Figure 1.0. It can be seen that $Fe^{2+/3+}$ are simply electron carriers that promote this cycle [18].

FIGURE 1.0

ELECTRON TRANSFER CYCLE
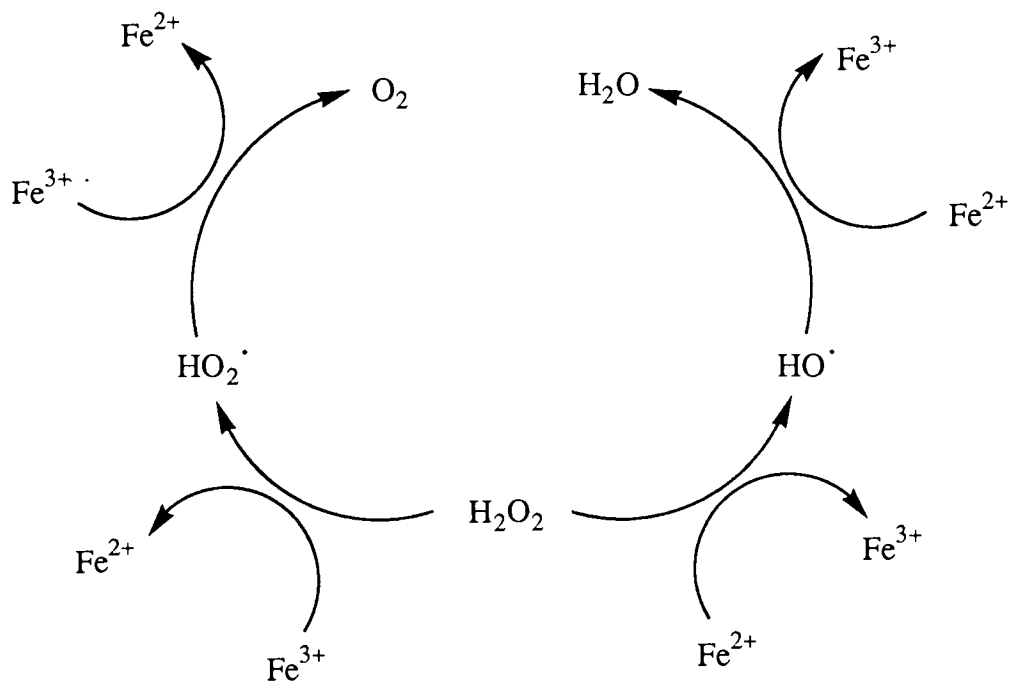
1.5.1.2.2 Problems of the Free Radical Scheme

a) It was suggested by Anbar in 1961 that the ·OH radical would be in rapid exchange with H_2O_2 [19].

$$\cdot OH + H_2O_2 \rightleftharpoons OH + H_2O_2^{\cdot}$$
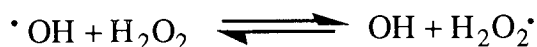
In response to this hypothesis, an experiment was devised in which $H_2(^{16}O)_2$ and $H_2(^{18}O)_2$ were decomposed together in solution. However, no $^{16}O^{18}O$ was observed, which would have been formed from two different molecules of H_2O_2. This indicates that the ·OH radical is not totally free to move around in solution or alternatively, that rapid exchange does not occur.

b) At low ratios, assuming steady state concentrations for Fe^{2+}, Fe^{3+}, and ·OH, the predicted rate law is as follows:

$$-\frac{d[H_2O_2]}{dt} = k [H_2O_2]^{\frac{3}{2}} [Fe^{3+}]^{\frac{1}{2}}$$

However, the free radical scheme does not correctly predict the experimentally observed kinetics at low $[H_2O_2] / [Fe^{3+}]$ ratios (although it does correctly predict the kinetics at high $[H_2O_2] / [Fe^{3+}]$ ratios) [19].

Nevertheless, it may be possible to model the system at low concentrations more accurately, for example by rejecting some simplifying assumptions about the steady state concentrations of species in solution.

c) The written reaction scheme suggests that HO^- or its daughter $^-O_2$ are converted to O_2 by oxidation with free Fe^{3+}. However, there is evidence that H_2O_2 forms stable complexes with Fe^{3+}, e.g. $[Fe(H_2O_2)(H_2O)_4]^{3+}$ or $[Fe(H_2O_2)(H_2O)_5]^{3+}$ [20]. This suggests that there is another oxidising agent present in solution, such as $[Fe^{(III)}O_2H]^{2+}$ or possibly $[Fe(H_2O_2)(H_2O)_6]^{3+}$ [21].

1.5.1.2.3 The Complex Scheme

The following reaction scheme, shown in Figure 1.1 (see overleaf), was suggested by Kremer in 1967 [22].

FIGURE 1.1

THE COMPLEX SCHEME

$$Fe^{3+} + HO_2^- \xrightarrow[k_2]{k_1} [Fe^{(III)} O_2H]^{2+}$$

$$[Fe^{(III)} O_2H]^{2+} \xrightarrow{k_3} FeO^{3+} + OH^-$$

$$FeO^{3+} + HO_2^- \xrightarrow{k_4} Fe^{3+} + O_2 + OH^-$$
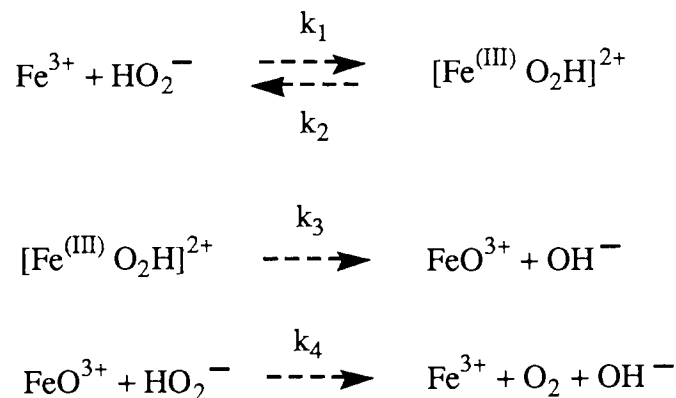
The complex scheme has been used to interpret the changes seen in the molar absorption of Fe^{3+} / H_2O_2 solutions [23]. Experimental data have been used to find the rate constants k_1 - k_4. The rate laws may be fitted to the experimental data over the full range of $[H_2O_2]$ / $[Fe^{3+}]$ ratios. Furthermore, there is strong evidence that the complex scheme is involved in haemoglobin and cytochrome oxidation [24]. It may be possible to draw an analogy between the two oxidation processes and the Fenton's reagent mechanism.

1.5.1.2.4 Problems of the Complex Scheme

Three main defects in the complex scheme have been pointed out by supporters of the free radical scheme. The most serious defect is

a) It has been reported that the rate of decomposition of H_2O_2 is altered by the presence of organic molecules. The rate of inhibition was calculated for various molecules and attributed to reactions between the organic species and the intermediates. These reactions compete with the decomposition pathway. Walling and Cleary claim that the complex scheme cannot account for the observed kinetics of competitive inhibition [25].

Other defects are

b) Using the rate constants produced by Kremer, it can be shown that a detectable amount of oxygen should remain in the form FeO^{3+} when all the H_2O_2 has decomposed. No oxygen deficit has been found [25].

c) It has been noted that the reaction rates between postulated decomposition intermediates and substrate molecules are the same as the rates measured for radiolytically generated ·OH radicals and the same substrate molecules [25,26].

The complex scheme has been re-evaluated since Walling's work, to explain the absence of an oxygen deficit. However, no explanation has been offered by supporters of the complex scheme for the correspondence between the rates of reaction of ·OH and the rate constants for FeO^{3+} [20]. Finally, there is no evidence in the literature for the existence of the two species FeO^{3+} and $[Fe^{(III)}O_2H]^{2+}$. All spectroscopic work carried out to date on the reaction system has failed to find any evidence that these two species exist [18].

1.5.1.2.5 A Summary of the Situation

Most workers in the area agree that free radicals are important in the $Fe^{2+/3+}$ / H_2O_2 decomposition, but it is recognised that the ·OH radical is not completely free to move through the reaction mixture. It is possible that a 'cage' reaction is occurring and the ·OH radical is not free to diffuse away from its site of generation, the $Fe^{2+/3+}$ ion [27].

Although the complex scheme has the advantage of fitting experimental kinetics data well, in the absence of more supporting data it must be considered suspect. Thus, it will be assumed that the ·OH radical scheme is correct from this point onwards.

1.5.1.3 The Action of Fenton's Reagent on Simple Organic Molecules

The first reaction between an organic molecule and ·OH radical generally takes one of two routes, depending on the type of organic molecule the ·OH radical is attacking.

1) A saturated molecule: - a hydrogen atom is abstracted

$$R_1 - \underset{\underset{R_2}{|}}{\overset{\overset{R_3}{|}}{C}} - H \quad + \ ^\bullet OH \quad \longrightarrow \quad H_2O + \quad R_1 - \underset{\underset{R_2}{|}}{\overset{\overset{R_3}{|}}{C}}\ ^\bullet$$
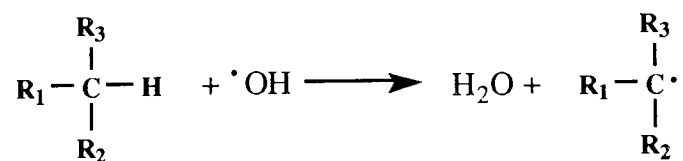
R_1, R_2, and R_3 can be hydrogen or various functional groups. The rate of the reaction of the ·OH radical with the molecule can depend on many factors. However, in general the main factor

45

affecting the reaction rate is the distribution of electrons in the molecule (which is affected by the type and arrangement of the functional groups in the molecule) [28].

2) An unsaturated molecule: - a ring addition reaction occurs
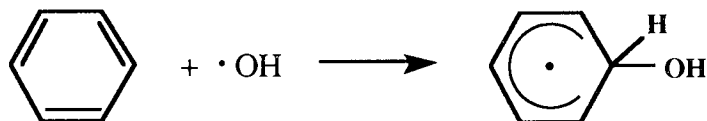
The products eventually formed depend on the ensuing fate of the substrate molecule [24]. It must also be remembered that there are several species in solution that can react with the substrate radical.

1.5.1.3.1 Common Reactions in a Fenton's Reagent / Organic Substrate Mixture

a) Oxidation by the Fe(III) ion

$$R^\cdot + Fe^{3+} \dashrightarrow R^+ + Fe^{2+} \xrightarrow{H_2O} ROH + H^+$$
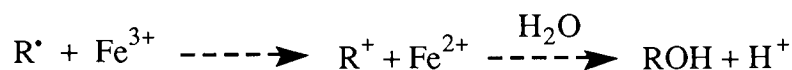
Here the Fe^{3+} ion oxidises the radical. This is the most important oxidation process in the Fenton's reagent system. The Fe^{2+} ion generated in this reaction releases more $\cdot$OH radicals when it reacts with H_2O_2.

$$Fe^{2+} + HO\text{-}OH \xrightarrow{k_1} Fe^{3+} + OH^- + {}^\cdot OH$$
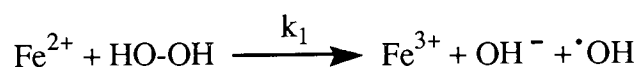
b) Reduction by the Fe(II) ion

$$R^\cdot + Fe^{2+} \dashrightarrow R^- + Fe^{3+} \xrightarrow{H_2O} RH + Fe^{3+} + OH^-$$
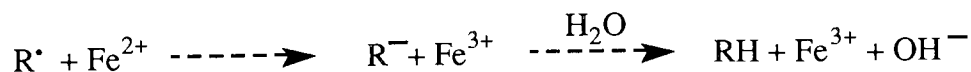
Many organic radicals are not easily oxidised to cations by Fe^{3+} due to the high energy barrier when the radical electron is removed [18]. This high energy barrier exists in two main types of radical.

i) An aromatic radical - the radical electron is in a low energy molecular orbital, delocalised around an aromatic ring, which stabilises the system.
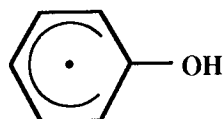
ii) When a delocalised orbital includes an electronegative atom such as oxygen. For example, the radical below would be resistant to further oxidation.

$$
\cdot\!\underset{\substack{|\\H}}{\overset{\substack{H\\|}}{C}} - \underset{}{\overset{\substack{O\\\|}}{C}} - \underset{\substack{|\\H}}{\overset{\substack{H\\|}}{C}} - H
\quad\longleftrightarrow\quad
\underset{\substack{|\\H}}{\overset{\substack{H\\|}}{C}} = \underset{}{\overset{\substack{\cdot O\\|}}{C}} - \underset{\substack{|\\H}}{\overset{\substack{H\\|}}{C}} - H
$$
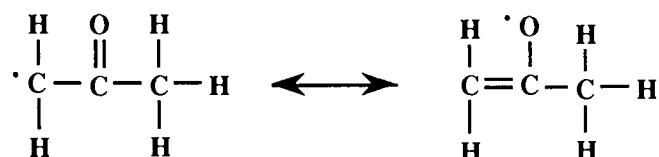
If a positive charge was formed by the loss of the radical electron to the Fe^{3+} ion, it would have to reside partially on the oxygen atom, which is energetically unfavourable. However, the enolate anion formed when the above radical is reduced by Fe^{2+} is known for its stability.

$$
\cdot\!\underset{\substack{|\\H}}{\overset{\substack{H\\|}}{C}} - \underset{}{\overset{\substack{O\\\|}}{C}} - \underset{\substack{|\\H}}{\overset{\substack{H\\|}}{C}} - H
\quad\xrightarrow{Fe^{2+}}\quad
\underset{\substack{|\\H}}{\overset{\substack{H\\|}}{C}} = \underset{}{\overset{\substack{O^-\\|}}{C}} - \underset{\substack{|\\H}}{\overset{\substack{H\\|}}{C}} - H
$$
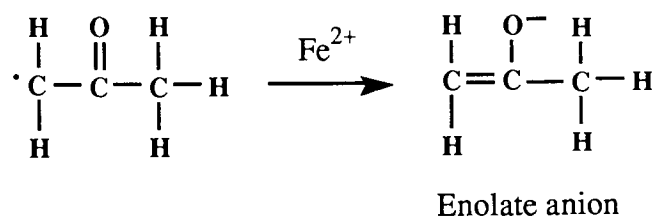
Enolate anion

The enolate anion subsequently abstracts a proton from solution to form the parent molecule.

$$
\underset{\substack{|\\H}}{\overset{\substack{H\\|}}{C}} = \underset{}{\overset{\substack{O^-\\|}}{C}} - \underset{\substack{|\\H}}{\overset{\substack{H\\|}}{C}} - H
\quad\xrightarrow{H^+}\quad
H - \underset{\substack{|\\H}}{\overset{\substack{H\\|}}{C}} - \underset{}{\overset{\substack{O\\\|}}{C}} - \underset{\substack{|\\H}}{\overset{\substack{H\\|}}{C}} - H
$$

Enolate anion
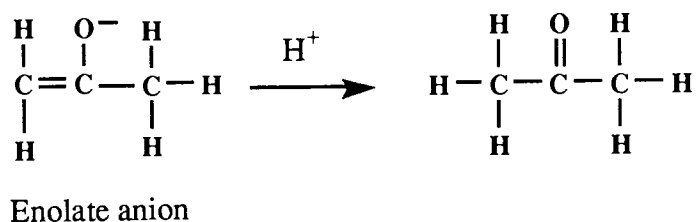
c) Radical combination

$$R^{\cdot} + {}^{\cdot}OH \dashrightarrow ROH$$

Since the concentrations of the radicals ·OH and R· in solution will be low due to their high reactivity, this reaction will not occur very often, but it is an important mechanism for the oxidation of various organic species, particularly those which are difficult to oxidise further[28].

e.g.

$$
R - \overset{\substack{O\\\|}}{C}\!\cdot + {}^{\cdot}OH \quad\longrightarrow\quad R - \overset{\substack{O\\\|}}{C} - OH
$$

d) Radical Rearrangement

$$R^{\bullet} \quad \text{-----} \rightarrow \quad A^{\bullet} + B$$

Radical fragmentation is an essential part of all oxidation schemes because the chain of carbon atoms comprising the substrate molecule must eventually break. This is the process that occurs when an aromatic radical undergoes side-chain scission, and when a carboxylic acid is decarboxylated [18].

e.g.

$$RCO_2^{\bullet} \quad \longrightarrow \quad R^{\bullet} + CO_2$$

e) Self Coupling

$$R_1^{\bullet} + R_2^{\bullet} \quad \text{-----} \rightarrow \quad R_1 - R_2$$
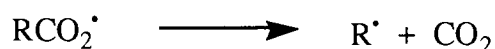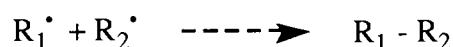
Due to the short lifetime of most radicals in solution, this reaction only occurs rarely. However, if aromatic radicals are involved this process becomes more important due to the relative stability (and therefore long life) of the aromatic radical [29].

e.g.
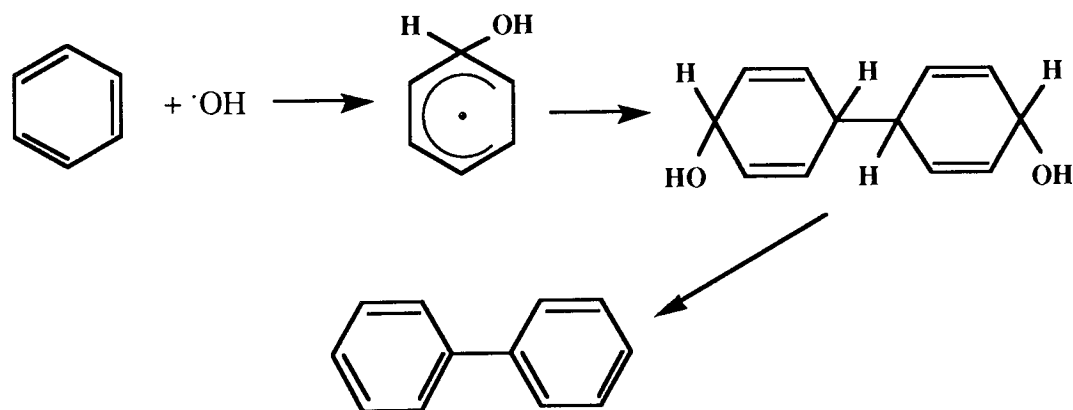
1.5.2 The Use of Fenton's Reagent to Digest Radioactive Ion Exchange Resins

In 1957, Wood reported that sulphonated co-polymers of styrene divinylbenzene, the basis of many types of cation exchange resins, could be degraded and destroyed by the addition of Fenton's reagent [30]. Further work by Bibler and Orebaugh in 1976 confirmed the potential of this technique [31]. More recent work by the Nuclear Electric Laboratories showed that Lewatit

DN could also be treated by this method [32].

1.5.2.1 Development of the Fenton's Reagent / Resin Treatment System by Nuclear Electric

Extensive preliminary work was carried out at Nuclear Electric to find the optimum reaction conditions of the Fenton's reagent / resin treatment system. This work showed that Fenton's reagent was very effective at converting the solid resin to CO_2, H_2O and H_2SO_4. If the reaction were stoichiometric, then it could be represented by the equation

$$C_7H_6O_4S + 16H_2O_2 \longrightarrow 7CO_2 + 18H_2O + H_2SO_4$$
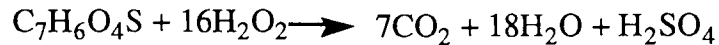
The work provided optimum values for catalyst levels and rate of hydrogen peroxide addition. However, during the course of the research it became obvious that there was a major problem with the process - a large drop in efficiency in the usage of H_2O_2, after the resin had solubilised. A collaborative project was set up with Aston University to look at this problem. The results of this collaboration are described in this thesis.

1.5.2.2 The Efficiency of Hydrogen Usage During the Reaction

FIGURE 1.2

HYDROGEN PEROXIDE USAGE DURING RESIN DIGESTION
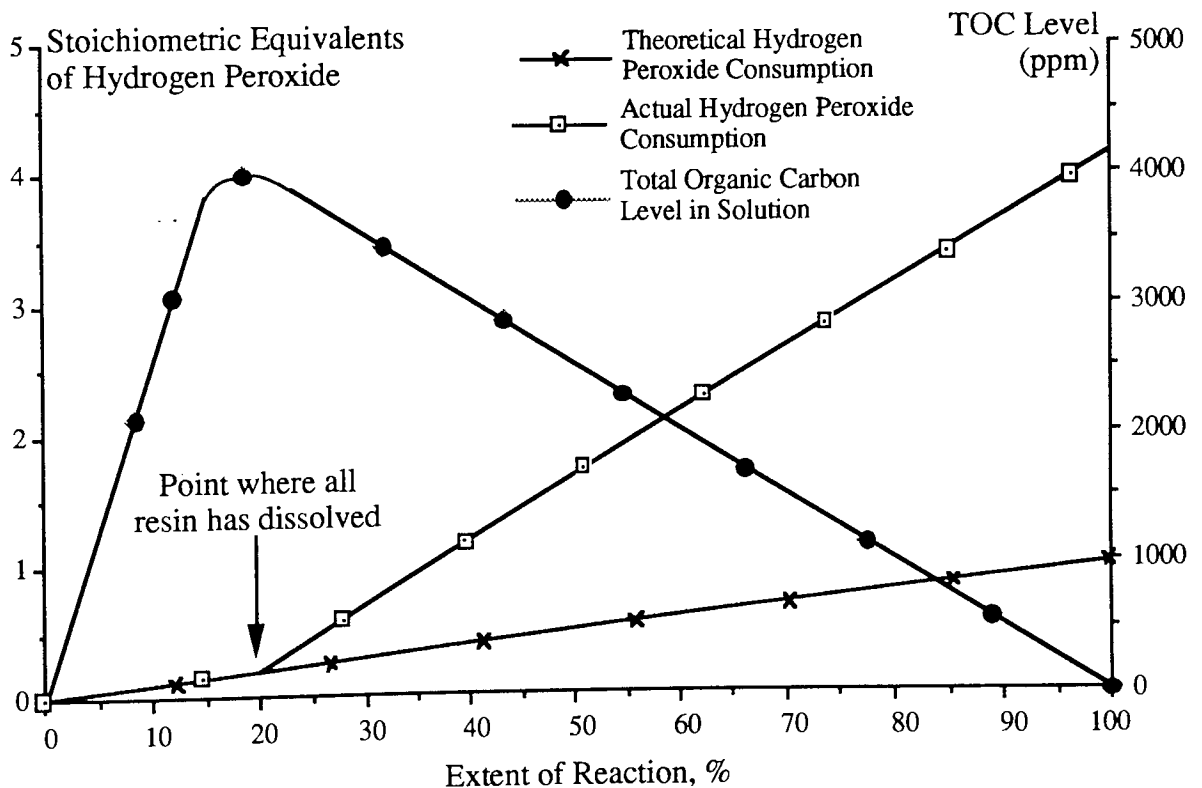
As seen in Figure 1.2, the actual efficiency of hydrogen peroxide use initially approximates to the theoretical efficiency until the resin has completely dissolved, releasing various organic molecules into solution. It is after this point the reaction starts to become wasteful, with increasing amounts of H_2O_2 dissociating into O_2 and H_2O, rather than following the desired path in which hydroxyl radicals attack organic molecules in solution. Since H_2O_2 is a major price component of the Fenton's reagent/resin destruction technique, this waste during the latter part of the reaction is a significant extra cost in the destruction process. It was therefore decided investigate methods for reducing or eliminating this inefficent use of H_2O_2.

1.5.2.3 Possible Methods for Reducing Inefficient Use of Hydrogen Peroxide

a) Stop or reduce the wasteful decomposition of H_2O_2 into O_2 and H_2O towards the end of the reaction by use of physical or chemical techniques e.g. different agitation regimes, different reaction environments. Research into this approach is detailed in Chapter 6 of this thesis.

b) Use an alternative organic molecule destruction technique to reduce the TOC (Total Organic Carbon) level in solution during the latter part of the Fenton's reagent / resin destruction reaction. This could be done either in conjunction with H_2O_2 addition or without the use of any H_2O_2 whatsoever. Research into this approach is detailed in Chapters 3,4, and 5 of this thesis.

To help evaluate each of these approaches for reducing the amount of Fenton's reagent wastage, the progress of the Fenton's reagent / resin destruction reaction was followed using various analytical proceedures (some of which were developed specifically for this work). The aim of this analytical work was to provide data for further research on efficiency improvement and TOC level reduction methods. The results of this analytical work are described in Chapter 7 of this thesis.

The literature was searched to find information on various methods of removing organic molecules from aqueous solutions. These techniques were then tested with the partly digested resin solutions, to see if they would reduce the TOC level. Where this was the case, the method was costed, and compared on economic and efficiency grounds with the Fenton's reagent / resin reaction. Details of the economic and technical aspects of the Fenton's reagent reaction and any potential TOC level reduction method are described in Chapter 8 of this thesis.

CHAPTER TWO

EXPERIMENTAL

2.0 EXPERIMENTAL

2.1 Chemicals

All chemicals used were at least "AnalaR" grade and obtained from Aldrich Chemicals (unless otherwise stated). Samples of "Lewatit DN" ion exchange resin were obtained from Nuclear Electric PLC. On receipt, resin samples were washed with distilled water and then dried at 70°C for 5 days.

Unless otherwise stated all "Ce^{4+}" solutions consist of a solution of 0.01M cerium(IV)sulphate in 1M sulphuric acid. The decision to use cerium sulphate in sulphuric acid was made because of the large amount of work carried out on this system by various workers.

2.2 Solvents

All solvents used were obtained from commercial sources. If further purification was required, they were purified according to the literature method as described by Perrin [33]. When a deoxygenated solvent was required, the solvent was placed in a flask, purged through with dinitrogen for at least 30 minutes, and the flask sealed. Distilled water was used for all aqueous reactions, unless otherwise stated.

2.3 Physical Measurements

2.3.1 Visible and Ultra-Violet Absorption Spectroscopy

Visible and ultraviolet absorption spectra and kinetic studies performed at Aston University were carried out using a Pye-Unicam UV-800 spectrophotometer. Spectra taken at Berkeley Nuclear Laboratories were obtained using a Cecil Instruments CE505 Double Beam UV spectrophotometer. The solution spectra were measured in the range 800-250 nm. The solution and reference solvent were contained either in:-

a) Matched 1cm path length glass cells, or

b) Matched 0.5cm path length quartz cells.

The cell compartment of the spectrophotometer was equipped with a water jacket to enable accurate temperature control by circulating water at the desired temperature through the cell holder.

2.3.2 Infra-Red Spectroscopy

Infra-red absorption spectra collected at Aston University were recorded on a Perkin-Elmer 1710 Infrared Fourier Transform Spectrometer. Infra-red absorption spectra collected at Berkeley Nuclear Laboratories were recorded on a Nicolet 5PC FT / IR spectrometer, with a Compac Deskpro 286 as the data station. Four sample analysis techniques were used to obtain IR spectra of organic materials:-

a) The sample was incorporated in a KBr disc.

b) An aqueous sample placed on a CaF_2 disc, and then the water was removed by heating in an oven at 50°C.

c) An aqueous sample was placed in a flow cell, between CaF_2 discs.

d) Horizontal ATR of aqueous samples

However, techniques (c) and (d) were ineffective, due to the masking of the signal from the organic solute by that of the solvent, water.

2.3.3 Nuclear Magnetic Resonance Spectroscopy

The ^1H and ^{13}C NMR spectra were recorded in various solvents by a Bruker Spectrospin AC 300MHz FT-NMR instrument.

Special pulsing techniques such as water pre-saturation and 1,3,3,1 jump and return were necessary to obtain ^1H spectra from samples of resin digestion mixture. These sequences were necessary to avoid the organic H signal being drowned out by the water H signal. Signal amplification techniques such as APT and DEPT were necessary to obtain ^{13}C spectra of resin digestion mixture, due to the low concentration of organic materials in these samples.

2.3.4 pH Measurements

pH measurements were carried out by using a PTI-6 Universal pH meter.

2.3.5 Melting Points

The melting points of all solid compounds were determined using a Gallenkamp melting points apparatus which was heated electrically and the temperature recorded using a mercury thermometer (calibrated at 100°C).

2.3.6 Mass Spectra

Mass spectra on aqueous samples were carried out on an AE1 MS9 spectrometer at an ionising potential of 70 eV. Mass spectra on non-aqueous samples were carried out by the SERC Mass Spectrometry Service Centre on a VG Masslab Model 12-253 [34].

2.3.7 Atomic Absorption

Atomic absorption spectroscopy on iron and cobalt ions in solution was carried out on a Varian Spectra AA-40 with a DS-15 Data Station.

2.3.8 Magnetic State

ESR spectra were recorded at room temperature using a JEOL JES-PE-1 spectrometer. A Gouy Balance, consisting of a Newport Instruments D104 magnet connected to a Stanton Instruments SM12 Balance, was used to detect the presence of paramagnetism in solid samples.

2.3.9 Total Organic Carbon (TOC)

The TOC level is a measurement of the amount of organic Carbon dissolved in water. The TOC levels of aqueous solutions were found by using an Ionics Total Organic Carbon Analyser Model 1270, which had an accuracy of plus or minus 2%. The TOC level results were output in the form of parts per million (ppm) of carbon.

2.3.10 Gas-Liquid Chromatography

The gas liquid chromatograph used was a Pye Unicam GCD Chromatograph fitted with a Flame Ionization Detector. The column was composed of 25% Silicone Grease absorbed on diatomite. The temperature of the column was varied between 100 and 225°C and the sensitivity between 4 and 4×10^3.

2.3.11 Particle Sizing

The diameter of particles suspended in water was found by using a Malvern Instruments Series 2600C Droplet and Particle Sizer.

2.3.12 Hydrogen Peroxide Concentration

Hydrogen peroxide levels in aqueous solution were found by using the method of Hawkins [35]. 1 cm^3 of the solution to be analysed was added to 20 cm^3 of 2M sulphuric acid, in a 250 cm^3 conical flask. 2 g of potassium iodide and 2 g of sodium hydrogen carbonate were then simultaneously added to the flask. The solution in the flask was then titrated with a solution of 0.1M sodium thiosulphate, using starch solution as an indicator.

2.4 Computation

All data analysis was performed using the program Cricket Graph on Apple Macintosh computers at Aston University. Graphs were created using a combination of the programs Cricket Graph, MacDraw II, and Superpaint 2.0.

2.5 Analysis

Micro analytical data for carbon, hydrogen, nitrogen and sulphur were obtained from Butterworths Laboratories Ltd, of Teddington, Middlesex, and also Medac Ltd, of Uxbridge, Middlesex. The presence of sulphate in aqueous solution was determined by the methods described by Vogel [36]:-

a) Lead Acetate Test (Sensitivity limit - 1 part in 10000)

b) Sodium Rhodizonate Test (Sensitivity limit - 1 part in 10000)

c) Potassium Permanganate / Barium Sulphate Test (Sensitivity limit - 1 part in 20000)

A quantitative determination of sulphate in solution was obtained by adding BaCl$_2$ solution to the solution to be tested. If the solution to be tested was not already acidic, HCl was added to acidify the solution. The precipitate formed was removed by filtration and dried at 130°C for 4 days. The precipitate was then weighed, heated by a bunsen burner for 15 minutes, and reweighed to obtain the amount of precipitate left. The amount of precipitate left was related to the amount of BaSO$_4$ precipitated from solution.

2.6 Description of Experimental Equipment Used

2.6.1 UV Photochemical Reactor

FIGURE 2.0

UV PHOTOCHEMICAL REACTOR
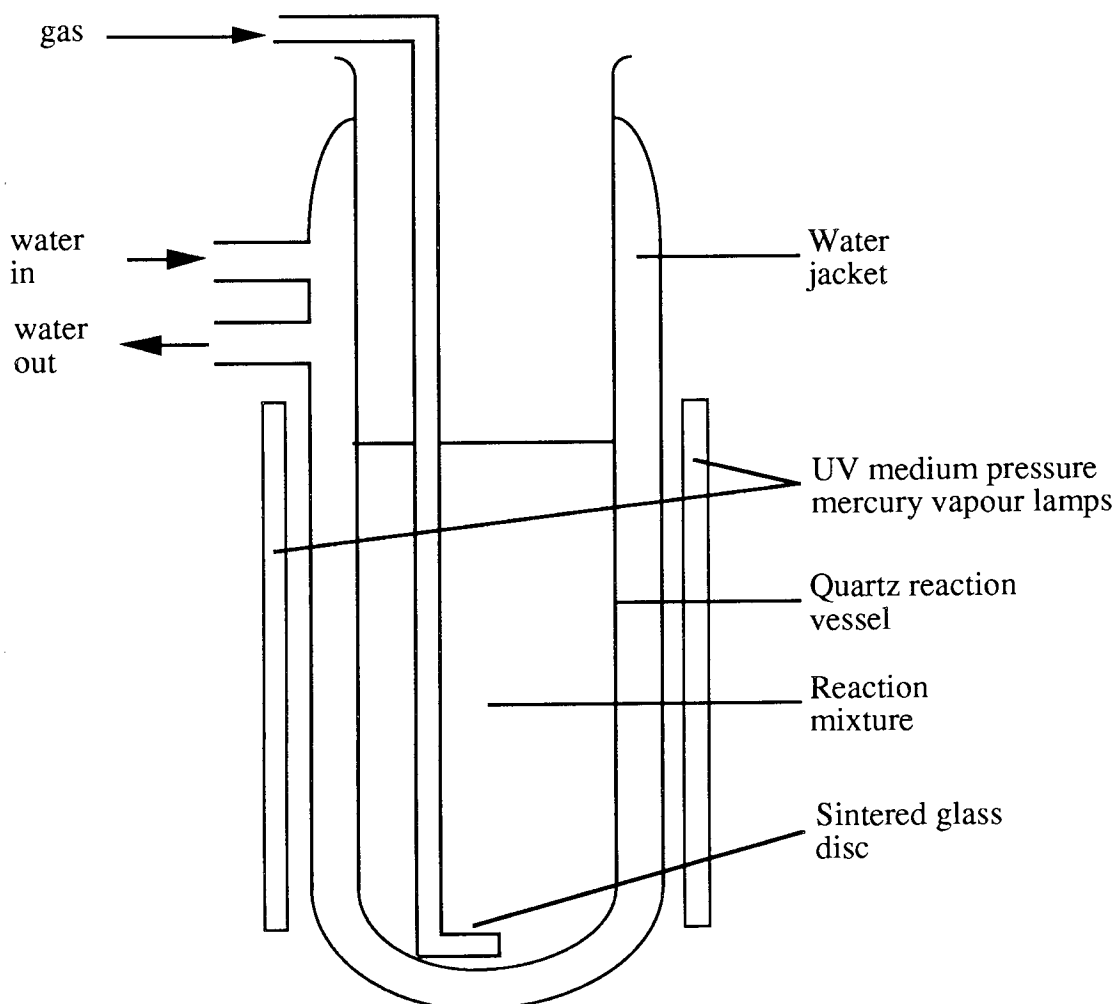
2.6.1.1 Start-up Procedure

1) The water jacket was connected either to the mains water supply or to a thermostated water pump.

2) The two medium pressure UV tubes were turned on and left to warm up for 10 minutes. If gas was being blown through the liquid then it was switched on at this point. The equipment was then left for a further 10 minutes to allow the temperature of the UV reactor and contents to stabilize.

2.6.1.2 Operational Procedure

The reactants were placed inside reaction vessel. Manual stirring was performed using a glass rod, or alternatively stirring was carried out by blowing a gas through a sintered glass tube immersed in the reaction mixture.

2.6.1.3 Important Safety Note

Intense UV light is produced by the two mercury vapour tubes, which have a peak emission wavelength of 366nm. UV goggles must be worn whenever near the reactor. There must also be no bare skin e.g. that of the hands, arms, exposed to the direct light of the tubes. Thus, thick rubber gloves and material covering the arms are essential items of apparel.

2.6.2 Bolt-Top-Reactor / Contact Thermometer

FIGURE 2.1

A 1 LITRE VOLUME BOLT-TOP REACTOR
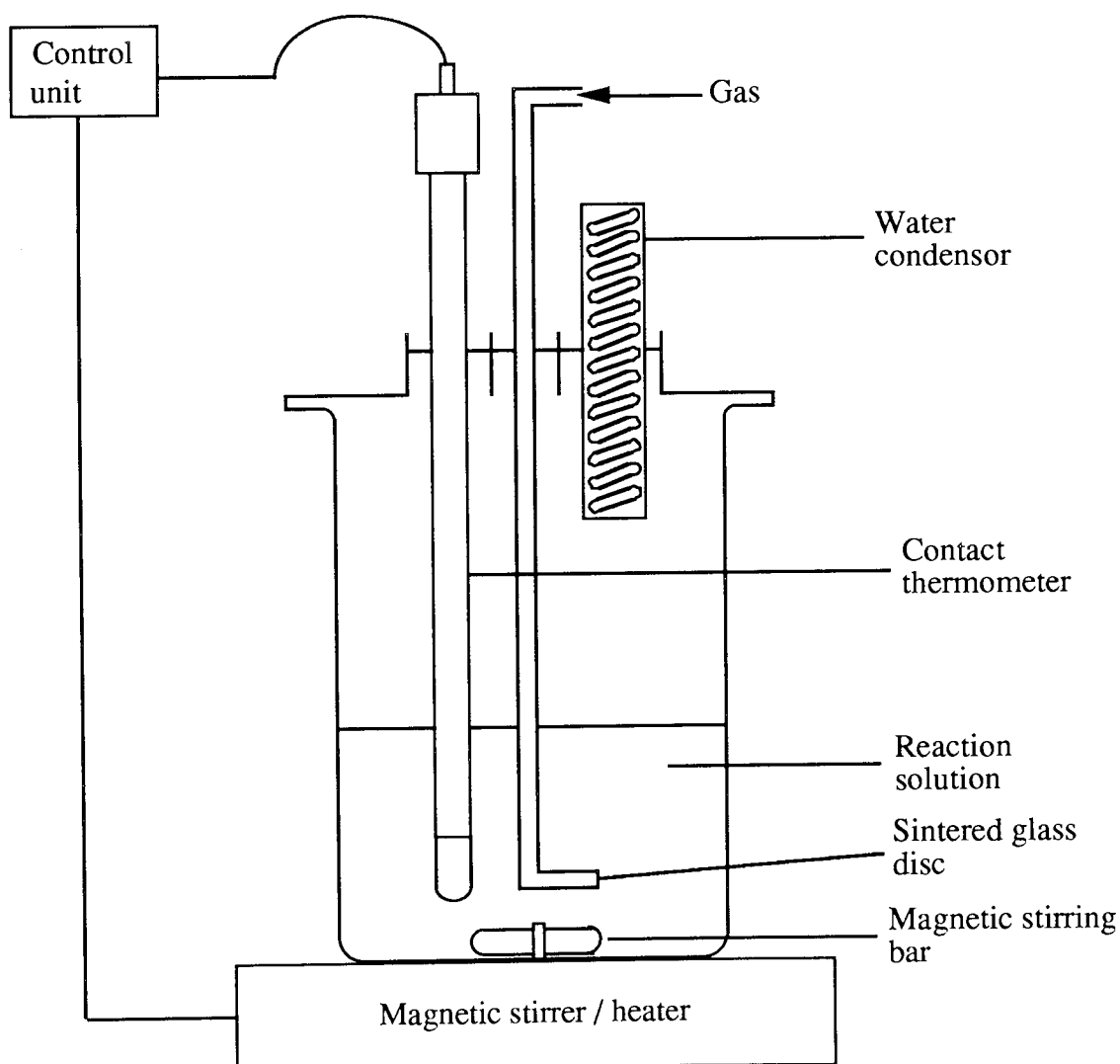
This equipment was used in all reactions that involved the use of Fenton's reagent. The contact thermometer was set at the desired temperature, and a feedback loop between the contact thermometer and magnetic stirrer / heater maintained this temperature to within $2^{\circ}C$. A glass tube with a p160 sintered glass disc at the end was used to bubble gases through the resin reaction mixture. The three gases bubbled through the resin reaction mixture at various times were air, O_2 and N_2. A standard set of conditions was defined for the resin digestion system to improve the reproducibility of results.

2.7 The Standard Resin Digestion Reaction

10 g of dry Lewatit ion exchange resin is placed in the bolt-top reactor. $400\,cm^3$ of distilled water is then added, together with 0.13 g of $FeSO_4.7H_2O$. The mixture is stirred and heated until either $85^{\circ}C$ (occasionally) or $95^{\circ}C$ (usually) is reached. $130\,cm^3$ of 30% w/v H_2O_2 is allowed to reach $25^{\circ}C$ (room temperature) and is then quickly added to the contents of the bolt-top reactor. The temperature is then maintained at a constant level until the end of the reaction. Samples taken were labelled as follows.

A sample taken from the standard resin digestion reaction mixture (reacting at $95^{\circ}C$) 140 minutes after the start of the reaction would be labelled 140 minutes resin.

This nomenclature is used throughout this thesis when describing samples taken at various times during the resin digestion reaction.

2.8 Stopping the Resin Digestion Reaction Prematurely

It was sometimes necessary to obtain large samples of resin reaction solution at a particular time during a reaction. To stop the progress of the reaction at a specific point, the reaction mixture was first cooled rapidly by placing the bolt-top reaction vessel in ice-water. Once the reaction mixture temperature had dropped below $80^{\circ}C$, the reaction rate was negligible [2]. The cooling was continued until room temperature was reached, and then a powder of 5% platinum on charcoal (supplied by Johnson Matthey Chemicals) was added. This catalytically decomposes any H_2O_2 in the reaction solution, forming H_2O and O_2. After 4 hours of stirring the mixture (4 hours was necessary to ensure that all of the H_2O_2 had been decomposed), the platinum catalyst was filtered out and the resin reaction solution stored in a glass vessel. It was found that

if the resin reaction solution was stored in a plastic container, contamination of the resin solution occurred after some weeks. It was also found that the resin reaction solution was slightly photosensitive (it was affected over a time scale of weeks), so the reaction solution was stored in the dark.

2.9 Experimental Techniques Specific To Chapter 3

2.9.1 Co(salen) / Oxygen / Resin Digestion Solution Experiments

2.9.1.1 Synthesis of Co(salen)

The method of Bailes and Calvin was used to synthesize Co(salen) [37]. For further details of Co(salen) please see p73 / 74.

2.9.1.2 The Use of Co(salen) to Oxidise Organic Molecules in Aqueous Solution

The resin digestion was stopped prematurely (as described in Section 2.8) to obtain a large quantity of solution for further study.

Typically, 100 cm^3 of this resin reaction solution was heated to 95°C in the bolt top flask / contact thermometer combination. O_2 was then blown through the resin reaction solution at the rate of 0.1 cubic litre per minute (via a p160 sintered glass disc). Samples of the solution were taken to determine the TOC level and Co concentration. Five minutes were allowed for the resin solution to become saturated with O_2. 1 g of Co(salen) was then added to the resin solution, and the mixture heated and stirred for 8 hours. At the end of this time, samples of the mixture were taken to determine the TOC level and Co concentration.

2.9.2 Palladium 1,4,7 Triazacyclononane / Oxygen / Resin Digestion Solution Experiments

2.9.2.1 Synthesis of the Triazacyclononane Ligand

The method of Richman and Atkins was used to synthesize the triazacyclononane (tacn) ligand [38]. Once the tacn ligand had been synthesised, palladium (III) triazacyclononane was made by adding PdCl$_2$ to a slightly alkaline solution of the ligand, as described by McAuley [39].

2.9.2.2 The Use of Palladium 1,4,7 Triazacyclononane to Oxidise Organic Molecules in Aqueous Solution

The procedure for these experiments was identical with that for the Co(salen) experiments (Section 2.9.1.2), except that 0.04 g of palladium 1,4,7, triazacyclononane was substituted for 1 g of Co(salen).

2.10 Experimental Techniques Specific To Chapter 4

The resin digestion reaction was stopped prematurely (as described in Section 2.8) to obtain a large quantity of solution for further study.

Typically, 100 cm^3 of resin digestion solution was then placed in the photochemical reactor and irradiated for 8 hours, with samples for TOC level analysis being taken regularly. If powdered TiO$_2$ (Anatase form) was added as a photocatalyst, 0.1 g was used. Undisturbed, the TiO$_2$ powder gradually settled out of solution, so every 30 minutes the mixture was stirred by blowing air through it, via a p160 sintered glass disc. When TiO$_2$ was used it was necessary to filter the samples taken for TOC level determination before injecting them into the TOC analysing equipment.

2.10.1 Calculation of the Light Output of the UV Photochemical Reactor

A potassium ferrioxalate solution-phase chemical actinometer system was used to find the light output of the photochemical reactor. In this system Fe^{3+} is reduced to Fe^{2+} by incident light in a reaction with a quantum yield (φ) of 1. The concentration of Fe^{2+} is found with a UV spectrophotometer by adding 1,10-phenanthroline which forms a strongly absorbing complex with Fe^{2+}.

e.g. if the absorbance of the Fe^{2+} complex, in a 1 cm path length cell, was found to be 1 after 60 seconds

$$A = \varepsilon \, C \, l$$

$$1 = (1.11 \times 10^4) \times C \times 1$$

rearranging this equation to find the concentration of Fe^{2+} we get

$$C = 1 / 1.1 \times 10^4$$

$$C = 9.09 \times 10^{-5} \text{ M}$$

$$C = 9.09 \times 10^{-5} \text{ M}$$

Since the quantum yield for the formation of Fe^{2+} is 1, this means that during the 60 seconds 9.09×10^{-5} M of photons were incident on the contents of the photochemical reactor.

2.11 Experimental Techniques Specific To Chapter 5

All stock solutions of 0.01M Ce^{4+} were replaced every 2 months due to absorption of Ce^{4+} onto the walls of the glass storage vessel. All kinetics experiments in this chapter were carried out at 25°C in the absence of light unless otherwise stated.

2.11.1 Reactions involving Ce(IV) and an End of Reaction Resin Digestion Solution

A stock solution of 0.01M Ce^{4+} was made up. Varying amounts of end of reaction resin digestion solution (300 minutes resin solution) were added to 100 cm^3 of cerium solution to obtain different Ce^{4+} : C in solution ratios. Samples were taken at intervals, diluted as necessary, placed in the UV spectrophotometer, and their absorbance at 317 nm was measured. 317 nm is the maximum absorption peak of the Ce^{4+} ion in sulphuric acid. The absorbance data were then converted to $[Ce^{4+}]$.

These reactions were also carried out under irradiation, in a UV photochemical reactor.

2.11.2 Reactions involving Ce(IV) and poly (sodium-4-styrene sulphonate)(PSS)

A stock solution of 0.01M Ce^{4+} was made up. Varying amounts of PSS were added to 100 cm^3 aliquots of cerium solution to obtain different Ce^{4+} : polymer ratios. Samples were taken at intervals, diluted as necessary, placed in the UV spectrophotometer, and their absorbance at 317 nm was measured.

These reactions were also carried out under irradiation, in a UV photochemical reactor.

2.11.2.1 The Analysis of PSS Oxidation Products

In order to analyse the organic products of the Ce^{4+} / PSS reaction by IR it was necessary to:-

a) remove any $Ce^{4+/3+}$ from solution.

b) neutralise the highly acidic reaction solution, to enable IR spectra to be obtained of the

This was done by slowly adding 7.5M NaOH solution to the reaction mixture, until it neutralised. This also had the effect of precipitating out all the $Ce^{4+/3+}$ ions from solution ($Ce^{4+/3+}$ ions are insoluble in neutral / basic solution). The precipitate was then removed by filtration, and a sample of the remaining liquid was placed on a CaF_2 disc. The disc was heated at 50°C until all the water had evaporated, leaving behind the organic constituents of the liquid. The CaF_2 disc was then placed in an IR spectrophotometer and a spectrum obtained.

2.11.2.2 The Detection of Any Gas Produced During the Ce(IV) / PSS/ UV Reaction

The following equipment was set up to detect any gas produced during the UV irradiation of PSS.

FIGURE 2.2

GAS COLLECTION EQUIPMENT
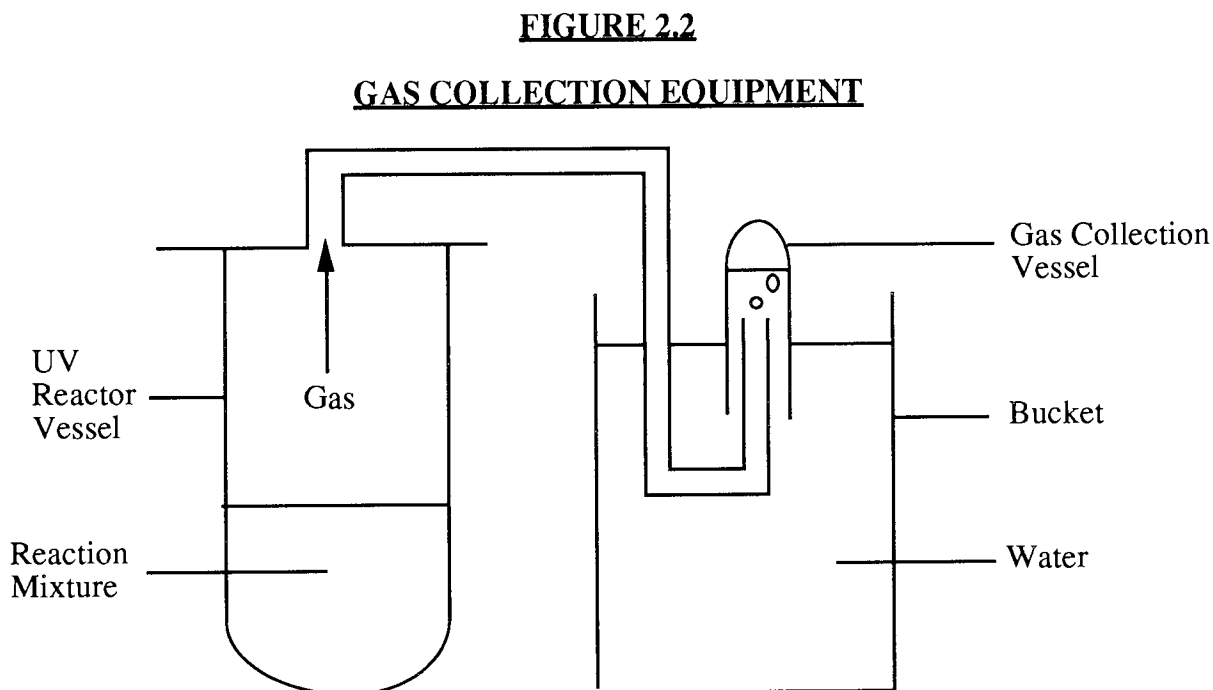
A solution of 0.01M Ce^{4+} was made up. 100 cm^3 was placed in the UV photochemical reactor, and 0.18 cm^3 of PSS was added to the Ce^{4+} solution. The top of the UV reactor vessel was then sealed, except for a tube leading to a gas collecting vessel held upside down in a bucket of water. The volume of any gas released during the reaction was noted.

2.11.3 Reactions involving Ce(IV) and calix[8]arene-p-octasulfonate (CALIX)

2.11.3.1 Synthesis of CALIX

The method of Gutsche was followed to produce the starting material, calix[8]arene (except for a doubling of the quantities of all starting reagents) [40].

To produce CALIX, the method of Shinkai was adapted slightly, because the starting material in Shinkai's synthesis was calix[6]arene [41].

p-t-Butylcalix[8]arene (6.0 g, 6.18 mmol) was mixed with concentrated sulphuric acid (34.5 g). To the stirred reaction mixture fuming sulphuric acid, "oleum," (60%, 10.2 g) was added dropwise. The temperature was maintained at 35-40°C, with the aid of a heating mantle and / or a flask of icewater. From time to time an aliquot was withdrawn from the solution and poured into water to monitor the progress of the reaction. The reaction was judged complete when no water insoluble material was detected on addition of the aliquot (this occurred after 4 hours). The reaction mixture was then poured into ice water (41 cm^3), and the precipitate formed was recovered by filtration. The precipitate was washed with a small amount of 50% sulphuric acid and then dissolved in 82 cm^3 of water. The solution was warmed at 60°C and granulated, activated charcoal was added. After filtering the solution, a white precipitate was obtained by salting out with NaCl. This precipitate was removed from the solution by centrifugation. The precipitate was impure, so it was redissolved in water, forming a concentrated solution. Ethanol was then added to precipitate out the product. Filtration using Whatman 542 filter paper then produced a pure product (as shown by NMR spectra of the product).

2.11.3.2 Calculation of Ce(IV) : CALIX ratios

All calculations of the ratio between Ce^{4+} and CALIX were based on the ratio of Ce^{4+} ions to the benzene repeat units in the CALIX molecule. Since there are 8 benzene units in the CALIX molecule, a '2 :1 Ce^{4+} : CALIX repeat unit' ratio would represent 2 Ce^{4+} ions per benzene unit, or 16 Ce^{4+} ions per CALIX molecule.

2.11.3.3 Stopped Flow Kinetics Experiments

2.11.3.3.1 Stopped Flow Apparatus

FIGURE 2.3

STOPPED FLOW EQUIPMENT
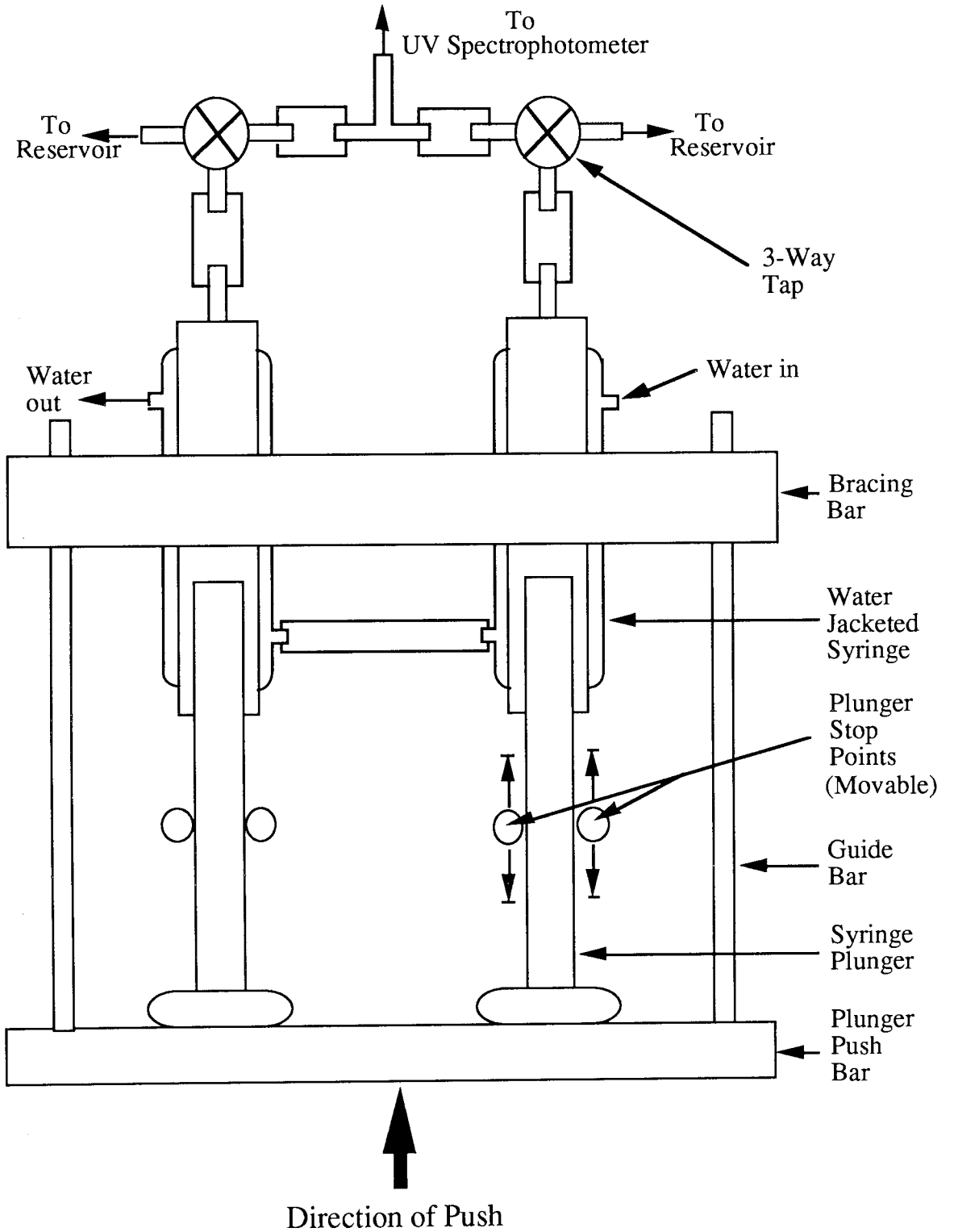
2.11.3.3.2 Start-up Procedures

1) The syringe water jackets were connected to a thermostated water pump and water run through the equipment at the chosen temperature for 10 minutes to ensure thermal equilibrium in the syringes.

2) The plungers were moved all the way into the syringes.

3) The two reservoirs were filled with the appropriate liquids.

4) The three way taps were opened, and the plungers pulled out slowly to draw the liquids from the reservoirs into the appropriate syringe.

5) The liquids were left in the syringes for a time to enable thermal equilibrium to be achieved throughout the syringes and their contents. This equilibrium time was dependent on the temperature of the water flowing through the water jacket, typical times - 2 minutes for $30^{\circ}C$ water, 3 minutes for $40^{\circ}C$ etc.

2.11.3.3.3 Operational Procedure

The three way taps were turned, and the plungers pushed rapidly into the syringes, being halted at the appropriate point by the plunger stop bars. This action rapidly mixed the two liquids, injecting them into and through a quartz flow cell in the UV spectrophotometer. The change in absorbance of the reacting liquids at 317 nm was then followed over time.

A 0.001M $Ce(SO_4)_2$ solution in 0.1M H_2SO_4 was made up along with a 6.6 x 10^{-5}M solution of CALIX (0.0175 g in 1000 cm^3 water). These solutions were used as reservoir solutions for the stopped-flow kinetics apparatus, giving a 15:1 $[Ce^{4+}]$: [CALIX repeat unit] ratio. To obtain a 2 : 1 ratio the Ce^{4+} solution was diluted a further 7.57 times. The reservoirs were filled, and the reactants injected into the flow cell in the UV spectrophotometer.

2.11.3.4 The Standard Ce(IV) / CALIX Reaction, Ce(IV) Variable

A stock solution of 0.01M Ce^{4+} in 1M H_2SO_4 was made up and diluted to varying concentrations, whilst maintaining the same total volume. A constant amount of CALIX (pre-dissolved in 5 cm^3 of water) was added to 229 cm^3 of each Ce^{4+} solution and the mixture stirred vigorously. All solutions were thermostated to $25^{\circ}C$.

TABLE 2.0

CE(IV) : CALIX RATIOS, WITH CE(IV) CONCENTRATION VARIABLE

Volume of Ce(IV) stock solution, cm^3	Volume of 1M H$_2$SO$_4$ dilutant, cm^3	Amount of CALIX, g	Ratio (Ce(IV) ions : CALIX repeat unit)
229	0	0.04	15 : 1
183.1	45.9	0.04	12 : 1
122.1	106.9	0.04	8 : 1
76.3	152.7	0.04	5 : 1
30.5	198.5	0.04	2 : 1

Samples of the reaction solution were taken regularly, and their absorbance at 317 nm measured. The same dilutions and procedures were used for the UV irradiated Ce^{4+} : CALIX reaction mixtures.

2.11.3.5 The Standard Ce(IV) / CALIX Reaction, CALIX Variable

A stock solution of 0.00333M Ce^{4+} in 1M H$_2$SO$_4$ was made up, and separated into vessels each containing 229 cm^3 of Ce^{4+} solution. Varying amounts of CALIX (pre-dissolved in 5 cm^3 of water) were added to each vessel and the mixture stirred vigorously. All solutions were thermostated to 25°C.

TABLE 2.1

CE(IV) : CALIX RATIOS, WITH [CALIX] VARIABLE

Volume of Ce(IV) stock solution, cm^3	Amount of CALIX, g	Ratio (Ce(IV) ions : CALIX repeat unit)
229	0.08	5 : 2
229	0.06	5 : 1.5
229	0.04	5 : 1
229	0.02	5 : 0.5
229	0.01	5 : 0.25

Samples of the reaction solution were taken regularly, and their absorbance measured at 317 nm. The same dilutions and procedures were used for the UV irradiated Ce^{4+} : CALIX reaction mixtures.

2.12 Experimental Techniques Specific To Chapter 6

2.12.1 Boiling the Resin in Dilute Mineral Acid

10 g of resin was boiled in 500 cm^3 of 0.1M H_2SO_4 and, in a separate experiment, boiled in 500 cm^3 of 0.2M HNO_3 (an equivalent H^+ concentration) for 8 hours. The acid solutions were then checked for TOC level and, for the HNO_3 solution, the presence of SO_4^{2-} (by addition of $BaCl_2$). The acidity of the acid was measured by titration against a 0.2M solution of NaOH before and after the resin had been boiled in acid. The resin was then dried at 70°C for 5 days and elemental analysis for C, H, O, and S carried out on a sample of the resin. 30 cm^3 of H_2O_2 was then added to 4 g of the H_2SO_4 and HNO_3 boiled resin, and also to 4 g of the unaltered resin, and the final TOC level of the solutions measured when all the H_2O_2 had been consumed.

2.12.2 Reducing the Concentration of Free Iron in Solution

It was decided to reduce the concentration of free iron in the resin digestion solution after all the resin beads had dissolved. This was done by adding various combinations of the chelating agents sodium silicate, sodium tungsten silicate, and $MgSO_4$ to a standard resin / Fenton's reagent solution, immediately after all the resin beads had dissolved. Half the normal quantities of reagents were used in the standard resin / Fenton's reagent reaction, i.e. 5 g of resin, 0.065 g $FeSO_4.7H_2O$, 65 cm^3 of H_2O_2, 200 cm^3 water.

2.12.2.1 Using a Combination of sodium tungsten silicate and $MgSO_4$ as Sequestering Agents

0.428 g of commercial grade sodium tungsten silicate, and 0.07 g of $MgSO_4$ were added to the resin / Fenton's reagent solution 70 minutes after the reaction had started. The quantities of sodium tungsten silicate and $MgSO_4$ added were based on work carried out by Bambrick[42]. TOC level and H_2O_2 concentration were monitored throughout the reaction.

2.12.2.2 Using a Combination of sodium silicate and MgSO₄ as Sequestering Agents

0.15 g of commercial grade sodium silicate and 0.07 g of $MgSO_4$ were added to the resin / Fenton's reagent solution 70 minutes after the reaction had started. The $NaSiO_3$ was added to the reaction mixture as a 27% solution in 14% NaOH. 0.291 cm^3 of this mixture was added to the resin / Fenton's reagent solution.

2.12.3 Making the Resin Digestion Solution More Alkaline

It was decided to make the resin digestion solution more alkaline by addition of solid NaOH. Solid NaOH (in pellet form), rather than a concentrated aqueous solution, was used to minimise any volume changes when the NaOH was added to the reaction mixture. In total, 2.5 g of solid NaOH was added intermittently from 2 minutes until 67 minutes into the reaction. TOC level, H_2O_2 concentration and Fe concentration were all measured throughout the reaction by the standard methods. However, the resin reaction solution was too acidic to obtain accurate pH measurements by using a pH meter so an alternative method was devised to measure the pH of the reaction mixture.

1 cm^3 samples of the resin reaction solution were taken and immediately placed in 100 cm^3 of distilled water. The pH of the distilled water was monitored before and after sample addition, and the change in pH enabled the original pH of the reaction mixture to be calculated (on the assumption that the activity coefficient of H^+ remained at 1.0 throughout).

2.12.3.1 Example Calculation of pH

$$pH = -\log [H^+]$$

pH of distilled water before sample addition = 5.34, therefore $[H^+] = 4.57 \times 10^{-6}$ mol / dm^3

pH of distilled water after sample addition = 4.10, therefore $[H^+] = 7.94 \times 10^{-5}$ mol / dm^3

Thus 1 cm^3 of resin solution added 7.48×10^{-5} moles of H^+ ($7.94 \times 10^{-5} - 4.57 \times 10^{-6}$) to the distilled water solution.

In 1000 cm^3 of the resin reaction solution there would be $1000 \times (7.48 \times 10^{-5})$ moles of H^+

$$= 7.48 \times 10^{-2} \text{ moles } H^+$$

Substituting into pH = -log [H⁺], we get

$$\underline{pH = 1.13}$$

2.12.4 Making the Resin Digestion Solution More Acidic

It was decided to make the resin digestion solution more acidic by addition of concentrated H_2SO_4. Concentrated H_2SO_4 was used to minimise any volume changes. Normally the pH of the resin digestion solution rises as soon as all the resin has dissolved, so drops of H_2SO_4 were added after all the resin had dissolved, with the aim of maintaining the pH at the same level throughout the reaction.

TOC level, H_2O_2 concentration and Fe concentration were all measured throughout the reaction by the standard methods. pH was measured by the method described in the previous section (Section 2.12.3.1).

CHAPTER THREE

THE USE OF DIOXYGEN AS AN OXIDANT OF ORGANIC MOLECULES IN AQUEOUS SOLUTION

3.0 INTRODUCTION

From a thermodynamic viewpoint, oxygen is capable of oxidising any organic molecules in the partially digested resin solutions. However, at standard pressure and temperature (25°C, 1 atmosphere) the oxidation of organic molecules by oxygen is very slow. This is mainly because oxygen has a triplet ground state and therefore its direct combination with singlet organic molecules is a spin-forbidden process [43]. This problem can, under certain circumstances, be overcome by using transition metal ions or transition metal complexes to catalyse the reaction [44]. Transition metals can catalyse these types of reaction because their multiple spin and oxidation states can readily interact with dioxygen, even to the extent of forming oxygen adducts that can be isolated [43].
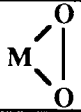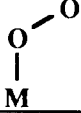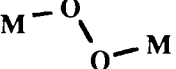
It was decided to investigate two catalytic systems involving the use of transition metals. The first system involved the use of a dioxygen-transition metal complex. The second system was based on the use of a variable oxidation state transition metal-ligand complex.

3.0.1 Dioxygen-Transition Metal Complexes

Many biologically produced oxygen carrying molecules are known, for example haemoglobin and haemocyanines. These biological molecules are based on a transition metal centre, which facilitates reversible oxygen binding to the molecule. Synthetically produced oxygen carrying molecules, generally based on a transition metal centre, have also been produced in great variety [45,46].

There are three main oxygenated forms of transition metal - oxygen complexes. The type of complex present in a system depends on the metal type and its oxidation state, as is shown in Table 3.0 (see overleaf) [43].

TABLE 3.0

OXYGENATED FORMS OF TRANSITION METAL COMPLEXES

Name	Shape	Example of Metal
Peroxo	$M \diagup\!\!\!\!\!\stackrel{O}{\underset{O}{\big|}}$	$Co^I, Ir^I, Ru^{II}, Rh^I$
Superoxo	$O\!\!\nearrow^{O}$ $\underset{M}{\big|}$	Fe^{II}, Co^{II}
μ-peroxo	$M\!-\!\!\underset{O\diagup\!\!M}{\overset{O}{\diagdown}}$	Fe^{II}, Co^{II}

where M = Metal and O = Oxygen

Once the complex forms, the metal acts as a reducing agent and can also polarize the dioxygen bond, facilitating its cleavage. It can also simultaneously bind the oxygen molecule and the substrate, thus creating favourable conditions for the oxidation of the substrate.

3.0.1.1 Anticipated Method of Use of a Transition Metal - Dioxygen Complex

The desired mode of operation would be that, when added to a solution of partly digested resin, the transition metal-O_2 complex interacts directly with an organic molecule in solution, adding oxygen to it. The deoxygenated transition metal molecule would then form another complex with O_2 from the reaction solution, and then add O_2 to another organic molecule. This catalytic cycle would continue until some or all organic molecules had been oxidised partially or completely to CO_2. Several workers have described the use of transition metal-O_2 complexes to oxidise organic substrates, so it was known that this behaviour could occur [47,48,49].

Figure 3.0 shows the catalytic cycle that occurs when an organic molecule is oxidised.

FIGURE 3.0

THE CATALYTIC OXIDATION OF AN ORGANIC MOLECULE BY A
TRANSITION METAL - DIOXYGEN COMPLEX

$$O_2 + Tr \rightleftharpoons Tr\text{-}O_2 \qquad (1)$$

$$Tr\text{-}O_2 + Or \longrightarrow Tr + Or\text{-}O_2 \qquad (2)$$

where Tr = Transition Metal

Tr-O_2 = Transition Metal - Oxygen Complex

Or = Organic Molecule
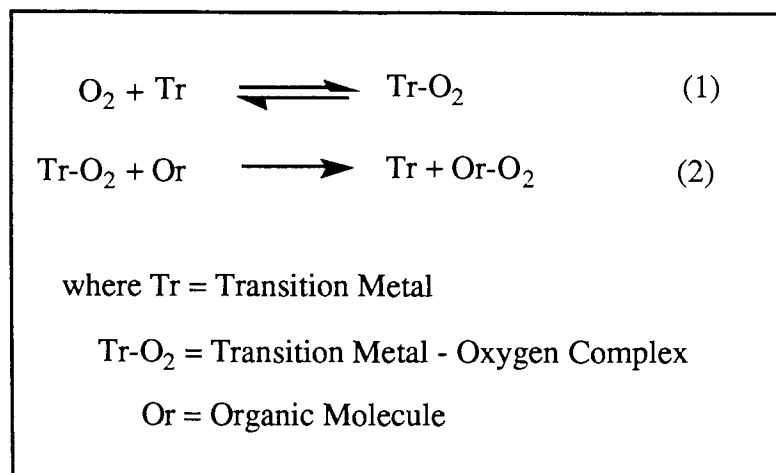
3.0.1.2 Cobalt Based Oxygen Carrying Molecules

The use of cobalt as the transition metal centre in synthetic oxygen carrying molecules has been widely investigated for many years. One of the earliest known complexes was a cobalt complex, [(NH$_3$)$_{10}$Co$_2$O$_2$]$^{4+}$, which was first described in 1893 [50]. However, this research was not followed up until 1938, when Tsumaki published a paper on the properties of the cobalt(II) chelate of Bis(salicylaldehyde)ethylenedi-imine, otherwise known as Co(salen) or "salcomine" [51]. Further work was carried out on this compound by Calvin and Bailes in 1947 [37].

Much of the initial work on Co(salen) and derivatives was carried out with the aim of developing a mechanically simple method for separating O$_2$ from the atmosphere. However, this aim was not achieved until 30 years after Calvin's work, when a fluorine-substituted Co(salen) chelate was developed as the basis of a successful oxygen supply system [52]. Other work on cobalt dioxygen complexes has used them as models for binuclear oxygen carrying and oxygen storage proteins [53]. Work has also been carried out on the use of complexes for the direct reduction of dioxygen to water in homogeneous solution and on electrode surfaces [50].
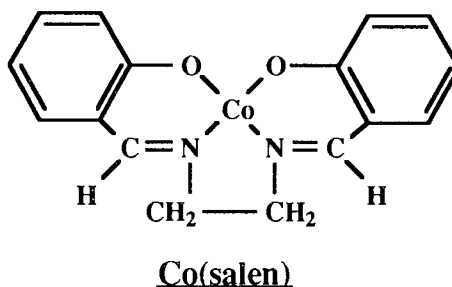
Co(salen)

It was decided to study the insoluble (in water) dioxygen complex Co(salen) because of the ease with which it can be synthesised, and the large quantity of research that has already been carried out on the complex. This research indicated that the Co(salen) molecule can be reversibly oxygenated and deoxygenated many thousands of times before the molecule eventually degrades [54].

Co(salen) is a perfectly planar compound, crystallising out in a layer lattice.

FIGURE 3.1

ELECTRON MICROSCOPE PHOTO OF A CO(SALEN) CRYSTAL
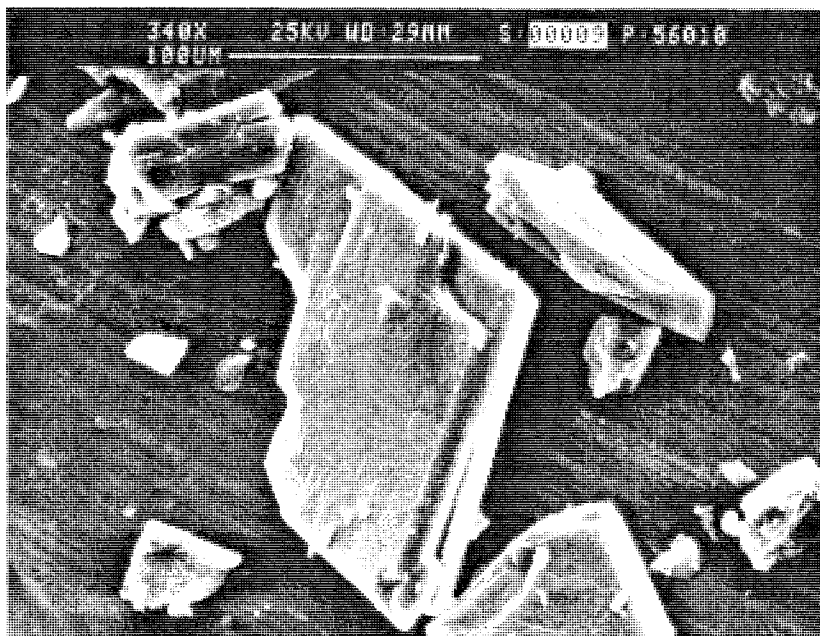
The oxygen uptake occurs in the ratio $Co:O_2 = 2:1$, in the solid state, and it is thought that the O_2 molecule is bound between two layers of cobalt atoms, with one atom attached to each layer. In organic solvents, the $Co:O_2$ ratio can either be 1:1, as in (A), or 2:1, as in (B) (see Figure 3.2) [55].

74

FIGURE 3.2

CO(SALEN)-OXYGEN CONFORMATIONS

$$
\begin{array}{c}
\text{N O} \\
\backslash / \\
\text{L}-\text{Co} \\
/ \backslash \\
\text{N O}
\end{array}
\quad + \quad \text{O}-\text{O} \quad \rightleftharpoons \quad
\begin{array}{c}
\text{N O} \quad \text{O} \\
\backslash / \quad / \\
\text{L}-\text{Co}-\text{O} \\
/ \backslash \\
\text{N O}
\end{array}
\qquad \text{(A)}
$$

$$
\begin{array}{c}
\text{N O} \quad \text{O} \\
\backslash / \quad / \\
\text{L}-\text{Co}-\text{O} \\
/ \backslash \\
\text{N O}
\end{array}
\quad + \quad
\begin{array}{c}
\text{O N} \\
\backslash / \\
\text{Co}-\text{L} \\
/ \backslash \\
\text{O N}
\end{array}
\quad \rightleftharpoons \quad
\begin{array}{c}
\qquad\qquad \text{O N} \\
\qquad\qquad \backslash / \\
\text{N O} \quad\quad \text{O}-\text{Co}-\text{L} \\
\backslash / \quad\; / \quad\; / \backslash \\
\text{L}-\text{Co}-\text{O} \quad\;\; \text{O N} \\
/ \backslash \\
\text{N O}
\end{array}
\qquad \text{(B)}
$$

$$
\text{where L = Ligand and} \quad
\begin{array}{c}
\text{N O} \\
\backslash / \\
\text{Co} \\
/ \backslash \\
\text{N O}
\end{array}
\; = \text{Co(salen)}
$$
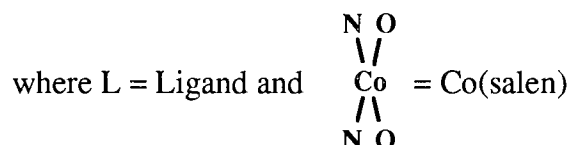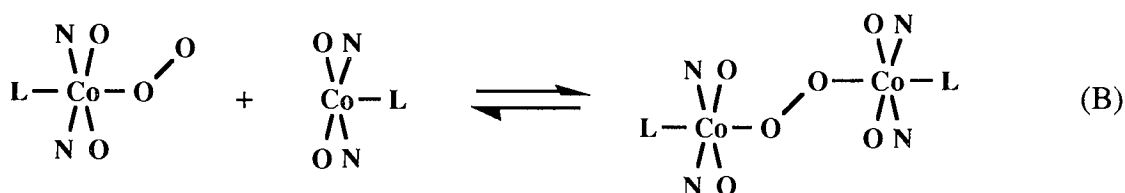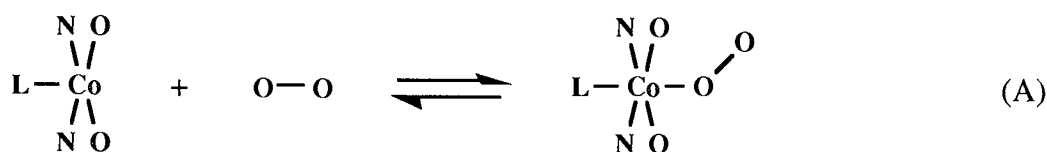
Factors that influence whether a 2:1 or 1:1 complex is formed include the relative concentrations of Co(salen) and O_2 in solution, temperature and solvent [50].

3.0.2 Variable Oxidation State Metal-Ligand Complexes

The presence of two or more stable oxidation states in transition metal ions is common e.g. $Ce^{4+/3+}$. Another example of this is the Pd ion, as part of the macrocyclic complex 'palladium 1,4,7 triazacyclonane'. The effect of the 1,4,7 triazacyclononane ([9]aneN$_3$) ligand, when complexed with a Pd^{II} ion, is to stabilise the Pd^{III} oxidation state. As a consequence of this stabilisation, O_2 will oxidise the Pd^{II} ion to the Pd^{III} ion. This Pd^{III} ion is then capable of acting as an oxidising agent. It was hoped that a catalytic system could be developed based on this property of the ([9]aneN$_3$) ligand when complexed to palladium.

3.0.2.1 Palladium 1,4,7 Triazacyclononane

The macrocyclic ligand 1,4,7-triazacyclononane ([9]aneN$_3$) has received attention recently for a variety of reasons, including its ability to stabilise unusual oxidation states, such as Ni^{III} [56]. The small size of the ring induces a facial disposition onto an octahedral structure, thus all the simple complexes involving first-row transition elements exhibit an MN_6 geometry [39].

However, the elements of the second and third transition series have increased crystal field stabilization energy and so are not always predisposed towards octahedral geometry. For Pt^{II}, the d^8 configuration exhibits almost exclusively a square planar geometry [57]. This d^8 configuration has been seen in the [Pt-([9]aneN$_3$)$_2$]$^{2+}$ complex. When this complex is then oxidised by molecular oxygen to [Pt-([9]aneN$_3$)$_2$]$^{4+}$, octahedral co-ordination is observed [57]. It is the ([9]aneN$_3$) ligand that facilitates the oxidation of the Pt centre.

The synthesis of the [Pd-([9]aneN$_3$)$_2$]$^{2+}$ complex was reported by McAuley in 1988 [58]. It was found that this complex could also be oxidised by oxygen, like the equivalent platinum complex, but to the III oxidation state rather than the IV oxidation state. The E^0 for the $Pd^{III/II}$ couple, at pH 1.5, is 0.53V (vs. NHE).

The crystal structure of the Pd^{II} complex has the ligand coordinated in a bidentate, square-planar manner (isomorphous with the Pt^{II} ion) [57]. However, there is some steric strain in this molecule. The axial lone pairs on the non-coordinated nitrogen atoms perturb the orbital energy levels, which encourages the formation of a Pd^{II} complex, which has a strain free octahedral geometry [39]. The [Pd-([9]aneN$_3$)$_2$]$^{3+}$ complex was the first example found of a monomeric Pd^{III} ion that is stable for long periods in aqueous solutions (pH $\approx$ 3-8). The Pd^{IV} ion has also been found, but it is far less stable than the Pd^{III} ion.

Triazacyclononane
ligand (formal
2-D respresentation)
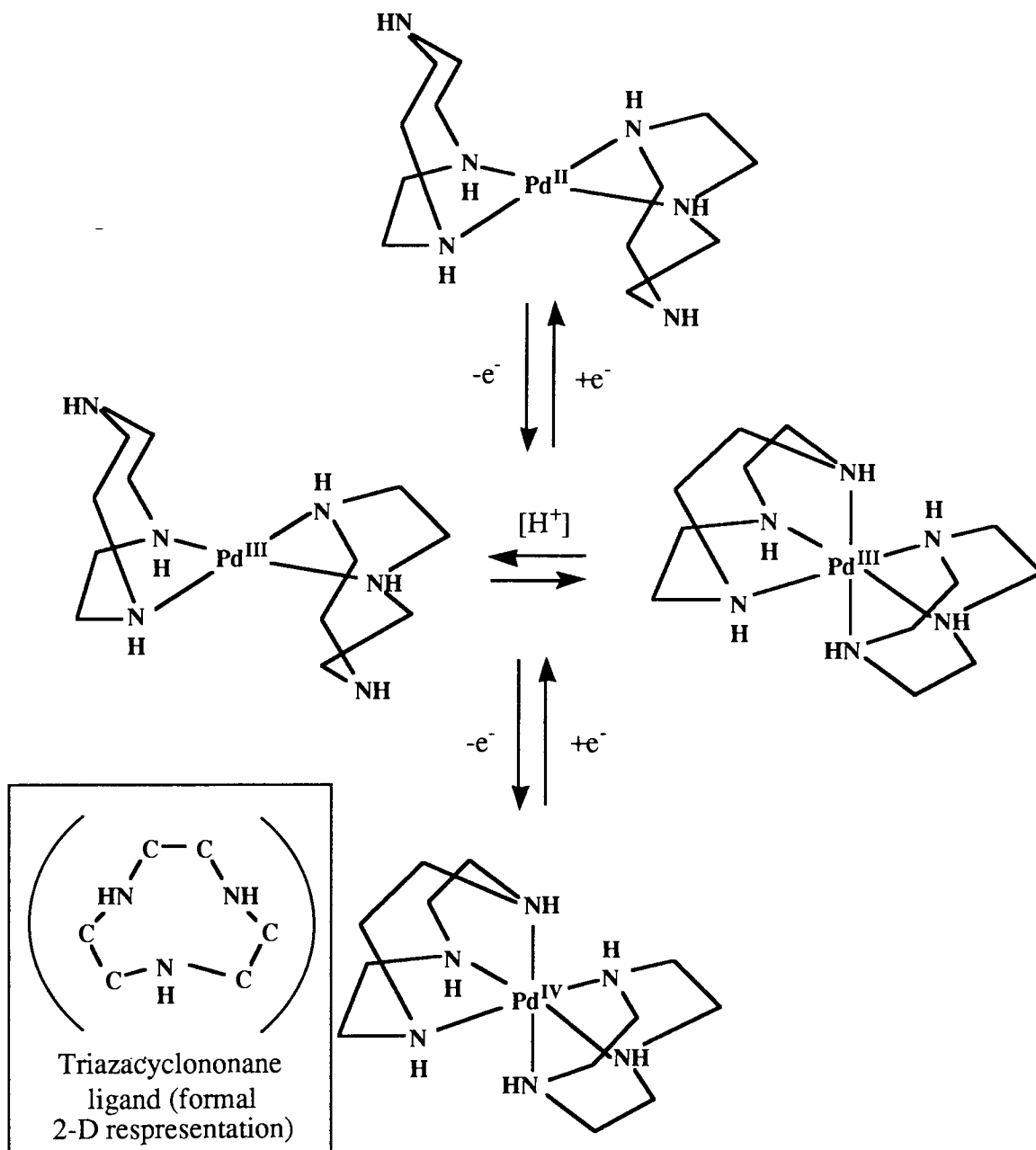
3.0.2.1.1 The Anticipated Method of Use of Palladium Triazacyclononane

The anticipated method of use for the [Pd-([9]aneN3)2] would be the addition of [Pd-([9]aneN3)2]$^{3+}$ to a partially digested resin solution. The complex would then oxidise an organic molecule, being itself reduced to [Pd-([9]aneN3)2]$^{2+}$ in the process. Oxygen blowing through the solution would reoxidise the complex back to [Pd-([9]aneN3)2]$^{3+}$, creating a catalytic cycle for the partial or complete oxidation of organic materials in solution, as shown in Figure 3.4.

FIGURE 3.4

THE CATALYTIC OXIDATION OF AN ORGANIC MOLECULE BY A
VARIABLE OXIDATION STATE METAL-LIGAND COMPLEX

$$Pd^{II} \xrightarrow{\quad O_2 \quad} Pd^{III} \qquad\qquad (1)$$

$$Pd^{III} + Or \longrightarrow Pd^{II} + \text{oxidised Or} \qquad (2)$$

where Pd = Palladium

Or = Organic molecule
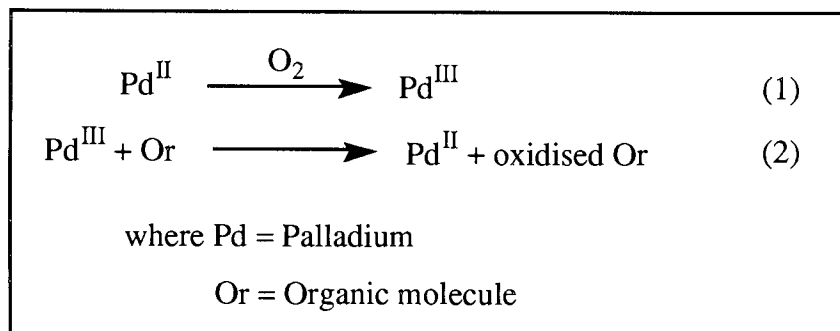
3.1 RESULTS

3.1.1 The Addition of Co(salen) to Resin Digestion Solutions

Co(salen) crystals were added to partly digested resin solutions and the mixture was then stirred and heated while O_2 was blown through the solution (Co(salen) is a heterogeneous catalyst in water). TOC level and Co concentration were monitored at the start and end of each experiment. Control experiments were carried out by blowing oxygen and nitrogen through the solutions under the same conditions, but in the absence of Co(salen).

3.1.1.1 TOC Level Changes

Over the course of several experiments, it was shown that the TOC level in the partly digested resin solutions was on average lower after O_2 or N_2 had been blown through the solution. A TOC level drop was also seen when O_2 was blown through the resin solution in the presence of Co(salen). Table 3.1 (see overleaf) presents a summary of the series of experiments carried out:-

TABLE 3.1

THE CHANGE IN TOC LEVEL OF 75 MINUTES RESIN SOLUTION

AFTER TREATMENT WITH OXYGEN OR NITROGEN, WITH AND

WITHOUT CO(SALEN)

Experiment	% Change, with O_2 sparge	% Change, with N_2 sparge	% Change, O_2 sparge, Co(salen)
1	-	-	0
2	-	-	+ 4.6
3	-	-	- 10.7
4	-	-	- 10.1
5	- 9.4	-	-
6	- 14.2	-	-
7	- 6.4	-	-
8	-	-10	-
Summary of results	**- 10**	**- 10**	**- 4**

On initial inspection of the experimental data shown in Table 3.1 it would seem that the Co(salen)-O_2 complex causes little or no further oxidation of organic molecules in aqueous solution. This is suggested by the 10% drop in TOC level when either O_2 or N_2 is blown through the resin solution, compared with a 4% drop in TOC level when O_2 is blown through the resin solution in the presence of Co(salen). The identical TOC level drop irrespective of whether N_2 or O_2 is blown through the resin solution, suggests that this TOC level drop is due to residual CO_2 and / or volatile organic molecules being swept out of the solution by a combination of the gas passing through the solution and the elevated temperature of the solution (95°C).

3.1.1.2 Further Analysis of Data from Table 3.1

Although the raw experimental data would suggest that the Co(salen)-O_2 complex is having little or no effect on the TOC level of the 75 minutes resin solution, (4% TOC level drop .vs. 10% drop for N_2 or O_2) it was decided to re-analyse the data. This was done as a result of experimental

data obtained on the concentration of Co in solution.

AA analysis of the resin solution before and after Co(salen) use showed that a very large increase in Co level had occurred during the experiment. Using typical experimental data (see Table 3.2) it can be seen that the Co concentration in solution increases from 1.5 ppm to 105 ppm, an increase of 70 times relative to the original concentration. Since the only possible source of Co in this system is the Co(salen) catalyst, it must be assumed that this Co increase is due to the Co(salen) crystal partially dissolving or degrading under the conditions used in the experiment. If this is happening then an increase in the TOC level of the resin solution due to the contribution of the carbon skeleton of the Co(salen) molecule can be expected.

To check whether the Co(salen) was in solution in the above system or alternatively in the form of fine particles, the resin solution was filtered through a p160 sintered glass disc. No change in Co level before and after was seen, indicating that the Co was in solution, and that parts of the Co(salen) crystals had degraded or dissolved into aqueous solution.

TABLE 3.2

TYPICAL CO(SALEN) / OXYGEN / RESIN SOLUTION TOC LEVEL AND COBALT CONCENTRATION DATA

TOC level before = 3720 ppm	TOC level after = 3320 ppm
Co level before = 1.54 ppm	Co level after = 105.4 ppm

Using the figures in Table 3.2 to calculate the effect on TOC level of Co(salen) dissolving or degrading into solution:-

a) The total ppm of Co in solution increases by 104 ppm, which represents an increase of 0.014 g of the Co loading in the resin solution (which has a constant volume of 100 cm^3).

b) Since the relative molecular mass of Co(salen), (molecular formula $C_{16}H_{14}N_2O_2Co$) is 325, this increase in Co level equates to the addition of 0.045 g of C into the resin solution (450 ppm C). This would increase the TOC level of the resin solution to 4120 ppm from its initial level of 3720 ppm, i.e., degradation of the Co(salen) crystals during passage of O_2 through the resin solution releases 0.045 g of C into solution.

c) If the total TOC level fall during passage of O_2 through the resin solution is calculated from 4120 ppm rather than 3720 ppm, a total drop of 20% is observed, compared with an average drop for O_2 alone of 10%.

If the data for all other non-Co(salen) experiments is analysed similarly then it is found that the average TOC level drop in the presence of O_2 and Co(salen) is 19.4%, whereas in the presence of O_2 alone the average TOC level drop is 10%.

This would suggest that 9.4% of the carbon in solution has been oxidised to CO_2 and H_2O by Co(salen), while a further 10% has been physically removed from solution by the gas passing through.

3.1.2 Blowing Oxygen Through a Resin Solution in the Presence and Absence of Co(salen) and Its Effect on Subsequent Hydrogen Peroxide Utilisation

Another series of experiments was carried out, in which the progress of a conventional Fenton's reagent / resin digestion reaction was again arrested 75 minutes after its start, to produce a large batch of '75 minutes resin solution'. The H_2O_2 concentration in this batch was found, and then the 75 minutes resin solution was split into 3 equal portions. The H_2O_2 in solution was removed from two of the portions by adding platinum catalyst. The final, unaltered portion was then allowed to react again by heating it to 95°C, to create a control experiment. O_2 was then blown through each of the other two portions of 75 minutes resin solution via a sintered glass gas bubbler, one portion in the presence and the other in the absence of Co(salen). The resin digestion reactions were then resumed from the points at which they had been stopped (after removal of Co(salen)) by addition of an amount of H_2O_2 equivalent to that removed by the platinum catalyst. The final TOC levels were found after the reactions had been completed. The aim of this series of experiments was to find out whether the presence of Co(salen) in solution (after using Co(salen) / O_2 to oxidise organic molecules in solution - see Section 3.1.1) would affect the later progress of the Fenton's reagent / organic molecules reaction.

3.1.2.1 The Results of the Use of a Co(salen) / Fenton's Reagent Combination

The TOC level of the unaltered 75 minutes resin solution was found to be 3450 ppm.

TABLE 3.3

THE EFFECT OF BLOWING OXYGEN THROUGH 75 MINUTES RESIN REACTION SOLUTION IN THE PRESENCE AND ABSENCE OF CO(SALEN), AND THEN CONTINUING A STANDARD RESIN DIGESTION REACTION

Experiment	Final TOC - standard digestion reaction	Final TOC - O_2 blown digestion reaction	Final TOC - O_2/Co(salen) digestion reaction
1	850 ppm	-	-
2	790 ppm	-	-
3	-	630 ppm	-
4	-	770 ppm	-
5	-	-	720 ppm
Summary of Data	820 ppm	700 ppm	720 ppm

The result of Experiment 5 (Table 3.3) shows that the presence of Co(salen) in solution has no adverse effect on the subsequent progress of the Fenton's reagent/resin reaction, after Co(salen) has been used mid-way through the reaction to oxidise organic molecules in solution. In fact, the final TOC level in this experiment was found to be 12% lower than the averaged final TOC level of the standard resin digestion reaction. Since the margin of error in TOC level measurements is about 2%, this TOC level fall is statistically significant. The final TOC level of 720 ppm represents a 79% drop in TOC level from the TOC level of the original 75 minutes resin solution.

The use of O_2 alone mid-way through the reaction, in Experiments 3 and 4, also had the effect of lowering the final TOC level of the resin solution relative to the standard resin digestion reaction. The final, averaged TOC level in these experiments was 15% lower than the averaged final TOC level of the standard resin digestion reaction. The final TOC level in this solution, 700 ppm, represents an 80% fall in TOC level from the 75 minutes resin value.

The final TOC level of the standard resin digestion solution, 820 ppm, represents a 76% drop in TOC level, relative to the 75 minutes resin.

3.2 Discussion of the Results

3.2.1 TOC Level Reduction by Gas Purging Alone (See Sections 3.1.1.2 and 3.1.2.1)

It seems that blowing either N_2 or O_2 through a heated solution of partially digested resin reduces the TOC level of that solution by removal of organic volatiles and CO_2. However, in the context of the Nuclear Electric project, this method of TOC level reduction may not be of any practical use, for two reasons.

The first reason is that at the end of any industrial process based on Fenton's reagent digestion of ion exchange resin, the end resin reaction solution would first be neutralised by addition of a base, and then heated until all water was lost (see Chapter 8, Section 8.6). It would be expected that any volatile organic molecules or CO_2 would be lost from the solution at this point, negating the beneficial effect of any earlier gas sparging of the solution. Secondly, I have suggested that air blown through the resin solution should be used to stir the reaction mixture in the full-scale industrial resin processing plant (see Chapter 8,.Section 8.3.1.2). This air would have the secondary effect of removing any volatile organic molecules or CO_2 from solution as soon as it was created.

3.2.2 TOC Level Reduction by Use of a Combination of Co(salen) and Dioxygen (See Section 3.12)

In my experiments, when O_2 was blown through the solution in the presence of Co(salen), there was a lower TOC level reduction than when O_2 alone was blown through the resin solution (4% against 10%). However, when the contribution of degrading Co(salen) molecules is taken into account, it seems that oxidation of the organic molecules in the resin reaction solution to CO_2 is occurring. The TOC level reduction due to O_2 / Co(salen) use might well be increased if the conditions of reaction were altered. If a large enough increase in the quantity of organic molecules oxidised were obtained, then the adverse increase in TOC level caused by dissolving Co(salen) would be counteracted, creating an overall reduction in TOC level through use of the O_2 / Co(salen) system. Alternatively, ways could be investigated of stabilising the Co(salen) crystals, to stop the addition of organic compounds to the resin solution by crystal degradation. If either of these approaches was successfully implemented, less H_2O_2 would be required to

oxidise the remaining organic molecules, resulting in savings in the use of this reagent. As shown by Table 3.3, the presence of Co in solution (from the dissolving Co(salen)) does not appear to have any adverse effect on the Fenton's reagent / resin reaction.

In summary, this area of research could be promising from an economic viewpoint because it seems that the use of the Co(salen) / O_2 oxidises some organic molecules present in the resin solution. Co(salen) is an easily and cheaply produced catalyst, and its use part of the way through the resin digestion reaction does not adversely affect the subsequent Fenton's reagent / organics reaction. O_2 is a fairly cheap gas, although the economics of using a Co(salen) / O_2 system would be greatly improved if it was found that air could be used instead of pure O_2. Unfortunately, it was not possible to perform further work on this system due to lack of time.

3.3 The Use of Palladium 1,4,7 triazacyclononane to Oxidise Resin Reaction Solutions

Palladium 1,4,7 triazacyclononane was added to partly digested resin solutions, which were then stirred and heated while O_2 was blown through the solution. The TOC level was monitored at the start and the end of the experiment.

3.3.1 Changes in TOC level

No significant change in TOC level values at the beginning and end of the experiment was seen in either 70 minutes resin solution or 300 minutes resin solution. However, the colour of the 70 minutes resin solution changed from light brown to dark brown / black during the experiment. This may indicate that some organic molecules in the resin solution are being partially oxidised.

3.4 Discussion of the Results

The TOC level results suggest that there is no conversion of aqueous organic molecules to CO_2 and water by palladium 1,4,7 triazacyclononane, in the presence of O_2. However, it might be that only partial oxidation of specific organic molecules is occurring, without complete oxidation of organic molecules to CO_2 and water occurring. This hypothesis may be supported by the colour change of the 70 minutes resin solution during the experiment. In fact, the colour change of the solution is an indication that partial oxidation of at least some of the organic

molecules in solution has occurred. For example, when phenols (likely components of the resin digestion mixture at this point) are oxidised there is a colour change from colourless to dark brown / black as variously coloured quinones are formed [59].

This hypothesis could be also investigated by analysis of the resin solution before and after the addition of palladium 1,4,7 triazacyclononane. Alternatively, subsequent H_2O_2 consumption could be measured, to find if it had been affected by use of palladium 1,4,7 triazacyclononane. These experiments were not carried out due to lack of time.

CHAPTER FOUR

THE USE OF UV LIGHT TO PROMOTE THE DESTRUCTIVE OXIDATION OF ORGANIC MOLECULES IN AQUEOUS SOLUTION

4.0 INTRODUCTION

UV irradiation of aqueous solutions, often in association with photocatalysts such as titanium dioxide, has been shown to be a very effective method of removing a large variety of organic compounds from solution [60,61].

It was suggested that irradiation of the partly digested resin solutions (with or without a photocatalyst) might produce a significant TOC level drop in the resin solution by conversion of the organic molecules to CO_2 and H_2O. This hypothesis was tested by irradiating two solutions of partly digested resin. The first sample solution irradiated was taken from a point just after all the resin had solubilised. The second sample solution irradiated came from the end of the reaction, after all the H_2O_2 had been consumed.

4.0.1 The Effects of UV Irradiation on Organic Molecules

If an atom or molecule absorbs UV light, it becomes energetically excited through the promotion of at least one electron to a higher energy orbital. Molecules in excited states are usually more easily oxidised than the equivalent ground state molecule due to the promotion of electrons to the higher energy, often anti-bonding, orbital (in which electrons are more weakly held). Excited states are also more easily reduced, because the photoexcitation generates an orbital vacancy in a low-energy orbital making the excited state highly electrophilic in the presence of an appropriate electron donor [62].

In aqueous solutions the excited state species often creates in turn a free radical, either by direct photolytic cleavage or by a photo-induced charge transfer reaction with another reagent. A major product of these reactions in water is the ·OH radical, which in turn initiates organic auto-oxidation [60].

$$OH^\bullet + RH \longrightarrow R^\bullet + HOH$$

$$R^\bullet + O_2 \longrightarrow ROO^\bullet$$

$$ROO^\bullet + RH \longrightarrow ROOH + R^\bullet$$

or, for aromatics

$$Ar^\bullet + O_2 \longrightarrow ArOO^\bullet$$

$$ArOO^\bullet + ArH \longrightarrow ArOOH + Ar^\bullet$$
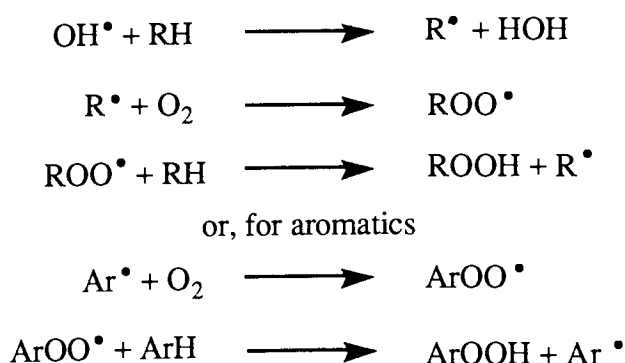
Auto-oxidation produces cleaved aromatic rings and small highly oxidised organic fragments such as low molecular weight carbonyl compounds [63]. Organic molecules which are particularly susceptible to auto-oxidation include phenols, compounds with electron rich centres, and molecules with easily oxidised functional groups [64].

4.0.2 The Effect of UV Irradiation on Organic Molecules in the Presence of Titanium Dioxide

Photoassisted heterogenous catalysis has been the focus of much research over the past 15 years, since it was shown that this technique could remove hydrocarbon and chlorocarbon contaminants from water [65]. For example, chloroform, benzene, phenol, poly-chlorinated biphenyls, and the herbicides atrazine and s-triazine can all be completely mineralised by a UV / semiconductor combination [66,67].

Various semi-conductors such as metal oxides (e.g. ZnO, WO_3) and metal sulphides (e.g. CdS) have been used as photocatalysts in the past. However, the semi-conductor TiO_2 was chosen for investigation as a catalyst for the destruction of organic molecules in the resin solution. This was because the UV / TiO_2 system has been studied by many workers and some of its properties and reactions are therefore well documented [68,69]. TiO_2 also has the benefits of being non-toxic, insoluble, and relatively cheap (all important factors to consider in an industrial process).

4.0.2.1 Chemistry of Semi-Conductor Photocatalysts

When photons of UV light fall on the semiconductor catalyst, they cause electron excitation within the solid. This excitation forms electron-hole pairs, some of which migrate to the surface of the semi-conductor [70]. Interaction of these conduction-band electrons and valence-band holes with water and oxygen in solution forms hydroxyl and other oxygen containing radicals. These radicals then attack and oxidise any organic molecules present [67,69].

FIGURE 4.0

FORMATION OF FREE RADICALS AT THE SURFACE OF AN IRRADIATED PHOTOCATALYST

electron

$$O_2 + e^- \longrightarrow O_2^-$$

$$O_2^- + H^+ \longrightarrow HO_2^\bullet$$

The surface of the semi-conductor

hole

$$H_2O + h^+ \longrightarrow {}^\bullet OH + H^+$$

$$2\,OH^- + h^+ \longrightarrow {}^\bullet OH + OH^-$$

where $h^+ =$ positive hole on surface of semi-conductor
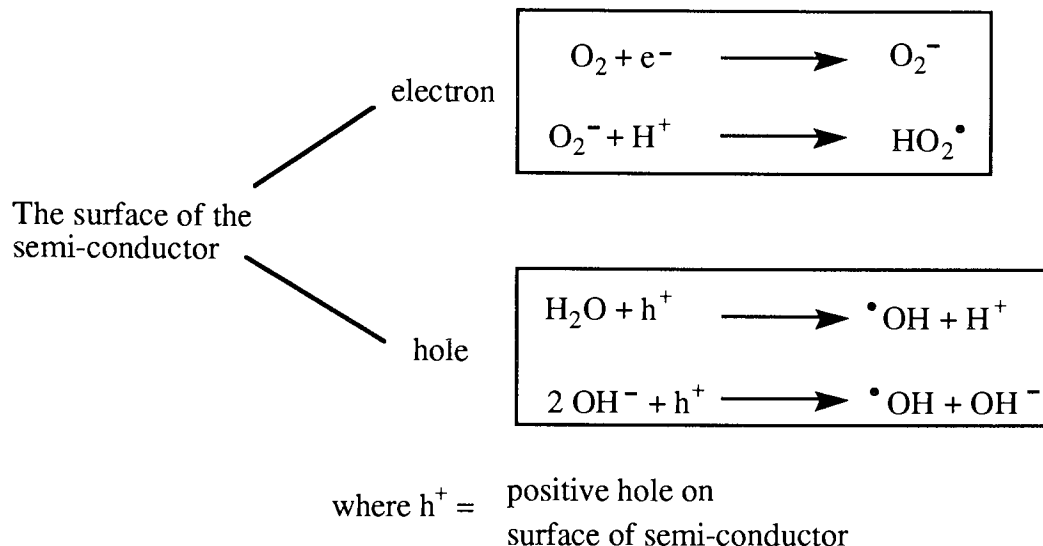
For example, Okamoto suggests the following reaction pathway for radical addition to phenol [67].

FIGURE 4.1

THE ADDITION OF FREE RADICALS TO PHENOL
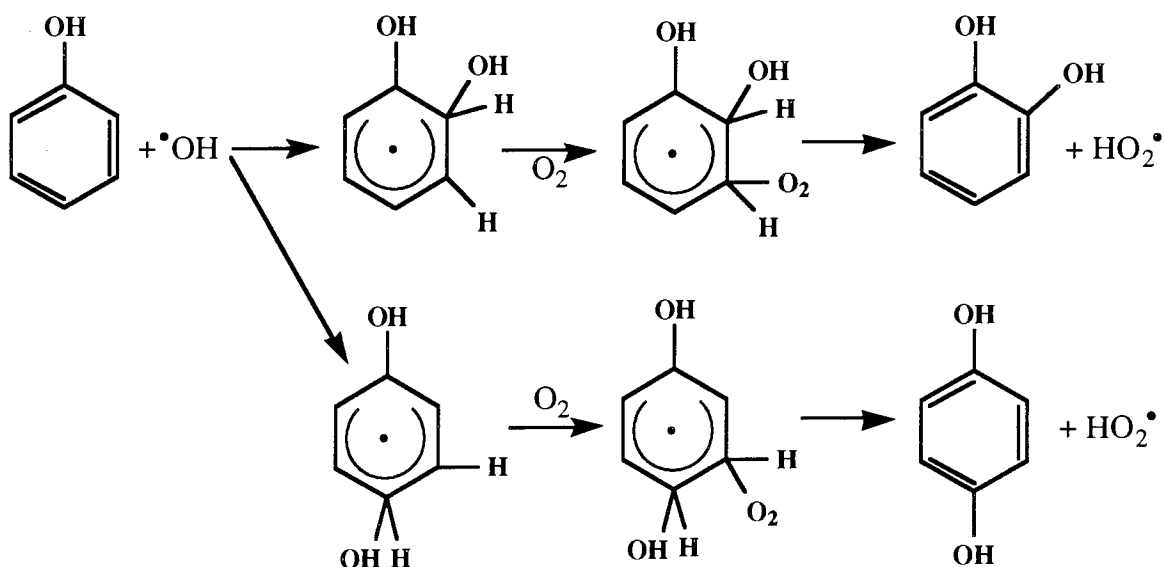
If irradiation is continued, eventually the phenol is completely converted to CO_2 and H_2O, in a process known as mineralisation.

$$C_6H_5OH + 7O_2 \longrightarrow 6CO_2 + 3H_2O$$

4.1 RESULTS

4.1.1 The Irradiation of Resin Digestion Solutions by UV Light

In 'Experiment 1' solutions of 75 minutes resin were irradiated in a UV photochemical reactor at room temperature while first oxygen, and then air was blown through the liquid. The TOC level was monitored throughout the reaction period.

In 'Experiment 2 ' the Fenton's reagent / resin reaction was halted at 75 minutes, part of the reaction mixture taken as a sample, and the reaction in the main part of the solution continued. The sample had its [H_2O_2] determined, and then all the H_2O_2 was removed from the sample, which was subsequently irradiated in a UV photochemical reactor for 1 hour. An equivalent amount of H_2O_2 to that originally removed was then added to the irradiated sample and a normal Fenton's reagent reaction continued until no H_2O_2 was left in the sample.

In 'Experiment 3 ' a solution of 300 minutes resin was irradiated in a UV photochemical reactor for 7 hours. The TOC level was measured at the start and end of the reaction.

4.1.1.1 TOC Level Changes

Experiment 1

TABLE 4.0

THE EFFECT OF UV IRRADIATION ON A 75 MINUTES RESIN SOLUTION

TOC (ppm) starting value	TOC (ppm) after 300 minutes UV irradiation	TOC (ppm) after 350 minutes UV irradiation + O$_2$	TOC (ppm) after 330 minutes UV irradiation + air
3720	3650	3750	3770

No statistically significant change in TOC level was observed during the 5-6 hours the 75 minute resin solutions were irradiated with UV light. However, the colour of the solution did change from light brown to dark brown / black during the period of irradiation.

Experiment 2

TABLE 4.1

THE EFFECT OF IRRADIATING A RESIN SOLUTION MIDWAY THROUGH THE STANDARD RESIN DIGESTION REACTION

TOC (ppm) at 75 minutes	TOC (ppm) after Fenton's reaction completion	TOC (ppm) of 75 minutes resin after 1 hour UV irradiation	TOC (ppm) of UV irradiated 75 minutes resin after Fenton's reaction completion
4170	1900	3930	1350

The sample that had been irradiated with UV and then reacted with Fenton's reagent had a final TOC level 29% lower than that of the unirradiated resin solution.

Experiment 3

TABLE 4.2

THE EFFECT OF UV IRRADIATION ON A 300 MINUTES RESIN SOLUTION

TOC (ppm) starting value	TOC (ppm) after 420 minutes UV irradiation
940	930

No statistically significant change in TOC level was observed during the 7 hours the 300 minute resin solution was irradiated with UV light.

4.1.1.2 Discussion of the Results

4.1.1.2.1 A Discussion of Experiment 1

Irradiation of the aqueous solution with UV light has no effect on the TOC level of the solution. However, this does not necessarily indicate that oxidation of organic molecules in solution is not occurring, only that any oxidation of organic molecules has not converted them to CO_2 and H_2O. In fact, the colour change of the solution is an indication that partial oxidation of at least some of the organic molecules in solution has occurred. For example, when phenols (likely components of the resin digestion mixture at this point) are oxidised there is a colour change

91

from colourless to dark brown / black [59].

In Chapter 3 it was described how, when gas was blown through a partly digested resin solution heated to 95°C, a TOC level drop of about 10% was noted. No similar TOC level drop was noted in Experiment 1 (75 minutes resin / gas sparge / UV light) indicating that a TOC level drop occurs only when the resin solution is heated. Heating the resin solution would be expected to reduce the solubility of volatile organic molecules in the solution, thus allowing some of the volatile organics to be removed by a gas stream.

4.1.1.2.2 A Discussion of Experiment 2

Assuming the results of this single experiment are reproducible, this experiment would tend to support the suggestion made above, in Section 4.1.1.2.1, that partial oxidation of the organic molecules in the resin solution is occurring. There appears to be a significant improvement in efficiency of the Fenton's reagent / resin reaction when the resin solution is irradiated for a time part of the way through the reaction. This improvement may be due to the UV light producing oxidised molecules which can be more easily oxidised by Fenton's reagent.

4.1.1.2.3 A Discussion of Experiment 3

Irradiation of the aqueous solution with UV light has no effect on the TOC level of the solution. However, this does not necessarily indicate that oxidation of organic molecules in solution is not occurring, only that any oxidation of organic molecules has not converted them to CO_2 and H_2O.

4.1.1.3 Conclusions

Although UV irradiation appears to have no direct effect on the TOC level of resin digestion solutions, it appears that oxidation of organic molecules does occur. It also appears that these molecules, once oxidised by UV light, are much less resistant to subsequent oxidation by Fenton's reagent. This could have important commercial implications, as UV irradiation of the resin mixture for one hour, just after resin solubilisation, eventually resulted in a large reduction in the final TOC level.

4.1.2 The Irradiation of Resin Digestion Solutions by UV Light, in the Presence of Titanium Dioxide

Solutions of 75 and 300 minutes resin were irradiated in a UV photochemical reactor in the presence of a suspension of TiO_2 (anatase form). The TOC level was monitored throughout the reaction. In Experiment 4, 10 second bursts of oxygen were blown through the irradiated resin solution every 15 minutes to purge the solution of any CO_2 formed by organic molecule degradation. In Experiment 5, oxygen was blown continuously through the resin solutions. In Experiment 6, 75 minutes resin was filtered prior to use to remove any suspended organic material, in an otherwise identical experiment to Experiment 5.

4.1.2.1 TOC Level Changes

4.1.2.1.1 Experiment 4 - with 75 minutes resin

TABLE 4.3

UV IRRADIATION OF A 75 MINUTES RESIN SOLUTION IN THE PRESENCE OF TITANIUM DIOXIDE

TOC (ppm) starting value	TOC (ppm) after 540 minutes UV irradiation
3800	3690

When 75 minutes resin was irradiated no statistically significant change in TOC level was observed after 9 hours irradiation. However, the colour of the solution did change from light brown at the start of the period of irradiation to dark brown / black at the end of the period of irradiation.

4.1.2.1.2 Experiment 4 - with 300 Minutes Resin

FIGURE 4.2

Graph showing the change in TOC level with time in a UV irradiated titanium dioxide / 300 minute resin solution
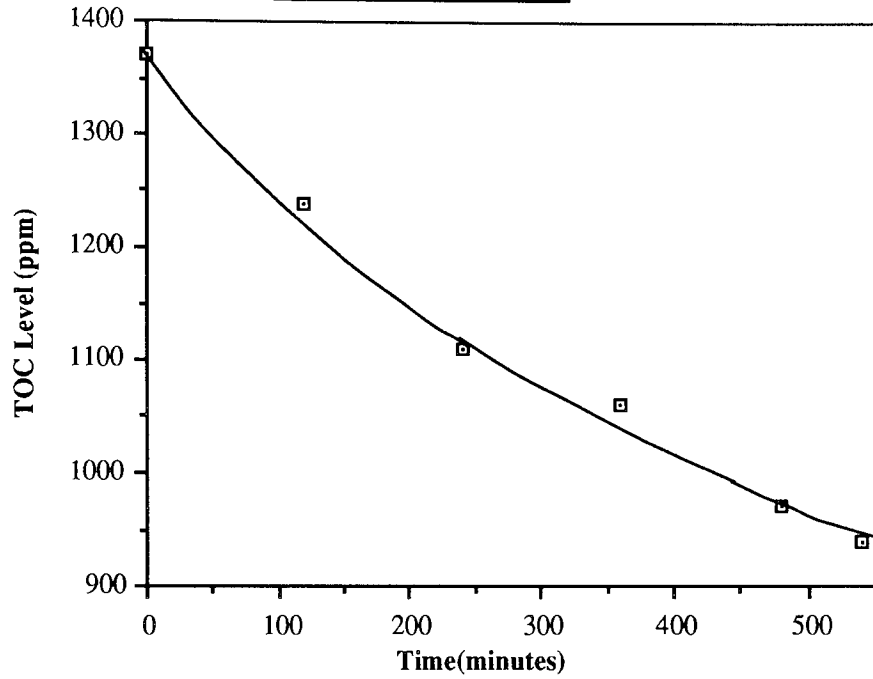
FIGURE 4.3

Graph showing the relationship of the logarithm of the TOC level to the time of irradiation for 300 minutes resin solution

Equation of the Line =
$y = 7.21 - 6.86e\text{-}4x$ $R^2 = 0.988$
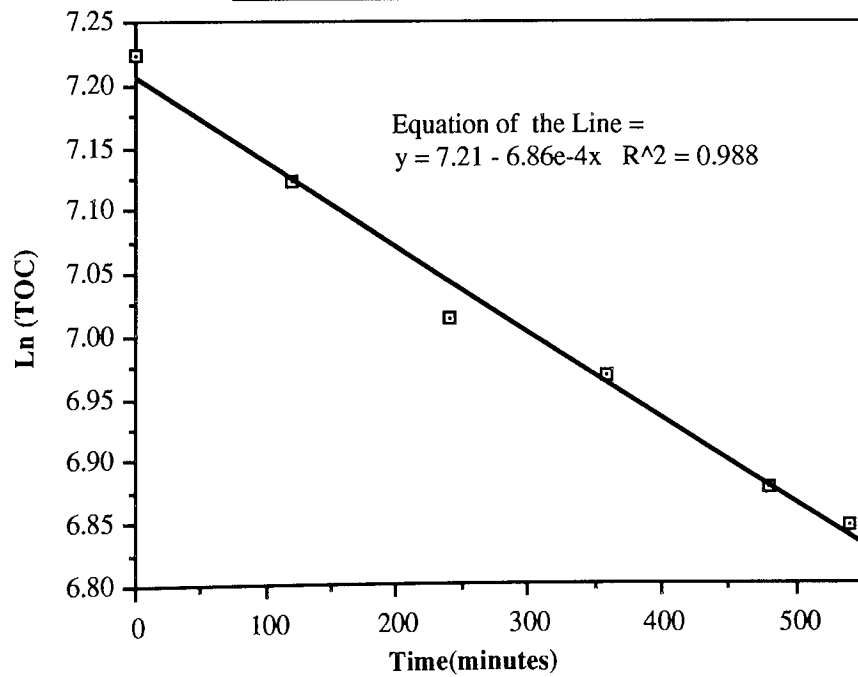
Figure 4.2 shows that when 300 minutes resin is irradiated, a smooth fall in TOC level is seen during the period of irradiation. When the logarithm of each of the points from Figure 4.2 is plotted against time, the points fall on a straight line, indicating that the rate of loss of carbon from solution is first order in carbon, this being shown in Figure 4.3.

4.1.2.1.3 Experiment 5 - with 75 Minutes Resin

TABLE 4.4

UV IRRADIATION OF A 75 MINUTES RESIN SOLUTION IN THE PRESENCE OF TITANIUM DIOXIDE AND A CONTINUOUS OXYGEN PURGE

TOC (ppm) starting value	TOC (ppm) after 540 minutes UV irradiation
3500	3400

When 75 minutes resin was irradiated no statistically significant change in TOC level was observed after 9 hours irradiation. However, the colour of the solution did change from light brown at the start of the period of irradiation to dark brown / black at the end of the period of irradiation.

4.1.2.1.4 Experiment 5 - with 300 Minutes Resin

FIGURE 4.4

Graph showing the change in TOC level with time in a UV irradiated titanium dioxide / 300 minute resin solution (constant oxygen purge)

95
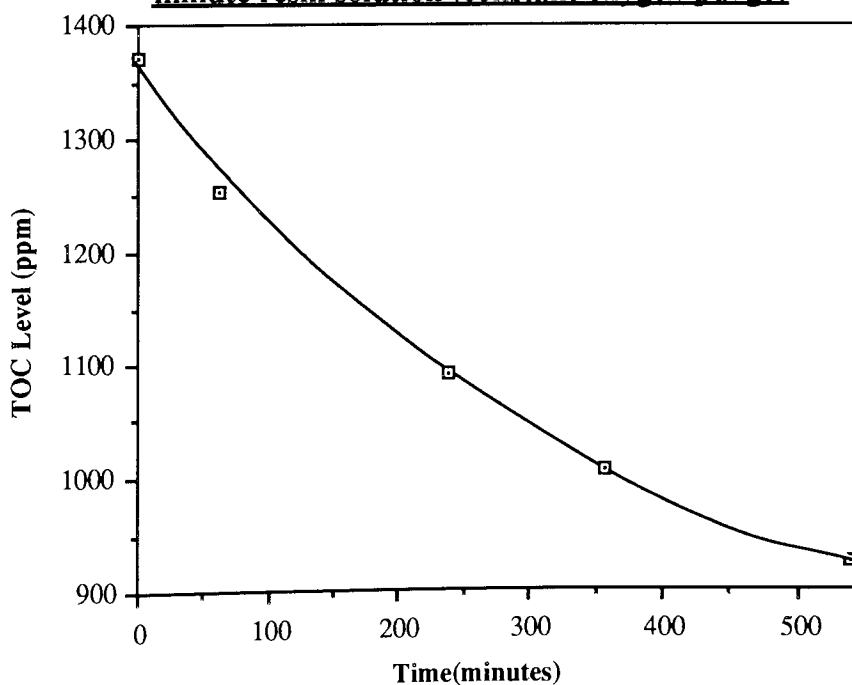
FIGURE 4.5

Graph showing the relationship of the logarithm of the TOC level to the time of irradiation for 300 minutes resin solution (constant oxygen purge)
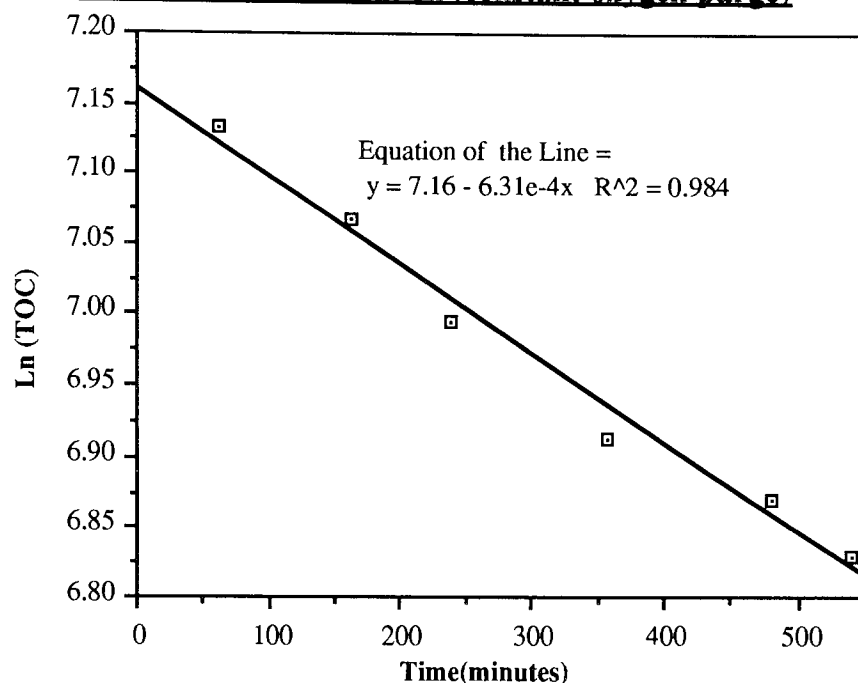
Figure 4.4 shows that when 300 minutes resin is irradiated a smooth fall in TOC level is seen during the period of irradiation. When the logarithm of each of the points from Figure 4.4 is plotted against time, the points fall on a straight line, indicating that the loss of carbon from solution is first order, this being shown in Figure 4.5. The gradient of this line is nearly the same as for the experiment in which O_2 was not constantly passed through the resin solution (6.3×10^{-4} .vs. 6.9×10^{-4}). This indicates that the progress of the reaction is not affected by the saturation of the resin solution with O_2 i.e., O_2 is not involved in the rate determining step in this reaction.

TABLE 4.5

UV IRRADIATION OF A PRE-FILTERED 75 MINUTES RESIN SOLUTION IN THE PRESENCE OF TITANIUM DIOXIDE AND A CONTINUOUS OXYGEN PURGE

TOC (ppm) starting value	TOC (ppm) after 540 minutes UV irradiation
3940	3970

When 75 minutes resin was irradiated in the presence of TiO_2 no statistically significant change in TOC level was observed after 9 hours irradiation. However, the colour of the solution did change from light brown at the start of the period of irradiation to dark brown / black at the end of the period of irradiation. Spectroscopic measurements in the UV / Visible region made during the reaction (see Figures 4.6 and 4.7) show this colour change clearly.

4.1.2.2.1 Changes in Absorption

FIGURE 4.6

Graph showing the change in absorbance with time at two wavelengths in a UV irradiated 75 minute resin / titanium dioxide system
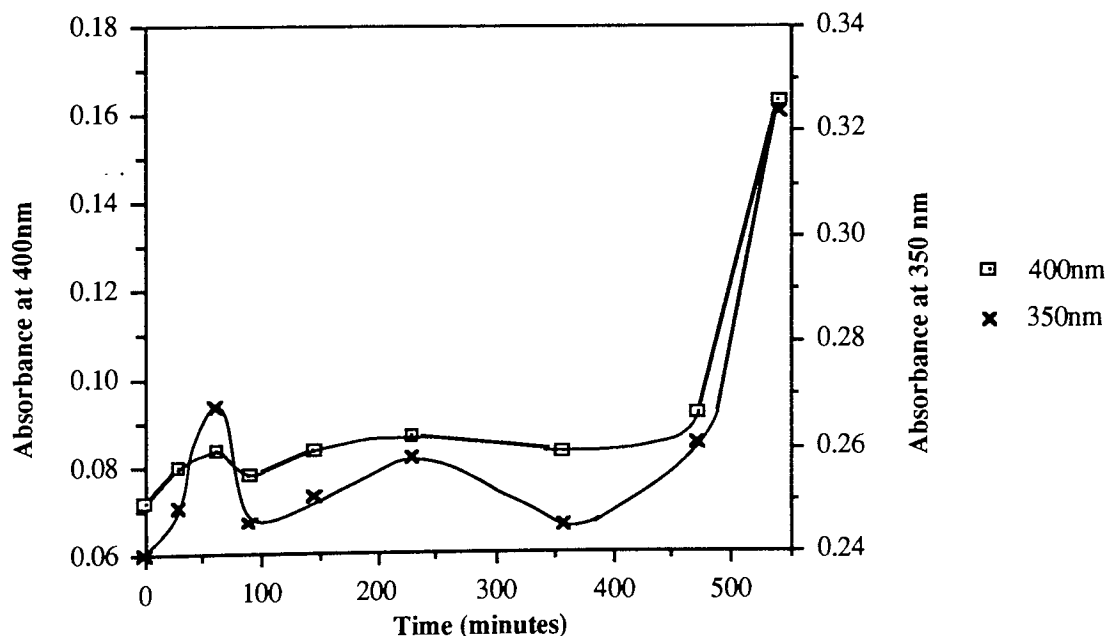
FIGURE 4.7

Graph showing the change in absorbance with time at two other wavelengths
in a UV irradiated 75 minute resin / titanium dioxide system
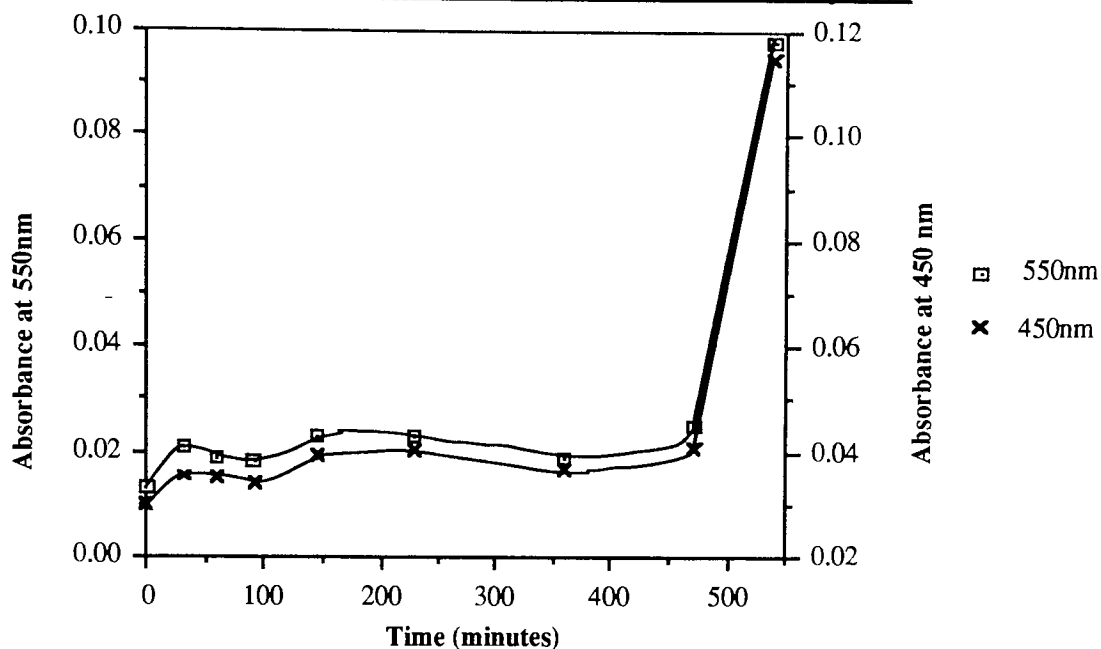
4.1.2.3 Calculation of the Quantum Yield for the 300 minutes / TiO_2 / UV reaction

A potassium ferrioxalate solution-phase chemical actinometer system, as described in Section 2.10.1, was used to find the quantum yield of the 300 minutes / TiO_2 / UV system. It was found that 0.022 moles of Fe^{3+} were reduced during 9 hours of irradiation.

Averaging the results for the two 300 minutes resin / TiO_2 / UV experiments carried out, 32.5% of the carbon is lost from solution in 9 hours, with a starting concentration of 1370 ppm, and a volume of 100 cm^3.

In 100 cm^3 of 300 minutes resin solution there is 0.137 g of carbon, of which 0.0445 g is oxidised to CO_2 in 9 hours.

0.0445 g of C represents 3.7×10^{-3} moles of C.

Thus for the UV / TiO_2 / 300 minute resin reaction,

φ = No. moles C oxidised / No. moles Fe^{3+} reduced

φ = 0.0037 / 0.022

φ = 0.17

0.17 represents a surprisingly high quantum yield for the 300 minutes resin / TiO_2 / UV system. The oxidation of CH_2O to CO_2 is a 4 e⁻ process,

$$CH_2O + H_2O \longrightarrow CO_2 + 4\,H^+ + 4\,e^-$$

and the figure for quantum yield implies that one molecule of C is removed for every 6 excited electrons i.e., excited electrons are used with an overall efficiency of around 67%.

4.1.2.4 Discussion of the Results

4.1.2.4.1 Oxidation of 75 Minutes Resin

It seems likely that partial oxidation of some organic molecules is occurring in this resin solution, as is indicated by the changing visible absorption with time at various wavelengths. These changes in absorption fit the obvious suggestion that various oxidation products are being formed and destroyed sequentially during solution irradiation.

The lack of any measurable TOC level drop in this solution, in contrast to 300 minute resin solution which exhibits a significant drop, can be explained by the high UV / visible absorption of the 75 minutes resin solution, relative to 300 minute resin. The anatase form of TiO_2 used in these experiments has a band gap of 3.23 eV (corresponding to 388 nm)[71]. At this wavelength the absorption of the 75 minutes resin is 4.4 times greater than that of the 300 minutes resin (0.102 v 0.023).

FIGURE 4.8

Graph showing the absorbance at different wavelengths of 75 and 300 minutes resin solution
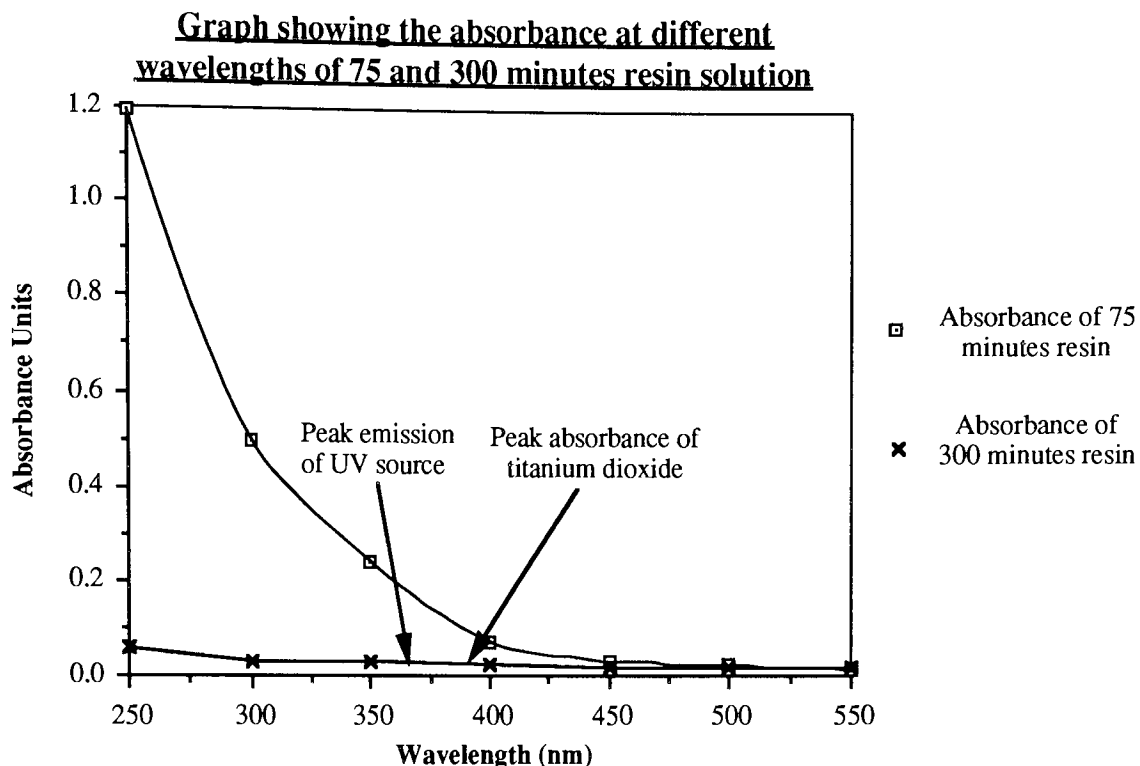
This would mean that radiation incident on the surface of the 75 minutes resin solution would penetrate a much shorter distance than radiation incident on the surface of the 300 minute resin solution. Thus, since less of the UV light of the appropriate wavelength reaches the TiO_2, fewer ·OH radicals will be created, and less oxidation of organic molecules in solution will occur.

4.1.2.4.2 Oxidation of 300 Minutes Resin

Some 30% of the organic components of this resin solution are being totally oxidised to CO_2 and H_2O by the combined action of TiO_2 and 9 hours of UV light. This is in contrast to the 75 minutes resin solution, in which little or no organic material appears to have been converted to CO_2 and H_2O. This difference in behaviour can be ascribed firstly to the different level of light absorption of each resin solution, as described earlier in Section 4.1.2.4.1. Secondly, it is likely that material in the 75 minutes resin solution is only being partly oxidised.

The rate at which organic material is converted to CO_2 and H_2O is very slow, even though the quantum yield for the reaction is good. This implies that the best way to speed up the conversion process would be to increase the rate of ·OH radical production. The simplest way to do this would be to increase the photon flux, thus increasing the number of radicals produced per

second. Alternative methods of increasing the rate of production of ·OH radicals are detailed below.

4.1.2.5 Possible Methods to Improve the Efficiency of Hydroxyl Radical Production in the Resin / TiO$_2$ / UV System

4.1.2.5.1 Combining at Least Two Types of Semi-Conductor

The effect of using other semi-conductors, such as ZnO or CdS, in conjunction with TiO$_2$ could be investigated. These semi-conductors would absorb radiation at different wavelengths to TiO$_2$ due to their different band gaps. This would increase the quantity of ·OH radicals produced in a solution illuminated by a relatively broad emission radiation source such as a mercury vapour lamp.

4.1.2.5.2 Alteration of the Surface of the Titanium Dioxide Catalyst

The surface of the TiO$_2$ catalyst could be altered either physically (to increase the surface area) or chemically to produce more ·OH radicals for the same amount of incoming radiation.

a) Physical Alteration

The surface area of a given mass of TiO$_2$ could be increased by using smaller particles, or by using particles with a rougher surface.

b) Chemical Alteration

Kondo has reported that the doping the TiO$_2$ particle surface with Ag increases the rate and degree of oxidation of chloroform in contaminated water [61]. It is feasible that similar effects would be seen in the resin / TiO$_2$ / UV system.

Another potential method is to exploit research carried out on the photodecomposition of water. In this research, applying Pt and RuO$_2$ to the surface of TiO$_2$ results in the decomposition of water to H$_2$O in a redox reaction [72]. If only RuO$_2$ were to be deposited on the surface of the TiO$_2$ then only an oxidation promoter would be present. This would further encourage oxidation of organic molecules in solution.

4.1.2.5.3 A Design Modification to Achieve an Increase in Degree of Organic Molecule Oxidation in the UV / TiO2 / 75 Minutes Resin System

If aspects of the experimental equipment design were altered it is likely that the degree of oxidation of the resin organic molecules could be increased.

FIGURE 4.9

POSSIBLE UV REACTOR DESIGN MODIFICATIONS

Experimental Design 1   Experimental Design 2

UV source

75 minutes resin/suspended titanium dioxide mixture

UV Source

Supported titanium dioxide catalyst

75 minutes resin solution
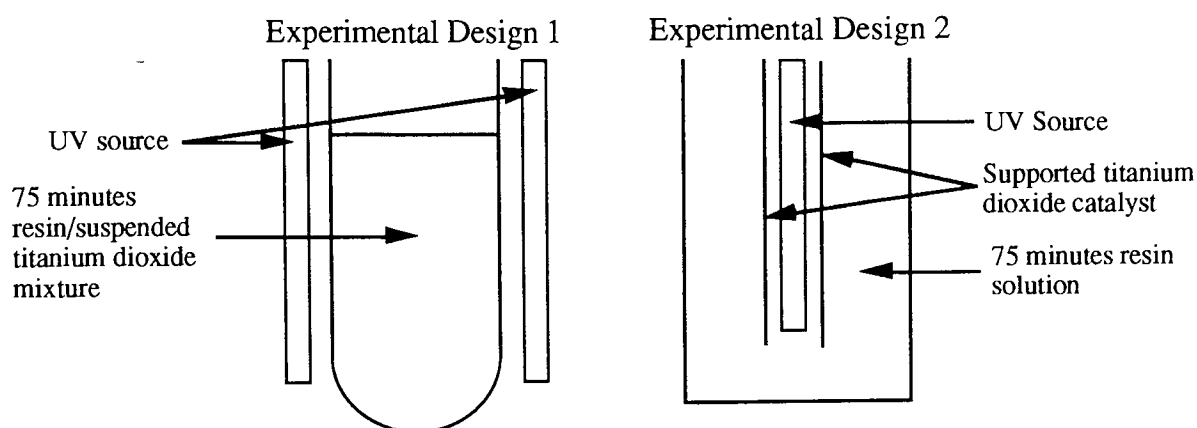
(In both designs the resin solution is continuously stirred)

In the experimental design used in the work for this thesis, Design 1, the TiO_2 is distributed throughout the 75 minutes resin solution. Due to the high degree of light absorption of the resin solution only a small fraction of the radiation emitted by the UV source is incident on the particles of TiO_2 in solution. If Design 2 were used, there would only be a small path length of resin solution for the UV radiation to travel through, from the UV source to the TiO_2, which would tend to increase the amount of ·OH radicals produced. However, the decreased surface area of TiO_2 in Design 2 might partially or completely counteract this potential improvement in ·OH radical production.

4.1.3 Conclusions

1) UV light alone appears to partially oxidise components of the concentrated resin digestion solutions seen early in the standard resin digestion reaction. These partially oxidised components may be more suseptible to subsequent attack by Fenton's reagent.

2) A UV / TiO_2 combination will effectively oxidise the smaller organic molecules seen towards the end of the Fenton's reagent digestion of Lewatit ion-exchange resin.

3) A UV / TiO_2 combination appears to partially oxidise components of the concentrated resin

102

digestion solutions seen early in the standard resin digestion reaction.

4) O_2 does not take part in the rate determining step in the UV / TiO_2 oxidation of the dilute end resin digestion mixture.

The irradiation of partly digested resin solutions in the presence of TiO_2 appears to be an effective method of directly reducing the carbon content of the resin solution. Further work on reaction variables would be required before the method could be used as part of a commercial ion-exchange resin treatment process. Nevertheless, the UV / TiO_2 research, along with the research on the effects of UV light on the progress of the Fenton's reagent reaction (Section 4.1.1) is very promising. Unfortunately, work was not started into these subjects until late into the PhD. Much more time would have been spent investigating the UV / Fenton's reagent and UV / TiO_2 systems if it had been available.

CHAPTER 5

THE USE OF CERIUM(IV) TO PROMOTE THE DESTRUCTIVE OXIDATION OF AQUEOUS ORGANIC MOLECULES

The Ce^{4+} ion has been used as a one-electron oxidant for many types of organic molecules [73]. Ce^{4+} solutions first emerged as important reagents when they became a successor to permanganate as the reagent of choice for oxidising organic molecules [74]. Standardised Ce^{4+} solutions in sulphuric acid were found to be stable for long periods and more easily prepared than permanganate solutions. Ce^{4+} solutions were also found to have the useful property of variable oxidation potentials, depending on the strength and type of acidic media present [75].

TABLE 5.0

VARIABLE CERIUM ELECTRODE POTENTIALS IN DIFFERENT ACIDIC MEDIA

$Ce^{4+} + e^- = Ce^{3+}$			
	Electrode Potential, E^0/V		
$[H^+]$/mol dm^3	$HClO_4$	HNO_3	H_2SO_4
1	1.70	1.61	1.44
2	1.71	1.62	1.44
4	1.75	1.61	1.43
6	1.82	-	-
8	1.87	1.56	1.42

Cerium is the only lanthanide species with a stable enough (IV) oxidation state to facilitate simple aqueous solution preparation, its chemistry being similar to that of Zr, Hf and tetravalent actinides, with the exception of its redox properties [76]. The hydrated ion of Ce^{4+}, $[Ce(H_2O)n]^{4+}$ would be a strong acid. However, hydrolysis and polymerisation can be expected to occur in all solutions, except at very low pH. Concentrated perchloric is the only acid in which it is likely that this ion could exist. In different acid media there is always co-ordination of anions, which accounts for the dependence of the potential of the Ce^{4+} / Ce^{3+} couple on the nature of the acid medium [76].

5.0.1 Details of reactions of Ce(IV) with Simple Organic Molecules

The oxidation by Ce^{4+} of a variety of organic compounds such as alcohols, aldehydes, and ketones has been extensively studied [73]. One example of this oxidising behaviour is the Ce^{4+} oxidation of aldehydes and ketones at the α-carbon atom. Other examples are the oxidation of benzaldehyde to benzoin, and the oxidation of substituted toluenes to aldehydes [77].

Sengupta et al. have shown that the following reactions occur when acetaldehyde is oxidised by Ce^{4+} [78].

$$CH_3CHO + 6Ce^{4+} + 3H_2O \longrightarrow 2HCOOH + 6Ce^{3+} + 6H^+ \quad --- \quad 50\% \text{ yield}$$

$$CH_3CHO + 2Ce^{4+} + H_2O \longrightarrow CH_3COOH + 2Ce^{3+} + 2H^+ \quad --- \quad 50\% \text{ yield}$$

Oxidation of alcohols by Ce^{4+} is generally thought to proceed by the following mechanism [79].

where A is probably
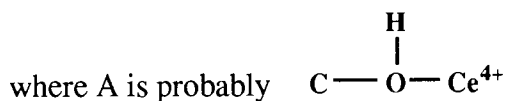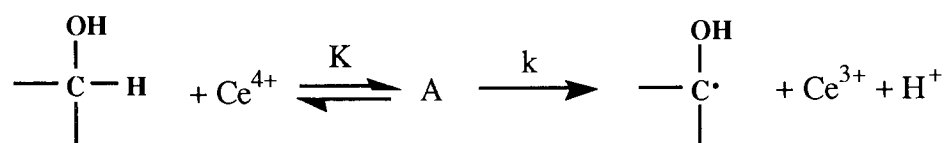
The rate determining step in this mechanism involves the unimolecular disproportionation of the complex, A, to yield a Ce^{3+} ion, a proton, and a free radical on the alcohol substrate. If the alcohol is a 1,2-diol, the C-C bond between the hydroxyl groups cleaves to yield an aldehyde or ketone, along with a free radical [80].
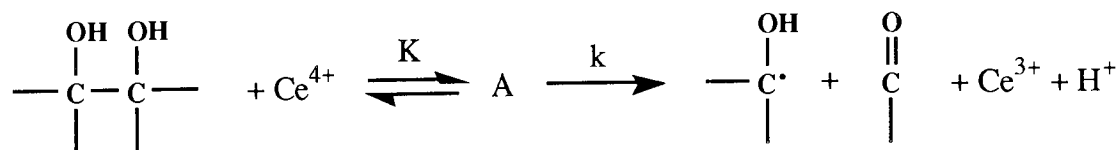
The fate of the free radical in both cases is probably fast oxidation by another Ce^{4+} ion to form an aldehyde or ketone.
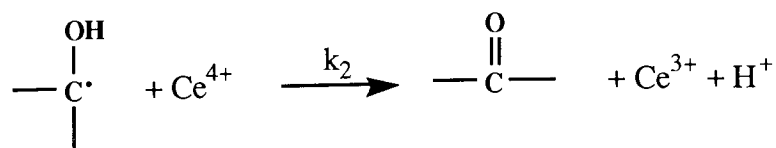
In its use as a TOC level reduction method, it was hoped that the Ce^{4+} ion would oxidise some or all organic molecules in solution, being reduced to Ce^{3+} in the process. The Ce^{3+} ions could then be oxidised back to Ce^{4+} in another process and so a redox cycle could be set up.

5.0.2 The Use of a Combination of Cerium(IV) and Ultraviolet Light

UV light forms ·OH radicals or molecules in an excited state in aqueous solution, as was described in Chapter 4 of this thesis. It was also known that when irradiated with UV light, a Ce^{4+} solution has more oxidising power than a non-irradiated solution. This is because UV light forms free radicals in aqueous solution, thus increasing the number of oxidising species in solution. Examples of molecules oxidised by a Ce^{4+} / UV light combination include alcohols and carboxylic acids [81].

It was thus decided to investigate the combined effect of Ce^{4+} ions and UV light on a partly digested resin solution and 2 model systems. It was hoped that a UV / Ce^{4+} combination would improve the rate and degree of degradation of organic substrates present in the partially digested resin solution.

5.0.2.1 The Effect of UV light on Solutions of Ce(IV) Containing Organic Molecules

Dogliotti and Hayon have elucidated the overall process that occurs when a solution of Ce^{4+} is irradiated with UV light [82].

$$Ce(IV)(H_2O) \xrightarrow{h\upsilon} Ce(III) + (H_2O)^+$$

$$(H_2O)^+ + H_2O \longrightarrow {}^\bullet OH + H_3O^+$$

$${}^\bullet OH + HSO_4^- \longrightarrow HSO_4^{\bullet} + OH^-$$
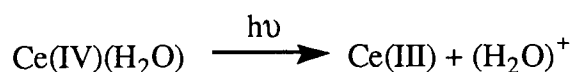
At 366 nm, the peak emission wavelength of medium pressure mercury vapour lamps, the $HSO_4^{\bullet}$ radical is the main oxidising species in solution, not the ·OH radical. This is due to both the quantum yield for Ce^{4+} reduction and the nature of the intermediate free radical species formed [83]. The ·OH radical is also subject to the following reaction in solution, which removes it as an oxidising species.

$$Ce(III) + {}^\bullet OH \longrightarrow Ce(IV) + OH^-$$

Dogliotti and Hayon found that the rate of formation of the $HSO_4^{\bullet}$ radical is independent of the presence of oxygen, slightly dependent on the concentration of cerium(IV)sulphate, and very dependent on the concentration of H_2SO_4. Dogliotti and Hayon also found that the decay of the

$HSO_4\cdot$ radicals in the presence of organic substrates was pseudo-first order.

Further ESR spectroscopy work by Greatorex et al. identified some of the intermediates formed when organic substrates are present [84].

TABLE 5.1

INTERMEDIATES FORMED BY THE REACTION OF ALCOHOLS WITH CE(IV) IN THE PRESENCE OF UV LIGHT

Substrate	Temperature (K)	Species Produced
$CH_3\text{-}CH_2\text{-}OH$	182	$\cdot CH_3$
$CH_3\text{-}CH_2\text{-}CH_2\text{-}OH$	190	$CH_3\text{-}CH_2\cdot$
$CH_3\text{-}CH_2\text{-}CH_2\text{-}CH_2\text{-}OH$	194	$CH_3\text{-}CH_2\text{-}CH_2\cdot$
$CH_3\text{-}CH_2\text{-}CH_2\text{-}CH_2\text{-}CH_2\text{-}OH$	210	$CH_3\text{-}CH_2\text{-}CH_2\text{-}CH_2\cdot$
$\begin{array}{c}CH_3\\ \diagdown\\ CH\text{---}OH\\ \diagup\\ CH_3\end{array}$	200	$\cdot CH_3$

From Table 5.1 it can be seen that the only radical formed from RCH_2OH is $\cdot CH_2OH$, suggesting that C-C bond cleavage is occurring. The results summarised in Table 5.2 (see overleaf) show how a Ce^{4+} / UV light combination oxidatively decarboxylates the acid RCO_2H.

TABLE 5.2

INTERMEDIATES FORMED IN THE REACTION OF CARBOXYLIC ACIDS WITH CE(IV) IN THE PRESENCE OF UV LIGHT

Substrate	Temperature ($^\circ$K)	Species Produced
$CH_3 - C \overset{OH}{\underset{H}{\diagdown}}$ (acetaldehyde acid structure)	190	$\cdot CH_3$
$CH_3 - CH_2 - C \overset{OH}{\underset{H}{\diagdown}}$	180	$CH_3\text{-}CH_2\cdot$
$\overset{CH_3}{\underset{CH_3}{\diagdown}} CH - C \overset{OH}{\underset{H}{\diagdown}}$	190	$\overset{CH_3}{\underset{CH_3}{\diagdown}} CH\cdot$
$CH_3 - \overset{CH_3}{\underset{CH_3}{\overset{\mid}{\underset{\mid}{C}}}} - C \overset{OH}{\underset{OH}{\diagdown}}$	195	$CH_3 - \overset{CH_3}{\underset{CH_3}{\overset{\mid}{\underset{\mid}{C}}}} \cdot$
Cyclo-$C_6H_{11}CO_2H$	203	$C_6H_{11}\cdot$

5.1 RESULTS

The oxidative behaviour of Ce^{4+} in aqueous solution towards soluble organic molecules was studied using three different organic substrates without UV irradiation. The first organic substrate studied was 300 minutes resin solution, the second a resin analogue, the sodium salt of poly(styrenesulfonate) (PSS) and the final substrate was another resin analogue, calix[8]arene-p-octasulphonic acid (CALIX). The action of Ce^{4+} towards all three substrates was also studied with irradiation by near UV light, in a photochemical reactor.

5.1.1 Calculation of the Degree of Absorption of Light by Ce(IV) in the UV Photochemical Reactor

The [Ce^{4+}] above which nearly all (99.9%) incoming energy at 317 nm (the maximum absorption peak of Ce^{4+}) was absorbed in the reactor used for this work was calculated by using the Beer-Lambert Law, $A = \varepsilon CL$. This was done to confirm that, at the concentrations of Ce^{4+}

used, all the incident light on the Ce^{4+} solutions would be absorbed. This information was necessary for some of the kinetics calculations made later in this chapter.

The extinction coefficient was found to be 4400 M^{-1} cm^{-1}, the path length for light in the photochemical reactor was 1.75 cm, and it was assumed that A = 3, equivalent to 99.9% of all incident light absorbed. Therefore any $[Ce^{4+}]$ higher than 3.90 x 10^{-4} M will absorb essentially all the light emitted at 317 nm by the mercury vapour lamps in the photochemical reactor.

5.1.2 The Reactions of Various Ratios of Ce(IV) and 300 Minutes Resin Solution

300 minutes resin solution is a complex mixture of aqueous organic molecules such as alcohols, aldehydes, and carboxylic acids. Details of the analysis of this mixture are given in Chapter 7. Due to the complexity of the 300 minutes resin solution the ratio of Ce^{4+} molarity to C molarity, rather than the concentration of any component, was used to illustrate the effect of varying $[Ce^{4+}]$ on the progress of the Ce^{4+} / resin reaction.

5.1.2.1 The Dark Reactions of Ce(IV) and 300 minute Resin Solution

Samples of a standard solution of Ce^{4+} and a 300 minute resin solution were mixed together in various ratios in the absence of light. The changes in $[Ce^{4+}]$ in solution (as determined by spectrophotometric measurement at 317 nm) with time were monitored. The TOC level and any changes in the oxidation state of the Ce in solution were also monitored during the reaction. The oxidation state of the Ce was measured by titrating the reaction solution against a standard solution of Fe^{2+}.

5.1.2.1.1 Changes in Ce(IV) Concentration

A fall in the $[Ce^{4+}]$ with time was observed at various ratios of Ce^{4+} and 300 minute resin solution when these two reagents were mixed together. When the data were analysed it was found that a plot of the natural logarithm of the $[Ce^{4+}]$ against time produced straight lines of similar gradient for all ratios tested (see Figure 5.0).

FIGURE 5.0

Graph showing the relationship of the logarithm of the [Ce(IV)] to the time of reaction for various ratios of Ce(IV) / 300 minute resin solution ([Ce(IV)] variable)

Initial Ce(IV):C in solution ratio

◻ 0.13:1

◆ 0.26:1

✕ 0.38:1

◈ 0.64:1

+ 0.77:1
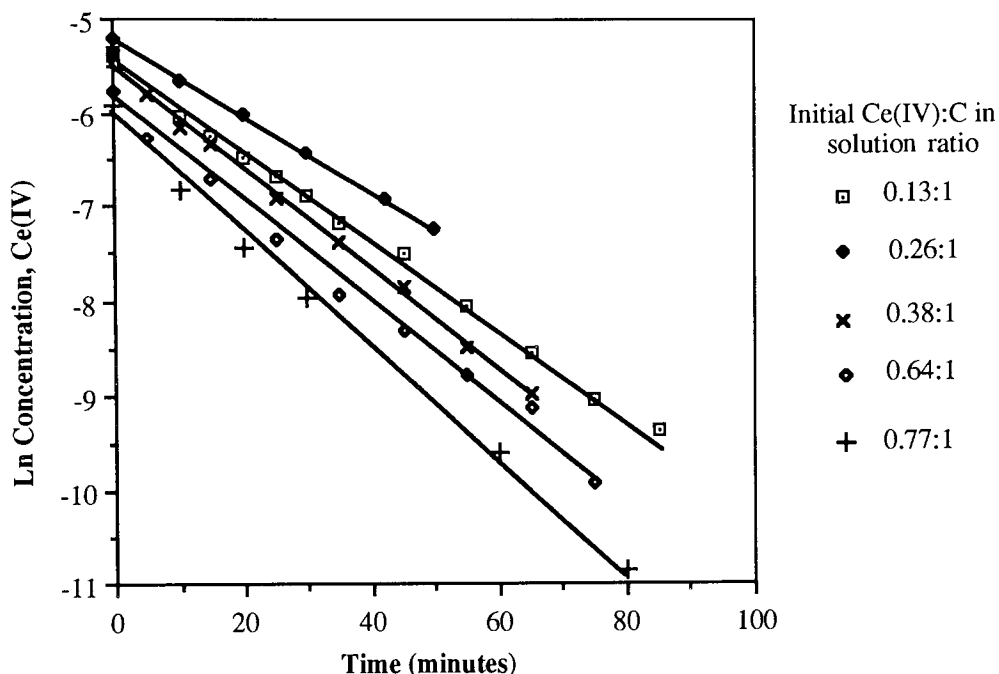
TABLE 5.3

GRADIENTS AND INTERCEPTS ON THE Y AXIS FOR VARIOUS CE(IV) : CARBON RATIOS

Ce(IV) ion : C in solution (mole / mole)	Rate of reaction (min^{-1})	Intercept on y axis
0.13 : 1	4.65×10^{-2}	-5.48
0.26 : 1	4.00×10^{-2}	-5.22
0.38 : 1	5.35×10^{-2}	-5.51
0.64 : 1	4.65×10^{-2}	-5.48
0.77 : 1	5.95×10^{-2}	-6.11

The average rate of reaction, k, was found to be

$$(4.9 \pm 1.0) \times 10^{-3} \text{ min}^{-1}$$

The results shown in Figure 5.0 mean that the rate of loss of Ce^{4+} from solution in the Ce^{4+} / resin reaction is first order in [Ce^{4+}] at all the ratios investigated and also that the rate of reaction

111

is independent of the initial Ce^{4+} : C ratio.

5.1.2.1.2 Changes in TOC Level

The TOC level of the resin solution was 940 ppm before Ce^{4+} addition, and 930 ppm 100 minutes after, thus within experimental error the TOC level was unchanged over this period of time.

5.1.2.1.3 Changes in Oxidising Power

The oxidising power of the Ce^{4+} in the resin solution was found to be reduced relative to an equivalent amount of Ce^{4+} in distilled water. This confirms the spectroscopic measurements, i.e., that the Ce^{4+} in the Ce^{4+} / resin solution mixture has been reduced to Ce^{3+}. This in turn suggests that some organic components of the resin have been partially oxidised, since the organic material in the resin solution is the only reductant present in large quantity.

5.1.2.2 Irradiation of the Ce(IV) / resin solutions with UV light

Samples of a standard solution of Ce^{4+} and a 300 minute resin solution, were mixed together at two ratios in the presence of UV light and the changes in the $[Ce^{4+}]$ with time were monitored. The results of these experiments were then compared with those from the 'dark', non-UV irradiated experiments.

FIGURE 5.1

Graph showing the relationship of the logarithm of the [Ce(IV)] to the time of reaction for two ratios of the Ce(IV) / 300 minute / UV system

Initial Ce(IV) : C in solution ratio

▣ 0.26:1
Equation of Line   y = - 5.35 - 3.50e-2x
Fit of Line   R^2 = 0.984

● 0.51:1
Equation of Line   y = - 5.17 - 2.01e-2x
Fit of Line   R^2 = 0.990
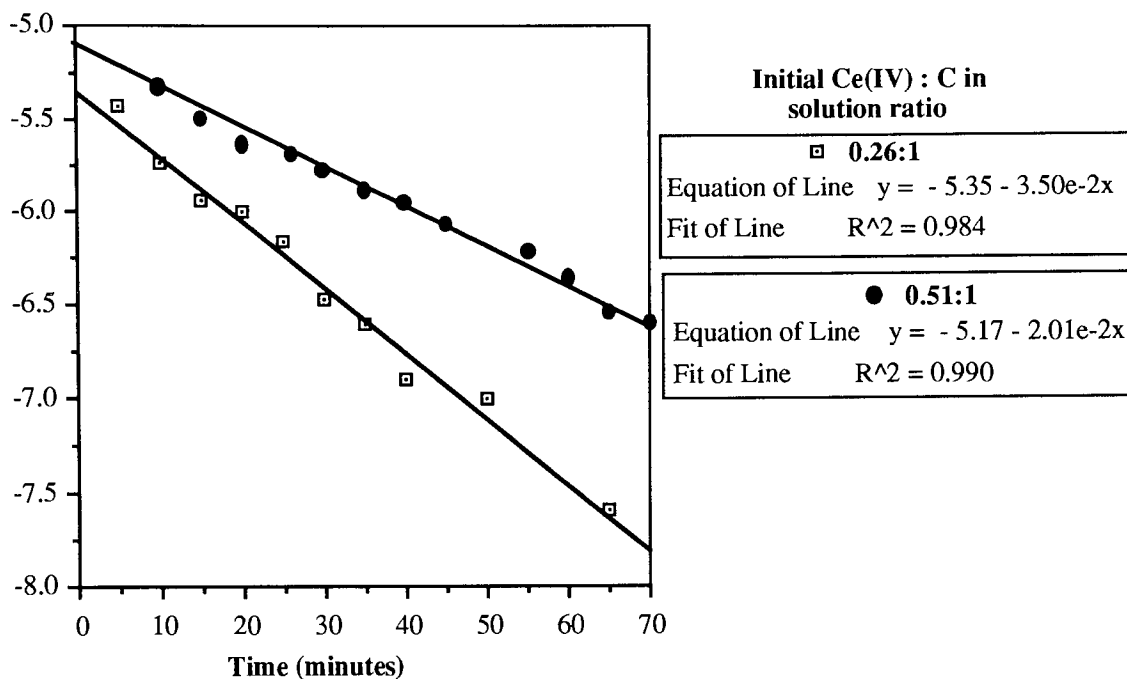
Figure 5.1 shows that the rate of loss of Ce^{4+} from solution in the Ce^{4+} / resin / UV system is first order in $[Ce^{4+}]$, as was the case in the non-irradiated solutions. However, insufficient data were obtained, due to lack of time, to decide whether the rate of reaction in this system is independent of initial Ce^{4+} : C (in the resin) ratio, as was found to be the case for the non-irradiated reaction.

FIGURE 5.2

Graph showing the relationship of the logarithm of the [Ce(IV)] to the time of reaction for a 0.26 : 1 (Ce(IV) : Carbon) ratio in the presence and absence of UV light

Initial Ce(IV) : C in
solution ratio

| □ 0.26:1 (Dark) |
| Equation y = - 5.28 - 1.79e-2x |
| Fit R^2 = 0.997 |

| ※ 0.26:1 (UV) |
| Equation y = - 5.35 - 3.50e-2x |
| Fit R^2 = 0.984 |
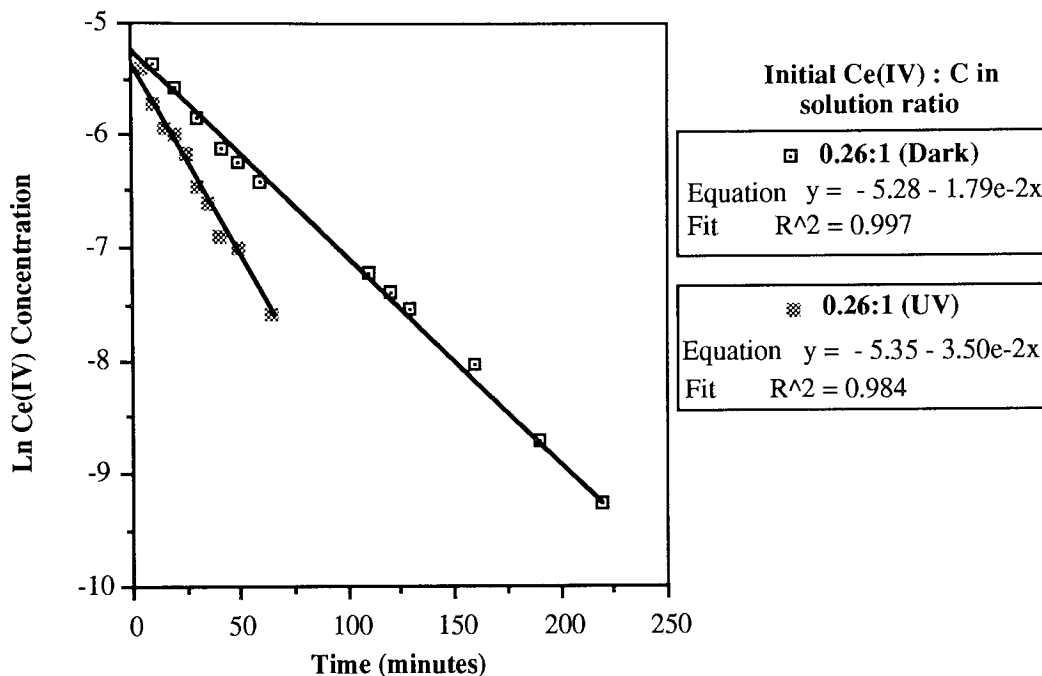
FIGURE 5.3

Graph showing the relationship of the logarithm of the [Ce(IV)] to the time of reaction for a 0.51 : 1 (Ce(IV) : Carbon) ratio in the presence and absence of UV light

Initial Ce(IV) : C in
solution ratio

| □ 0.51:1 (Dark) |
| Equation y = - 5.01 - 6.97e-3x |
| Fit R^2 = 0.992 |

| ※ 0.51:1 (UV) |
| Equation y = - 5.17 - 2.01e-2x |
| Fit R^2 = 0.990 |
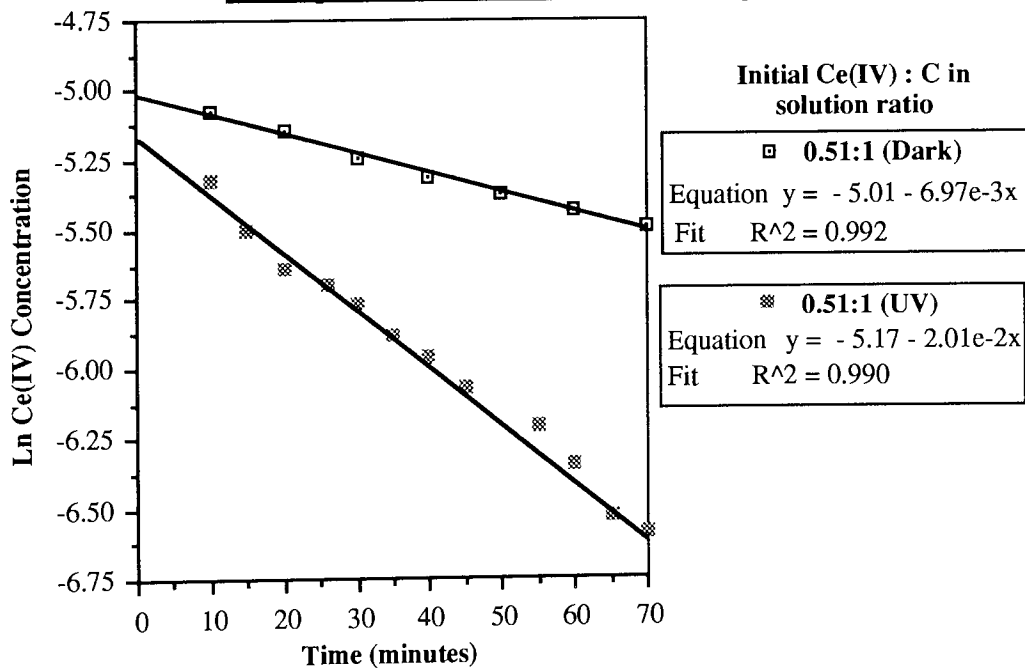
Figures 5.2 and 5.3 show that there is a small difference in the rate of reaction for irradiated and non-irradiated solutions, factors of 2 x and 3 x in these instances. For both ratios of Ce^{4+} : resin solution tested, the [Ce^{4+}] in the irradiated solution falls faster than in the non-irradiated solution.

5.1.2.4 Discussion of the Results

5.1.2.4.1 The Oxidation of the Organic Material in the 300 Minute Resin Solution

It has been shown in Section 5.1.2.1.3 that Ce^{4+} is being reduced to Ce^{3+} when it is added to 300 minute resin solution. There are two potential explanations for this observation.

1) "The Ce(IV) could be being reduced by the Fe(II) in solution."

This is not the case, for two reasons. Firstly, even if the all the Fe in solution was in the Fe^{2+} oxidation state, there would only be sufficient Fe^{2+} present to reduce 1 percent of the Ce^{4+} present at the start of the reaction. Secondly, the reduction of Ce^{4+} to Ce^{3+} by Fe^{2+} is a very fast reaction (a time scale of milliseconds), whereas the observed reduction occurs over a period of several minutes [85].

2) "The Ce(IV) could be oxidising the organics in solution"

This is the most likely explanation for the reduction of Ce^{4+} to Ce^{3+}. No TOC level change was noted on addition of Ce^{4+}, so the Ce^{4+} can only be partially oxidising the organic molecules in the resin solution.

5.1.2.4.2 The Mechanism of Reaction in the UV Irradiated and Non-UV Irradiated Ce(IV) : Resin Mixtures

The loss of Ce^{4+} was shown to be 1st order in both systems i.e.,

$$-\frac{d}{dt}[Ce(IV)] = k\,[Ce(IV)]^1$$

The non-appearance of the reductant concentration in the rate equation probably reflects its large excess over oxidising agent, as there were more moles of C present than moles of Ce(IV). Also

C will only be lost from solution when it is converted to CO_2 or another volatile end product.

A mechanism was developed for the Ce^{4+} / resin / UV system, and is detailed below.

For the general reaction

$$A + B \xrightarrow{k} C \qquad \text{where B is in very large excess}$$
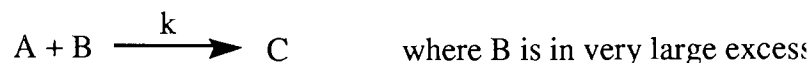
then

$$\frac{d\,[C]}{dt} = -\frac{d\,[A]}{dt} = k_{obs}\,[A]^1$$

but

$$\underline{k_{obs} = k\,[B]}$$

If k_{obs} is independent of [B] then it means that B is not involved in the slow, rate determining step. That occurs in the present case therefore a reasonable mechanism is the system shown in Figure 5.4 for the reaction of Ce^{4+} and 300 minute resin solution.

FIGURE 5.4

A MECHANISM FOR THE OXIDATION OF '300 MINUTE RESIN SOLUTION' BY CE(IV) IN THE PRESENCE OF UV LIGHT

$$Ce^{4+} + S \underset{}{\overset{K}{\rightleftharpoons}} S\text{--}Ce^{4+} \qquad \text{where S = co-ordination site on a 'resin solution' molecule}$$

$$\text{i.e., the } [S\text{--}Ce^{4+}] \approx [Ce^{4+}]$$

$$S\text{--}Ce^{4+} + h\upsilon \underset{k_1}{\overset{k_0}{\rightleftharpoons}} [S\text{--}Ce^{4+}]* \qquad [\ ]* = \text{activated complex}$$

$$[S\text{--}Ce^{4+}]* \xrightarrow{k_2} S'\text{--}Ce^{3+} \qquad S' = \text{oxidised co-ordination site}$$

$$S'\text{--}Ce^{3+} \xrightarrow[\textit{fast}]{+Ce^{4+}} S'' + 2\,Ce^{3+} \qquad S'' = \text{further oxidised co-ordination site}$$
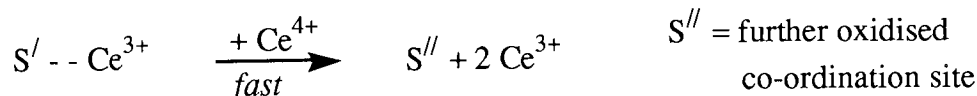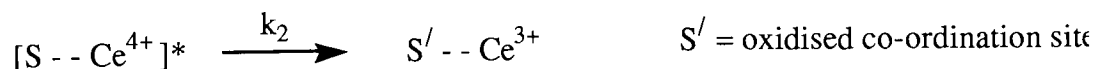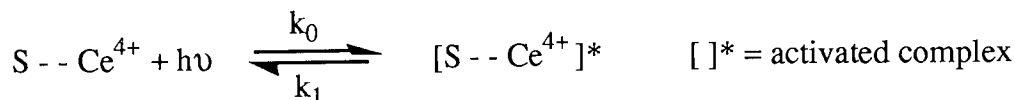
$$\text{which leads to} \quad -\frac{d[Ce^{4+}]}{dt} = \frac{2\,k_2\,k_0\,[Ce^{4+}]}{k_2 + k_1}$$

116

5.1.2.4.3 Future Work on the Ce(IV) / Resin Reaction

It has been shown that addition of Ce^{4+} to a solution of 300 minutes resin causes partial oxidation of the organic components in solution. I would suggest that any future work on this system should proceed as follows:-

1) Investigate the effect of higher Ce^{4+} : C ratios i.e., would more Ce^{4+} result in complete oxidation of organic molecules in solution, with a consequent TOC level reduction ?

2) If it were found that Ce^{4+} could completely oxidise organic molecules the next step would be to find a method of re-oxidising the Ce^{3+} formed back to Ce^{4+}. If this could be done cheaply and efficiently a catalytic cycle for the destruction of organic molecules might be devised.

5.1.2.4.4 The Use of Ce(IV) in Combination with Fenton's Reagent

It would probably not be possible to set up a combination Ce^{4+} / H_2O_2 resin destruction system, equivalent to a UV / H_2O_2 resin destruction system such as that described Chapters 4 and 8. This is because the presence of Ce^{4+} in solution was found to severely decrease the efficiency of utilisation of H_2O_2 during the resin destruction process, possibly by catalysing the decomposition of H_2O_2 to H_2O and O_2. This means that Ce^{4+} used to oxidise organic molecules at an earlier point in the resin destruction process would have to be completely removed before any more H_2O_2 could be added.

5.1.3 The Reactions of Various Ratios of Ce(IV) and PSS

Poly(styrenesulfonate) (PSS)
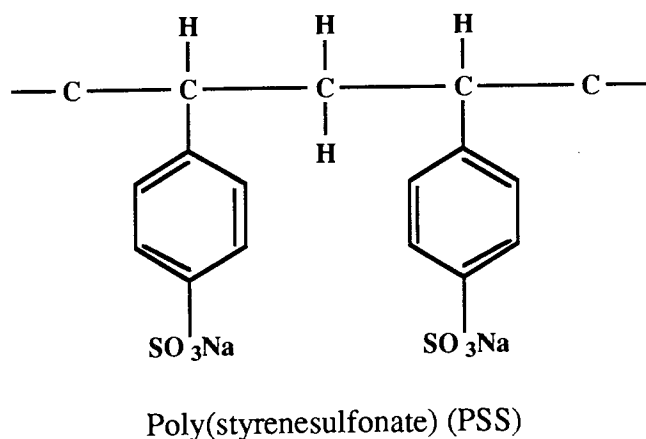
The organic substrate PSS was chosen for use as a resin analogue because it has a similar chemical structure to Lewatit and other ion-exchange resins, and is soluble in water. This water

solubility allows study of a homogeneous system from the start of any reaction.

The PSS : Ce^{4+} ratio was calculated on the basis of the PSS repeat unit to Ce^{4+} ion ratio.

5.1.3.1 The Dark Reactions of Mixtures of Ce(IV) / PSS

Samples of solutions of PSS and Ce^{4+} were mixed together in a 5 : 1 ratio. Using the same terminology as was used for the Ce^{4+} / resin experiments, this is a 0.0225 Ce^{4+} : C ratio. The changes in concentration of Ce^{4+} were monitored by following the changing absorbance of the mixture at 317 nm. PSS does not absorb strongly at this wavelength.

5.1.3.1.1 Changes in Ce(IV) Concentration

FIGURE 5.5

Graph showing how the logarithm of the [Ce(IV)] changes with time, in a 5 :1 ratio PSS : Ce(IV) system

Equation of Line =
$y = -4.87 - 4.75e-5x$ $R^2 = 0.994$
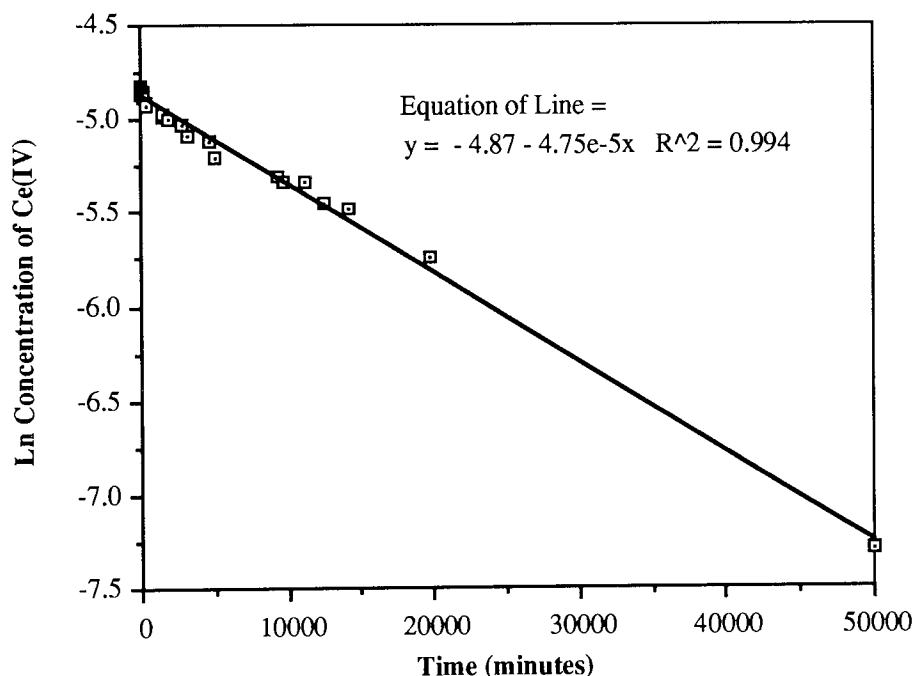
When PSS was added to solutions of Ce^{4+} in the dark, a very slow fall in $[Ce^{4+}]$ was seen. If the natural logarithm of the concentration was then calculated and plotted against time, a straight line was produced (see Figure 5.5). The rate of loss of Ce^{4+} can be seen to be first order, but the non-irradiated reaction occurred too slowly to be of interest as a method of oxidising organic materials. Only the one ratio of PSS : Ce^{4+} was tested, due to this very slow rate of reaction.

5.1.3.2 Irradiation of Ce(IV) / PSS mixtures with UV light

PSS and Ce^{4+} were mixed together at various ratios in a UV photochemical reactor and the changes in $[Ce^{4+}]$ with time were monitored. The reaction solution was constantly stirred by blowing air through the solution. Separate experiments were also carried out to find out if

a) there was any change in TOC level after the mixture had been irradiated, or

b) if any gas was being produced by the irradiated solution.

5.1.3.2.1 Changes in Ce(IV) Concentration

FIGURE 5.6

Graph showing the change in [Ce(IV) with time for various ratios of PSS repeat unit : Ce(IV) in a PSS / Ce(IV) (UV irradiated) system

Initial PSS repeat unit to Ce(IV) ion ratio

▫	1.25:1
◆	2.08:1
✕	3.12:1
◇	5:1
+	8.3:1
●	12.5:1
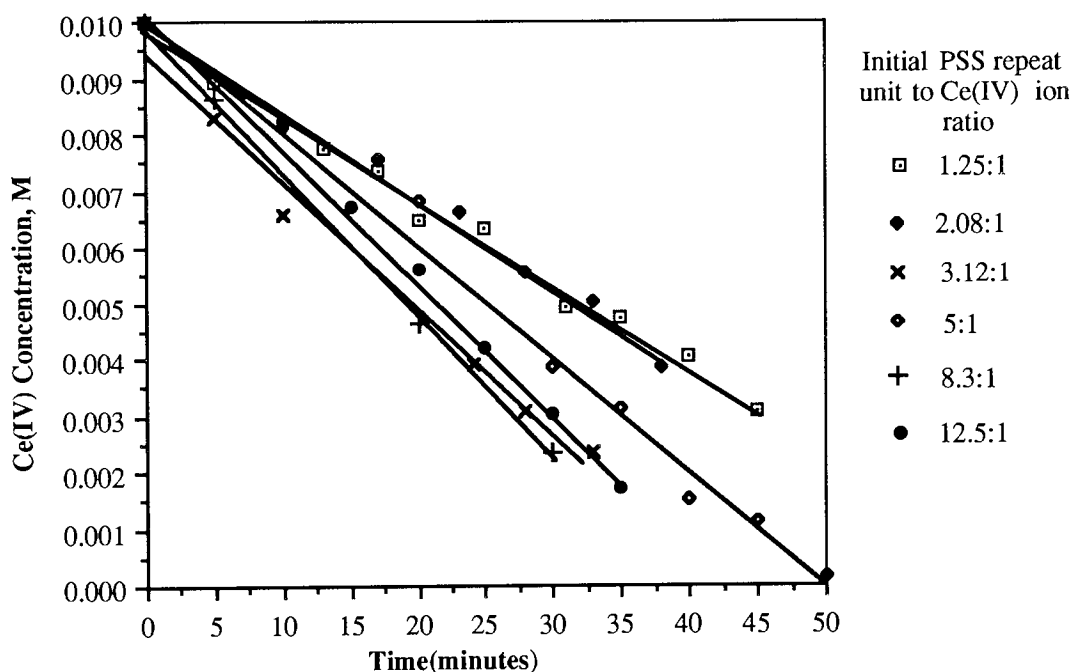
TABLE 5.4

GRADIENTS AND INTERCEPTS ON THE Y AXIS FOR

VARIOUS PSS : CE(IV) RATIOS

PSS : Ce(IV) (moles / moles)	PSS repeat unit : Ce(IV) ion ratio	Rate of reaction (min $^{-1}$)	Intercept on y axis (M)
0.00250 : 0.002	1.25 : 1	1.48 x 10^{-4}	9.78 x 10^{-3}
0.00416 : 0.002	2.08 : 1	1.56 x 10^{-4}	1.00 x 10^{-2}
0.00624 : 0.002	3.12 : 1	2.26 x 10^{-4}	9.47 x 10^{-3}
0.01 : 0.002	5 : 1	2.05 x 10^{-4}	1.03 x 10^{-2}
0.0166 : 0.002	8.3 : 1	2.57 x 10^{-4}	9.93 x 10^{-3}
0.025 : 0.002	12.5 : 1	2.41 x 10^{-4}	1.03 x 10^{-2}

Figure 5.6 shows that for all ratios tested of PSS repeat units to Ce^{4+} ions, the rate of loss of Ce^{4+} from solution is zero order in $[Ce^{4+}]$ (and [PSS]). The average rate of reaction, k, is

$$(2.1 \pm 0.58) \times 10^{-5} \text{ min}^{-1}$$

This result is surprising, as it implies that the rate determining step in the reaction mechanism involves neither Ce^{4+} or PSS. However, a mechanism was devised to explain this observation (see Section 5.1.3.3.2).

5.1.3.3 Suggested Mechanisms for the Irradiated and Non-Irradiated PSS / Ce(IV) Systems

5.1.3.3.1 The Non-Irradiated PSS / Ce(IV) System

The loss of Ce^{4+} was shown to be 1st order i.e.,

$$-\frac{d}{dt}[Ce(IV)] = k [Ce(IV)]^1$$

This probably reflects the very large excess of reducing agent over oxidising agent. In the 5 : 1 ratio PSS / Ce^{4+} system there are 5 PSS repeat units per Ce^{4+} ion. Each PSS repeat unit is potentially able to act as a 41 electron reductant, as shown below.

$$C_8H_9SO_3 + 17 H_2O \longrightarrow 8 CO_2 + SO_4^{2-} + 43 H^+ + 41 e^-$$

120

<u>5.1.3.3.2 The Irradiated PSS / Ce(IV) System</u>

The loss of Ce^{4+} has been shown to be 0 order, i.e.,

$$-\frac{d}{dt}[Ce(IV)] = k\,[Ce(IV)]^0$$

while the [PSS] does not appear within the rate constant, k.

This indicates that the mechanism of reaction is different from that of the non-irradiated system where the Ce^{4+} ion is involved in the rate determining step (r.d.s).

PSS has a maximum absorption peak at 229 nm, well away from the peak emission of the mercury vapour lamps used in the photochemical equipment, so it was assumed that all incident light was absorbed by Ce^{4+} in solution, forming photo-excited Ce^{4+} ions.

$$Ce^{4+} \xrightarrow{\;h\upsilon\;} {}^*Ce^{4+}$$
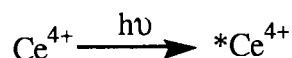
A model mechanistic scheme (see Figure 5.7) for the reaction of photo-excited Ce^{4+} with any reducing agent was devised.

FIGURE 5.7

REACTION PATHWAYS FOR PHOTO-EXCITED CE(IV)
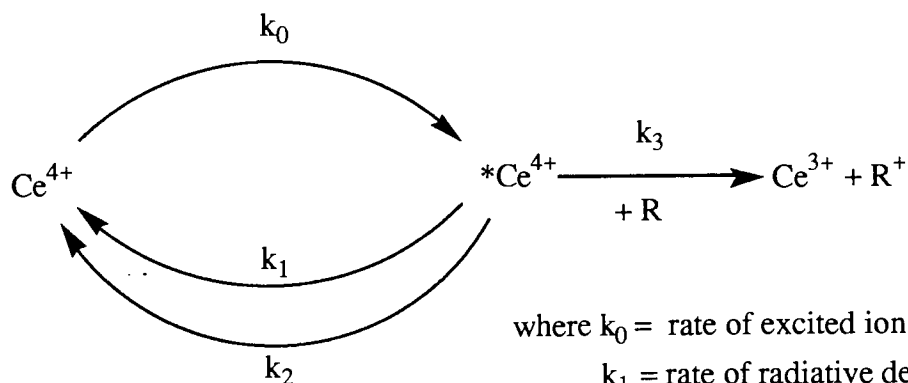
where k_0 = rate of excited ion formation
k_1 = rate of radiative deactivation
k_2 = rate of non-radiative deactivation
k_3 = rate of photochemical reaction
${}^*Ce^{4+}$ = photo-excited Ce^{4+} ion
R = Reducing agent (unspecified)

The steady state assumption was made for the concentration of activated ${}^*Ce^{4+}$.

All light incident on the reaction solution is absorbed, so therefore the rate of formation of ${}^*Ce^{4+}$ is constant and independent of $[Ce^{4+}]$.

Therefore, in the system shown in Figure 5.7,

$$k_0 = [*Ce^{4+}] \{k_1 + k_2 + k_3 [R]\}$$

Rearranging,

$$[*Ce^{4+}] = \frac{k_0}{\{k_1 + k_2 + k_3 [R]\}}$$

Now we can also see from Figure 5.7 that

$$-\frac{d [R]}{dt} = k_3 [R] [*Ce^{4+}]$$

Substituting for the $[*Ce^{4+}]$,

$$-\frac{d [R]}{dt} = \frac{k_0 k_3 [R]}{(k_1 + k_2 + k_3 [R])}$$

Since, as can be seen from Figure 5.7

$$-\frac{d [R]}{dt} = \frac{d [Ce^{3+}]}{dt}$$

it follows that

$$\frac{d [Ce^{3+}]}{dt} = \frac{k_0 k_3 [R]}{(k_1 + k_2 + k_3 [R])}$$

Finally,

$$k_{obs} = \frac{k_0 k_3 [R]}{(k_1 + k_2 + k_3 [R])} \qquad \text{where } k_{obs} = \text{Observed rate constant}$$

If we then substitute PSS for the general reducing agent, R, described above, we get

$$k_{obs} = \frac{k_0 k_3 [PSS]}{(k_1 + k_2 + k_3 [PSS])}$$

By substituting values for PSS in the equation above, a graph of the form shown in Figure 5.8 (see overleaf) is produced.

FIGURE 5.8

THE GENERAL FORM OF A SATURATION CURVE
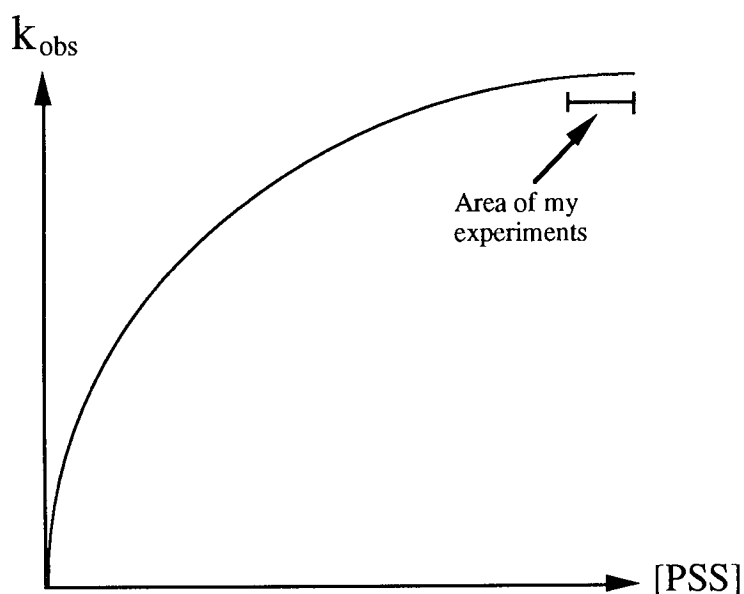
This graphical form, often called a "saturation curve" is first order in PSS when

$$(k_1 + k_2) \gg k_3 \,[PSS]$$

but becomes zero order when

$$k_3 \,[PSS] \gg (k_1 + k_2)$$

which is apparently the situation in my experiments.

5.1.3.4 An Increase in Absorbance at 317 nm after UV Irradiation

It was also noted that after reaching a minimum absorbance value, the absorbance at 317 nm in the PSS / Ce^{4+} / UV system appeared to rise again at a very slow rate, as is shown in the following Figures, 5.9 and 5.10.

FIGURE 5.9

Graph showing the changes in absorbance at 317 nm with time in a 5 : 1 ratio PSS : Ce(IV) (UV irradiated) system

Equation of Line
$y = 34.9 - 0.7x$ $R^2 = 0.991$

UV Irradiation
Stopped

Liquid heated
to 60 deg. C

(X-axis: Time (minutes); Y-axis: Absorbance at 317 nm)
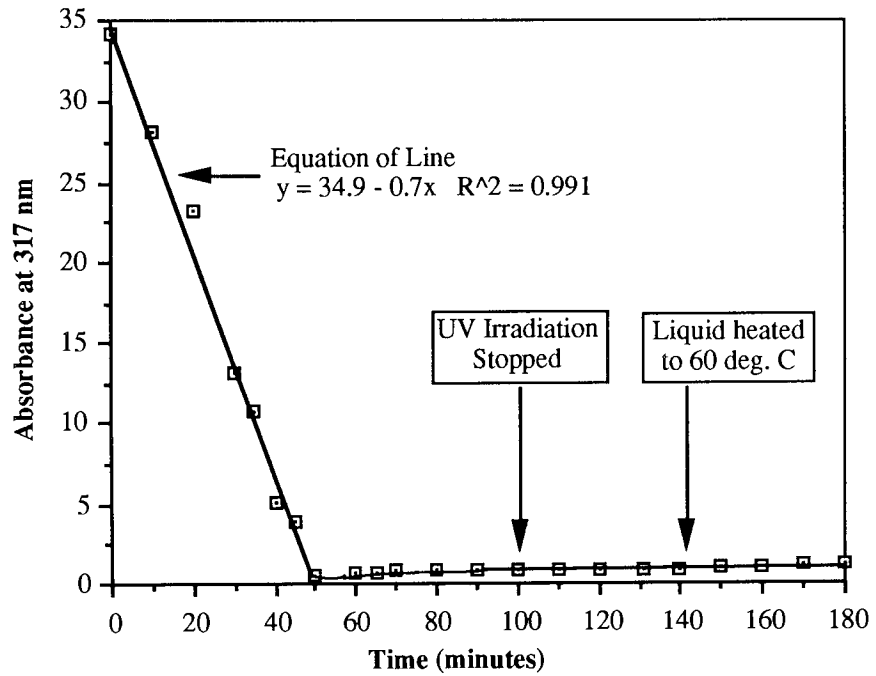
FIGURE 5.10

Graph showing the absorbance at 317 nm of a 5 : 1 ratio PSS : Ce(IV) (UV irradiated) system - from 40 minutes into the reaction

UV Irradiation
Stopped -
Point A

Liquid heated
to 60 deg. C -
Point B

(X-axis: Time (minutes); Y-axis: Absorbance at 317 nm)
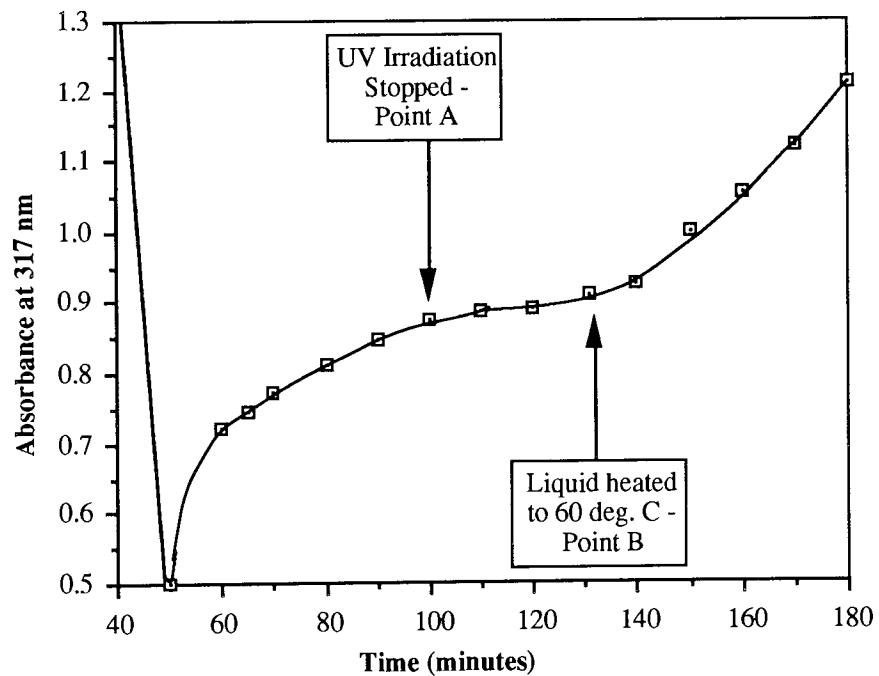
Figure 5.10 shows that there was a rise in absorbance even while the UV lamp was still on, once a minimum absorbance value had been reached.

The reduction in rate of rise of absorbance seen when the UV lamp was turned off, at Point A, is probably due to the fall in temperature of the reaction mixture upon extinguishing the lamp. Even though the quartz photochemical reaction vessel is water jacketed, the temperature of the reaction mixture has been found to rise by approximately $10^{\circ}C$ when the lamp is on, due to the large quantity of heat produced when medium pressure mercury vapour lamps are operated. When the temperature is raised, at Point B, it can be seen that the rate of absorbance rise increases again.

A similar experiment was carried out over a much longer period, for a 8.3 : 1 PSS / Ce^{4+} ratio.

FIGURE 5.11

Graph showing the change in absorbance at 317 nm after UV irradiation of a 8.3 : 1 ratio PSS : Ce(IV) system
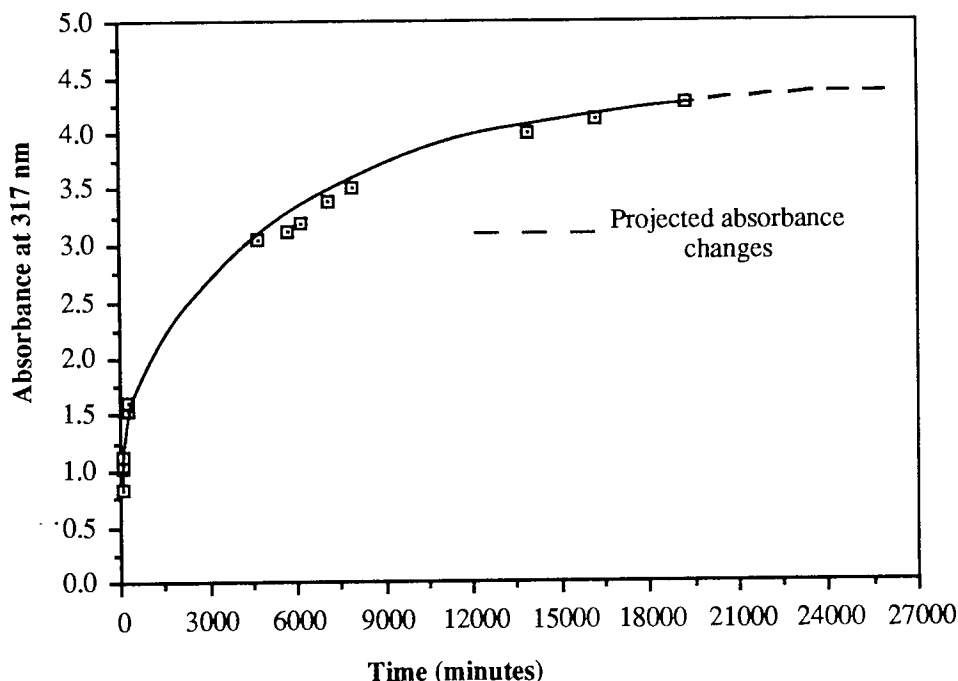
If the experimental data in Figure 5.11 are extrapolated, a constant absorbance of around 4.5 is reached at about 17 days (24500 minutes) from the start of the reaction after rising from a minimum absorbance of about 0.7 (0.7 represents about 2% of the starting absorbsorbance). During the initial UV irradiation, it took 11 minutes for the absorbance to fall from 4.5 to 0.7, which is 2000 times faster than the slow subsequent absorbance rise.

125

Two possible explanations for this (slow!) rise in measured absorbance after UV irradiation are detailed below.

1) The Ce^{3+} in the reaction solution is being oxidised to Ce^{4+} by the oxygen in the air, causing an increase in the absorbance measured at 317 nm. Since O_2 does not normally oxidise Ce^{3+} to Ce^{4+}, the Ce^{4+} state would have to be being stabilised by co-ordination with an organic ligand (in a similar manner to $Pd^{II/III}$, as described in Chapter 3, Section 3.0.2).

2) The oxygen in the air is slowly oxidising the products of the PSS / Ce^{4+} reaction. It is possible that the oxidised products of PSS could have a greater absorbance at 317 nm than the original reaction products of PSS (a solution of PSS alone was found to be completely stable over an equivalent period of time). This explanation would account for the shape of the curve shown in Figure 5.11, i.e., the rate of change in absorbance falls as the concentration of oxidised reaction products of PSS falls, so I would suggest that this is the correct explanation for the absorbance rise.

This absorbance rise after irradiation was not studied further because the rise's small size and slow rate of increase was not considered likely to be commercially useful.

5.1.3.5 IR Analysis of the Ce(IV) / PSS Mixture Before and After UV Irradiation

Drops of the PSS / Ce^{4+} mixture (with the $Ce^{4+/3+}$ removed before analysis by making the mixture slightly alkaline) were placed on a ZnSe Horizontal ATR Crystal before and after the mixture had been irradiated in a UV photochemical reactor. IR spectra were collected, and compared to find if any change had occurred. A change would indicate that oxidation of the PSS had been caused by the Ce^{4+}.

FIGURE 5.12

IR SPECTRA OF A CE(IV) / PSS MIXTURE BEFORE UV IRRADIATION
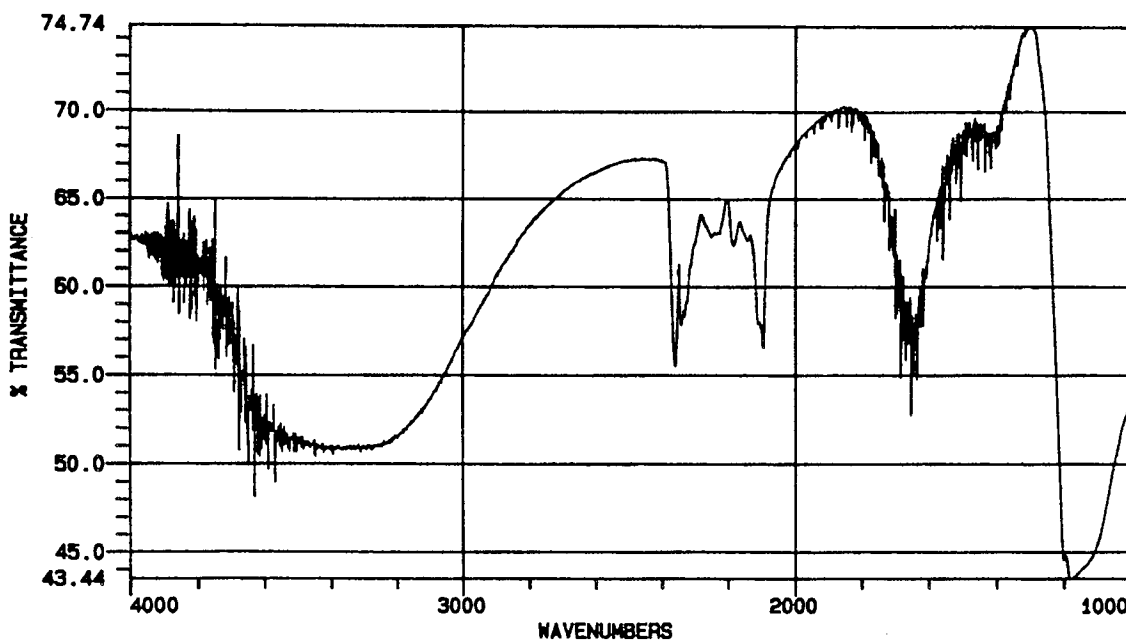
FIGURE 5.13

IR SPECTRA OF A CE(IV) / PSS MIXTURE AFTER UV IRRADIATION
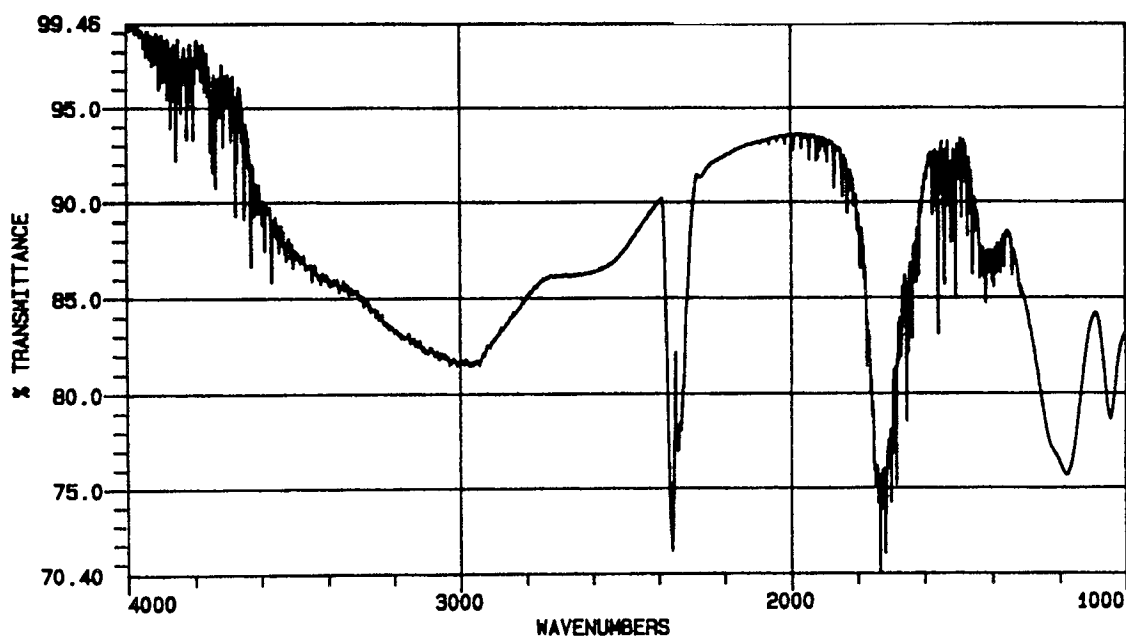
The spectra show that there are two regions of the spectrum where major changes have occurred. The first region is between 2100 and 2300 cm^{-1}, and the second is between 1000 and 1400 cm^{-1} (ZnSe does not transmit IR radiation below 1000 cm^{-1}, so data from this region was

not available). These differences between the two spectra indicate that partial oxidation of the PSS had occurred in this system. Due to the cut off of data below 1000 cm^{-1} the only absorbance peak that could positively be assigned in Figures 5.12 and 5.13 is the peak at 1190 cm^{-1}, which is the sulphonate peak. It can be seen that this peak is much larger, relative to the other peaks, in the spectrum obtained before irradiation than in the spectrum collected after irradiation. This suggests that one of the processes occurring during oxidation of PSS in the Ce^{4+} / UV system is removal of the SO$_3^-$ group from the PSS molecule.

5.1.3.6 Other Observations

Within experimental error the TOC level remained unchanged during irradiation of the PSS / Ce^{4+} solution, indicating that complete oxidation of the PSS in solution was not occurring to any significant extent. No off-gas was detected from the reaction mixture, showing that the Ce^{4+} / UV combination was not oxidising water, and that Ce^{4+} must therefore be oxidising the organic component of the mixture.

5.1.3.7 Discussion of the Results

As was the case in the Ce^{4+} / resin system, partial oxidation of the organic material in solution appears to be occurring. However, unlike the Ce^{4+} / resin system, the non-irradiated reaction is very much slower than the irradiated reaction (465 times slower). This indicates that the PSS / Ce^{4+} reaction is light catalysed. The process occurring might be summarised as
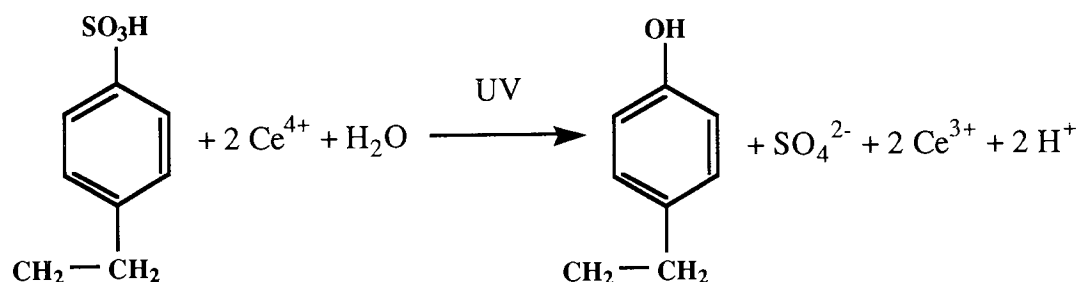
FIGURE 5.14

CALIX[8]ARENE-P-OCTASULPHONIC ACID
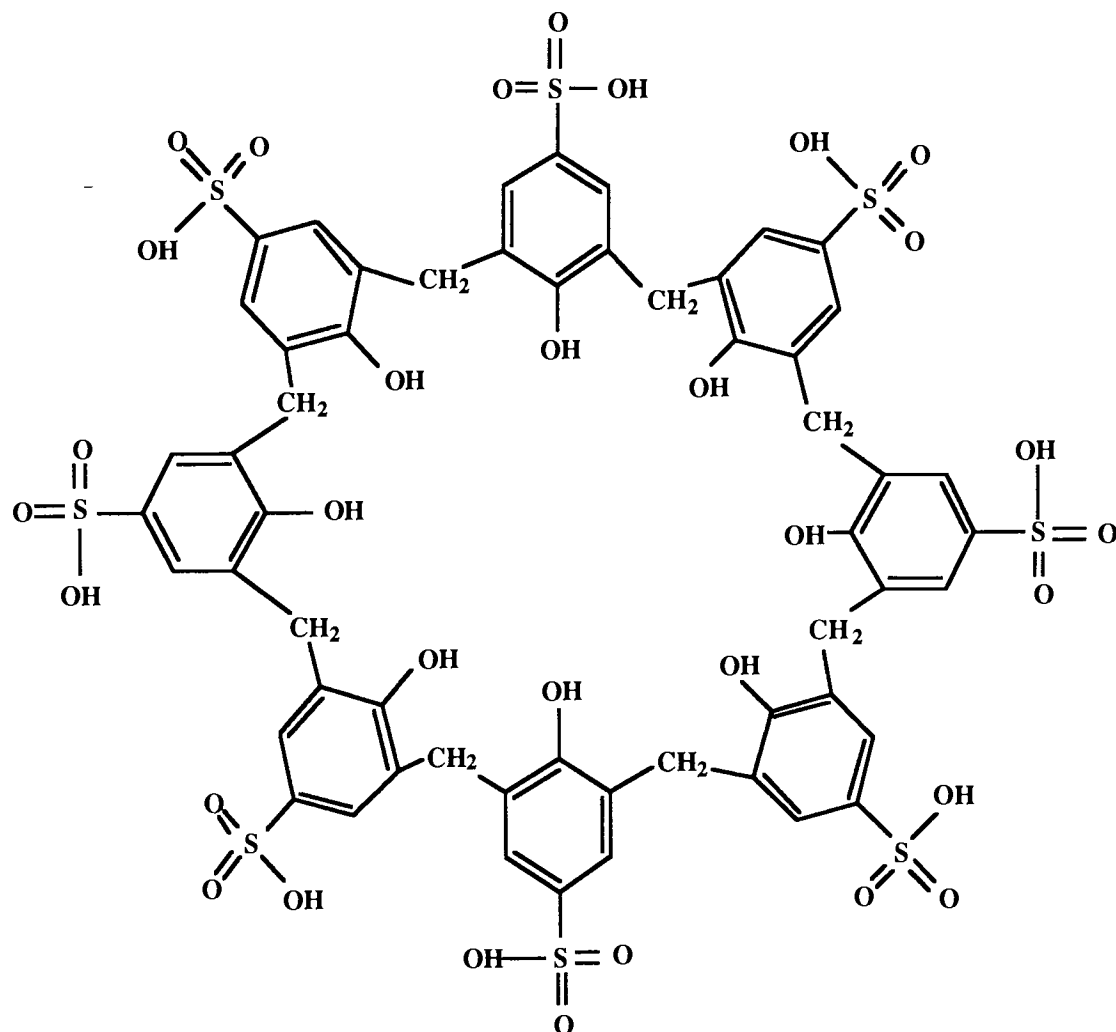
It was decided to use the cyclic oligomer calix[8]arene-p-octasulphonic acid as a model compound. This was because of its close resemblance to Lewatit ion exchange resin (which has a sulphonated, phenol-formaldehyde, cross-linked structure), and also because of its solubility in water, like PSS. This means that a homogeneous, well defined reaction system can be studied from the beginning of any reaction. A formal structural diagram of CALIX is shown in Figure 5.14, and further details of the CALIX molecule are described in Chapter 7, Section 7.03.

<u>5.1.4.1 The Ce(IV) / CALIX System</u>

Samples of solutions of Ce^{4+} and CALIX were mixed together at various concentrations and under various conditions. Most calculations of the ratio between Ce^{4+} ions and CALIX were based on the ratio of Ce^{4+} ions to the benzene repeat units in the CALIX molecule. Since there are 8 benzene units in the CALIX molecule, a '2 :1 Ce^{4+} : CALIX repeat unit' ratio would represent 2 Ce^{4+} ions per benzene unit (or alternatively 16 Ce^{4+} ions per CALIX molecule). The changes in concentration of Ce^{4+} were followed by measuring the absorbance of the reaction solution at 317 nm.

FIGURE 5.15

<u>Graph showing the changes in absorbance with
time for a typical Ce(IV) : CALIX ratio</u>
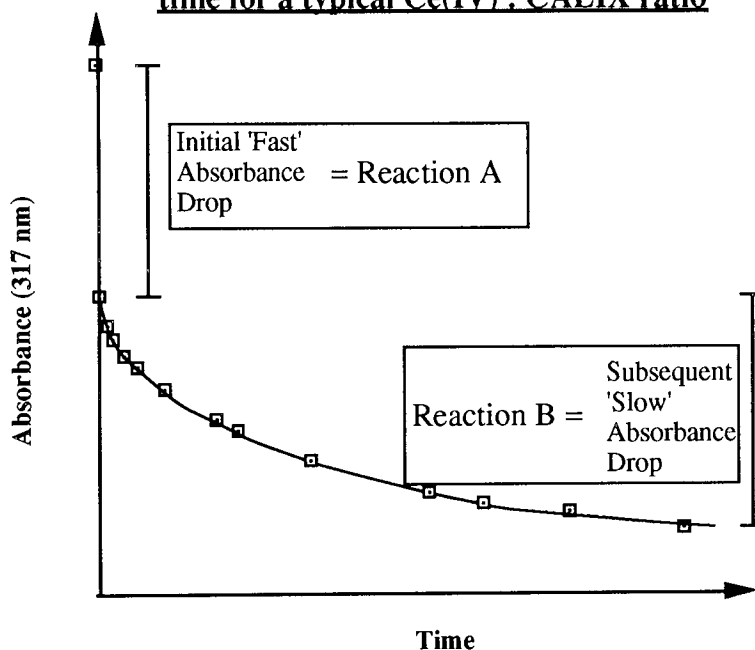
Figure 5.15 shows the typical pattern of absorbance changes found for the Ce^{4+}/CALIX system. Upon addition of CALIX (pre-dissolved in a small quantity of water) a fast initial drop in absorbance is seen. This drop in absorbance was found to occur over a period of less than 0.5 second (by use of simple stopped-flow kinetics apparatus). This rapid drop was followed by much slower drop in absorbance, which typically occurred over a time scale of hours. It was also found that this subsequent absorbance drop occurred several times faster if the Ce^{4+}/CALIX mixture was irradiated by UV light during the period of the experiment.

130

mixture was irradiated by UV light during the period of the experiment.

5.1.4.2 The Investigation of the Mechanisms of Reactions 'A' and 'B' (Figure 5.15)

Unlike the practice used in the rest of this PhD, in my descriptions of the Ce^{4+} / CALIX system my conclusions on the implications of the results will be given before the results themselves. This has been done because the argument that follows is demanding and I believe that it will make it easier for the reader to follow my chain of thought if the reader is aware of my conclusions when reading through the results.

The mechanisms of both Reaction A and B were primarily elucidated by analysis of the way the absorbance of the reaction solution changed with time. The rapid initial absorbance drop seen during Reaction A was assumed to be a measure of the loss of 'free' Ce^{4+}. This loss of free Ce^{4+} could either occur by complexation of Ce^{4+} with CALIX, or by its reduction to Ce^{3+}. Additional information was obtained on the mechanism of Reaction A by finding the oxidising power of the reaction solution immediately after CALIX had been added to the Ce^{4+} solution. The oxidising power of the solution was found by adding it to a known volume and concentration of Fe^{2+} solution, and then measuring the change in the $[Fe^{2+}]$.

An overall mechanism (see Figure 5.16) was developed using experimental data, which appears to describe the behaviour of the Ce^{4+} / CALIX system (as summarised in Figure 5.15).

FIGURE 5.16

AN OVERALL MECHANISM FOR THE CE(IV) / CALIX REACTION

$$Ce^{4+} + \text{Receptor Site (CALIX)} \xrightleftharpoons{K_1} \text{Complex}^{3+}$$

$$\text{Complex}^{3+} \xrightarrow{k_2} Ce^{3+} + \text{Intermediate}$$

$$Ce^{4+} + \text{Intermediate} \xrightarrow[\text{(fast)}]{k_3} Ce^{3+} + \text{First product}$$
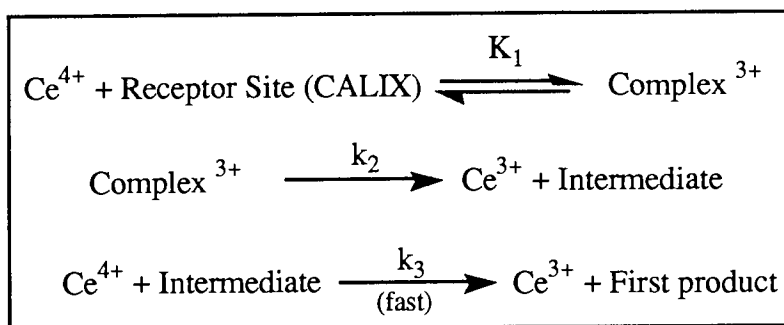
5.1.4.2 A Suggested Mechanism for the Early Part of the Ce(IV) / CALIX Reaction (Reaction A)

Let

$$[Ce^{4+}]_{t=0} = m$$

$$[\text{Receptor Site}]_{t=0} = r$$

$$[\text{Complex}] = c$$

$$[\text{Repeat Unit}]_{t=0} = u$$

Consider an equilibrium forming a 1 : x complex

$$Ce^{4+} + x \text{ Repeat Units} \quad \overset{K}{\underset{}{\rightleftharpoons}} \quad 1 : x \text{ complex}$$

$$(m - c) \qquad (u - xc) \qquad\qquad\qquad c$$
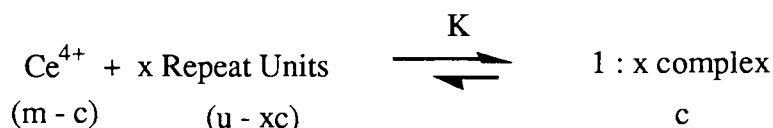
Under the experimental conditions used here

$$2 < m/u < 20$$

If the equilibrium lies well over to the right, the concentration of uncoordinated repeat units will be small

$$(u - xc) = \rho$$

and the complex concentration will be approximately

$$\frac{u}{x}$$

Therefore the fractional drop in initial absorbance will be

$$= \frac{c}{m}$$

$$= \frac{u}{mx}$$

Or using reciprocals

$$\left(\frac{m}{c}\right) = x\left(\frac{m}{u}\right)$$

Figures 5.17 and 5.18 (see pages 135, 136) show plots of this equation with gradients close to one half. Therefore, even though they show non-zero intercepts it is reasonable to deduce that $x =$ one half. This is an acceptable value, as each repeat unit has two ionisable protons and thus anionic coordination sites, i.e. $u = 2r$

If we now re-consider our proposed equilibrium in this new light we can say

$$Ce^{4+} + Receptor\ Site^- \underset{}{\overset{K_1}{\rightleftharpoons}} Complex^{3+}$$

$$(m-c) \qquad (r-c) \qquad\qquad c$$
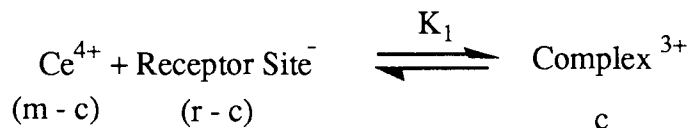
or

$$K_1 = \frac{c}{(m-c)(r-c)}$$

Rearranging this equation,

$$c = K_1 mr - K_1 c\,(m+r) + K_1 c^2$$

It will normally be the case that $mr \gg c^2$, (m and r are the starting concentrations of Ce^{4+} and

repeat unit). The only time when this will not be the situation is when K_1 is very large, and also

$m \approx r$.

Thus we can state

$$c \approx K_1 mr - K_1 c(m+r)$$

Rearranging this equation,

$$c + K_1 c(m+r) = K_1 mr$$

$$c[1 + K_1(m+r)] = K_1 mr$$

we obtain

$$c = \frac{K_1 mr}{1 + K_1(m+r)}$$

If the complex absorbs a negligible amount at 317 nm (the monitored wavelength), then the

fractional drop (f),

$$f = \frac{c}{m} = \frac{Drop\ in\ absorbance}{Original\ absorbance}$$

or, alternatively

$$\delta = c = Drop\ in\ absorbance\ converted\ to\ [Ce^{4+}]$$

can be related to reagent ratios.

The relationships will be as follows.

The equation in this situation is

$$\delta = \frac{(K_1 m)r}{(1 + K_1 m) + (K_1)r} \qquad \text{(brackets round constants)}$$

or, alternatively

$$\frac{1}{\delta} = \frac{(1 + K_1 m) + K_1 r}{(K_1 m)r}$$

Separating out the fraction,

$$\frac{1}{\delta} = \frac{K_1 r}{(K_1 m)r} + \frac{(1 + K_1 m)}{(K_1 m)r}$$

and then rearranging we obtain,

$$\frac{1}{\delta} = \frac{1}{m} + \left(\frac{1 + K_1 m}{K_1 m} \right) \frac{1}{r}$$

Now, we know that

$$\frac{1}{f} = \frac{m}{\delta}$$

therefore

$$\frac{m}{\delta} = 1 + \left(\frac{1 + K_1 m}{K_1} \right) \frac{1}{r}$$

If we wish to plot this on a graph,

$$\frac{1}{f} = 1 + \left(\frac{1 + K_1 m}{K_1 m} \right) \frac{m}{r}$$

with the

$$\text{Gradient} = 1 + \frac{1}{K_1 m}$$

and the intercept being at 1. The gradient will be halved if u, rather than r, is plotted; as in Figures 5.17 and 5.18.

2) When [repeat unit] is constant, but $[Ce]_0$ varies, i.e 'r' is constant, 'm' varies

The equation in this situation is

$$\delta = \frac{(K_1 r)\, m}{(1 + K_1 r) + K_1 m}$$

Or, alternatively,

$$\frac{1}{\delta} = \frac{1}{r} + \left(\frac{1 + K_1 r}{K_1 r}\right)\frac{1}{m}$$

$$\frac{1}{f} = \frac{m}{\delta} = \left(\frac{1 + K_1 r}{K_1 r}\right) + \frac{m}{r}$$

The intercept on the y axis will be

$$= 1 + \frac{1}{K_1 r}$$

and the gradient of the line will be 1, or 0.5 plotting u.

5.1.4.2.1 CALIX Concentration Variable, Ce(IV) Concentration Constant (3.33 x 10^{-3}M)

FIGURE 5.17

**Graph showing the relationship between initial [Ce(IV)]
drop and the Ce(IV) : CALIX (benzene repeat unit) ratio
in the Ce(IV) / CALIX system ([CALIX] variable)**

Equation of Line =
y = 0.74 + 0.46x   R^2 = 0.996

y-axis: Reciprical of [Ce(IV)] Fraction Lost

x-axis: $\frac{[Ce(IV)]_{t=0}}{[Repeat\ Unit]_{t=0}}$

135
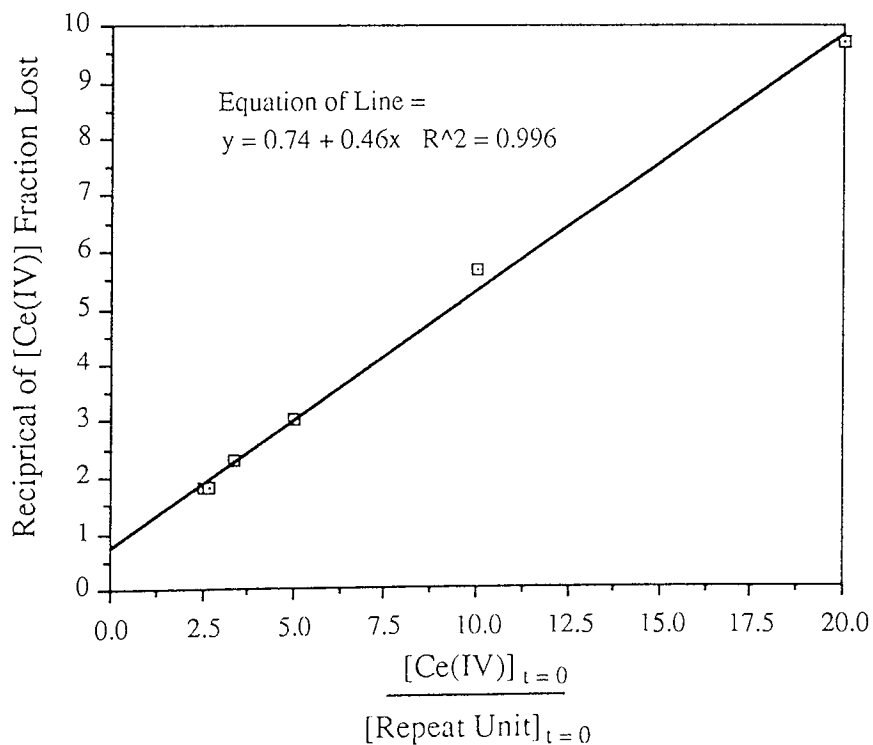
FIGURE 5.18

Graph showing the relationship between inital [Ce(IV)] drop and the Ce(IV) : CALIX (benzene repeat unit) ratio in the Ce(IV) / CALIX system, ([Ce(IV)] variable)

Equation of Line =
y = 0.86 + 0.48x   R^2 = 0.979

y-axis: $\dfrac{[Ce(IV)]_{t=0}}{[Ce(IV)]_{lost}}$

x-axis: $\dfrac{[Ce(IV)]_{t=0}}{[Repeat\ Unit]_{t=0}}$
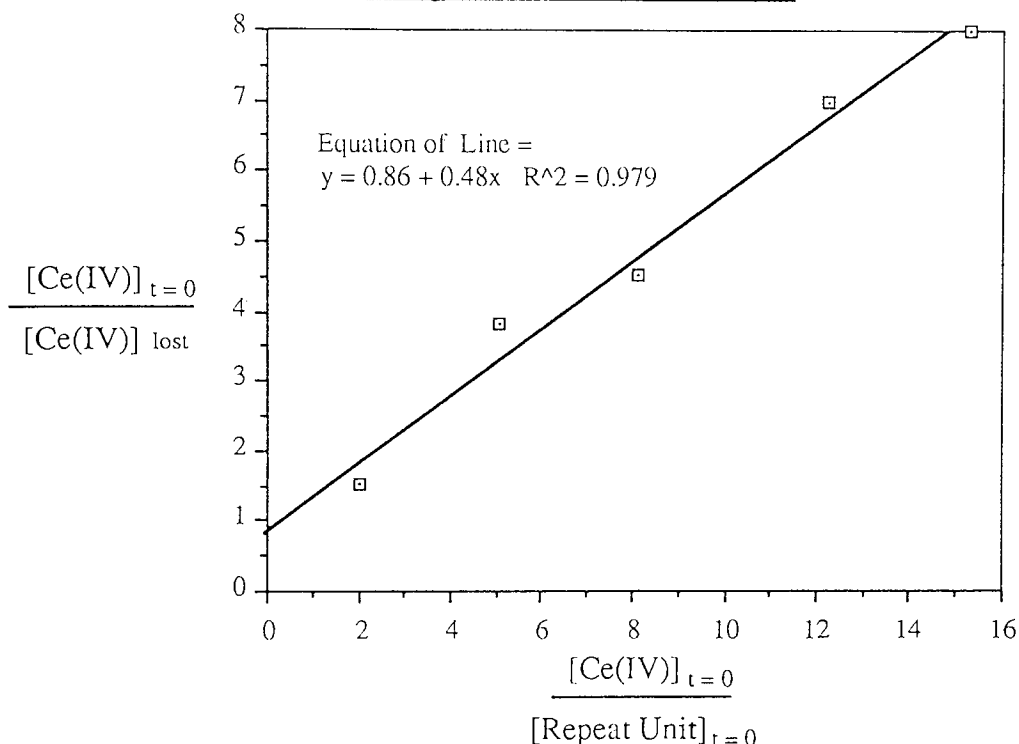
Figures 5.17 and 5.18 show that there is a good correlation between the predicted results and the experimental results, suggesting that the mechanism developed is consistent with the experimental data and probably correct.

5.1.4.2.3 Estimation of the Value of K_1

It was not possible to obtain a value of K_1 directly from the experimental data because of experimental errors. However it is reasonable to estimate that if ρ, the concentration of non-coordinated receptor sites defined on p 132, is always < u/10, i.e.

$$\rho < 10^{-4} \text{ M, then}$$

$$K_1 > \frac{10^{-3}}{3 \times 10^{-3} \times 10^{-4}} \text{ M}^{-1}$$

$$K_1 > 3 \times 10^3 \text{ M}^{-1}$$

Since there are two different sites, phenolate and sulphonate, this treatment must be over-

simplified, as the two sites will have different values of their stability constants. However, given the accuracy of the data a more complete treatment is not warranted.

5.1.4.2.4 The Oxidising Power of a Ce(IV) / CALIX Reaction Mixture Immediately After CALIX Addition

In an attempt to understand further the fast initial reaction (Reaction A) a 4 cm^3 sample of a 7.5 : 1 ratio Ce^{4+} : CALIX reaction solution (immediately after the CALIX had been added) was rapidly mixed with 100 cm^3 of Fe^{2+} / bipyridyl solution, to check if this initial absorbance drop was due to the co-ordination reaction (1) or if it was due to the fast oxidation reaction (2).

<u>Fast initial reaction</u>

$$Ce^{(IV)} + C \longrightarrow Ce^{(IV)}C \quad ---------- \quad (1)$$

$$Ce^{(IV)} + C \longrightarrow Ce^{(III)} + C^{(oxidised)} \quad ---- \quad (2)$$
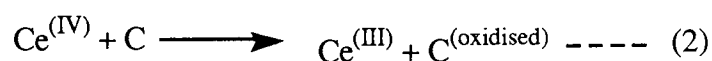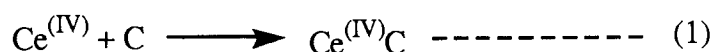
where C = CALIX

5.1.4.2.5 Calculation of the Oxidative Power of the Ce(IV) / CALIX Reaction Solution Immediately After Calixarene Addition

Absorbance, at 532 nm, of a 0.0005 M Fe^{2+} / bipy complex = <u>1.562.</u>

<u>The Oxidising Power of the Ce(IV) Solution</u>

Absorbance of 100 cm^3 of the Fe^{2+} / bipy complex after the addition of 4 cm^3 of Ce^{4+} solution = <u>0.481.</u>

0.481 x 1.04 (correction for dilution) = 0.500, this represents 0.00016M Fe^{2+} i.e., <u>4 cm^3 of Ce^{4+} solution has oxidised 0.00034 moles of Fe^{2+}</u>

<u>Oxidising Power of the Ce(IV) / CALIX Solution</u>

Absorbance, of 100 cm^3 of Fe^{2+} / bipy complex, after the addition of 4 cm^3 of Ce^{4+} / CALIX solution = <u>0.760.</u>

0.760 x 1.04 = 0.79, this represents 0.00025M Fe^{2+} i.e., <u>4 cm^3 of Ce^{4+} / CALIX solution has oxidised 0.00025 moles of Fe^{2+}.</u>

If the amount of oxidation caused by the Ce^{4+} solution, (0.00034 moles Fe^{2+}) is regarded as "100%", then the Ce^{4+} / CALIX solution has 74% of the oxidising power of the Ce^{4+} solution alone.

i.e., the Ce^{4+} sample had 26% more oxidising power than the Ce^{4+} / CALIX sample.

These calculations were repeated for a full, identical, experimental run, giving a figure of 20% for the greater oxidising power of the Ce^{4+} sample. If the two results are averaged, a figure of 23% is obtained.

If Figure 5.19 is inspected, a 22.6 % 'initial' drop in absorbance for a 7.5 :1 ratio can be seen. This is almost identical to the reduction in oxidising power of the Ce^{4+} /CALIX mixture, suggesting that the fast initial reaction (Reaction A) is a fast oxidation reaction.

FIGURE 5.19

Graph showing the relationship between the initial absorbance drop (Reaction A) and the Ce(IV) : CALIX (benzene repeat unit) ratio
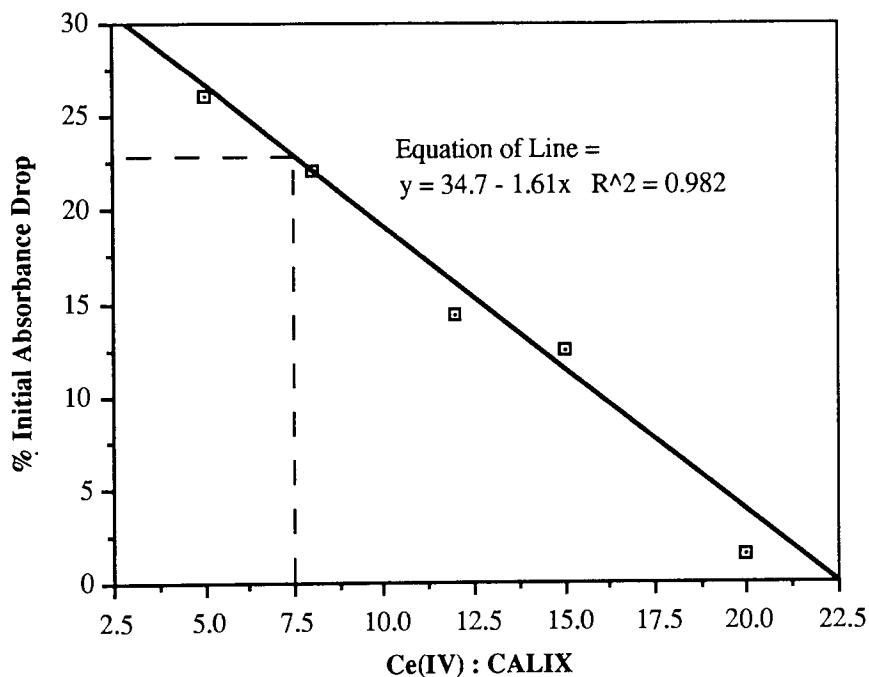
5.1.4.2.6 Conclusions

The results described and interpreted in Sections 5.1.4.2.1 to 5.1.4.2.3 suggest that the initial Ce^{4+} / CALIX reaction is a complexation whilst Sections 5.1.4.2.4 and 5.1.4.2.5 suggest that the initial Ce^{4+} /CALIX reaction involves a rapid oxidation of the CALIX. These results at first sight seem to contradict each other. However, on further consideration, these results may not

The results of Sections 5.1.4.2.4 and 5.1.4.2.5 may be interpreted as the coordinated ligand in a Ce^{4+} / CALIX complex masking the effect of the Ce^{4+} ion i.e., the E^o of the Ce^{4+} is reduced to a point where it will no longer oxidise Fe^{2+} to Fe^{3+}.

There are three reasons that make this suggestion seem likely.

1) The experimental results in Sections 5.1.4.2.1 to 5.1.4.2.3 strongly suggest that an equilibrium has been set up.

2) Oxidation of organic molecules is generally a slow process (because it is an inner sphere reaction), and it is difficult to imagine a 2 e⁻ oxidation of CALIX occurring in milliseconds.

3) If oxidation were occurring then it would be expected that the loss of Ce^{4+} would be stoichiometric i.e. 2 Ce^{4+} per CALIX. However, the loss of Ce^{4+} can be seen to be directly related to the Ce^{4+} / CALIX ratio (Figure 5.19).

5.1.4.3 Investigation of the Slow Absorbance Drop (Figure 5.15, Reaction B)

This reaction was studied in the absence of light (the 'dark reaction'), and also in the presence of intense UV light, in the UV photochemical reactor.

5.1.4.3.1 The Dark Reactions of the Ce(IV) / CALIX System

Two series of experiments were carried out on the Ce^{4+} / CALIX dark system. In the first series of experiments the [CALIX] was varied while the [Ce^{4+}] remained the same. In the second series of experiments the [Ce^{4+}] was varied while the [CALIX] remained at the same level.

A mechanism was developed to describe the observed behaviour of the slow [Ce^{4+}] drop in the Ce^{4+} / CALIX system.

5.1.4.3.2 Suggested Mechanism for the Ce(IV) / CALIX Reaction (Dark, Reaction B)

If k_3 is very fast (see Figure 5.16) as might be expected for an organic radical reaction, then

$$\frac{d}{dt}[Ce^{3+}] = 2k_2[complex] = 2k_2c$$

However, we know (see Section 5.1.4.2) that

$$c = \frac{K_1 mr}{1 + K_1(m + r)}$$

Because we are now dealing with conditions that change with time we need to amend our nomenclature slightly from that used above by using m for initial $[Ce^{4+}]$ and m_t for total $[Ce^{4+}]$ at t.

Thus

$$m = [Ce^{4+}] + [Complex] + [Ce^{3+}]$$

and therefore

$$m = m_t + [Ce^{3+}]$$

$$m_t = m - [Ce^{3+}]$$

but we know that

$$\frac{d}{dt}[Ce^{3+}] = 2k_2 c = \frac{2K_1 k_2 m_t r}{1 + K_1(m_t + r)}$$

Substituting,

$$-\frac{d\left\{m - [Ce^{3+}]\right\}}{dt} = \frac{2K_1 k_2 r \left\{m - [Ce^{3+}]\right\}}{1 + K_1 r + K_1 \left\{m - [Ce^{3+}]\right\}}$$

All experimental data were obtained for experiments with m/r > 2, and only the early stages of Ce^{4+} reduction were monitored. Therefore it is possible to assume that the $[Ce^{3+}]$ containing term in the denominator is negligible compared to the other terms. This allows us to use a simple first order rate equation

$$-\frac{d[Ce^{4+}]}{dt} = k_{obs}[Ce^{4+}]$$

where

$$k_{obs} = \frac{2K_1 k_2 r}{1 + K_1(m + r)}$$

When plotting graphs of experimental data, the relationships will be as follows.

1) When [repeat unit] is constant, but [Ce]$_0$ varies, i.e 'r' is constant, 'm' varies (see Figure 5.20)

$$\frac{1}{k_{obs}} = \left(\frac{1 + K_1 r}{2 K_1 k_2} \right) + \left(\frac{1}{2 k_2} \right) \frac{m}{r}$$

i.e., 1 / k$_{obs}$ will vary linearly with m

2) When [Ce]$_0$ is constant, but [repeat unit] varies, i.e 'm' is constant, 'r' varies (see Figure 5.22)

$$\frac{1}{k_{obs}} = \left(\frac{1}{2 k_2} \right) + \left(\frac{1 + K_1 m}{2 K_1 k_2 m} \right) \frac{m}{r}$$

i.e., 1 / k$_{obs}$ will vary linearly with 1 / r

5.1.4.3.3 Ce(IV) Concentration Variable, CALIX Repeat Unit Concentration Constant (6.655 x 10^{-4}M)

FIGURE 5.20

Graph showing the relationship of the logarithm of the [Ce(IV)] to the time of reaction for various ratios of Ce(IV) : CALIX (benzene repeat unit) ([Ce(IV)] variable)

Initial Ce(IV) : CALIX repeat unit ratio

▣	15:1
◆	12:1
✕	8:1
■	5:1
✛	2:1
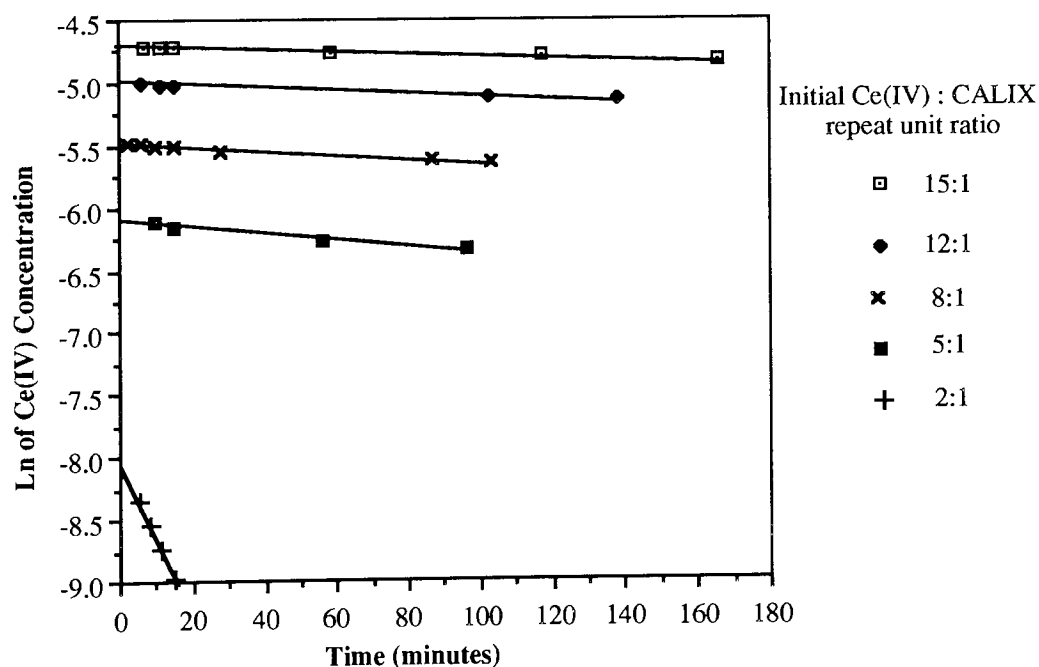
TABLE 5.5

GRADIENTS AND INTERCEPTS ON THE Y AXIS FOR VARIOUS CE(IV) : CALIX RATIOS, [CE(IV)] VARIABLE

Ce(IV) : CALIX repeat unit (mole / mole)	Ce(IV) ion : CALIX repeat unit ratio	Rate of reaction (min^{-1})	Intercept on y axis
$1.00 \times 10^{-2} : 6.55 \times 10^{-4}$	15 :1	7.45×10^{-4}	-4.71
$8.00 \times 10^{-3} : 6.55 \times 10^{-4}$	12 : 1	9.60×10^{-4}	-5.00
$5.33 \times 10^{-3} : 6.55 \times 10^{-4}$	8 : 1	1.56×10^{-3}	-5.48
$3.33 \times 10^{-3} : 6.55 \times 10^{-4}$	5 : 1	2.51×10^{-3}	-6.11
$1.33 \times 10^{-3} : 6.55 \times 10^{-4}$	2 : 1	6.52×10^{-2}	-8.02

FIGURE 5.21

Graph showing the relationship between the Ce(IV) : CALIX (benzene repeat unit) ratio and the rate of reaction for the Ce(IV) / CALIX system, [Ce(IV)] variable

Equation of line =
$y = -151 + 98x$ $R^2 = 0.997$

(x-axis) $\dfrac{[\,Ce(IV)\,]}{[\,Repeat\ Unit\,]}$

(y-axis) Reciprical of the rate of reaction
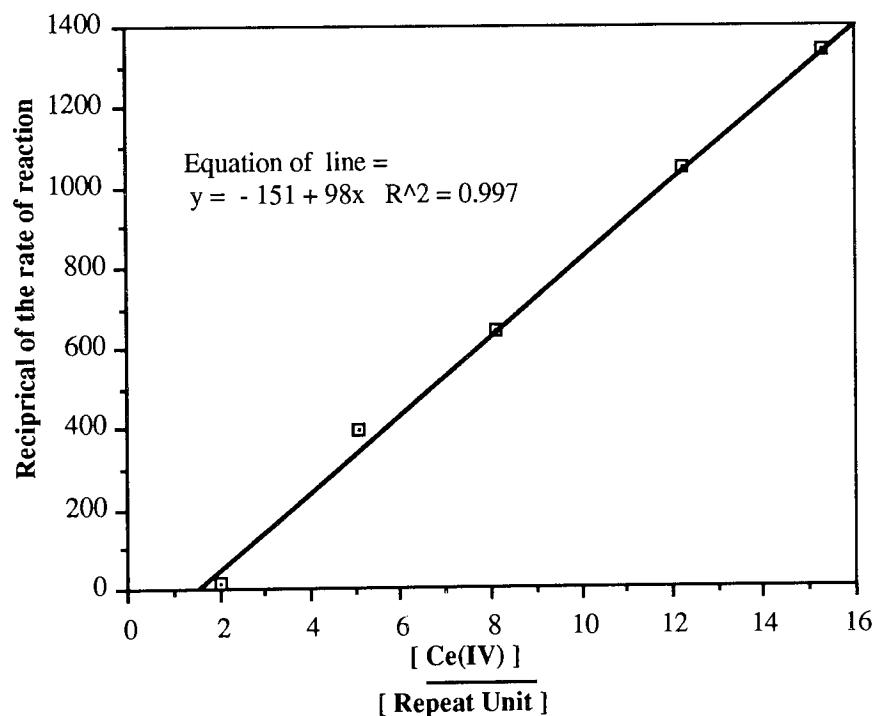
FIGURE 5.22

Graph showing the relationship of the logarithm of the [Ce(IV)] to the time of reaction for various ratios of Ce(IV) : CALIX (benzene repeat unit) ([CALIX] variable)
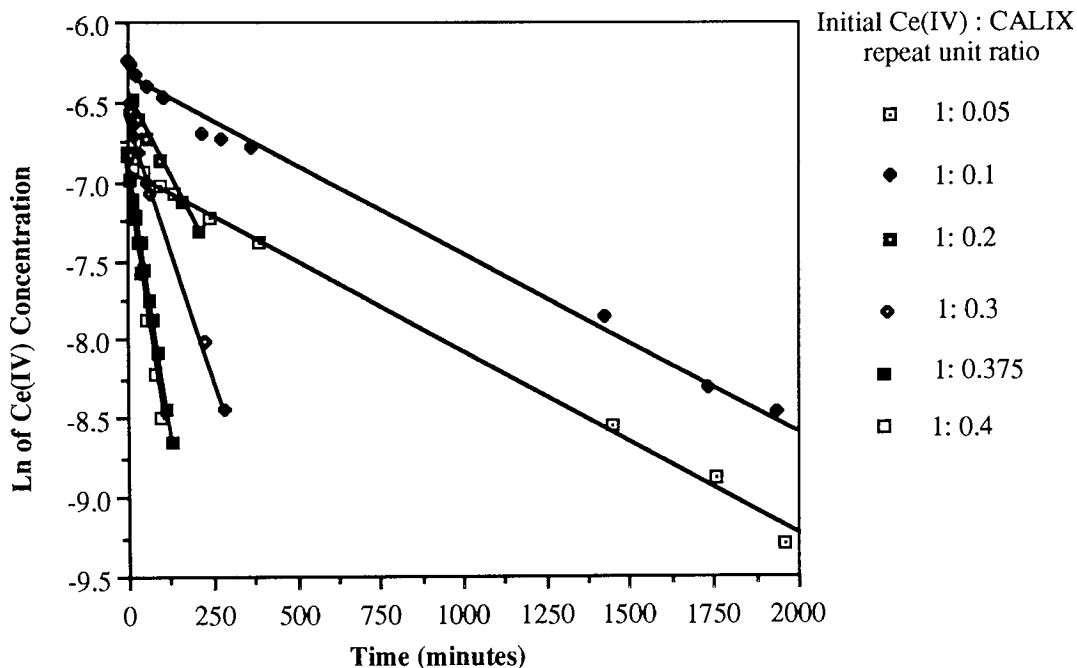
TABLE 5.6

GRADIENTS AND INTERCEPTS ON THE Y AXIS FOR VARIOUS CE(IV) : CALIX RATIOS, [CALIX] VARIABLE

Ce(IV) : CALIX repeat unit (mole / mole)	Ce(IV) ion : CALIX repeat unit ratio	Rate of reaction (min $^{-1}$)	Intercept on y axis
3.33 x 10^{-3} : 1.66 x 10^{-4}	1 : 0.05	1.18 x 10^{-3}	-6.88
3.33 x 10^{-3} : 3.33 x 10^{-4}	1 : 0.1	1.11 x 10^{-3}	-6.34
3.33 x 10^{-3} : 6.66 x 10^{-4}	1 : 0.2	4.06 x 10^{-3}	-6.47
3.33 x 10^{-3} : 1.00 x 10^{-4}	1 : 0.3	6.61 x 10^{-3}	-6.56
3.33 x 10^{-3} : 1.25 x 10^{-3}	1 : 0.375	1.37 x 10^{-2}	-6.85
3.33 x 10^{-3} : 1.33 x 10^{-3}	1 : 0.4	1.64 x 10^{-2}	-6.87

FIGURE 5.23

Graph showing the relationship between the Ce(IV) : CALIX (benzene repeat unit) ratio and the rate of reaction for the Ce(IV) / CALIX system, [CALIX] variable
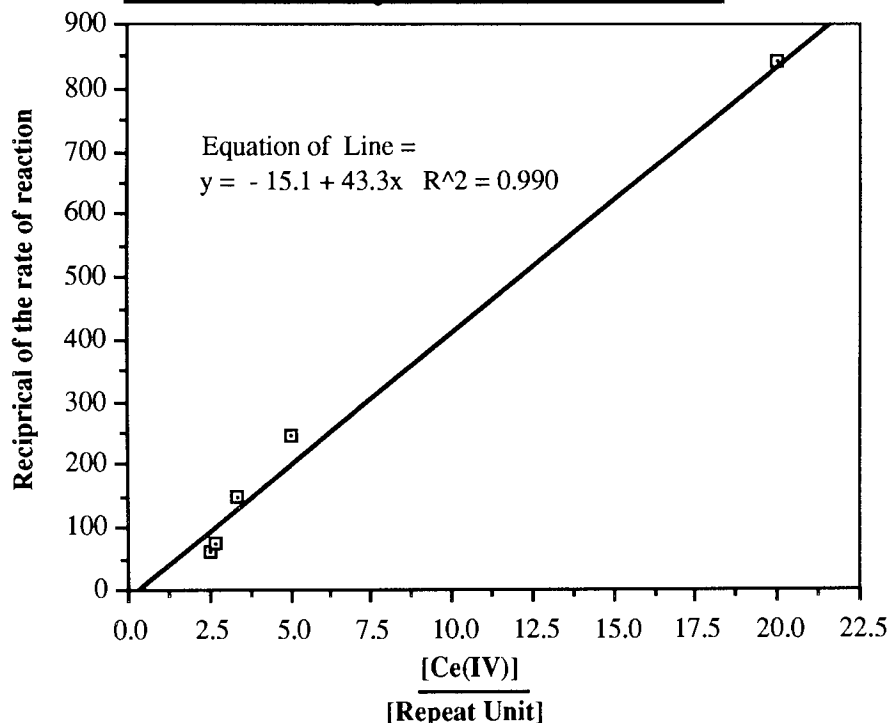
5.1.4.3.5 Calculation of the Rate Constant k_2 from Experimental Data Shown in Figures 5.21 and 5.23

[CALIX Repeat Unit] Constant (Figure 5.21)

The equation for this line in this graph was shown to be

$$\frac{1}{k_{obs}} = \left(\frac{1 + K_1 r}{2 K_1 k_2}\right) + \left(\frac{1}{2 k_2}\right) \frac{m}{r}$$

where K_1 is the equilibrium constant and k_2 is the rate of reaction (see Figure 5.16 for definitions of K_1 and k_2).

The gradient of this line is

$$= \frac{1}{2 k_2} \quad (\text{units} = \text{mol. min. dm}^{-3})$$

So, substituting into this equation from Figure 5.21, we obtain

$$k_2 = \frac{1}{2 (98)} = 5.10 \times 10^{-3} \text{ dm}^3 \text{ mol}^{-1} \text{ min}^{-1}$$

144

<u>[Ce(IV)] Constant (Figure 5.23)</u>

The equation for this line in this graph was shown to be

$$\frac{1}{k_{obs}} = \left(\frac{1}{2k_2}\right) + \left(\frac{1 + K_1 m}{2K_1 k_2 m}\right)\frac{m}{r}$$

where K_1 is the equilibrium constant and k_2 is the rate of reaction (see Figure 5.16)

The intercept of this line is

$$= \frac{1}{2k_2}$$

However, when Figure 5.23 is inspected, it can be seen that the intercept on the y axis is a negative value (-15). This means that this graph cannot be used to find the rate of reaction, k_2. This negative value is probably due to experimental error (15 represents 1.7% of the maximum y axis value in Figure 5.23). Given the oversimplifications used, such as assuming that only one step was involved in the early stages, this is a reasonable set of results.

5.1.4.3.6 The UV Irradiated Reactions of the Ce(IV) / CALIX System

The experimental method used in the previous section was repeated for this series of experiments. The only change was that the Ce^{4+}/CALIX reaction solutions were continuously irradiated with UV light throughout the reaction.

5.1.4.3.7 The Mechanism of the Ce(IV) / CALIX / UV Reaction

It was observed experimentally (see Figures 5.25 and 5.27) that the pseudo first order rate constant observed obeys the relationship.

$$k \propto \frac{[Rpt\ Unit]_{t=0}}{[Ce^{4+}]^2_{t=0}}$$

A mechanism was developed to explain this relationship.

There was a large excess of Ce^{4+} in the experiments carried out. If, as before, all light incident on the reaction mixture is absorbed, it will be mainly due to the absorbance of Ce^{4+}. However, suppose that the mechanism requires UV absorption by the complex or by uncoordinated CALIX. In this case the size of the small fraction of the UV light so used will depend on the

145

relevant concentrations of the complex or uncoordinated CALIX.

If the pre-equilibrium is represented as

$$Ce^{4+} + Receptor\ Site \underset{}{\overset{K_1}{\rightleftharpoons}} Complex \quad \left[\begin{array}{l} where\ \underline{m = constant} \\ \underline{K_1 = As\ in\ Previous\ Sections} \end{array} \right]$$
$$\quad m \qquad (r - c) \qquad\qquad\qquad c$$
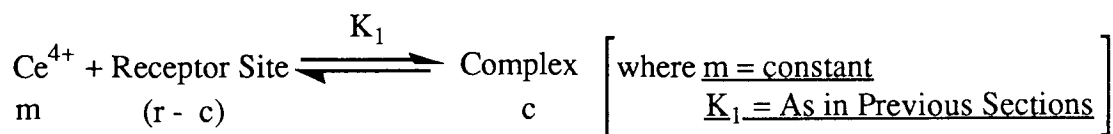
then

$$c = K_1 m(r - c)$$

Rearranging this equation,

$$c = K_1 mr - K_1 mc$$

$$c + K_1 mc = K_1 mr$$

$$c(1 + K_1 m) = K_1 mr$$

we finally reach

$$c = \frac{K_1 mr}{1 + K_1 m} \quad ------- Equation\ 1$$

It is also true that

$$r - c = \frac{c}{K_1 m}$$

Substituting and simplifying we obtain first

$$r - c = \frac{K_1 mr}{(1 + K_1 m)(K_1 m)}$$

and then

$$r - c = \frac{r}{1 + K_1 m} \quad ------- Equation\ 2$$

The equations that have been derived are for the general case of two reactants in equilibrium with a complex. However, it is often possible to use the simplifying assumption that the equilibrium is far over on one side or other of the equation.

The lower limit of K_1 was estimated to be $3 \times 10^3\ dm^3\ mol^{-1}$ in Section 5.1.4.2.4. Since the value of m is 0.01 M, the value of $K_1 m$ is therefore $>>30$. In order to simplify the following equations, we may be entitled to assume that $1 << K_1 m$, which leads to

$$c = r \qquad\qquad (from\ Equation\ 1)$$

146

$$(r - c) \cong \frac{r}{K_1 m} \qquad \text{(from Equation 2)}$$

5.1.4.3.8 A Mechanism Based on the Above Equations

If photo-excitation of uncoordinated CALIX repeat unit is occurring then we can expect the following steps to be involved, where an asterisk is used to indicate an excited state.

I have not been able to devise a totally satisfactory explanation of the observed reaction profile. The main problem is clearly that a differential equation of the form

$$-\frac{d[Ce^{4+}]}{dt} = k_{obs} \frac{[Ce^{4+}]}{[Ce^{4+}]^2{}_{t=0}}$$

is very unlikely to be a completely correct representation of a rate equation. However, there is no justification in believing that any alternative would be more trustworthy, as the pseudo-first order equation provides such a good fit for the experimental data. I am not particularly happy with the mechanism I have devised, but it produces a good fit for the experimental data available. The argument that follows gives an equation which can be simplified to the observed form.

If we have experimental conditions such that all incident radiation is absorbed, mainly by Ce^{4+}, with photochemical reaction occurring only when excitation of non-complexed repeat units occurs, i.e., a mechanistic scheme such as that shown in Figure 5.24.

FIGURE 5.24

AN OVERALL MECHANISM FOR THE CE(IV) / CALIX / UV REACTION

$$Ce^{4+} \xrightarrow{h\upsilon} {}^*Ce^{4+} \longrightarrow Ce^{4+}$$

$$R \xrightarrow{h\upsilon} {}^*R \xrightarrow{k_2} R$$

$$^*R + Ce^{4+} \xrightarrow{k_3} R^+ + Ce^{3+}$$

$$R^+ + Ce^{4+} \xrightarrow[fast]{k_4} Product + Ce^{3+}$$
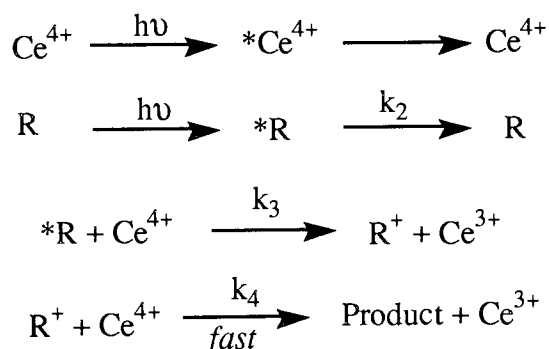
then the rate at which excited units, *R, are formed can be approximated to be

$$\approx k_0 \ \frac{\varepsilon_R \ [R]}{(\varepsilon_R \ [R] + \varepsilon_{Ce(IV)} \ [Ce^{4+}])}$$

where k_0 is the zero order rate constant for the absorption of incident radiation. As the first term in the denominator is negligible then

$$\approx \alpha \ \frac{[R]}{[Ce^{4+}]} \quad \text{where } \alpha \text{ is a constant.}$$

But we have already seen that

$$[R] = r - c = \frac{r}{K_1 m}$$

therefore the rate of formation of *R is

$$\approx \frac{\alpha \ r}{K_1 \ m^2}$$

both r and m decrease with time, and so the approximation that the rate of formation of *R is constant should hold for a considerable portion of the overall reaction. If that is so, and if the steady state hypothesis can be applied to [*R], i.e.,

$$\frac{d[*R]}{dt} = 0$$

then

$$\frac{\alpha \ r_0}{K_1 (m_0)^2} = [*R] \ (k_2 + k_3 \ [Ce^{4+}])$$

therefore

$$[*R] = \frac{\alpha \ r_0}{K_1 m_0^2 \ (k_2 + k_3 \ [Ce^{4+}]}$$

but

$$-\frac{d[Ce^{4+}]}{dt} = 2 \, k_3 [Ce^{4+}] \ [*R]$$

i.e.,

$$-\frac{d[Ce^{4+}]}{dt} = \frac{2 \, k_3 \, \alpha \ r_0 [Ce^{4+}]}{K_1 (m_0)^2 \ (k_2 + k_3 \ [Ce^{4+}])}$$

Given the additional assumption that $k_2 >> k_3$ $[Ce^{4+}]$ then we have a psuedo-first order rate equation with

$$k_{obs} = \frac{2 k_3 \alpha [Rpt]_0}{K_1 [Ce^{4+}]_0^2}$$

and, of necessity, a low quantum yield.

5.1.4.3.9 Ce(IV) Concentration Variable, CALIX Repeat Unit Concentration Constant (6.655 x 10^{-4}M) for Ratios between 2 to 1 and 15 to 1

FIGURE 5.25

Graph showing the relationship of the logarithm of the [Ce(IV)] to the time of reaction for various ratios of Ce(IV) : CALIX (benzene repeat unit) ([Ce(IV)] variable, UV Irradiated System)
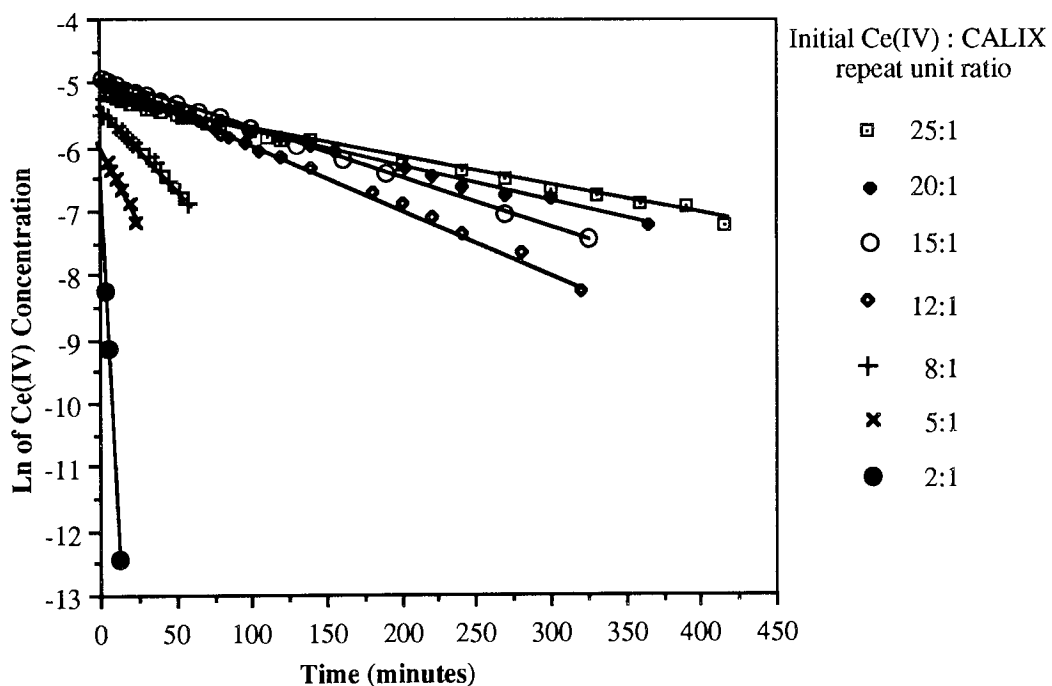
FIGURE 5.26

The first 100 minutes of four Ce(IV) : CALIX ratios, (an expansion of Figure 5.25)
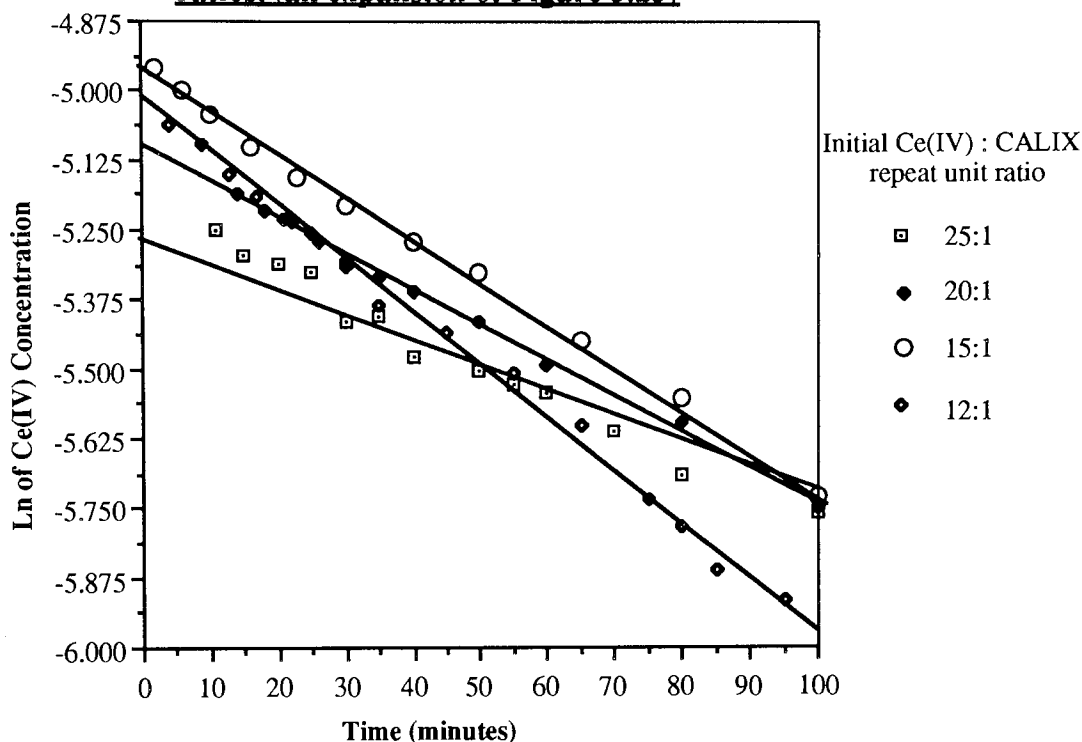
TABLE 5.7

GRADIENTS AND INTERCEPTS ON THE Y AXIS FOR VARIOUS CE(IV) : CALIX RATIOS, [CE(IV)] VARIABLE, UV IRRADIATED REACTION

Ce(IV) : CALIX repeat unit (mole / mole)	Ce(IV) ion : CALIX repeat unit ratio	Rate of reaction (min $^{-1}$)	Intercept on y axis
$1.00 \times 10^{-2} : 4.36 \times 10^{-4}$	25 : 1	4.51×10^{-3}	-5.27
$1.00 \times 10^{-2} : 5.40 \times 10^{-4}$	20 : 1	5.82×10^{-3}	-5.12
$1.00 \times 10^{-2} : 6.55 \times 10^{-4}$	15 : 1	7.61×10^{-3}	-4.96
$8.00 \times 10^{-3} : 6.55 \times 10^{-4}$	12 : 1	9.64×10^{-3}	-5.01
$5.33 \times 10^{-3}: 6.55 \times 10^{-4}$	8 : 1	2.40×10^{-2}	-5.42
$3.33 \times 10^{-3} : 6.55 \times 10^{-4}$	5 : 1	5.09×10^{-2}	-5.95
$1.33 \times 10^{-3}: 6.55 \times 10^{-4}$	2 : 1	4.70×10^{-1}	-6.81

(Different amounts of CALIX had to be used for the 20 : 1 and 25 :1 ratios, due to problems with Ce(IV) solubility in solutions more concentrated than 0.01M).

150

FIGURE 5.27

Graph showing the relationship between the CALIX : Ce(IV) ratio and rate of reaction for the Ce(IV) / CALIX / UV system, [Ce(IV)] variable

Equation of Line =
y = - 7.36e-3 + 11.0x   R^2 = 0.994
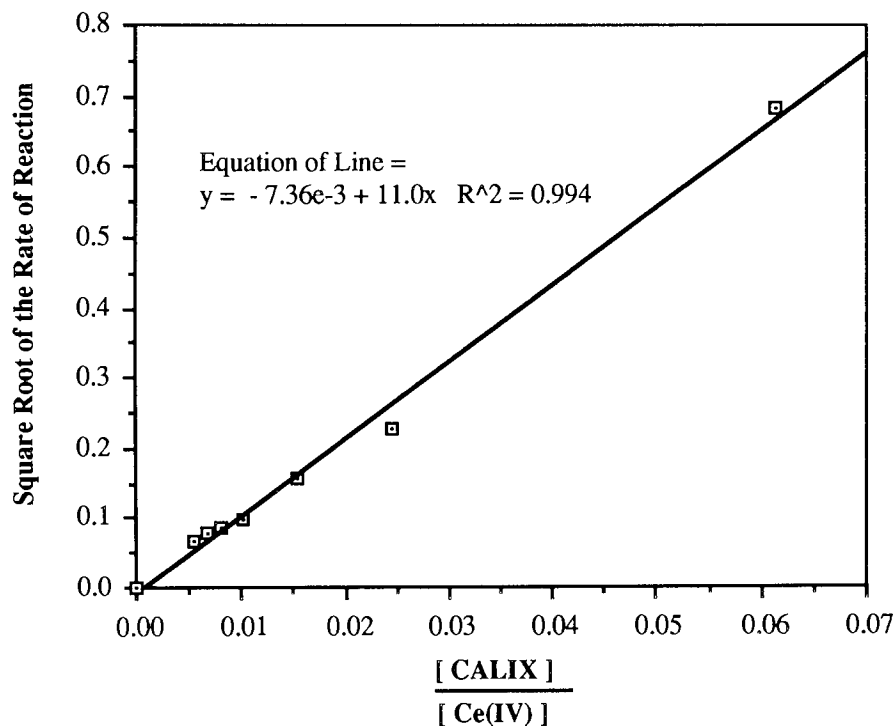
5.1.4.3.10 CALIX Concentration Variable, Ce(IV) Concentration Constant (3.33 x 10^{-3} M)

FIGURE 5.28

Graph showing the relationship of the logarithm of the [Ce(IV)] to the time of reaction for various ratios of Ce(IV) : CALIX (benzene repeat unit), [CALIX] variable, UV irradiated system

Initial Ce(IV) : CALIX
repeat unit ratio

□   1:0.4

●   1:0.2

✗   1:0.1

+   1:0.05
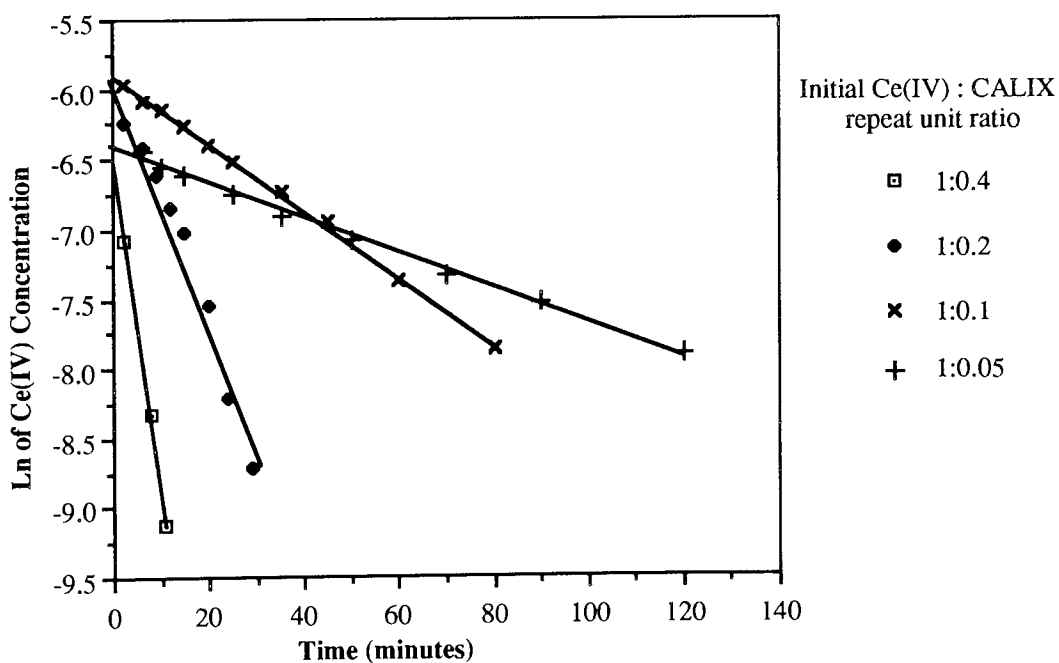
TABLE 5.8

GRADIENTS AND INTERCEPTS ON THE Y AXIS FOR

VARIOUS CE(IV) : CALIX RATIOS, [CALIX] VARIABLE,

UV IRRADIATED REACTION

Ce(IV) : CALIX repeat unit (mole / mole)	Ce(IV) ion : CALIX repeat unit ratio	Rate of reaction (min $^{-1}$)	Intercept on y axis
$3.33 \times 10^{-3} : 1.66 \times 10^{-4}$	1 : 0.05	1.25×10^{-2}	-6.43
$3.33 \times 10^{-3} : 3.33 \times 10^{-4}$	1 : 0.1	2.41×10^{-2}	-5.91
$3.33 \times 10^{-3} : 6.66 \times 10^{-4}$	1 : 0.2	9.41×10^{-2}	-5.83
$3.33 \times 10^{-3} : 1.33 \times 10^{-3}$	1 : 0.4	2.23×10^{-1}	-6.62

FIGURE 5.29

Graph showing the relationship between the CALIX : Ce(IV) ratio and rate of reaction for the Ce(IV) / CALIX / UV system, [CALIX] variable

Equation of Line =
y = - 2.84e-2 + 4.99x   R^2 = 0.993
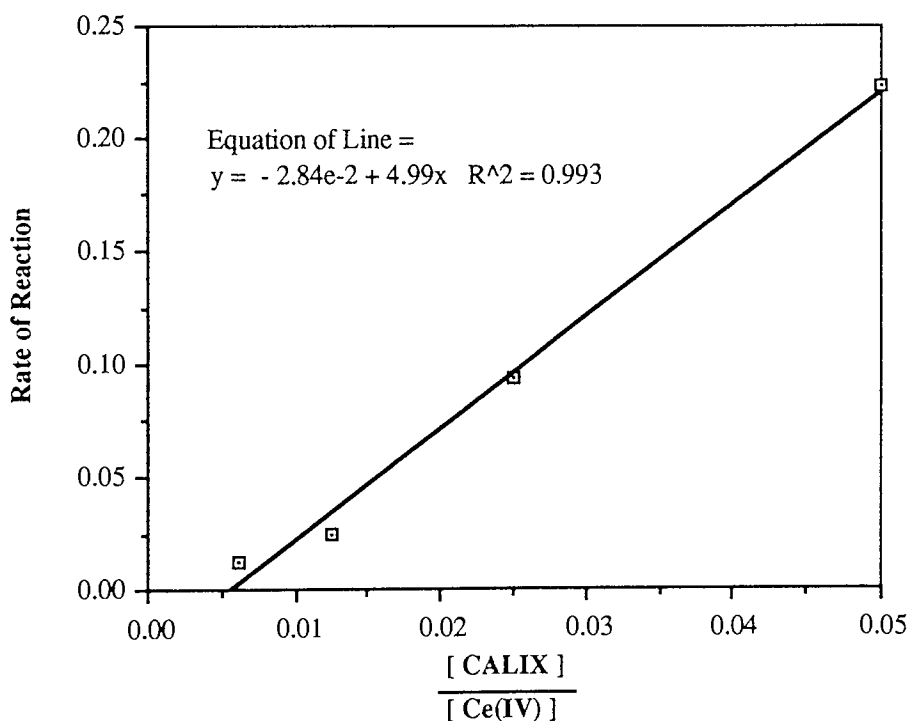
5.1.4.4 The Changes in Absorbance of the Reaction Solution after Irradiation Had Ceased

As in the Ce^{4+}/PSS system, changes in absorbance of the Ce^{4+}/CALIX system, after a minimum

absorbance value was reached, were monitored at 317 nm.

FIGURE 5.30

Graph showing the changes in absorbance at 317 nm with time in a 3 : 1 ratio Ce(IV) : CALIX system (UV Irradiated)
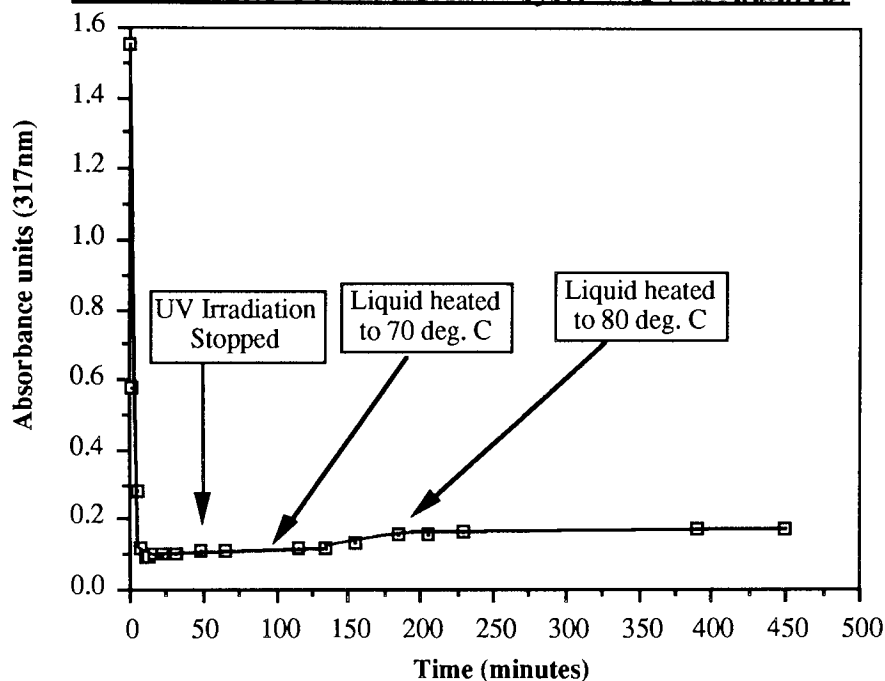
FIGURE 5.31

Graph showing the changes in absorbance at 317 nm with time in the same 3 : 1 ratio Ce(IV) : CALIX system (UV Irradiated) (expanded y axis)
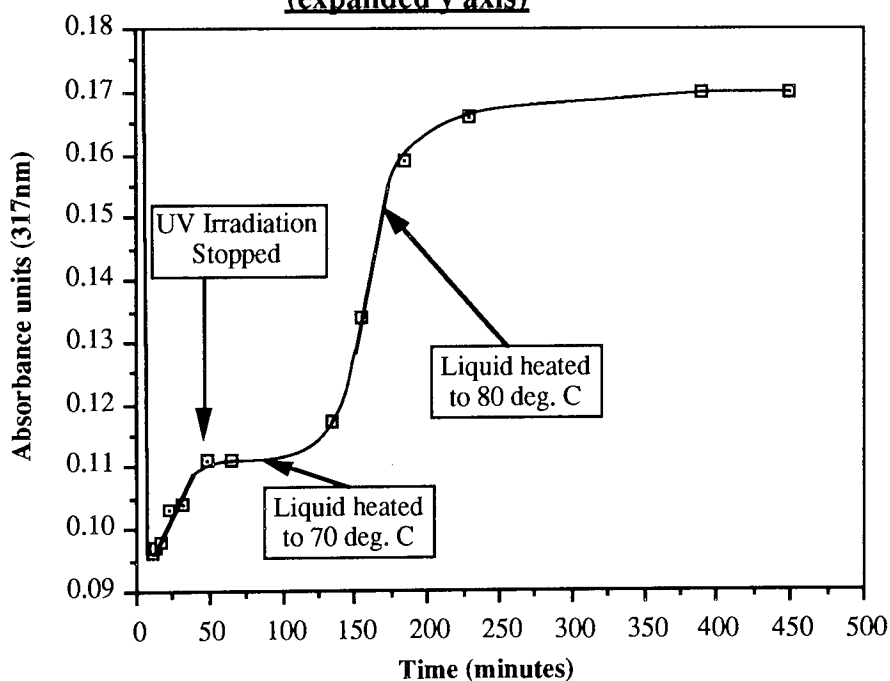
Figures 5.30 and 5.31 show that, as was seen in the Ce^{4+}/PSS system, after UV irradiation the absorbance of a Ce^{4+} / CALIX mixture at 317 nm increases from a minimum value, until a plateau is reached. It can also be seen that the rate of rise of absorbance increases when the mixture is warmed.

In this system the absorbance of the reaction mixture after irradiation reaches 0.170 about 400 minutes after the start of the reaction, 0.170 being 11% of the starting absorbance. During the initial UV irradiation it took only 4 minutes for the absorbance to fall from 0.170 to the minimum absorbance value of 0.096. It took 380 minutes for the absorbance to reach an absorbance of 0.170 again, that is, the rate of rise in absorbance is approximately 100 times slower than at the initial fall in absorbance under the influence of UV light. If the mixture had not been warmed the differential in reaction rates would have been much greater, as warming the reaction mixture increases the rate of absorbance rise.

The same two possible explanations for the rise of absorbance after irradiation, as suggested for the Ce^{4+}/PSS system, can be invoked for the Ce^{4+}/CALIX system i.e., Ce^{3+} is being oxidised to Ce^{4+}, or products of CALIX oxidation are themselves being oxidised by air. In this system it is likely that oxidation of Ce^{3+} to Ce^{4+} is the operative process. This is because CALIX, at the low concentrations used in these experiments, has a very small absorbance at all UV / Visible wavelengths, making it unlikely that any breakdown product would absorb significantly in the UV / Visible region.

5.1.5 A Summary of the Ce(IV) / Organic Substrate Reactions

I have developed various mechanistic schemes for the Ce^{4+} / 300 minutes resin solution, Ce^{4+} / PSS, and Ce^{4+} / CALIX systems. These mechanistic schemes all have their differences, but they also have their similarities. These similarities are particularly noticeable between the Ce^{4+} / resin and Ce^{4+} / CALIX systems. In these two systems a major part of the mechanism is the formation of a complex between the Ce^{4+} and organic substrate before oxidation occurs. One similarity between all 3 systems is that photoactivated Ce^{4+} ions are one of the main oxidising species. The diffences of the Ce^{4+}/PSS system from the other two systems are probably because of the large excess of reducing agent present. If lower PSS : Ce^{4+} ratios had been used then the mechanistic schemes of all 3 systems would probably have been more similar.

CHAPTER SIX

IMPROVING THE EFFICIENCY OF HYDROGEN PEROXIDE USE IN THE

FENTON'S REAGENT / ION EXCHANGE RESIN REACTION

6.0 INTRODUCTION

Some of the optimum reaction conditions for the Fenton's reagent / resin destruction reaction had already been determined by the CEGB and other workers at the start of my research project [86]. The variables that had been investigated and optimised were the initial concentration of iron catalyst, temperature, and the initial acidity level of the reaction solution. The use of various co-catalysts such as Cu^{2+} had been found to have no effect on the efficiency of the reaction. It was therefore decided to investigate the effect of other factors on reaction efficiency, such as pre-treatment of the resin, and alteration of the pH of the standard resin reaction.

6.1 Pre-Treatment of the Solid Resin

6.1.1 Boiling the Resin in Dilute Mineral Acid

Desulphonation of aromatic molecules is known to occur when a sulphonated aromatic ring is boiled in a dilute aqueous solution of mineral acid [87]. Since one of the two major monomer units of Lewatit DN is
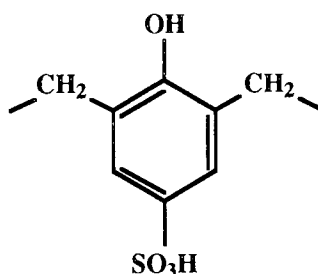
the resin was boiled in dilute acid to see if the sulphonic acid group on the benzene ring would pass into solution. Since it is known that unsulphonated, cross-linked polystyrene is unreactive to Fenton's reagent, if desulphonation of the aromatic ring in the resin occurred it would be expected that the overall efficiency of the Fenton's reagent / resin would fall [88].

6.1.1.1 The Chemistry of Desulphonation in Aqueous Solution

Many types of aromatic sulphonates are hydrolytically desulphonated by heating in an aqueous medium, as is shown by the following overall reaction.

SO$_3$H
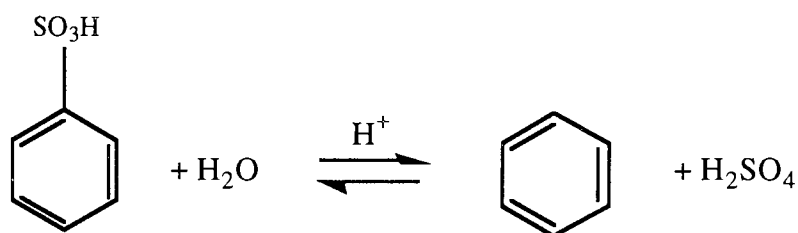
This type of reaction can proceed rapidly, particularly in the presence of a mineral acid (for example sulphuric or nitric), which catalytically accelerates the reaction [89]. Studies of the desulphonation of hydroxy-benzenesulphonic acid have shown that the rate of reaction is independent of the nature of the inorganic anion. However, the rate of reaction is proportional to the hydrogen ion activity of the solution. The reversible relation between sulphonation and desulphonation can be summarised as follows: -

$$C_6H_5SO_3^- + H_3O^+ \rightleftharpoons C_6H_6^{---}OH_2 \rightleftharpoons C_6H_6 + H_2O\text{-}SO_3$$
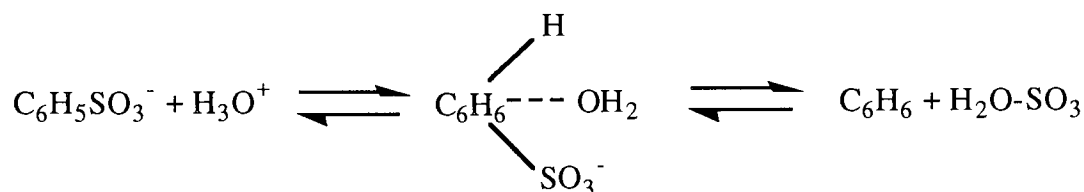
6.1.1.2 Results

Lewatit resin was boiled in distilled water, dilute H_2SO_4 and, in a final experiment, boiled in dilute HNO_3 (of equivalent [H^+] to the dilute H_2SO_4) for 8 hours. The solutions were then checked for TOC level. The relative acidity of each acid was measured before and after the resin had been boiled by titrating it with NaOH. The resin was then dried and elemental analysis for C, H, O, and S was carried out on a sample of the resin. A standard amount of Fenton's reagent was then added to a set amount of each resin sample, and the final TOC level of the solutions measured when all the H_2O_2 had been consumed.

6.1.1.2.1 TOC Level and Sulphate Level Changes

Table 6.0 summarises the results of the experiments carried out on boiling the resin in acids.

TABLE 6.0

TOC LEVEL CHANGES WHEN LEWATIT RESIN IS BOILED IN ACID AND THEN TREATED WITH FENTON'S REAGENT

Resin Type	TOC Level (ppm) - After 8 hours boiling	TOC Level (ppm) - After all H_2O_2 Consumed
Boiled in water	0	3520
Boiled in H_2SO_4	32	5150
Boiled in HNO_3	210	3690

6.1.1.2.2 Sulphuric Acid Boiled Resin

Table 6.0 shows that a very small amount of carbon is released into solution when the resin is boiled with a solution of H_2SO_4. No increase in [H^+] in the H_2SO_4 solution was seen after the resin had been boiled, suggesting that no sulphonic acid groups had been lost from the resin structure. When a standard amount of H_2O_2 was then added the final TOC level was 55% higher than when untreated resin was used indicating that a loss in efficiency in the Fenton's reagent / resin reaction has occurred.

6.1.1.2.3 Nitric Acid Boiled Resin

After boiling the resin in HNO_3 a 7-fold increase in the TOC level of the HNO_3 solution was seen, relative to the H_2SO_4 treated resin. The TOC level after Fenton's reagent addition was nearly the same for both the HNO_3 treated resin and for the untreated resin. After boiling the resin, the HNO_3 solution was titrated with NaOH. No change was seen in the acidity of the HNO_3 solution.

Elemental analysis of the resin after treatment with acid was also carried out with the results being shown in Table 6.1.

TABLE 6.1

ELEMENTAL ANALYSIS OF RESIN SAMPLES

Element, %	Water Boiled Resin	H_2SO_4 Boiled Resin	HNO_3 Boiled Resin
C	58.6	60.2	60.8
H	4.9	5	4.8
N	0.07	0.3	0.3
S	4.1	4.3	3.8
O (by difference)	32.3	30.2	30.2

The data provided by these elemental analytical tests are somewhat variable. For example C represents 58.6% of the untreated resin, and 60.8% of the HNO_3 treated resin. The C content of the resin cannot have been increased by boiling in a solution of pure acid, and in fact should have decreased due to C loss to solution. It seems likely that this result is due to a slightly higher water content in the untreated resin sent for analysis, relative to the treated resin samples.

6.1.1.3 Discussion of the Results

It seems possible that the C in the H_2SO_4 boiled resin solution is simply due to the dissolution of trace organic impurities present in the resin. This hypothesis would be supported by the similar elemental analysis results for both untreated and H_2SO_4 boiled resin. However, when the resin is boiled in HNO_3 significantly more carbon is found in solution. The TOC level of this solution represents 0.105 g of dissolved carbon, which is 2.3% of the original mass of carbon in the resin. This suggests that boiling the resin in 0.2 M HNO_3 dissolves part of the resin structure. Since nitric acid is an oxidising agent it seems likely that oxidative degradation of the resin has occurred. The elemental analytical data in Table 6.1 do show a decrease in sulphur level in the HNO_3 boiled resin, but the decrease is within experimental error.

For the H_2SO_4 treated resin, there has been a dramatic loss in efficiency in the Fenton's reagent / resin reaction. This could be explained by loss of sulphonic acid groups from the resin, a process described in Section 6.1.1. However, the elemental analytical data of resin before and

after treatment with dilute H_2SO_4 suggests that there has not been a loss of sulphonic acid groups from the resin. There was also no increase in $[H^+]$ after the resin had been boiled in dilute H_2SO_4, which is another indication that no sulphonic acid groups were lost from the resin. It seems, therefore, that the loss in efficiency in this system is not due to the loss of sulphonic acid groups from the resin, and must instead have been caused by some other factor. The loss in efficiency may instead be due to residual metal ions in the resin being leached out by the H_2SO_4 acid. This factor might result in less efficient degradation of the resin, resulting in a higher final TOC level.

6.1.2 Crushing the Resin Prior to Fenton's Reagent Addition

It has been suggested by Morioka in a recent patent that crushing the resin before H_2O_2 addition would improve the overall efficiency of the resin digestion reaction [90]. The patent suggests that crushing the ion exchange resin serves to increase the surface area, which allows the H_2O_2 to react with the resin much more efficiently than would otherwise be the case. This claim was investigated by crushing Lewatit DN and then comparing the efficiency of its degradation relative to uncrushed resin. It was recognised that a large improvement in reaction efficiency would have to be achieved for the crushing process to be economically viable due to the high cost and complexity of crushing equipment capable of dealing with radioactive materials.

6.1.2.1 Results

The resin was ground in a ball mill for 15 hours, which resulted in production of a fine powder with the particle size distribution shown in Figure 6.0 (found by using a laser particle sizer). Data from the particle sizer also indicated that the crushing process had increased the total surface area of the resin by 18 times (assuming that the resin particles before and after grinding were spheres).

FIGURE 6.0

Graph showing the particle size distribution for
Lewatit ion-exchange resin crushed in a ball mill

Centre of Size Band (microns)

136.6
98.5
74.5
57.4
44.6
34.7
27.1
21.1
16.5
13.1
10.2
8.1
6.5
2.9

0.0   2.5   5.0   7.5   10.0   12.5   15.0

Percent of Particles in Band
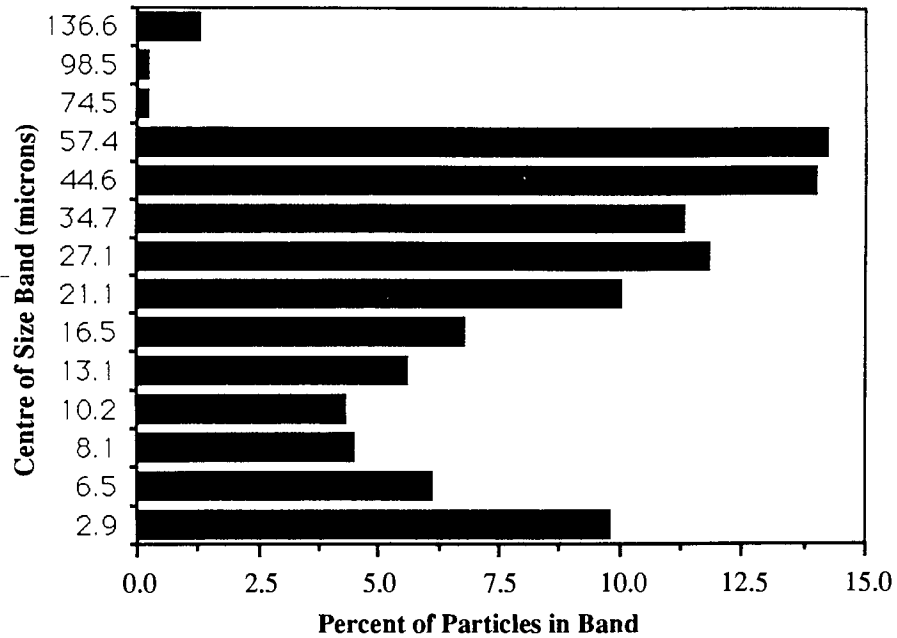
The crushed resin was also photographed at medium and high magnification with an electron microscope (resin on an aluminium base, single layer of gold sputtered on).

FIGURE 6.1

PHOTOS OF THE CRUSHED RESIN (MEDIUM AND HIGH MAGNIFICATION)

Medium Magnification
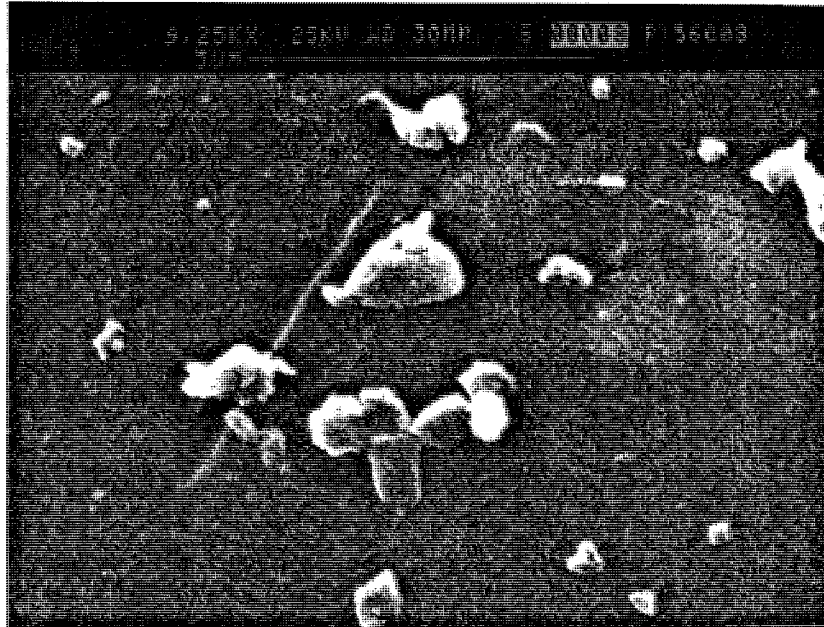
High Magnification

The crushed resin was then reacted with Fenton's reagent at 95°C, and the results compared with those for the uncrushed resin / Fenton's reagent reaction.

FIGURE 6.2

Graph showing change in organic carbon level with time, in two resin solutions

□ TOC Level (standard resin reaction)

✗ TOC Level (crushed resin reaction)
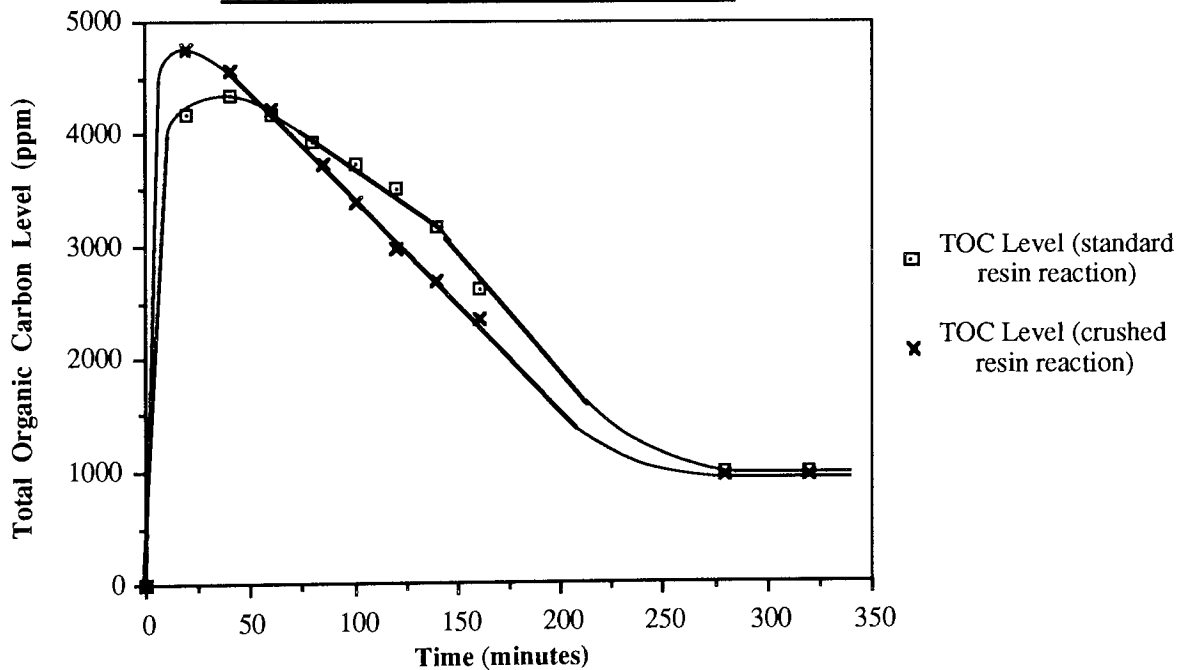
FIGURE 6.3

Graph showing change in Hydrogen Peroxide concentration with time, in two resin solutions
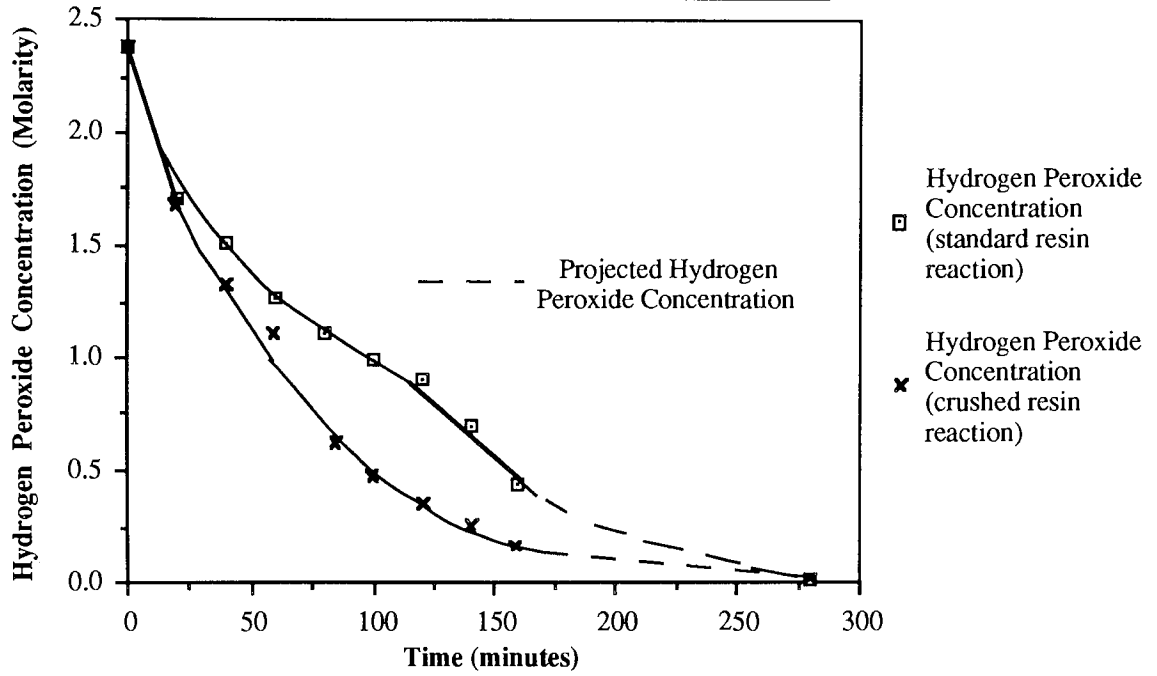
FIGURE 6.4

Graph showing the changes in apparent iron concentration with time, in two resin solutions
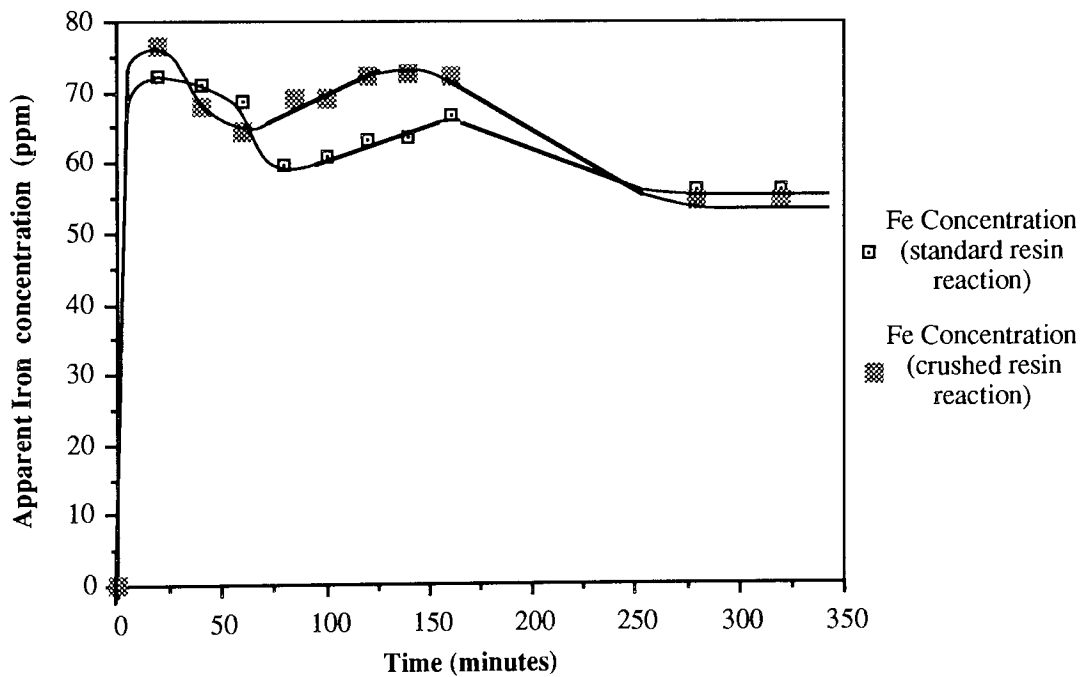
Figures 6.2 to 6.4 show the variations in TOC level, $[H_2O_2]$, and apparent [Fe] clearly. The main feature to note, in all 3 graphs, is that the changes in the 'crushed resin reaction' experimental variables lead those of the 'standard resin reaction' by several minutes for most of the reaction. The variations in the apparent [Fe] measured during both reactions are likely to be caused by the changing chemical environment of the reacting resin solution, as there is only a fixed amount of iron in solution. This hypothesis is developed further in Chapter 7, Section 7.1.2.

6.1.2.2 Discussion of the Results

The experimental data for TOC level and H_2O_2 concentration show that crushing the resin prior to H_2O_2 addition has no effect on overall efficiency of H_2O_2 usage. Although the crushed resin initially reacts faster than the uncrushed resin, by the end of the reaction a nearly identical final TOC level is reached. The faster initial reaction rate with crushed resin (about 10% faster) presumably occurs because crushing the resin creates a greater surface area and so a faster initial rate of reaction.

The lack of improvement in the efficiency of H_2O_2 utilisation might be expected, because the decrease in efficiency in the standard Fenton's reagent / resin reaction occurs only once the resin has completely dissolved (See Chapter 1, Figure 1.2). It would be difficult to propose a mechanism by which the initial particle size of the resin would effect the efficiency of the reaction once all the resin had solubilised.

6.2 Altering the Conditions in the Reaction Solution

6.2.1 Blowing Oxygen and Nitrogen Through a Reacting Resin Digestion Solution

It was decided to investigate the effects of blowing oxygen and nitrogen through the Fenton's reagent / resin solution during reaction. There were three reasons for carrying out this work.

1) Blowing a gas through the resin solution while simultaneously stirring it using a magnetic stirrer mixes the solution more thoroughly than is the case with only a magnetic stirrer. For the 'standard' reaction only magnetic stirring is used to agitate the solution.

2) It was hoped that blowing dioxygen through the resin solution would oxidise, either partially or totally, some of the organic molecules present in the solution. Nitrogen was blown through

the resin solution to check if this was happening (nitrogen would not cause any oxidation of organic molecules)

3) It is likely that any industrial size resin destruction plant would be stirred by blowing air and nitrogen through the resin solution, so it was necessary to find if blowing gas through the resin solution would make any difference to the reaction efficiency.

6.2.1.1 Results

The N_2 and O_2 were blown through a p160 sintered glass gas bubbler at a rate of 0.16 l per minute into the reacting resin solution, which was heated to 85°C (not the more normal 95°C). All other experimental parameters were identical to those of the standard resin reaction. TOC level, H_2O_2 concentration, and the absorbance of the resin solution at various visible wavelengths were monitored during the reaction, with the following graphs showing the changes that occurred.

FIGURE 6.5

Graph showing change in organic carbon level with time, in various resin solutions

Legend:
- TOC Level (Oxygen blow)
- TOC Level (Nitrogen blow)
- TOC Level (Standard)

X-axis: Time (minutes)
Y-axis: Total Organic Carbon Level (ppm)
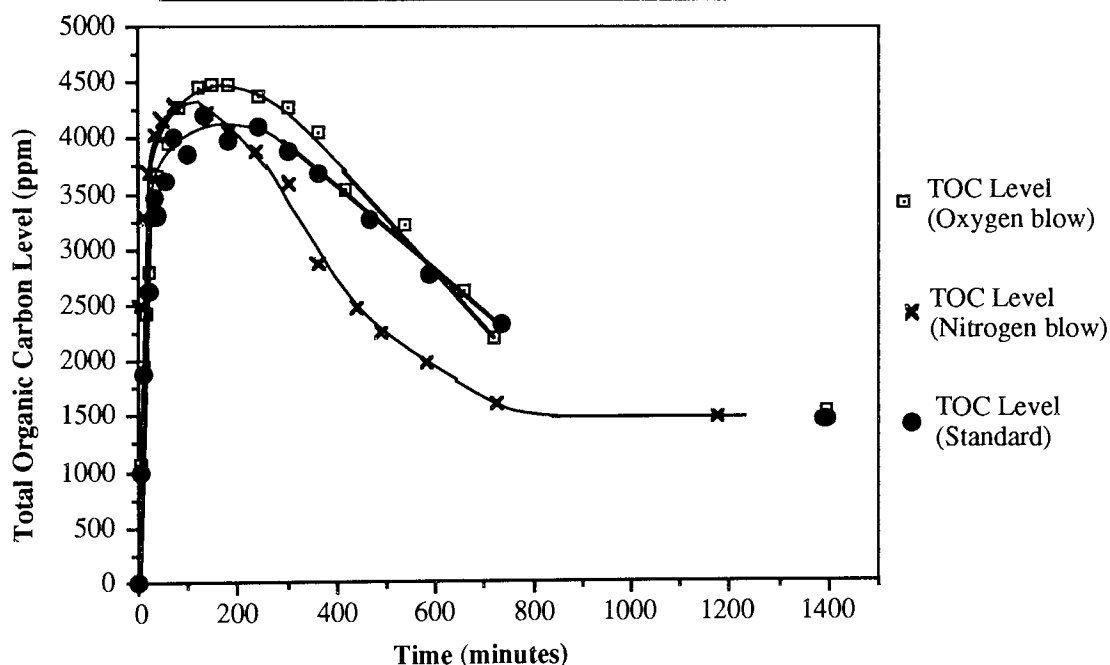
FIGURE 6.6

Graph showing changes in Hydrogen Peroxide concentration with time, in various resin solutions

Peroxide Concentration (Oxygen blow)
Peroxide Concentration (Nitrogen blow)
Peroxide Concentration (Standard)
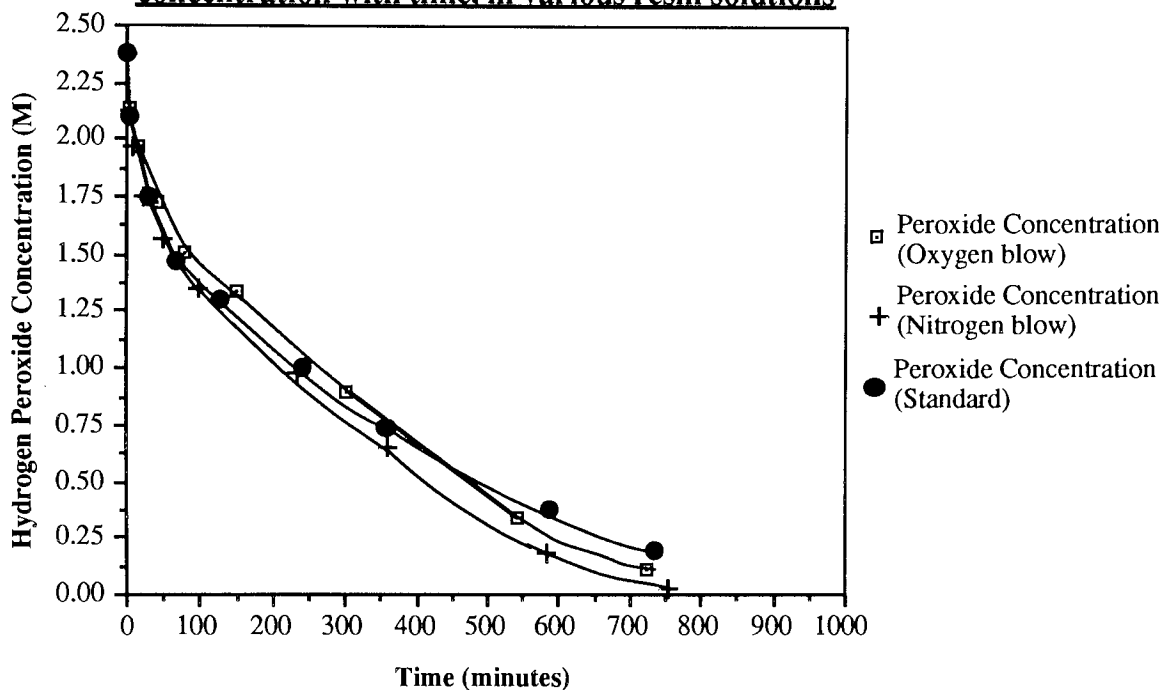
FIGURE 6.7

Graph showing change in absorbance with time measured at 450 nm in various resin solutions

Absorbance (Oxygen blow)
Absorbance (Nitrogen blow)
Absorbance (Standard)

166
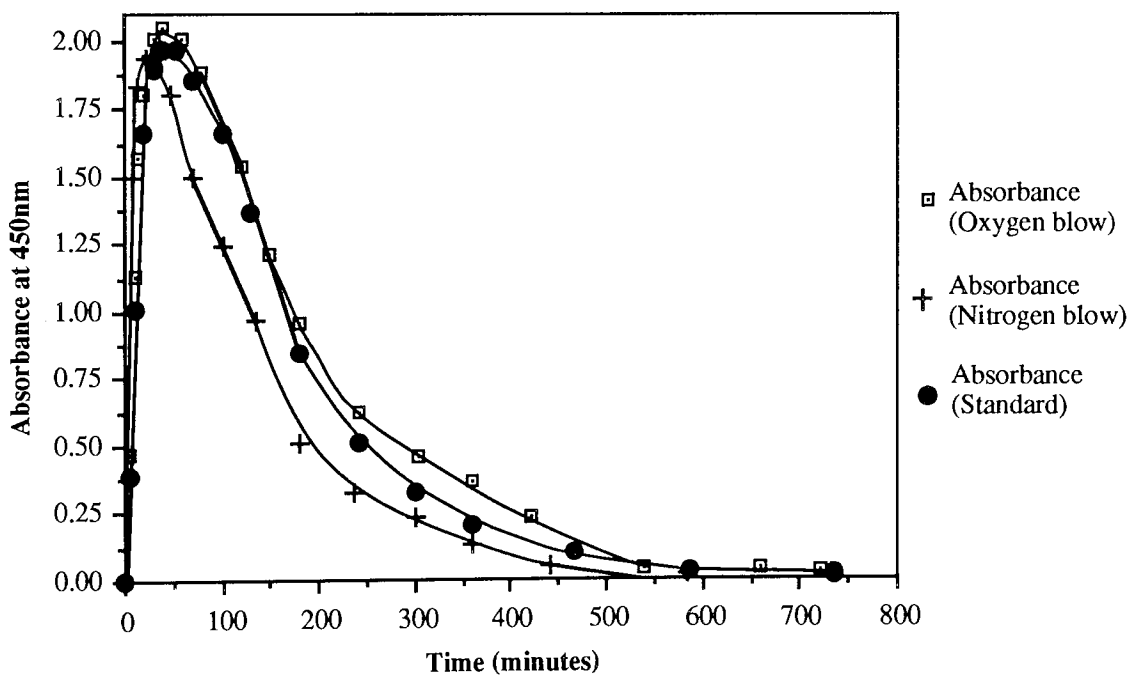
FIGURE 6.8

Graph showing change in absorbance with time measured at 500 nm in various resin solutions

Legend:
- □ Absorbance (Oxygen blow)
- + Absorbance (Nitrogen blow)
- ● Absorbance (Standard)
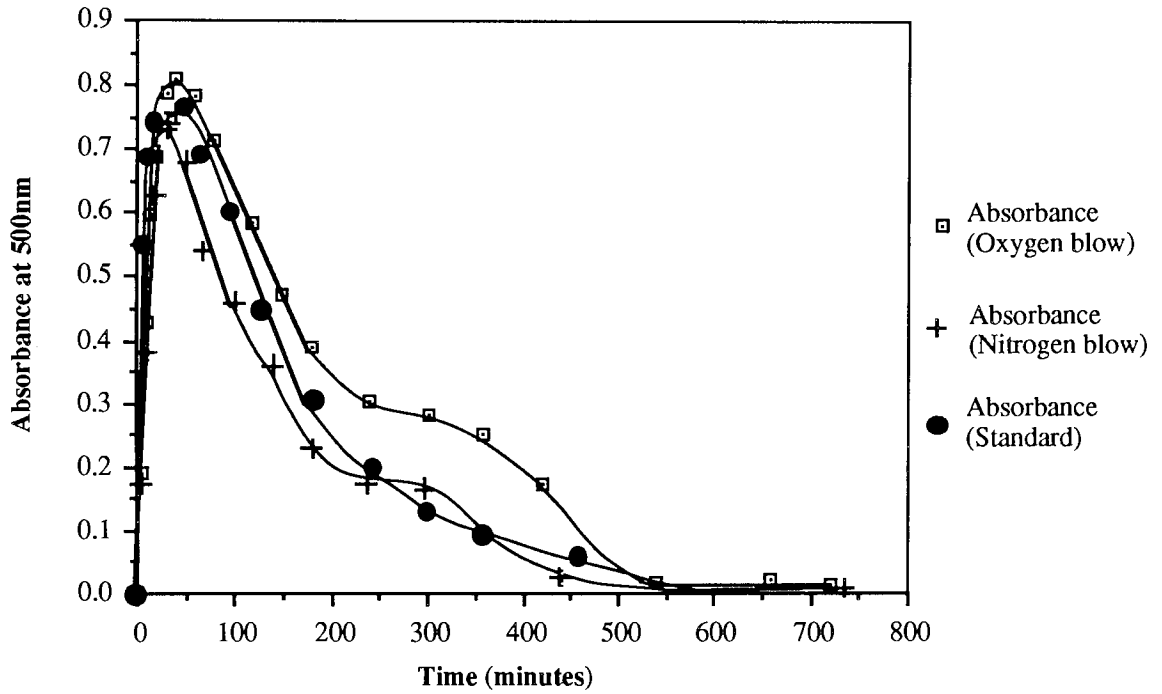
FIGURE 6.9

Graph showing change in absorbance with time measured at 550 nm in various resin solutions

Legend:
- □ Absorbance (Oxygen blow)
- + Absorbance (Nitrogen blow)
- ● Absorbance (Standard)
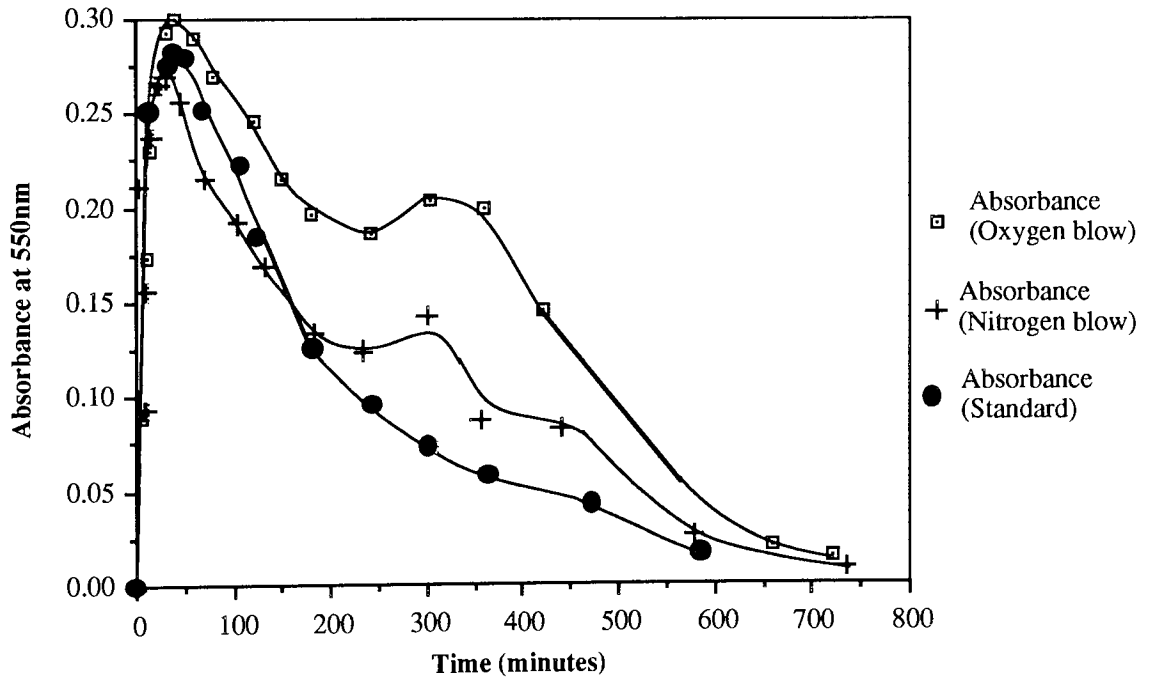
Figures 6.5 and 6.6 show that blowing O_2 or N_2 through the reaction mixture has little effect on either the final TOC level or on the way H_2O_2 concentration changes with time. However, the digestion of the resin appears to occur faster in the N_2 blown reaction. This may indicate that O_2 in solution has an inhibitory effect on the rate of the Fenton's reagent / resin reaction.

The graph for absorbance changes at 450 nm (Figure 6.7) shows little difference between the O_2, N_2 and standard reactions. However, significant differences between these 3 systems are seen when the absorbance changes are measured at 500 nm and 550 nm (Figures 6.8 and 6.9). In the O_2 and N_2 blown systems, an absorbance 'bump' over a period of around 150 minutes is seen, starting at about 300 minutes from the start of the reaction. The bump is particularly pronounced in the O_2 blown system. These 'bumps' must represent the formation of oxidised, coloured, organic molecules in solution, which are not created in equivalent concentrations in the standard reaction. The smaller 'bump' in the N_2 blown system presumably reflects the lower concentration of O_2 (and therefore lower concentration of oxidised, coloured molecules) dissolved in the reaction solution.

6.2.1.2 Discussion of the Results

These experiments indicate that blowing N_2 or O_2 through the Fenton's reagent / resin solution has no effect on the final TOC level although N_2 blown through the reaction solution may increase the rate of reaction. If N_2 is increasing the rate of reaction it must be as a result of its removal of O_2 from the reaction solution in both the standard and O_2 blown reaction. There is a large amount of O_2 in solution in the standard resin reaction due to the dissociation of H_2O_2 into H_2O and O_2.

The inhibitory effect of O_2 may be due to the scavenging of organic free radicals by O_2.

e.g.

$$R^{\bullet} + O_2 \longrightarrow RO_2$$
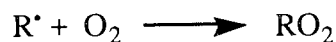
The products formed in this reaction, such as RO_2H, may themselves be more resistant to $\cdot OH$ radical radical attack, again slowing down the rate of oxidation of organic material.

6.2.2 Reducing the Concentration of Free Iron in Solution

Although the optimum starting concentration of Fe had been found in previous work at the CEGB, it was felt that altering the Fe concentration in solution after resin solubilisation had occurred might result in an increase in the overall efficiency of the reaction. This suggestion was due to the development of a hypothesis to explain the decrease in efficiency of H_2O_2 use during the reaction.

It was considered possible that this efficiency drop might be due to an increasing concentration of free $Fe^{2+/3+}$ ions in solution (as compared with $Fe^{2+/3+}$ ions complexed with organic molecules in the resin solution). These free ions would react with H_2O_2 to form ·OH radicals away from the organic molecules to be oxidised. This is in contrast with the $Fe^{2+/3+}$ ions complexed with organic molecules. Many of the ·OH radicals formed at the site of these ions would have time to attack the organic molecule before being deactivated by other processes. Thus if the concentration of free $Fe^{2+/3+}$ ions could be reduced, the relative ratio of $Fe^{2+/3+}$ ions associated with organic molecules would increase, and the efficiency of H_2O_2 usage would be increased. Work carried out by Bambrick suggested that a combination of sodium silicate and magnesium sulphate would act effectively to remove free $Fe^{2+/3+}$ ions from solution (see Table 6.2, overleaf), so an experiment using these sequestering agents was devised [91].

TABLE 6.2

EFFECT OF DIFFERENT COMBINATIONS OF CHELATING AGENTS ON THE RATE OF DECOMPOSITION OF HYDROGEN PEROXIDE IN THE PRESENCE OF IRON [91]

	Chelating Agent Concentration			Residual H_2O_2 % (hours at $60^\circ C$)				
Iron, ppm	DTPA %	Silicate %	$MgSO_4$ %	Time 0 hr	Time 0.5 hr	Time 1 hr	Time 1.5 hr	Time 2 hr
0	0.2	-	-	100	93	67	43	31
40	0.2	-	-	96	0	-	-	-
0	-	3	0.08	100	98	97	96	96
40	-	3	0.08	94	92	88	85	82
0	0.2	3	0.08	100	99	98	97	96
40	0.2	3	0.08	99	93	89	86	82

Table 6.2 shows that a solution of H_2O_2 with 40 ppm Fe dissolved in it decomposes completely to H_2O and O_2 in half an hour. In comparison, an identical solution with sodium silicate and $MgSO_4$ added as $Fe^{2+/3+}$ sequestering agents loses only 18% of the original H_2O_2 in 2 hours. The addition of DTPA to the sodium silicate and $MgSO_4$ has no effect on the concentration of H_2O_2 left after 2 hours, so it was decided not to add DTPA. The compound sodium tungsten silicate was also used, in a separate experiment, in the place of sodium silicate to find out if it increased or decreased the reaction efficiency.

FIGURE 6.10

Graph showing change in organic carbon level with time, in three different resin solutions

TOC Level
▣ (standard resin reaction)

Toc Level
✗ (Sodium silicate reaction)

Toc Level
● (Sodium tungsten silicate reaction)
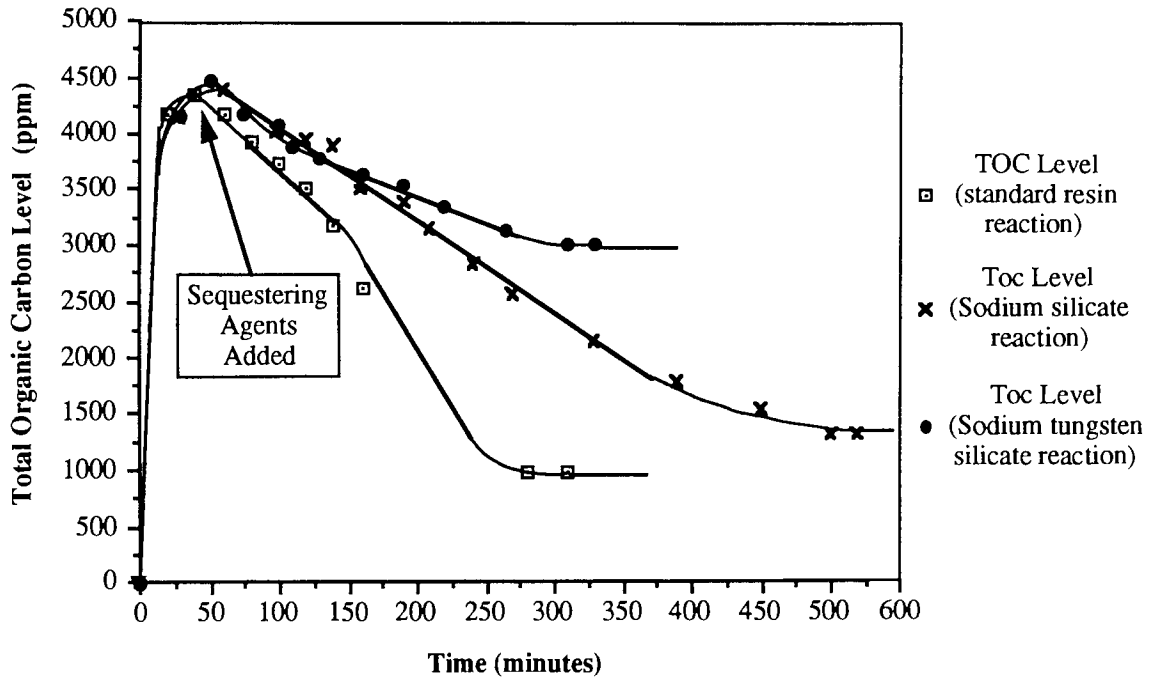
FIGURE 6.11

Graph showing change in hydrogen peroxide concentration with time, in three different resin solutions

Hydrogen Peroxide
Concentration
▣ (standard resin reaction)

Hydrogen Peroxide
Concentration
✗ (sodium silicate reaction)

Hydrogen Peroxide
Concentration
● (sodium tungsten silicate reaction)
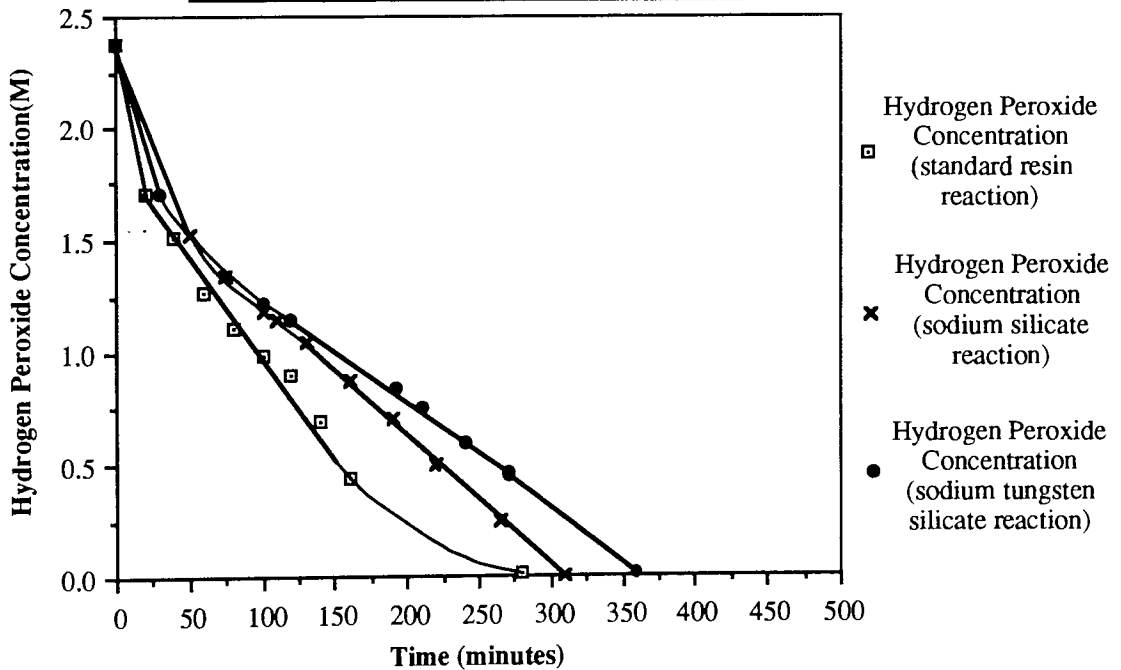
Figure 6.10 shows that, as expected, the plots of TOC level .vs. time are the same for all three solutions until the sequestering agents are added, whereupon they begin to deviate. The final TOC level for the sodium silicate reaction was found to be 34% higher than for the standard reaction, and the final TOC level for the sodium tungsten silicate reaction was found to be three times greater than that of the standard reaction (310%).

In Figure 6.11, it can be seen that the rate of H_2O_2 consumption is fastest for the standard reaction, with the sodium silicate reaction next, and the rate of consumption in the sodium tungsten silicate reaction being the slowest. These data on their own might be promising, but if these results are compared with the TOC level results it can be seen that H_2O_2 is being used much less efficiently in the sodium silicate and sodium tungsten silicate reactions.

6.2.2.2 Discussion of the Results

The results show clearly that adding sodium silicate or sodium tungsten silicate to a resin reaction solution has two effects.

1) A slight but real reduction in the rate of loss of H_2O_2 from solution. This is a good indication that these compounds are acting as sequestering agents, and reducing the concentration of free $Fe^{2+/3+}$ ions in solution. This reduction in Fe concentration would in turn be expected to slow the rate of H_2O_2 loss.

2) A large reduction in the amount of carbon removed from solution, relative to the standard reaction.

These effects can be explained by postulating the following explanation for H_2O_2 consumption in the Fenton's reagent / resin reaction.

In this system there will be at least two mechanisms by which H_2O_2 is being lost from solution, a Fe catalysed mechanism (Fenton's reagent) in which ·OH radicals are created, and also one or more non-Fe catalysed mechanism/s in which ·OH radicals are not created. Examples of such mechanisms might be thermal decomposition, or the presence of low levels of various metal ions, released into solution by degradation of the solid resin.

If the Fe catalysed mechanism is slowed by removal of some Fe ions as ·OH radical producers, then the non-Fe catalysed mechanism/s will become relatively more important. The Fe

catalysed mechanism will be slowed even more if the inorganic sequestering agents are not only removing free $Fe^{2+/3+}$ from solution, but also the $Fe^{2+/3+}$ associated with the organic molecules in solution. Thus, in a given time, a greater amount of the H_2O_2 present in solution will be wasted producing H_2O and O_2.

If the sequestering agents are removing $Fe^{2+/3+}$ from organic molecules then an efficiency gain might be obtained by using less efficient sequestering agents, that would only remove free $Fe^{2+/3+}$, and not $Fe^{2+/3+}$ associated with organic molecules.

6.2.3 Making the Resin Digestion Solution Less Acidic

During this work another hypothesis was developed to account for the fall in efficiency of hydrogen peroxide usage in the latter part of the resin digestion process.

At the start of the standard Fenton's reagent / resin reaction the pH of the mixture is about 5. However, during the reaction the pH changes dramatically, falling to a low of around 0.7 when all the resin has dissolved, and then gradually rising until the end of the reaction (see also Chapter 7, Section 7.1.6).

FIGURE 6.12

GRAPHS SHOWING CHANGES IN THE pH DURING THE FENTON'S REAGENT / RESIN REACTION

Graphs showing the changes in the pH during the Fenton's reagent / resin reaction

pH Changes During Reaction

pH Changes During Reaction (pH scale expanded)
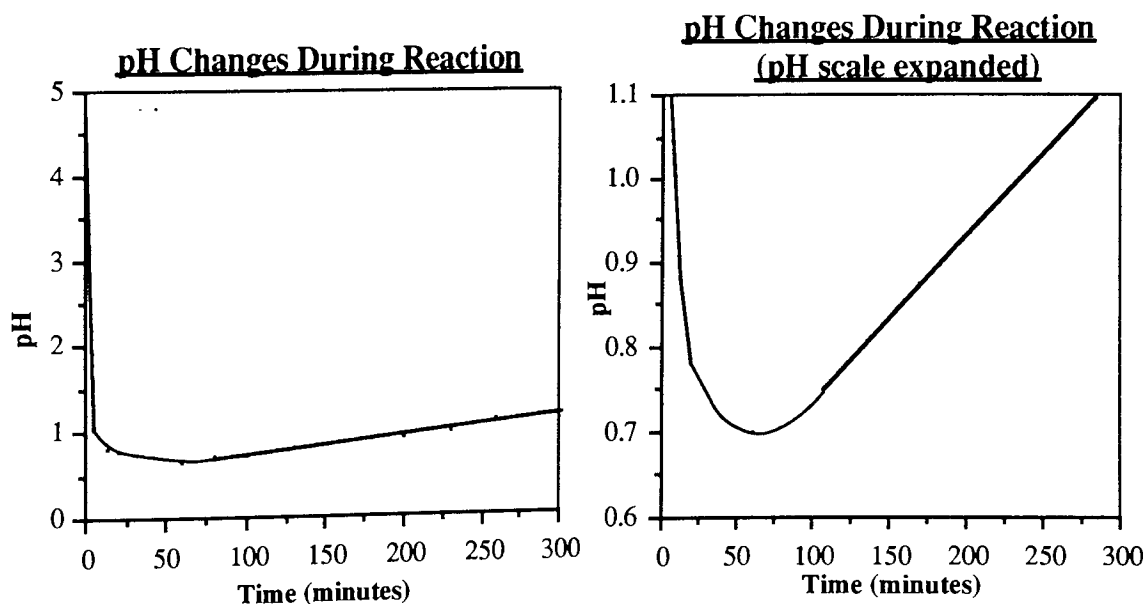
I hypothesise that it is desirable for $Fe^{2+/3+}$ ions to be close to the organic molecule so that when ·OH radicals are formed they can more readily attack the adjacent organic molecule [27]. In the resin the metal ion is mainly held at the active site of the cation exchange resin, the sulphonic acid group. As the sulphonic acid groups are converted to sulphate ions, after cleavage from the aromatic ring, H^+ ions are produced making the solution more acidic. This acidic solution would then catalyse the cleavage of more sulphonic acid groups from the organic molecules in solution (see Section 6.1.1.1). As the sulphonic acid groups are lost from the organic molecule, $Fe^{2+/3+}$ ions are also removed from the vicinity of the organic molecule. This reduces the fraction of ·OH radicals that will interact with the organic substrate.

As a consequence of this hypothesis it was suggested that if the resin reaction solution could be made more alkaline by adding NaOH, loss of sulphonic groups from organic molecules could be slowed or stopped. This would hopefully keep the $Fe^{2+/3+}$ ions close to the organic molecules in solution, thus increasing the efficiency of H_2O_2 use. However, care would have to be taken not to increase the pH of the resin reaction solution beyond about 4, because above this pH Fe^{3+} compounds start to precipitate out if they are not complexed, and the Fenton's reagent gradually becomes inactive [2].

6.2.3.1 Results

Solid NaOH was used during the reaction to adjust the pH, so as to minimise the change in volume of the reaction mixture as alkali was added. In all other respects the reaction was identical to the standard resin digestion reaction.

FIGURE 6.13

Graph showing the change in organic carbon level with time, in a standard and a NaOH adjusted resin digestion digestion reaction

Graph showing Total Organic Carbon Level (ppm) versus Time (minutes), with legend: TOC Level - in acidity adjusted resin digestion (□); TOC Level - in standard resin digestion (✗)
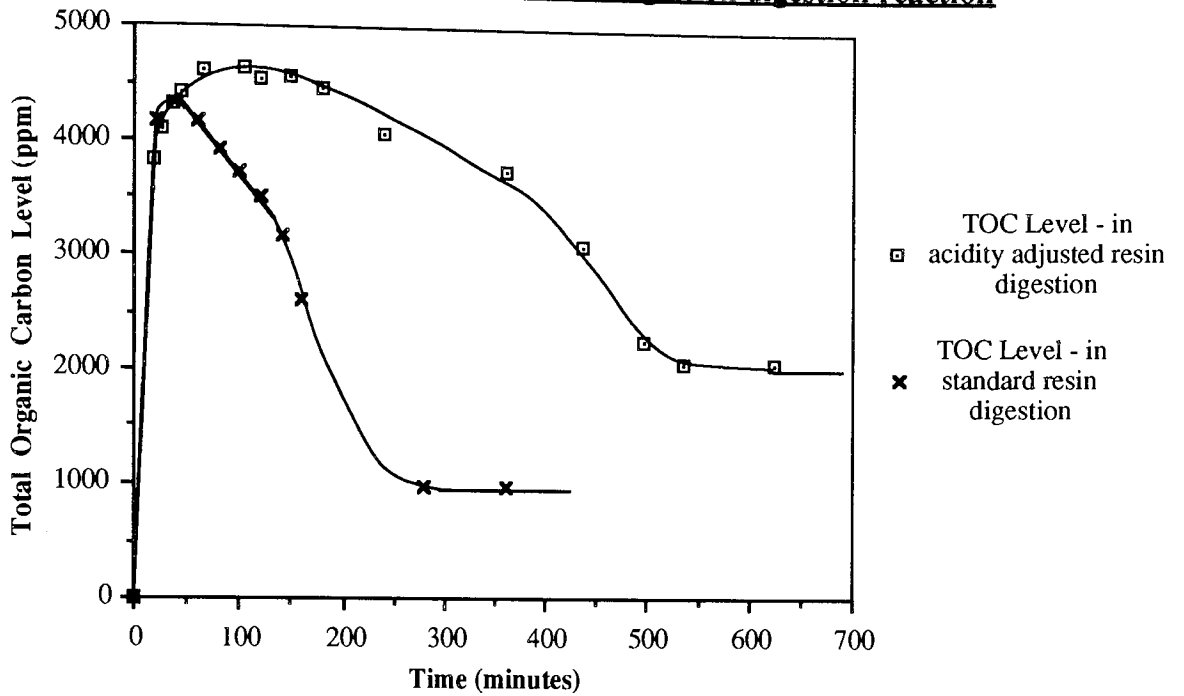
FIGURE 6.14

Graph showing the change in hydrogen peroxide concentration with time, in a standard and a NaOH adjusted resin digestion reaction

Graph showing Hydrogen Peroxide Concentration (Molarity) versus Time (minutes), with legend: Hydrogen Peroxide Concentration -in acidity adjusted resin digestion (□); Hydrogen Peroxide Concentration -in standard resin digestion (✗)
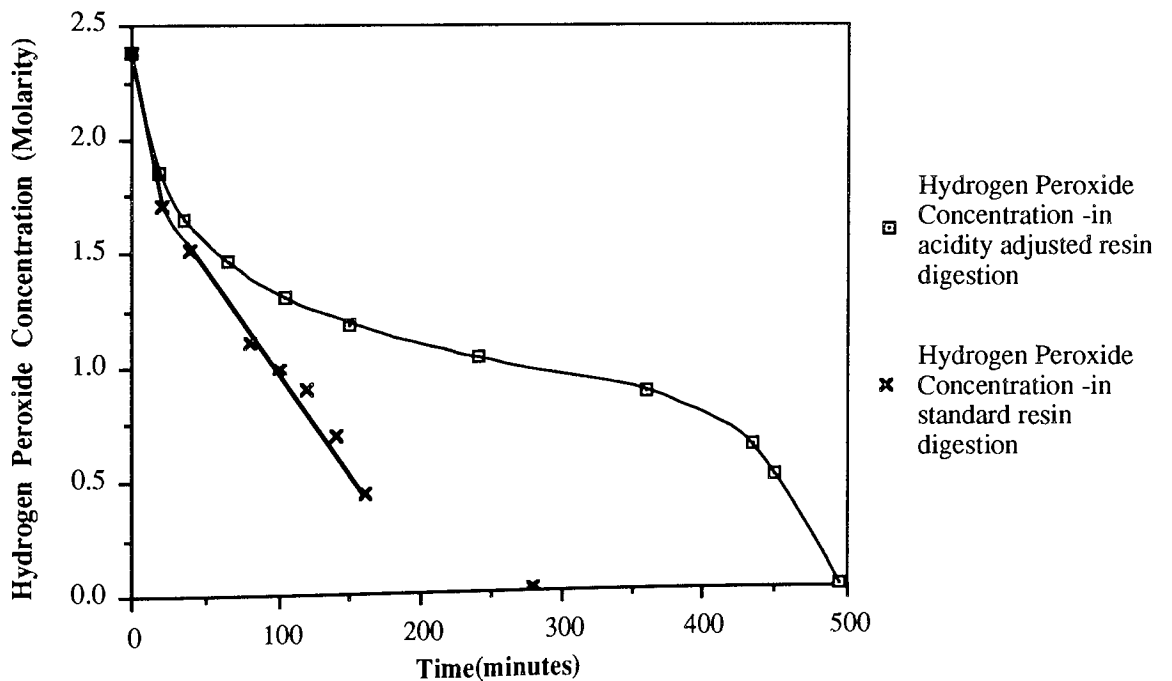
FIGURE 6.15

Graph showing the change in apparant iron concentration with
time, in a standard and a NaOH adjusted resin digestion reaction
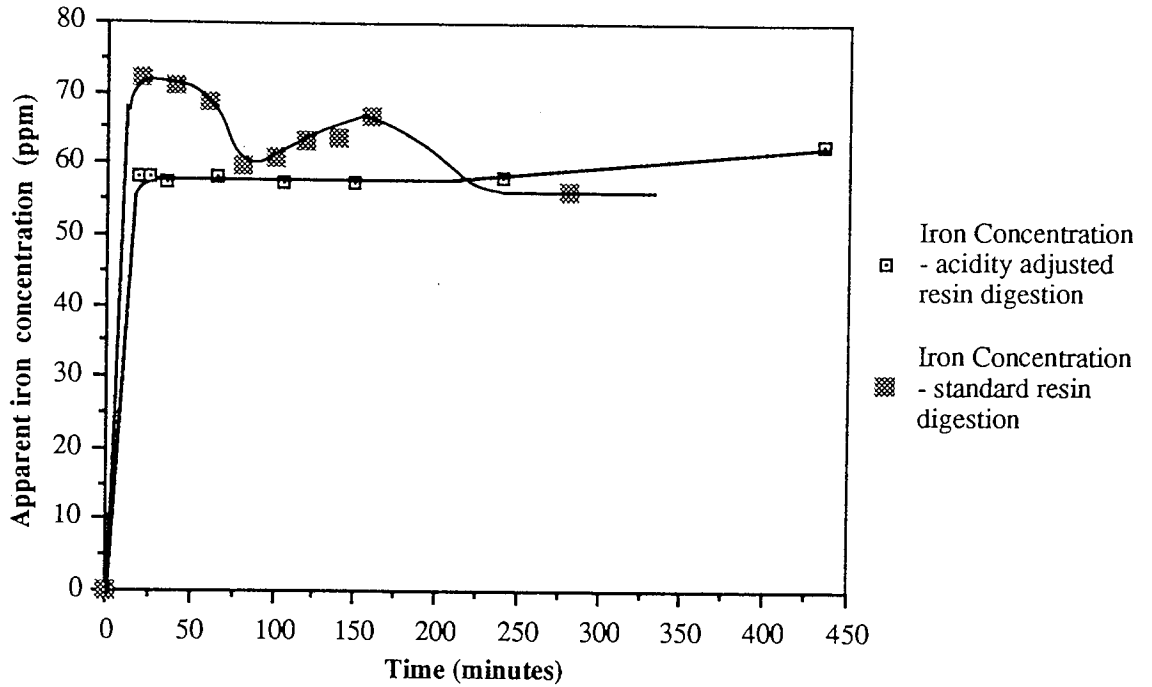
FIGURE 6.16

Graph showing the change in pH level with time, in a
standard and a NaOH adjusted resin digestion reaction

A = Intermittent NaOH addition started

B = NaOH addition halted

176
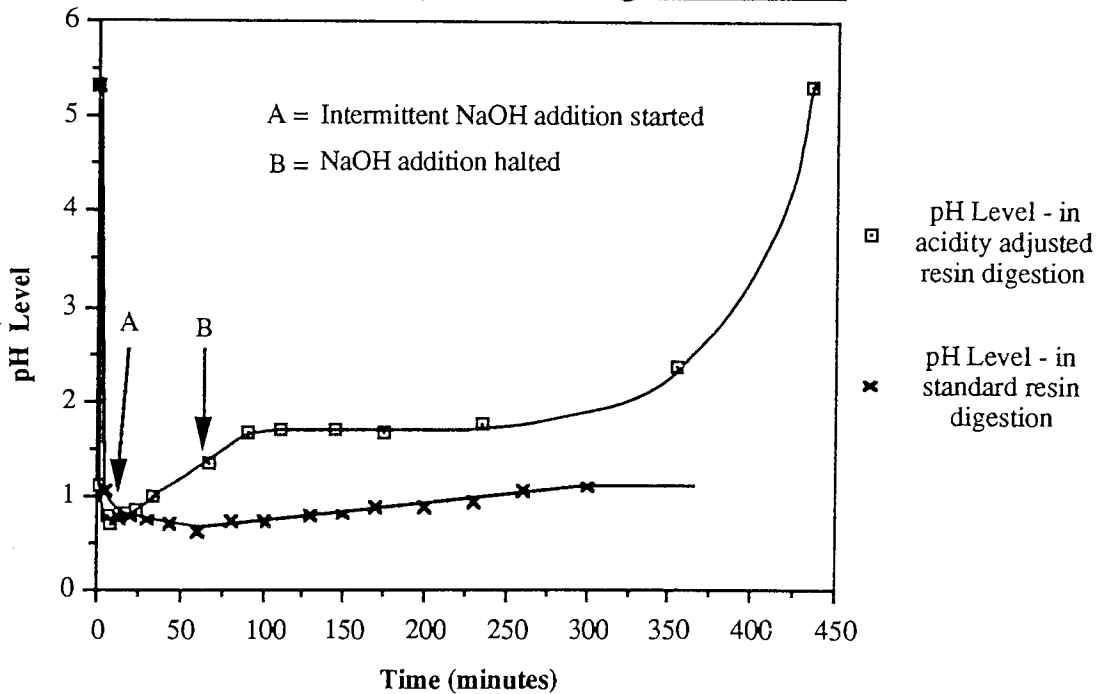
Figures 6.13 and 6.14 show that the effect of using NaOH to alter the pH of the reaction mixture is to slow and reduce the efficiency of the Fenton's reagent / resin reaction, with the final TOC level of the acidity controlled reaction being 210% higher than that of the standard reaction.

Figure 6.15 shows that the apparent Fe concentration in the acidity controlled resin reaction is

a) more stable than the standard reaction

b) lower than the standard reaction for most of the time of reaction

Since for both experiments there is only a fixed amount of Fe in solution (primarily from the Fe catalyst) the variation in apparent Fe concentration must reflect changes in the chemistry of the reaction solution, caused by the higher pH. This higher pH is likely to favour the formation of deprotonated organic ligands, which will coordinate strongly with the Fe in solution, causing the Fe AA signal to be depressed relative to uncoordinated Fe. Citric acid, for example, is known to depress an Fe AA signal by up to 50% (see also Chapter 7, Section 7.1.2).

Figure 6.16 shows that the pH levels of the respective solutions start to diverge rapidly at 25 minutes, after NaOH addition is started. This rapid divergence continues until just before 100 minutes, in spite of the fact that the NaOH addition is stopped at 75 minutes. This time lag indicates that some type of kinetically slow process is occurring in the resin digestion system. After 100 minutes the pH of the NaOH resin reaction is stable for a time, rising rapidly at the end.

6.2.3.2 Discussion of the Results

The results from this experiment show that the hypothesis that "reducing $[H^+]$ would improve the efficiency of H_2O_2 use" is incorrect, at least under the conditions used in my experiment. As the reaction mixture becomes less acidic (in the NaOH reaction) the rate of H_2O_2 loss from solution decreases but the reaction becomes more inefficient. This effect is particularly noticeable when the acidity of the reaction solution moves above pH2 at around 350 minutes from the start of the reaction. At this point the concentration of H_2O_2 in the resin reaction solution is about 0.88 M. Table 6.3 shows clearly how inefficient the NaOH resin digestion reaction becomes after this point.

TABLE 6.3

CHANGE IN TOC LEVEL FOR EQUIVALENT STARTING LEVELS

OF HYDROGEN PEROXIDE IN TWO DIFFERENT RESIN

DIGESTION SOLUTIONS

	TOC Level (ppm) -when [H_2O_2] (M) = 0.884	TOC Level (ppm)-when [H_2O_2] (M) = 0	% drop in TOC Level
Standard Resin Reaction	3470	980	70
NaOH Resin Reaction	3750	2270	40

It seems likely that the same process as described in Section 6.2.2.2 is occurring in this system. This is the process in which the rate of the iron catalysed decomposition of H_2O_2 is slowed while other H_2O_2 decomposition mechanisms are unaffected, resulting in a decrease in overall reaction efficiency i.e, as the Fenton's reagent / resin solution becomes more alkaline, the iron catalysed decomposition of H_2O_2 is slowed.

6.2.4 Making the Resin Digestion Solution More Acidic

As a result of data gathered for the previous experiment, it was noted that the pH of the resin solution affected the efficiency of the resin digestion reaction (see Section 6.2.3.2). It was therefore decided to investigate the effect of making the resin solution more acidic by the addition of concentrated H_2SO_4 just after the resin had solubilised. The pH at the point of resin solubilisation was taken as the pH to be maintained for the duration of the experiment.

FIGURE 6.17

Graph showing change in organic carbon level with time, in a standard and a sulphuric acid adjusted resin digestion reaction
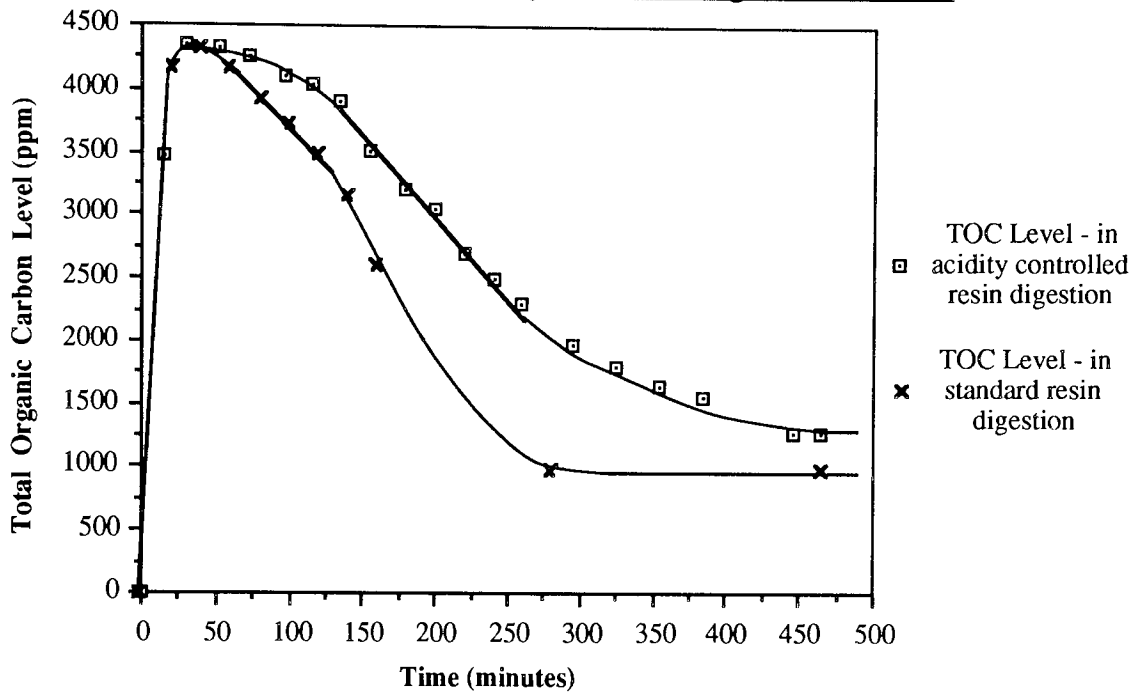
FIGURE 6.18

Graph showing change in hydrogen peroxide concentrationwith time, in a standard and a sulphuric acid adjusted resin digestion reaction
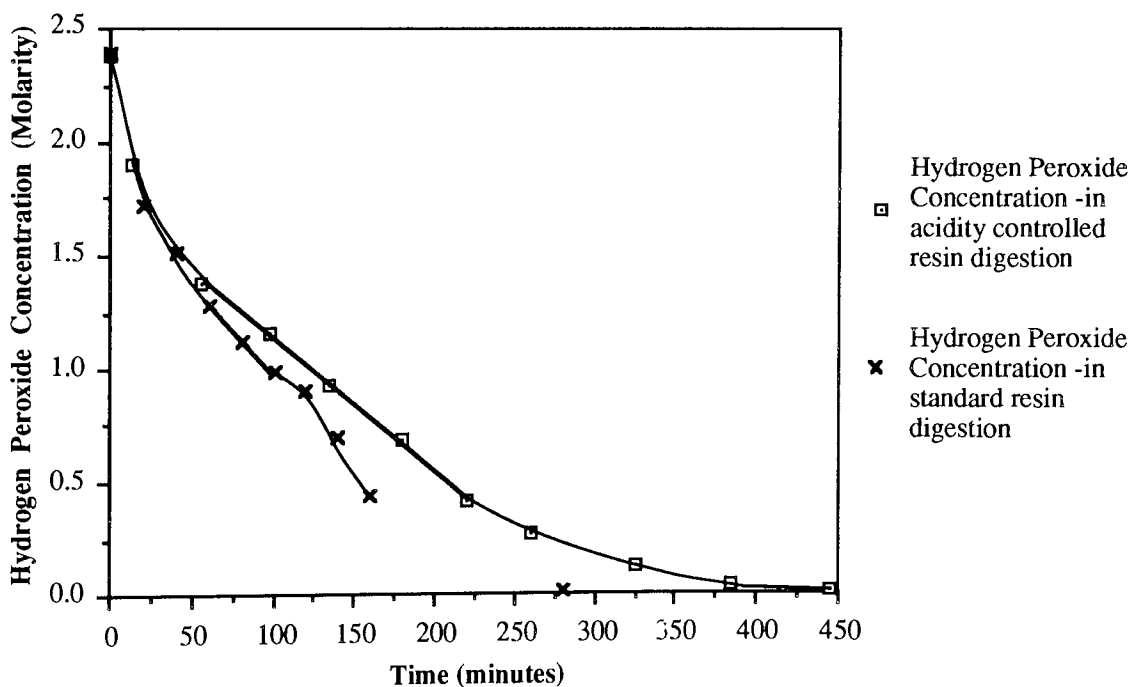
FIGURE 6.19

Graph showing change in apparent iron concentrationwith time, in a standard and a sulphuric acid adjusted resin digestion reaction

Iron Concentration
- acidity controlled
resin digestion

Iron Concentration
- standard resin
digestion
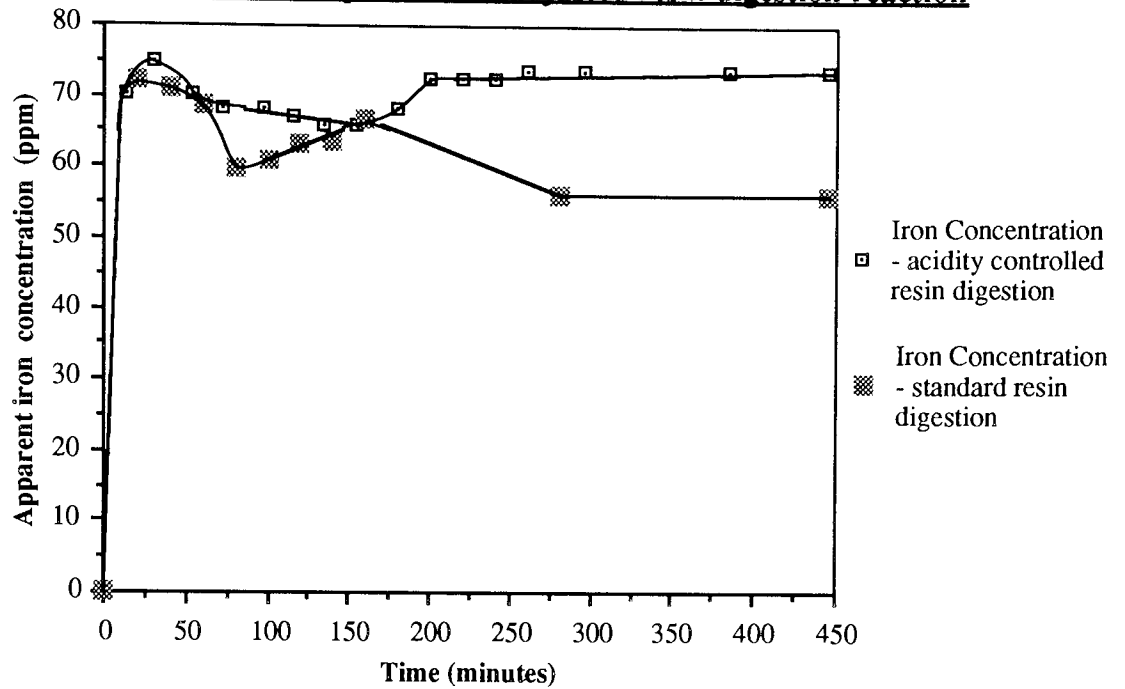
FIGURE 6.20

Graph showing change in pH Level with time, in a standard and a sulphuric acid adjusted resin digestion reaction

Intermittent Sulphuric Acid
Addition Started at 17 minutes

Sulphuric Acid
Addition Stopped

pH Level - in
acidity adjusted
resin digestion

pH Level - in
standard resin
digestion
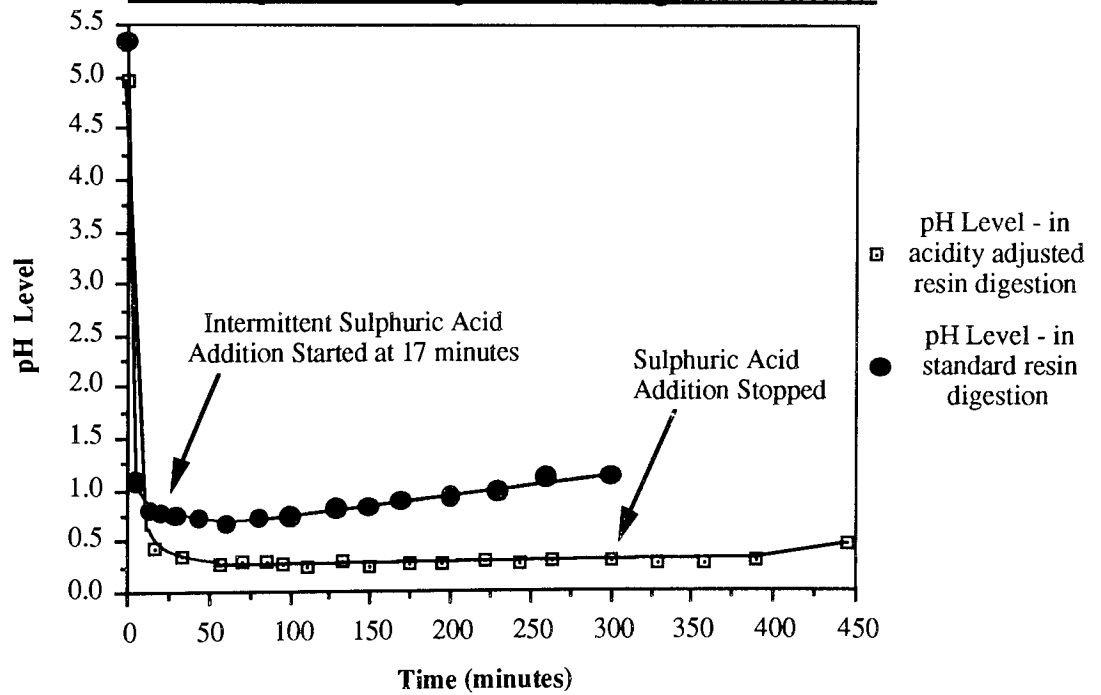
Figures 6.17 and 6.18 show that the effect of using H_2SO_4 to alter the pH of the reaction mixture is to slow and reduce the efficiency of the Fenton's reagent/resin reaction. The final TOC level of the H_2SO_4 acidity controlled reaction is 130% higher than that of the standard reaction. Figure 6.19 shows that adding acid the reaction solution has altered the pattern of apparent Fe concentration change during the reaction. This must mean that the added acid has affected the quantity and/or type of organic acids produced during the reaction (see Chapter 7, Section 7.1.2) Figure 6.20 shows that once the maximum pH level of the resin reaction solution was reached, addition of concentrated H_2SO_4, when required, maintained this pH level until just before the end of the reaction.

6.2.4.2 Discussion of the Results

It seems likely that the same process as described in Section 6.2.2.2 is occurring in this system. This is the process in which the rate of the iron catalysed decomposition of H_2O_2 is slowed while other H_2O_2 decomposition mechanisms are unaffected, resulting in a decrease in overall reaction efficiency i.e the stabilisation of the pH of the Fenton's reagent/resin solution causes the iron catalysed decomposition of H_2O_2 to slow.

6.2.5 Suggestions for Reducing the Loss of Hydrogen Peroxide in Inefficient Side Reactions

Further research would be required to understand the processes by which H_2O_2 is lost from solution. If thermal decomposition was found to be a major factor in the loss of H_2O_2, then the temperature of the reaction mixture could be altered, until the best balance of reaction efficiency .vs. rate of resin degradation was obtained. If the presence of low levels of metal ions is a major cause of H_2O_2 loss, then the possibility of using chelating agents specific for those ions could be investigated.

6.2.6 Conclusions

1) Boiling the resin in acid before addition of Fenton's reagent has no beneficial effect on overall efficiency of the resin digestion reaction.

2) Crushing the resin has no effect on the overall efficiency of the resin digestion reaction, its

only effect being to increase the initial rate of reaction.

3) Blowing O_2 or N_2 through a reacting resin digestion solution appears to have no adverse effect on the progress of the reaction. This means that air stirring is a suitable method for agitating the reaction mixture in a full scale resin destruction plant.

4) Removal of $Fe^{2+/3+}$ from the resin reaction solution reduces the efficiency of the reaction.

5) Both increasing and reducing the pH of the Fenton's reagent / resin solution, relative to that seen in the standard reaction, results in a decrease in the efficiency of H_2O_2 use.

6) If any method developed in an attempt to improve the efficiency of H_2O_2 usage slows the rate of the Fenton's reaction / resin reaction down, consideration must be given to ways of reducing the rate of decomposition of H_2O_2 in inefficient side reactions.

CHAPTER SEVEN

ANALYSIS OF THE FENTON'S

REAGENT / ION EXCHANGE RESIN REACTION

7.0 INTRODUCTION

Analytical work was carried out on the Fenton's reagent / ion exchange resin system to provide data for the efforts to find a more efficient way to use H_2O_2. This analytical work was concentrated in two main areas:-

a) Direct analysis of the various stages of the Fenton's reagent / ion exchange resin reaction.

b) Substitution of a model compound, calix[8]arene-p-octasulphonic acid (CALIX), for the ion-exchange resin in the Fenton's reagent/resin reaction. This substitution was carried out because while CALIX has a close chemical resemblance to Lewatit ion exchange resin (both have a sulphonated, phenol-formaldehyde, cross-linked structure), CALIX is soluble in water (the resin is insoluble in water). This solubility in water allows a homogeneous system to be studied from the moment of first H_2O_2 addition. There is also the advantage that the structure of CALIX is known precisely, thus aiding the subsequent interpretation of the degradation of the CALIX.

7.0.1 The Structure of Lewatit DN

FIGURE 7.0

AN IDEALISED STRUCTURE OF LEWATIT ION-EXCHANGE RESIN
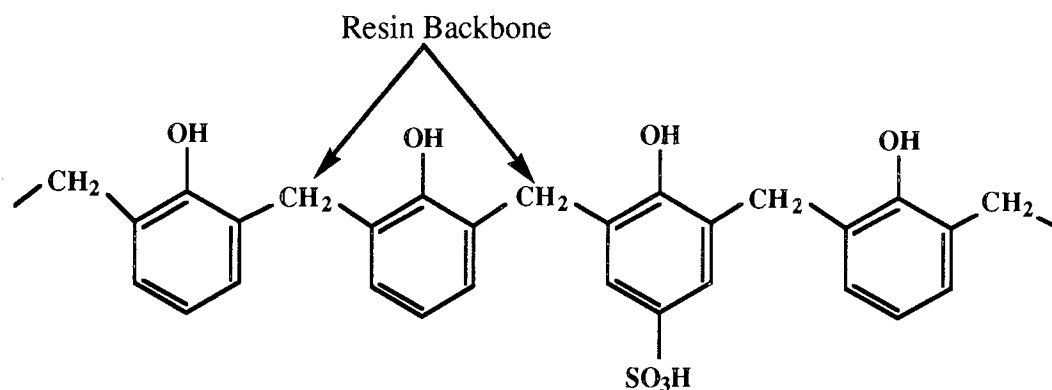
As Figure 7.0 shows, only some benzene rings have a sulphonic acid group attached. Elemental analysis of the resin shows that 20% of the benzene rings are sulphonated. The whole resin is heavily cross-linked (not shown in Figure 7.0), which unfortunately complicates the chemistry of the breakup of the resin.

7.0.2 A Prediction of the Decomposition Products of the Fenton's Reagent / Lewatit Resin System

The known reactions of ·OH radicals with simple molecules, as described in Chapter 1, Section 1.5.1.3, combined with knowledge of common organic reactions, can be used to predict the kind of molecules that will be created as the resin is gradually decomposed into CO_2, water, and inorganic sulphate.

7.0.2.1 The Initial Hydroxyl Radical Attack of the Ion Exchange Resin

FIGURE 7.1

POSSIBLE SITES OF INITIAL HYDROXYL RADICAL ATTACK AT A SULPHONATED BENZENE RING IN LEWATIT DN
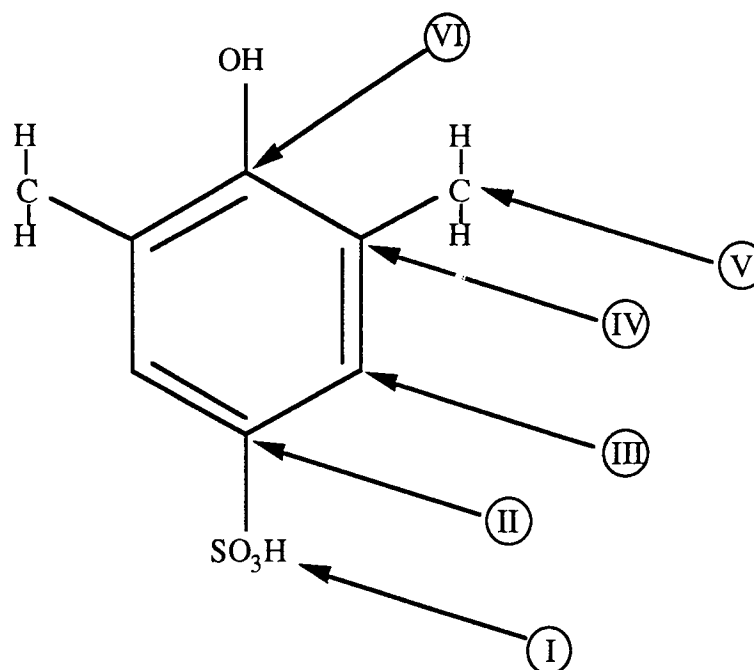
There are 6 possible sites for attack by the hydroxyl radical, four at the benzene ring, one at the carbon backbone that holds the resin together, and one at the sulphonic acid group. All 6 sites will be attacked by the ·OH radical, but it is possible to predict which sites are statistically the most likely to be attacked, using molecular orbital theory.

7.0.2.2 Orbital Bonding Theory Applied To Hydroxyl Radical Ring Addition [92]

As an ·OH radical approaches the ring there will be a small initial overlap between the highest occupied molecular orbital (HOMO) of the radical, and the lowest unoccupied molecular orbital

185

of the ring (LUMO). This causes a new bonding molecular orbital to start forming and the unpaired electron occupies this new orbital. This process happens very rapidly as there is no activation energy to overcome. As the overlap increases, the energy released will increase, until a full chemical bond results. The great speed of this series of reactions was shown by Dorfmann, who demonstrated that the ·OH radical will attack benzene in aqueous solution [93]. ·OH radical attack has a rate that is nearly diffusion controlled (k = from 3 to 8 x 10^9 l mol^{-1} s^{-1}) [29].

For substituted ring compounds there is competition between sites during hydroxyl addition reactions, due to the effect of electron-withdrawing substituents on the ring [29]. An electron withdrawing group reduces the overlap between the hydroxyl radical HOMO and ring LUMO at positions meta to itself, explaining why most attacks occur at position 2, relative to the electron withdrawing group. Other factors that affect hydroxyl radical are equilibriation, rearrangement and reversion to the starting material [29].

In contrast to ring hydroxylation, when hydrogen abstraction takes place there is an activation energy barrier to be surmounted. In this case activation energy is required as the C-H bond must break before the O-H bond can be formed. This energy barrier slows the whole reaction down, making hydrogen abstraction less likely compared with ring hydroxylation. Studies of ·OH radical addition to toluene have shown that only 3% of the ·OH radicals abstract hydrogen from the methyl group of the toluene, with the other 97% adding to the aromatic ring [94]. Similarly when ·OH radicals add to phenylacetic acid solutions more than 90% of the radicals add to the aromatic ring [95].

Finally there are also mechanistic considerations that favour ring hydroxylation as the first attack process [18]. It has been shown in a model system (mandelic acid / FeSO$_4$) that around 50% of the ·OH radicals formed in the reduction of H$_2$O$_2$ by Fe^{2+} are held temporarily within a 'solvent cage' around the metal ion. These ·OH radicals are held in place for a long enough time to react with the nearby functional group of mandelic acid (phenyl hydroxyacetic acid), forming benzaldehyde and benzene carboxylic acid at pH<1. If the pH of the reaction solution is increased, phenols are formed in increasing yield [27].

FIGURE 7.2

THE OXIDATION OF MANDELIC ACID BY HYDROXYL RADICALS

Mandelic Acid/Fe^{2+} Complex

$\xrightarrow[\text{pH}<1]{\text{OH}^{\cdot}}$

Benzaldehyde

+

Benzene Carboxylic Acid
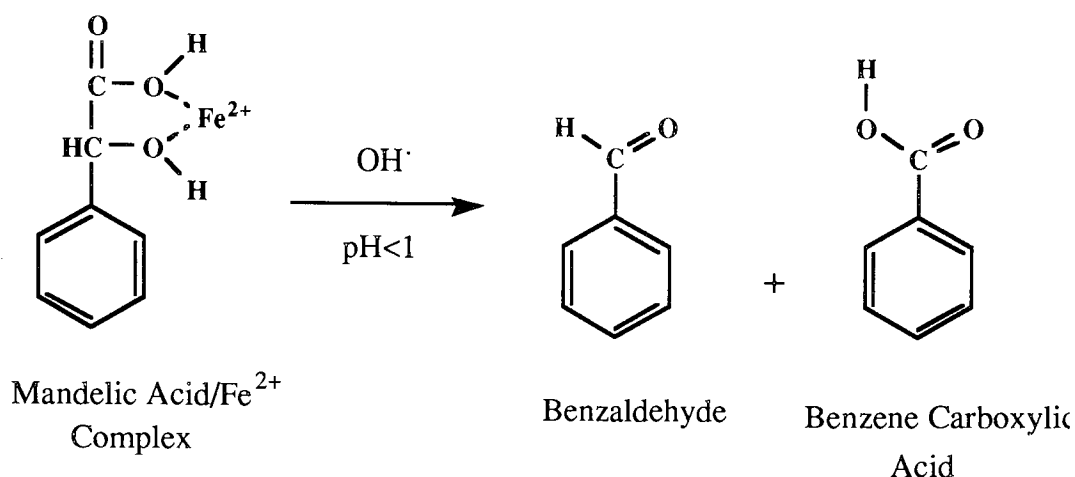
TABLE 7.0

THE PRODUCTS OF OXIDATION OF MANDELIC ACID BY HYDROXYL RADICALS UNDER VARIOUS CONDITIONS

	Yield [a], %				
pH	C$_6$H$_5$CHO	C$_6$H$_5$COOH	Phenols [b]	Other[c]	Total
<1	63.6	2.3	-	-	65.9
1.2	55.6	3.4	1.6	2.9	63.5
1.9	39.4	11.4	7.0	-	57.8
2.7	20.5	9.3	13.5	-	43.3

[a] based on oxidant used, [b] hydroxymandelic acids, [c] hydroxybenzaldehydes and hydroxybenzoic acids

Since in the Lewatit resin the Fe^{2+} ion is held close to the aromatic ring, (primarily at the sulphonic acid group), newly formed ·OH radicals would mainly attach themselves to the ring rather than the more distant polymer backbone.

Bibler suggested that the backbone of the polymer chain in a cross-linked polystyrenesulfonate cation resin would be the first part of an ion-exchange resin to be attacked by ·OH radicals[31]. However, the work on mandelic acid would not support this. Also, other work by Walling has shown that aromatic side chain cleavage (the process by which resin cross linkages are destroyed) is mechanistically dependent on previous ring hydroxylation[29].

187

7.0.2.3 The Hydroxyl Radical Attack of Aliphatic Chains

The environment in which all the resin destruction reactions occur is fiercely oxidising, thus the general reaction pathway, starting from an alkane chain, will be as follows [96]:-

$$\textbf{Alkane or Alkene} \xrightarrow{\text{Oxidation}} \textbf{Alcohol} \xrightarrow{\text{Oxidation}} \textbf{Aldehyde or Ketone} \xrightarrow{\text{Oxidation}} \textbf{Carboxylic Acid}$$
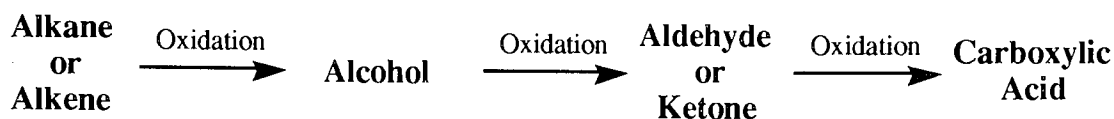
Once the carboxylic acid has been formed, decarboxylation will occur, shortening the C backbone by one C atom, and creating a new alkane, in the following general reaction

$$\underset{\text{Carboxylic Acid}}{R-\overset{\overset{\textstyle O}{\|}}{C}-OH} \longrightarrow \underset{\text{Alkane}}{R-H} + CO_2$$
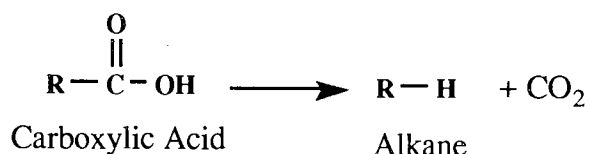
Normally the decarboxylation of carboxylic acids is a slow process, but under special circumstances the reaction very fast. These circumstances are:-

a) When the carboxylic acid has a carbonyl group one carbon removed from the carboxylic acid group, in β-keto acids.

$$\underset{\text{A β-keto acid}}{R-\overset{\overset{\textstyle O}{\|}}{C}-\overset{\overset{\textstyle H}{|}}{\underset{\underset{\textstyle H}{|}}{C}}-\overset{\overset{\textstyle O}{\|}}{C}-OH} \longrightarrow R-\overset{\overset{\textstyle O}{\|}}{C}-\overset{\overset{\textstyle H}{|}}{\underset{\underset{\textstyle H}{|}}{C}}-H + CO_2$$
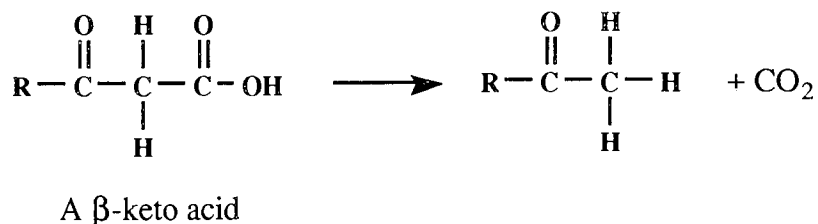
b) When a malonic acid has been formed.

$$\underset{\text{A Malonic acid}}{HO-\overset{\overset{\textstyle O}{\|}}{C}-\overset{\overset{\textstyle R}{|}}{\underset{\underset{\textstyle R}{|}}{C}}-\overset{\overset{\textstyle O}{\|}}{C}-OH} \longrightarrow H-\overset{\overset{\textstyle R}{|}}{\underset{\underset{\textstyle R}{|}}{C}}-\overset{\overset{\textstyle O}{\|}}{C}-OH + CO_2$$
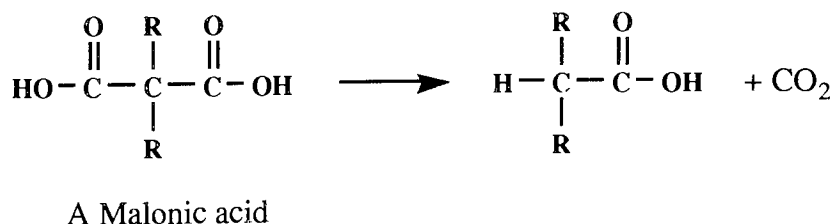
c) When a carboxyl radical has been formed.

$$\underset{\text{Carboxyl Radical}}{RCO_2 \cdot} \longrightarrow R \cdot + CO_2$$
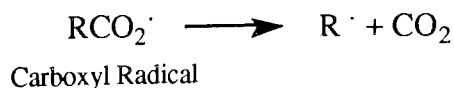
The decomposition of carboxyl radicals will probably be the main source of CO_2 detected during

the digestion of the resin, as they will be very common in the reaction solution.

7.0.2.4 A Summary of the Ring Degradation Processes

It is probable that the dominant process in resin degradation will be ring hydroxylation followed by side-chain scission, producing multiply hydroxylated products. Baxter produced the following reaction scheme for the ·OH radical attack of a resin similar in structure to Lewatit (see Figure 7.3, overleaf) [18].

The fragments of backbone can be expected to have the groups CH_2OH, CHO, and $COOH$ at the terminal positions of the fragments, with further degradation prodcuts such as oxalic $((COOH)_2)$ and crotonic acid $(CH_3CH=CHCOOH)$ also being commonly present during the reaction.

Aromatic sulphonic acids would be expected to break down to $(COOH)_2$, $HCHO$, and $HCOOH$. However, it would not be expected that much aliphatic sulphonic acid will be present in solution as non-aromatic sulphonic acids are oxidised to sulphates [97]. Eventually, if excess H_2O_2 is supplied, all organic species in solution are converted into CO_2 and water in the process known as mineralisation.

FIGURE 7.3

A SUGGESTED PATHWAY FOR THE FRAGMENTATION OF A RESIN POLYMER

Attack by
·OH on ring
gives

Oxidation
by Fe^{3+} then
occurs

Elimination of
the Side-Chain
follows

2 Major Products
of the Reaction
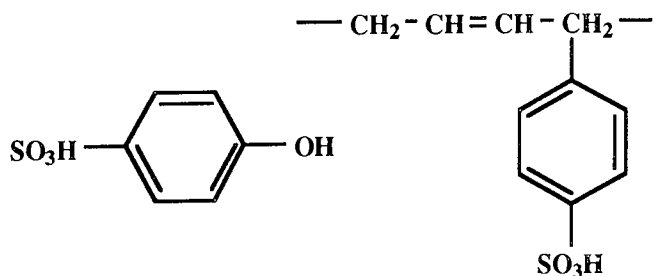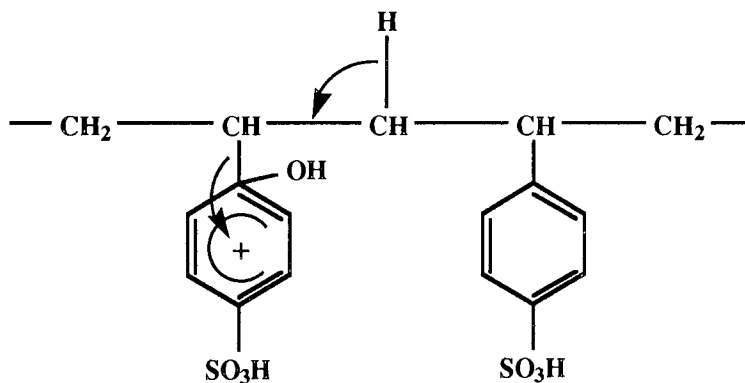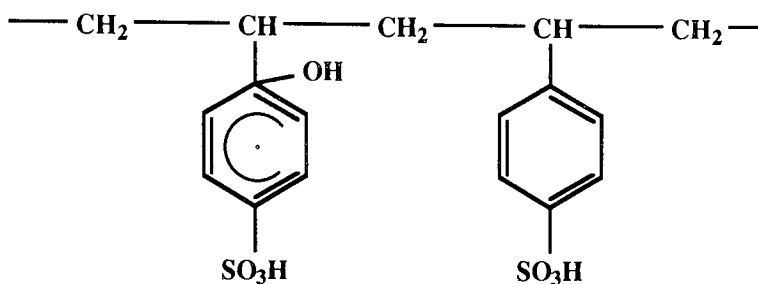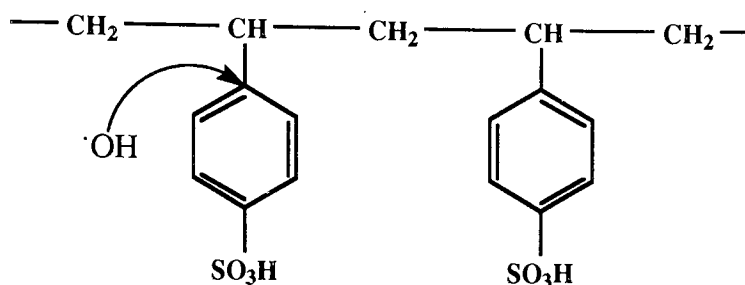
The structure and an efficient synthesis of a new class of molecules, 'calixarenes' was first described by Gutsche in 1981[40]. Gutsche produced calixarenes by reaction of p-tert-Butylphenol with para-formaldehyde, using potassium hydroxide as a catalyst, to form a class of cyclic oligimers, an example of which is shown in Figure 7.4.

FIGURE 7.4

CALIX[8]ARENE

where R = methyl
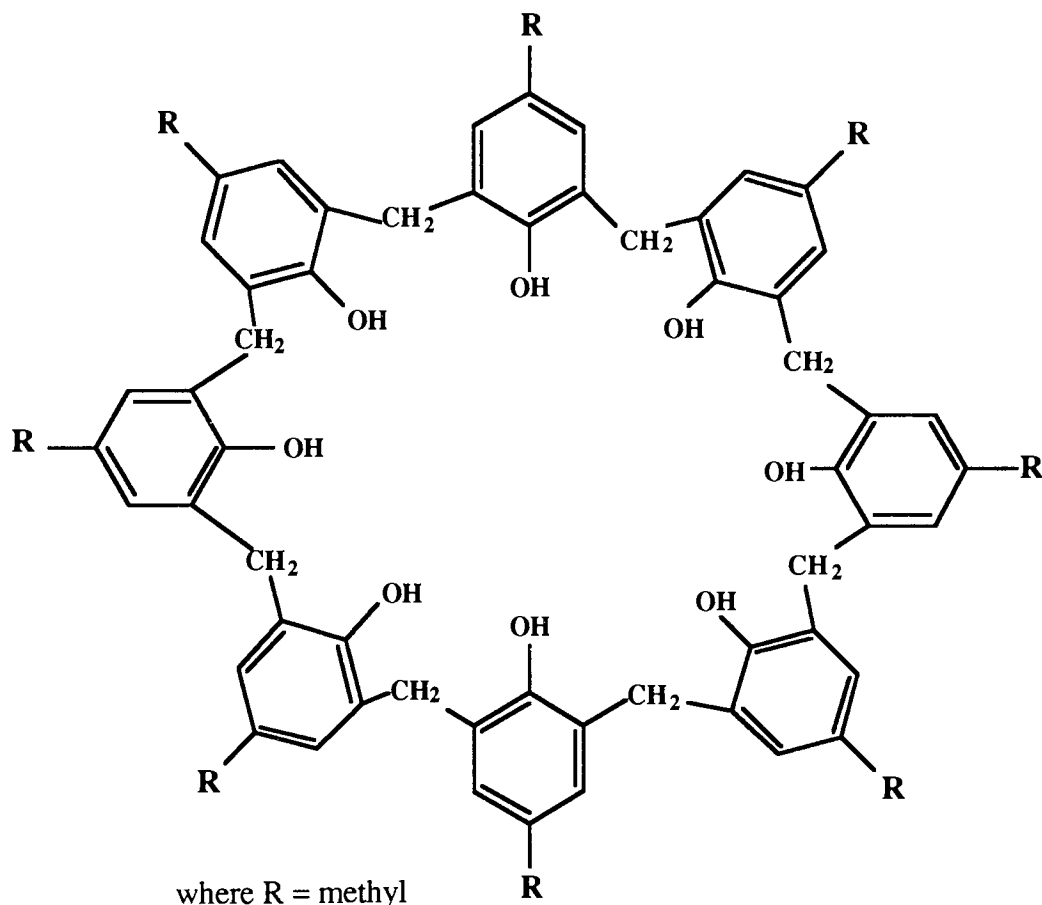
Calixarenes are made up of benzene units, having the same cylindrical architecture as cyclodextrins (which are made up of glucose units). The number within the name of the calixarene shows how many benzene units there are in the ring i.e., calix[6]arene-p-hexasulphonic acid has 6 benzene units. Since the cyclodextrins are well known for host-guest chemistry in solution, it was expected that calixarenes would have similar properties. However, very few examples of this behaviour were reported, until a paper of Shinkai's was published in 1989, describing the use of calix[6]arene-p-hexasulphonic acid in this area of chemistry[98].

This work was based on the work first published in 1984, in which Shinkai described the

discovery of a water soluble calixarene, calix[6]arene-p-hexasulphonic acid, made by replacing the CH3 groups on the outer rim of the calixarene with sulphonate groups [99]. Shinkai's method was adapted for this thesis to produce calix[8]arene-p-octasulphonic acid.

FIGURE 7.5

CALIX[8]ARENE-p-OCTASULPHONIC ACID
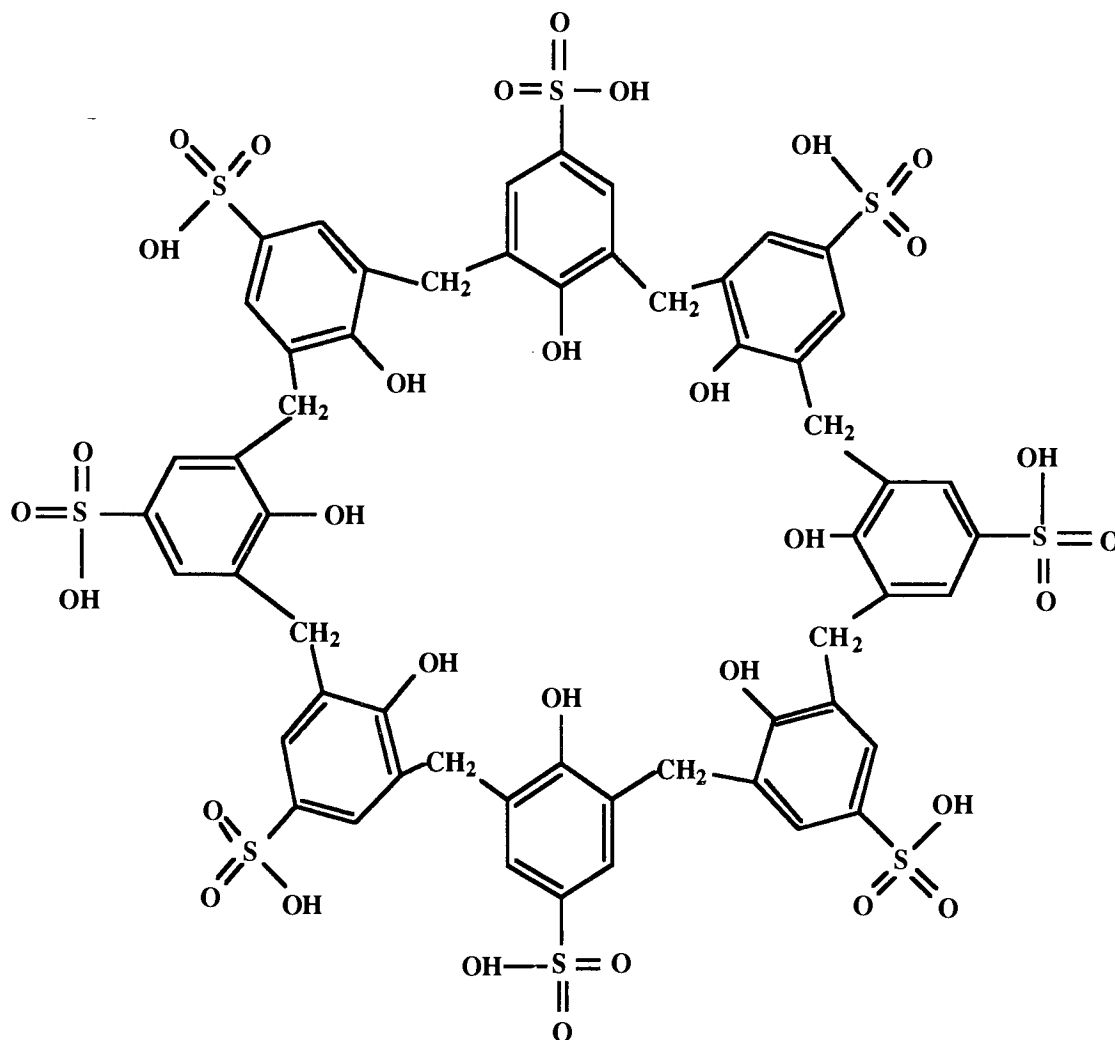
7.0.3.1 The 3-D Conformation of Calix[8]arene-p-octasulphonic Acid

Shinkai describes calix[6]arene-p-hexasulphonic acid as having a flattened cone shape, or possibly a winged or hinged structure (see Figure 7.6) [100].

FIGURE 7.6

3D CONE STRUCTURE OF CALIX[6]ARENE OCTASULPHONIC ACID

'Cone' structure   'Winged or hinged' structure
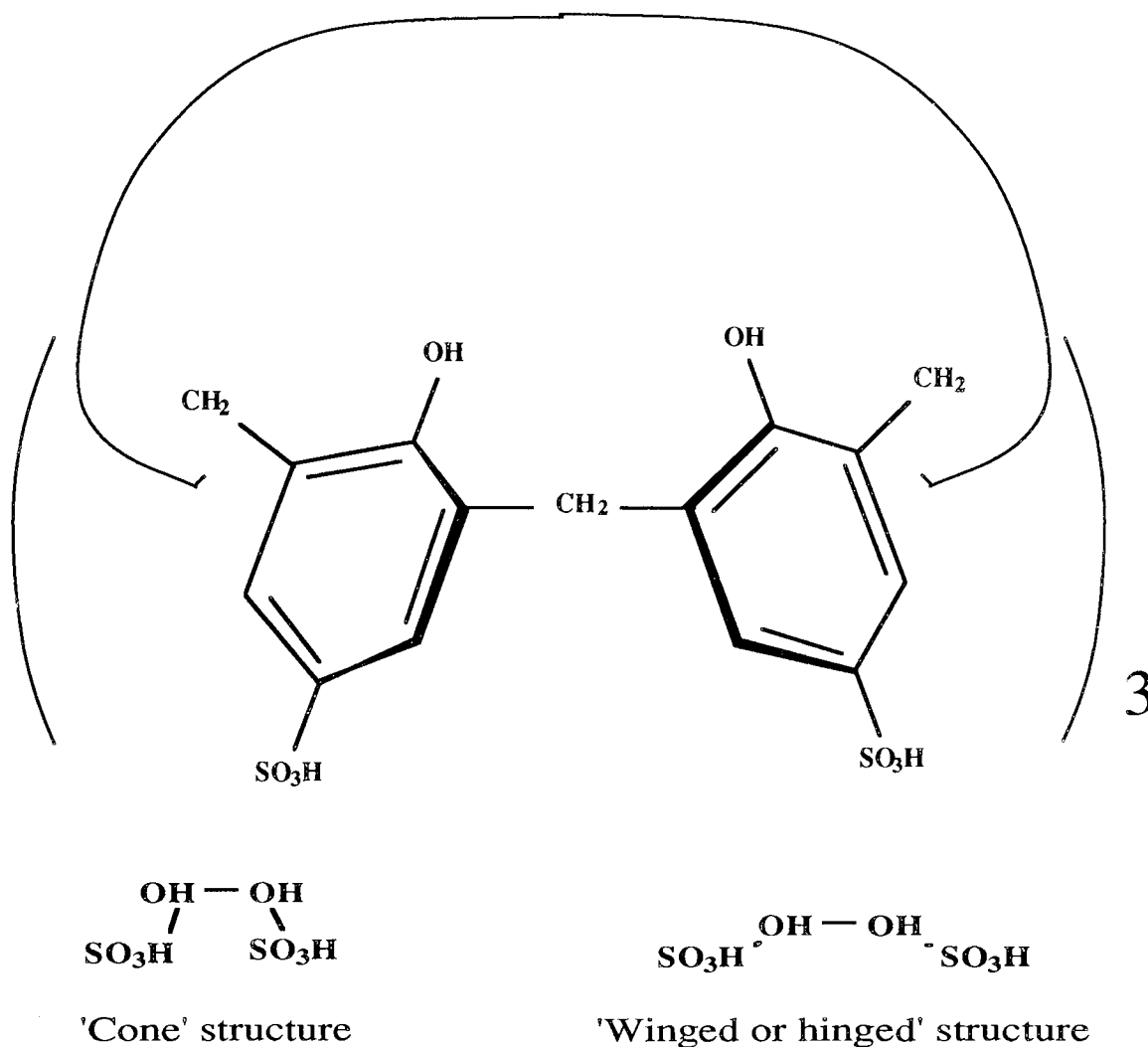
However, Gutsche reports that calix[8]arene, the precursor for calix[8]arene-p-octasulphonic acid, has a 'pleated loop' structure [101]. This is a disc shape, with the OH groups pointing in and out of the plane of the molecule. Hydrogen bonding between the OH groups on the inner rim of the calixarene helps maintain the flattened shape of the calixarene molecule. It would be expected that due to the electrostatic repulsion of the sulphonate groups, the sulphonated version of calix[8]arene would be more 'pleated', as the sulphonate groups try to move apart.

7.0.4 Analytical Procedures and Techniques Used in the Analysis of the Fenton's Reagent / Ion Exchange Resin Reaction

The nature of the reaction between Fenton's reagent and Lewatit ion-exchange resin is very complex, with many types of organic molecule being present in solution at any one time. This

is particularly the case for the first part of the resin digestion process, when there is a high Total Organic Carbon (TOC) level.

To attempt to elucidate the course of the reaction it was decided to approach the analysis of the reaction solution in two stages. The first stage of analysis involved measuring the changes of physical characteristics of the resin reaction solution eg pH, TOC level, Fe concentration, SO_4^{2-} concentration and relating these changes to the type of chemical reactions occurring in solution. The second stage of analysis involved using spectroscopy and GC-MS to try to find which kind of organic molecules are being formed during the reaction. Finally the results from the two parts of the analytical process were combined with the results obtained from the analysis of the Fenton's reagent digestion of CALIX, to give a suggested overall reaction mechanism for the Fenton's reagent / resin reaction.

7.1 RESULTS

7.1.1 Observations of the Resin Beads During Their Solubilisation by Fenton's Reagent

The Lewatit ion-exchange resin supplied by Nuclear Electric is in the form of black, irregularly shaped beads, approximately 1 mm in diameter.

FIGURE 7.7

A PHOTO OF A RESIN BEAD
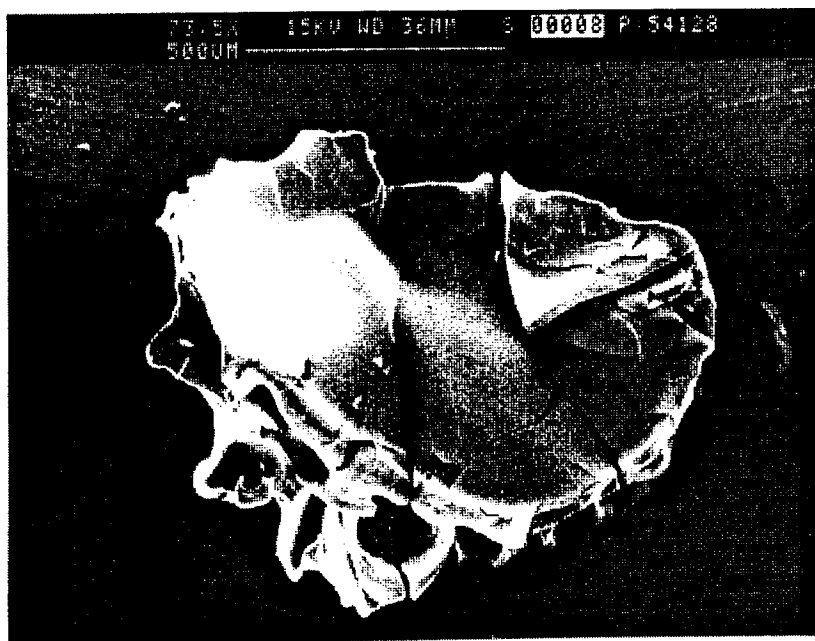
Within 20 seconds of the initial addition of H_2O_2 to the reaction vessel, the solution above the resin can be seen to become discoloured, indicating that the Fenton's reagent is immediately attacking the resin beads. The beads then become sticky and clump together if not stirred vigorously. This is probably due to the formation of multiple OH groups on the surface of the resin bead (multiple OH groups are common in the substances used to make adhesives). The presence of polyhydroxylate structures would be expected in this system (See Section 7.0.2.4). As the resin dissolves a smell reminiscent of organic carbonyl groups is detected. This smell is present during the whole of the reaction.

If a resin bead sampled at 5 minutes after the start of the reaction is observed at low magnification in an electron microscope, extensive pitting of the surface of the bead can be seen. As the magnification is increased it can be seen that some of pits on the surface of the bead are very deep.

FIGURE 7.8

MEDIUM AND HIGH MAGNIFICATION PHOTOS OF A RESIN BEAD 5 MINUTES AFTER ADDITION OF FENTON'S REAGENT

Medium Magnification

195
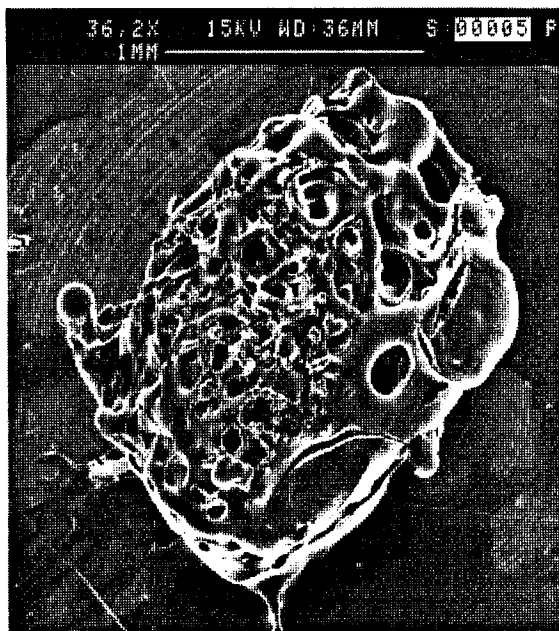
High Magnification

These pits are probably formed by the enlargement of microscopic pits that already exist on the surface of the resin bead, in a process shown in Figure 7.9 (see overleaf).

FIGURE 7.9

THE INITIAL STAGES OF THE FENTON'S
REAGENT DEGRADATION OF A RESIN BEAD

(1)

HO-OH

HO-OH   HO-OH

HO-OH   HO-OH

Water and hydrogen peroxide

Fe   Fe   Fe Fe   Fe Fe   *Surface of resin bead*
         Fe
      Fe   *Resin bead*

Microscopic, pre-existing pit on resin bead surface

(2)

HO-OH

HO-OH   HO-OH

HO-OH   HO-OH

Water and hydrogen peroxide

Fe   .OH   Fe→.OH   Fe   *Surface of resin bead*
         Fe
.OH   .OH .OH   Fe   .OH .OH   *Resin bead*
   .OH   .OH   .OH   .OH
          .OH   .OH
       .OH .OH
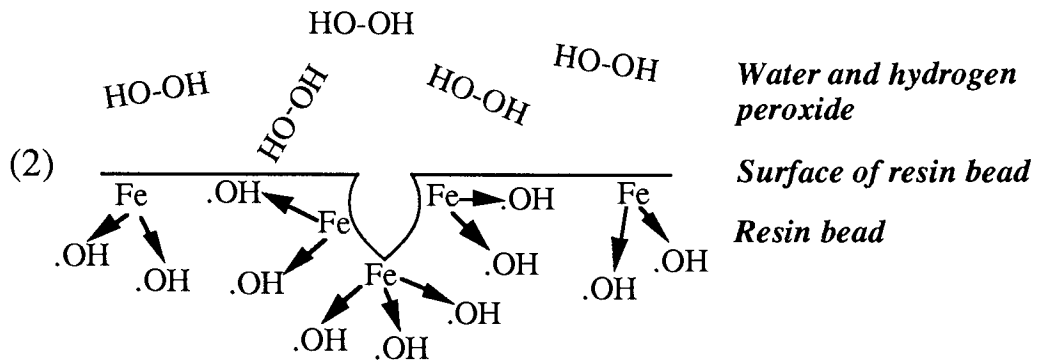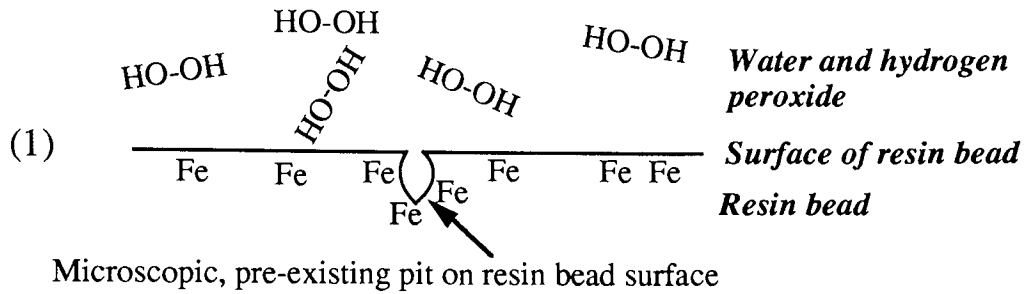
The hydrogen peroxide diffuses rapidly into the resin bead, whereupon Fe ions catalyse the production of .OH radicals, wh'ch travel out in all directions away from the Fe ions. The .OH radicals attack the resin, forming water soluble organic molecules.

(3)

HO-OH   HO-OH   .OH

HO-OH   HO-OH   Fe

HO-OH

Water and hydrogen peroxide

.OH   Fe   HO-OH   .OH   *Surface of resin bead*
.OH← Fe   HO-OH   .OH   *Resin bead*
          HO-OH   Fe →.OH
.OH   Fe
   .OH   .OH   Fe   .OH

.OH
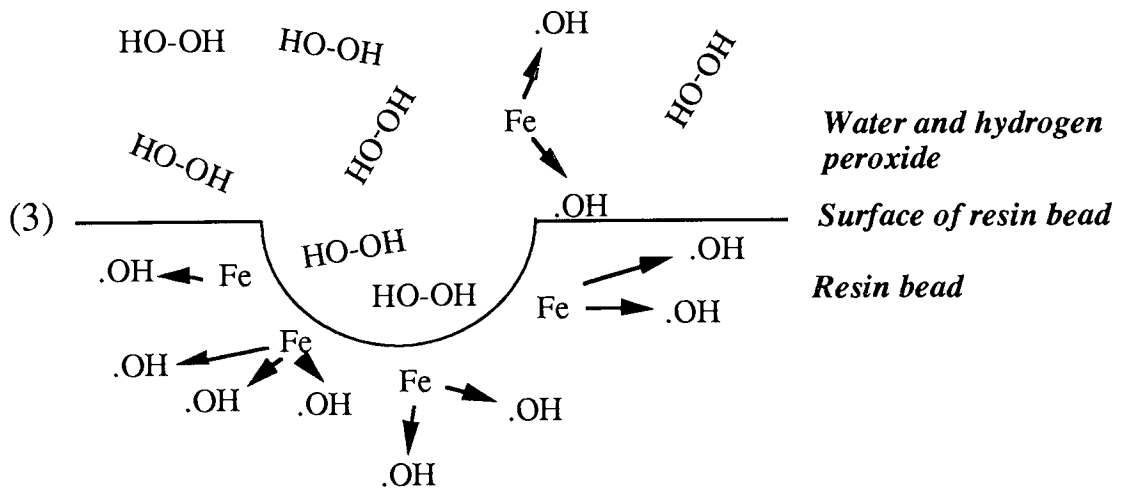
There would be a higher rate of .OH radical attack at locations with a microscopic hole in the resin bead surface, due to the higher surface area at these points. This would result in enlargement of these holes. Fe would also tend to be temporarily trapped in these holes, rather than diffuse away into solution, again resulting in enlargement of the holes.

If a resin bead sampled at 30 minutes after the start of the reaction is observed at low magnification it can be seen that, unlike the resin bead from 5 minutes into the reaction, there is no longer any surface pitting, with only a smooth surface being seen (up to a magnification of 2000 times).

FIGURE 7.10

A PHOTO OF A RESIN BEAD 30 MINUTES AFTER ADDITION
OF FENTON'S REAGENT
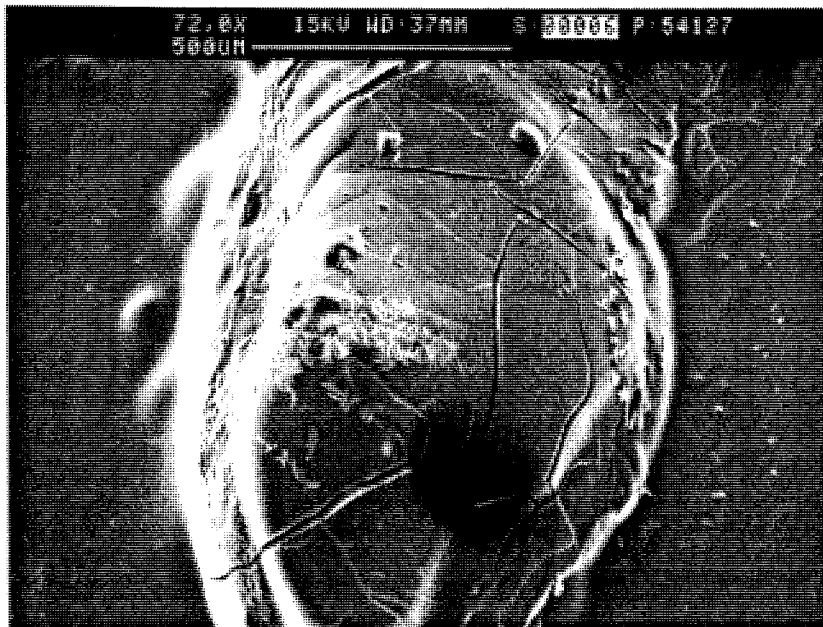
This observation suggests that by this time there are no longer any sites in the structure in which iron catalyst can be trapped. Instead, the ·OH radicals must be being created solely in solution by reaction of H_2O_2 with Fe ions. Since the resin beads are completely surrounded by water, the surface of the resin bead would be attacked by ·OH radicals from all directions at an equal rate, resulting in the completely smooth surface observed.

On visual inspection of the reaction vessel, the average size of the beads is seen to reduce, as more and more of the bulk of the bead is dissolved, with complete dissolution of the resin occurring at 65 to 75 minutes after the start of the reaction. The colour of the resin reaction solution gradually fades from dark brown as the reaction proceeds until at the end it is a pale brown / yellow colour.

FIGURE 7.11

Graph showing typical changes in apparent iron concentration with time, in the standard resin digestion reaction
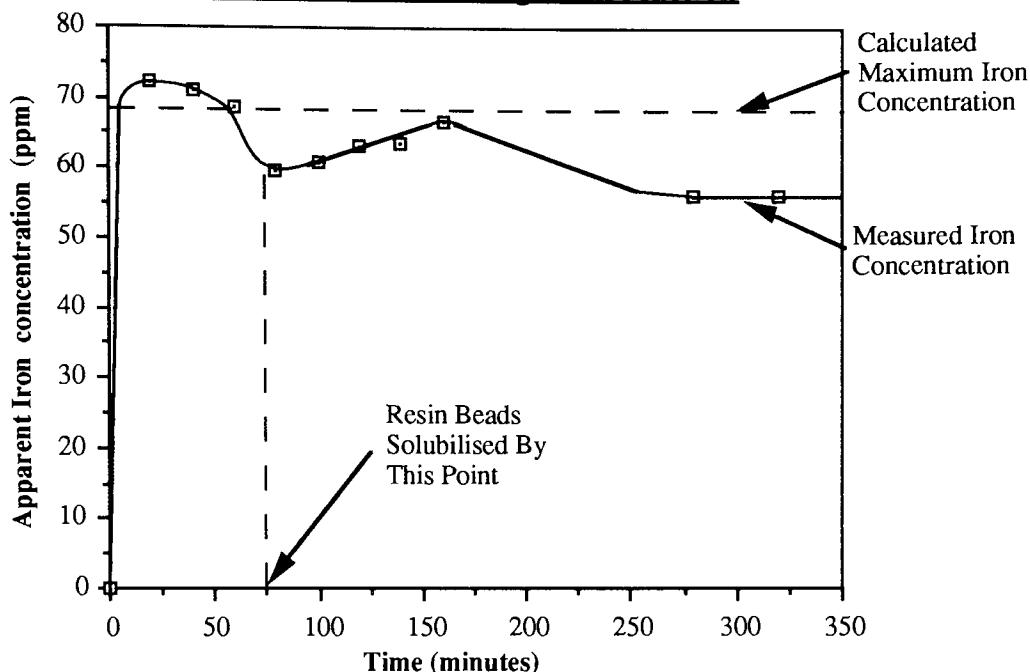
Figure 7.11, which is typical of many such sets of data, shows that the measured Fe concentration reaches its maximum at 20 minutes after the start of the reaction. This indicates that at this point all the iron has been removed from the resin, even though substantial quantities of ion-exchange resin are still present in the reaction vessel. This in turn implies that, under the conditions used in my experiments, the Fe catalyst does not permeate the whole of the resin bead and reside throughout it, but is only localised at or near the surface of the bead.

The maximum Fe concentration at 20 minutes also indicates that the Fe released from the resin is not re-absorbed, to any significant extent, onto the surface of the resin. By this stage there is a variety of organic molecules in solution, and it seems likely that the Fe is being ligated by these organic molecules as soon it is released into solution, thus being prevented from returning to the resin. An alternative explanation is that when a resin sulphonic acid group is exposed to the reaction environment, by dissolution of resin material above it, the sulphonic acid group is immediately lost from the benzene backbone of the resin. This would reduce the chances of any free Fe in the reaction solution being bound onto the resin surface.

FIGURE 7.12

THE LOSS OF IRON FROM THE ION EXCHANGE RESIN

(1) [Reaction scheme showing sulphonated phenol-formaldehyde resin with $O\text{--}Fe^{2+}$ reacting with $^{\cdot}OH$ to give dihydroxy product $+ Fe^{3+} + SO_4^{2-}$]

(2) $Fe^{3+} + L \longrightarrow Fe^{3+}L$ where L=Organic Ligand
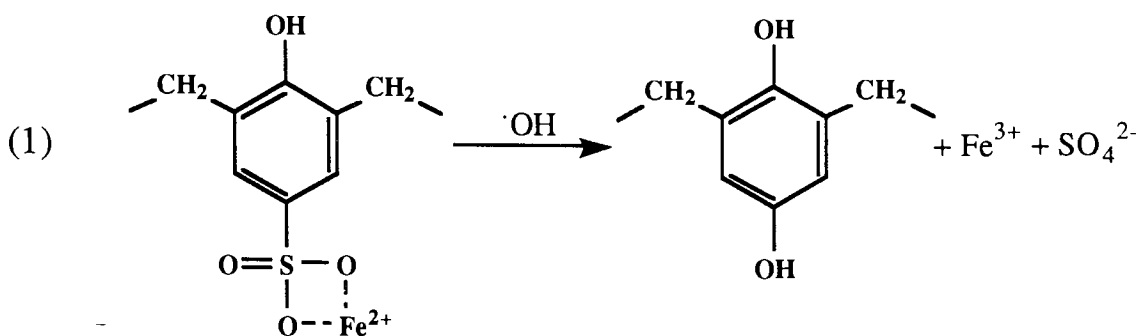
Although the replacement group for SO_3H, OH, can itself act as a ligating group for iron in solution, the stability constants for phenol and benzene sulphonic acid, with respect to H^+, suggest that OH is inferior to SO_3H in the ligation of iron. The stability constant is the reciprocal of the dissociation constant. No data were available for the relative stability of Fe / HO_3SPh and Fe / HOPh complexes.

TABLE 7.1

THE STABILITY CONSTANTS OF BENZENE

SULPHONIC ACID AND PHENOL [102]

Compound	Acid Dissociation Constant (mol dm-^{3})	Log of Acid Dissociation Constant	Log of Stability Constant
$C_6H_6O_3S$	2×10^{-1}	-0.7	0.7
C_6H_5OH	1.28×10^{-10}	-9.9	9.9

After the apparent Fe concentration maximum has been reached, the apparent Fe concentration varies slowly until the end of the reaction (Figure 7.11). At this point the final Fe concentration is 78% of the maximum measured Fe concentration.

The resin solution is very acidic, and the iron catalyst concentration is very low, so it seems unlikely that this variation is caused by iron precipitating out of, and then solvating back into solution. Since there appears to be no other possible mechanism for the removal of Fe from solution after the resin has solubilised, the variations in apparent Fe concentration must be a

reflection of the changing chemical environment of the reaction mixture. The chemical environment affects the rate at which monatomic Fe ions are formed in the flame of the AA equipment, and thus the Fe concentration reading produced by the AA (see Section 7.1.2.1).

7.1.2.1 Chemical Interference in AA

It is well known that the chemical matrix of a sample can affect the reading obtained when atomic absorption spectroscopy is used. Chemical interference occurs when compounds or radicals containing the element being measured are not broken down into individual atoms at the temperature of the flame being used [103]. There are several chemical environments known to effect the AA reading obtained for samples containing iron. Mineral acids cause a slight depression in the reading obtained, whilst organic acids (in particular citric acid) can cause a depression of up to 50% in the iron concentration measured by an AA spectrophotometer (see Figure 7.13) [104,105].

FIGURE 7.13

Graph showing the effect of citric acid on the determination of iron

Citric acid concentration, ppm
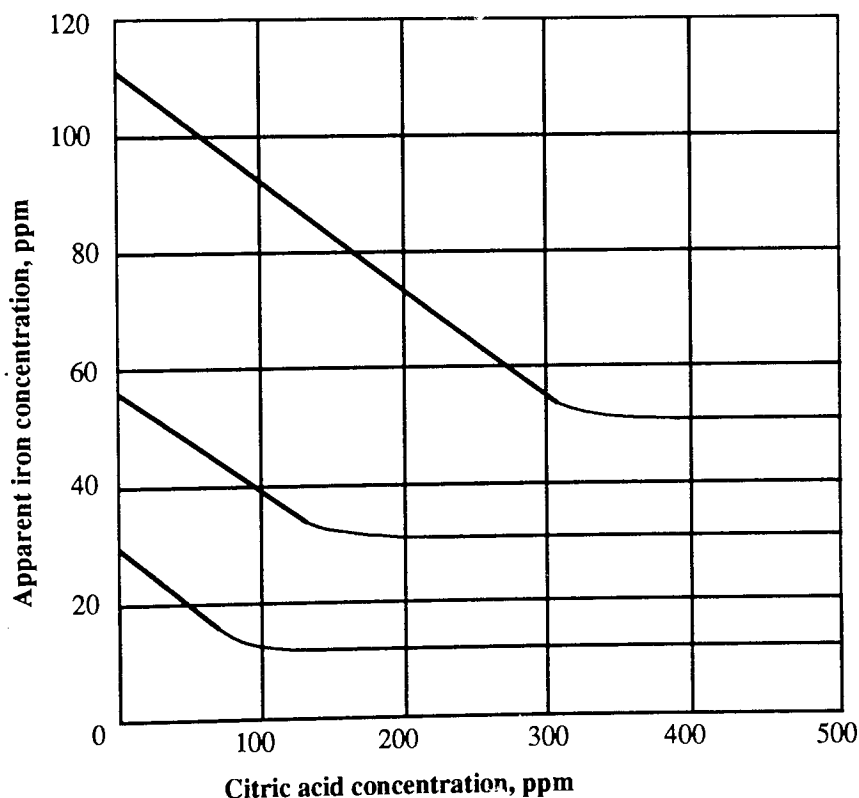
Both organic acids and H_2SO_4 are present in varying concentrations in the samples analysed for iron (see Sections 7.1.13.1 and 7.1.6) suggesting strongly that chemical interference accounts

for the variations in the measured [Fe].

7.1.2.2 Calculation of the Expected Iron Concentration in Solution

It is possible to calculate the expected iron concentration in the reaction solution, based on the iron content of the resin, plus the amount of iron added in the form of the catalyst.

3 g of resin had H_2O_2 added to it, without Fe being used as a catalyst, until a reaction mixture similar in appearance to that of solutions seen at the end of the standard reaction was obtained. 330 cm^3 of solution with an Fe concentration of 7.85 ppm (measured by an AA spectrometer) remained at this point.

Assuming that this concentration was itself depressed by chemical interference, to the same extent seen at the end of the standard resin reaction (78%), then the actual Fe concentration would be 10 ppm.

$$10.0 \text{ ppm Fe} = 0.01 \text{ g of Fe per litre}$$

However, there was only 330 cm^3 of solution, so

$$0.01 / 3.03 = \underline{0.0033 \text{ g of Fe in 3 g of resin}}$$

In the standard reaction 0.13 g of $FeSO_4.7H_2O$ is added to 10 g of resin, along with 541 cm^3 of liquid (water + H_2O_2).

Amount of Fe in 0.13 g of $FeSO_4. 7H_2O$ = 0.0262 g

Amount of Fe in 10 g of resin = 0.011 g

Total amount of iron in 541 cm^3 of liquid = 0.0372 g

$$\underline{\text{Calculated maximum Fe concentration} = 68.7 \text{ ppm}}$$

$$\underline{\text{Observed maximum Fe concentration reading} = 71.8 \text{ ppm}}$$

The slightly higher observed Fe concentration maximum may result from slight contamination of the apparatus used for the resin digestion.

FIGURE 7.14

Graph showing typical changes in organic carbon level with time, in the standard resin digestion reaction
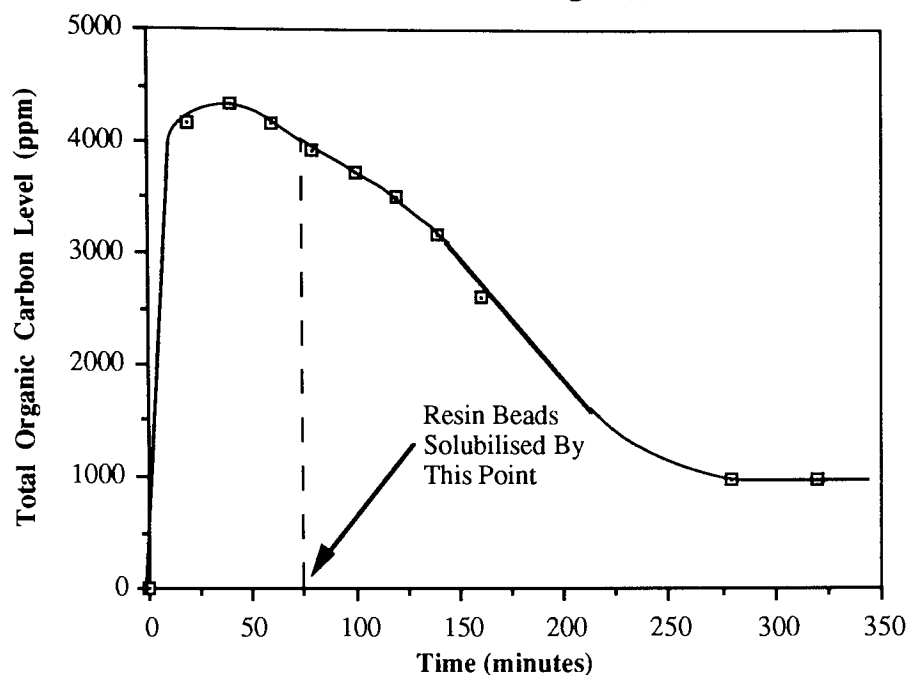
Figure 7.14, which is typical of many such sets of data, shows that the TOC level starts falling before the resin beads are totally dissolved. This indicates that at this point the rate of destruction of organic molecules in solution exceeds the rate of resin bead dissolution. In heterogeneous reactions the reacting molecules are transferred from one phase to the other, and rate of transfer will depend on the surface area of the interface between the phases. As the bead dissolves a reduction of the surface area of the bead will occur and the quantity of organic material going into solution in a given time will fall as the beads dissolve.

An attempt was made to mathematically model the dissolution of the resin, and compare the results with the actual TOC level readings obtained.

7.1.3.1 Assumptions Made in Model of Resin Dissolution

1) The bead is a perfect sphere, and dissolution occurs only at the surface.

2) The [H_2O_2] is constant during the dissolution of the bead.

3) Organic material that is released into solution is not oxidised to CO_2.

4) The rate of loss of mass from the bead is proportional to the surface area.

Assuming (4) is correct, then

$$\frac{-dr}{dt} = k_1$$

Integrating this equation we get

$$r = -k_1 t + k \quad \cdots\cdots\text{Equation 1}$$

When r_0 = radius at time 0, then

$$r_0 = k$$

Substituting into Equation 1,

$$r = -k_1 t + r_0$$

and rearranging,

$$r - r_0 = -k_1 t \text{, and } -r + r_0 = k_1 t$$

and

$$r_0 - r = k_1 t \quad \cdots\cdots\text{Equation 2}$$

If T = the time when the resin bead has been totally destroyed, then

$$r = k_1 (T - t) \quad \cdots\cdots\text{Equation 3}$$

From Equation 2 we know that

$$k_1 = \frac{r_0 - r}{t}$$

Substituting for k_1 in Equation 3,

$$r = \frac{(r_0 - r)}{t}(T - t)$$

and rearranging,

$$rt = (r_0 - r)(T - t) \text{, and } rt = r_0 T - r_0 t - rT + rt \text{, and } 0 = r_0 T - r_0 t - rT \text{ and } rT = r_0 T - r_0 t$$

followed by,

$$rT = r_0(T-t) \text{, and } \frac{rT}{r_0} = T-t \text{, and } \frac{r}{r_0} = \frac{T-t}{T} \text{, finally } \frac{r}{r_0} = 1-\frac{t}{T}$$

The volume of a sphere is

$$= \frac{4}{3}\pi r^3$$

therefore the amount of carbon left at any point will be

$$= \frac{4}{3}\pi (r_0{}^3 - r^3)$$

Rearranging,

$$= \frac{4}{3}\pi r_0{}^3 \left(1 - \frac{r^3}{r_0{}^3}\right)$$

But,

$$\frac{r}{r_0} = 1 - \frac{t}{T} \text{ so therefore } \frac{r^3}{r_0{}^3} = \left(1 - \frac{t}{T}\right)^3$$

Thus, the amount of carbon left is equal to

$$= \frac{4}{3}\pi r_0{}^3 \left[1 - \left(1 - \frac{t}{T}\right)^3\right]$$

The fraction of the resin bead that has been dissolved at time t will be

$$= \frac{\frac{4}{3}\pi r_0{}^3 \left[1 - \left(1 - \frac{t}{T}\right)^3\right]}{\frac{4}{3}\pi r_0{}^3}$$

$$= \left[1 - \left(1 - \frac{t}{T}\right)^3\right]$$

If the fraction dissolved is multiplied by the maximum observed TOC level, C, then the model TOC values and actual TOC values can be compared.

$$= C \left[1 - \left(1 - \frac{t}{T}\right)^3\right]$$

FIGURE 7.15

Graph showing a comparison of theoretical and actual
TOC level changes during resin bead dissolution
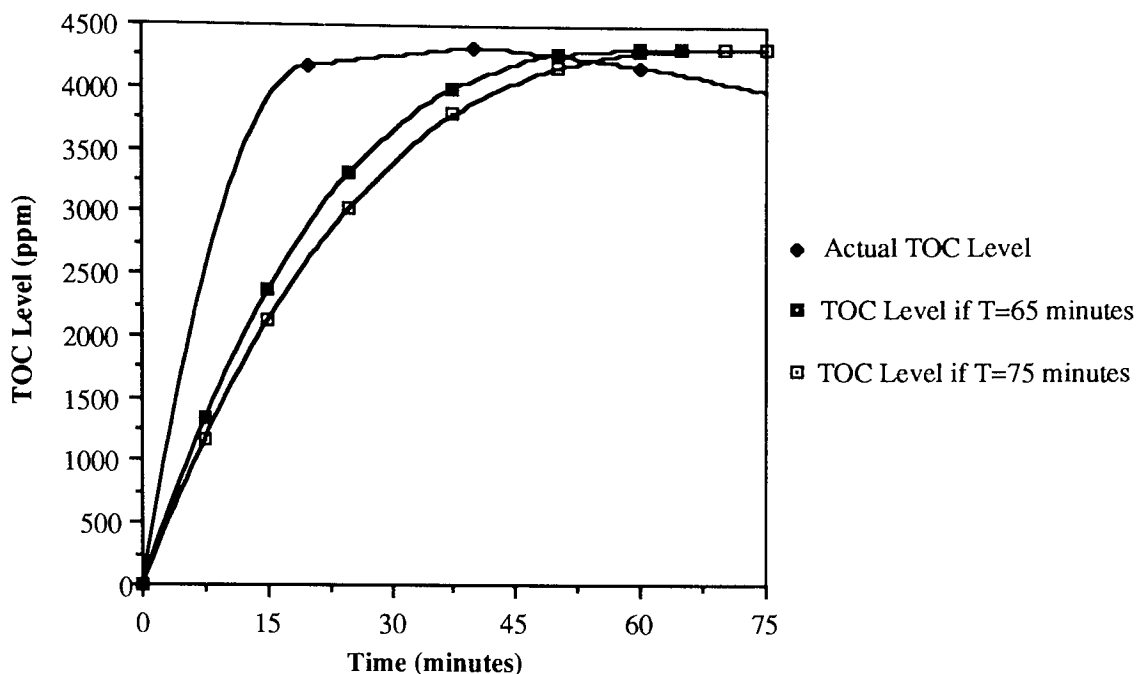
Figure 7.15 shows that the actual TOC level rises to a peak much faster than the modelled TOC

levels. The most probable explanations for this disparity are the assumptions made about the

shape and surface area of the resin bead. The real beads are irregular in shape, and pits and deep

channels develop in the structure of the bead soon after the start of the reaction (see Figure 7.8).

This will substantially increase the surface area available for ·OH radical attack, relative to the

perfect sphere assumed in my model.

The data for the fall in TOC level after all the resin had solubilised were analysed next and the

results are shown in Figure 7.16.

FIGURE 7.16

Graph showing a typical fall in organic carbon level after all the resin
beads have dissolved, in the standard resin digestion reaction
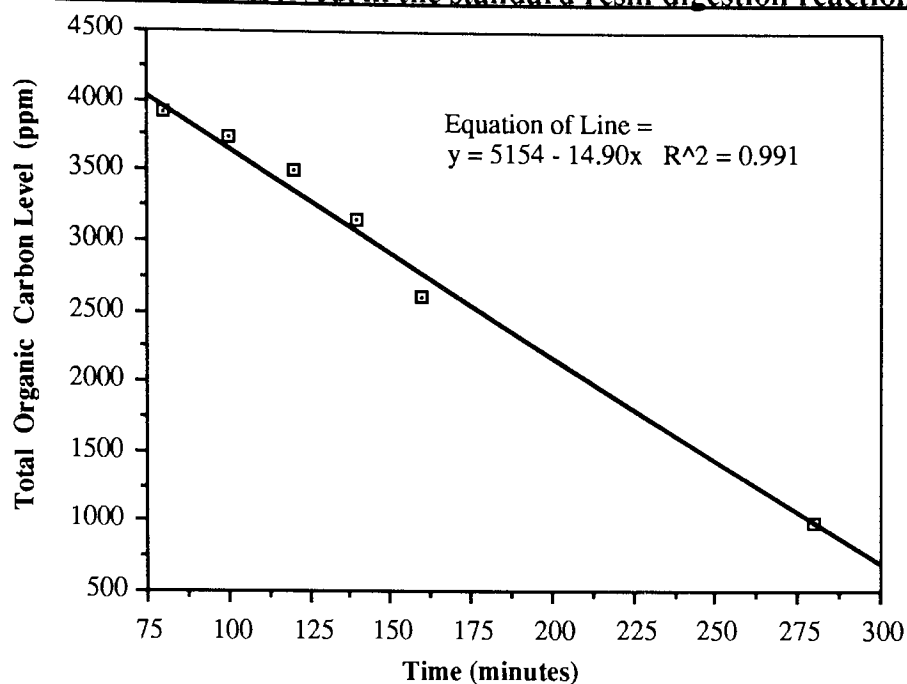
Figure 7.16, which is typical of many such sets of data shows that the rate of loss of C from solution after all the resin beads have dissolved is approximately 0 th order, i.e., the rate of removal of C from solution is not dependent on the concentration of C present in solution. This means that the rate determining step in the removal of C from solution does not involve C, that is

$$\frac{d\,[Carbon]}{dt} = k\,[Carbon]^0$$

FIGURE 7.17

Graph showing change in hydrogen peroxide concentration with time, in the standard resin digestion reaction
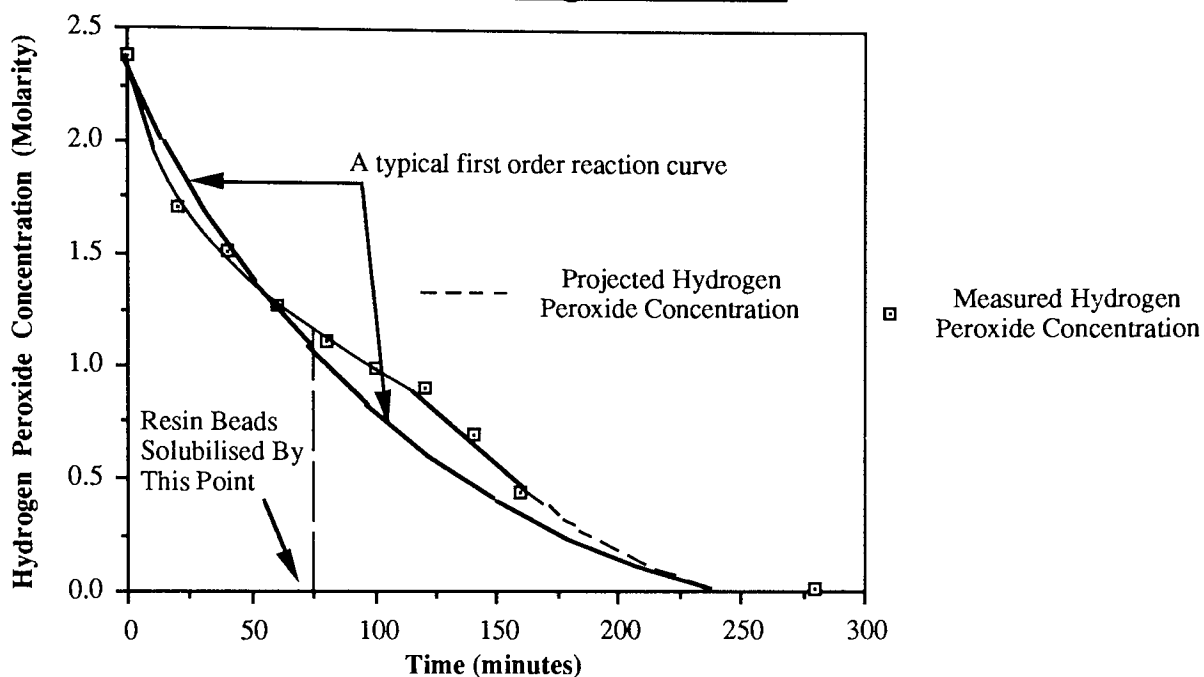
Figure 7.17 shows that the general form of the H_2O_2 concentration plot matches that of a 1st order plot of concentration . The variations of the H_2O_2 concentration plot from the 'ideal' 1st order plot, in particular the increase in the rate of H_2O_2 seen at about 125 minutes, can be explained as follows:-

Normally as time passes the rate of H_2O_2 consumption would fall. However, as the degree of oxidation of organics in solution increases, then the average C backbone length of organic fragments will fall. If shorter chain length molecules are easier to oxidise, then the rate of H_2O_2 consumption is likely to increase, as is seen at 125 minutes.

The first order nature of Figure 7.17 is confirmed in Figure 7.18, in which data is analysed for 3 'standard resin reactions'.

FIGURE 7.18

Graph showing the relationship between time and the logarithm of the hydrogen peroxide concentration, for 3 separate standard resin digestion reactions
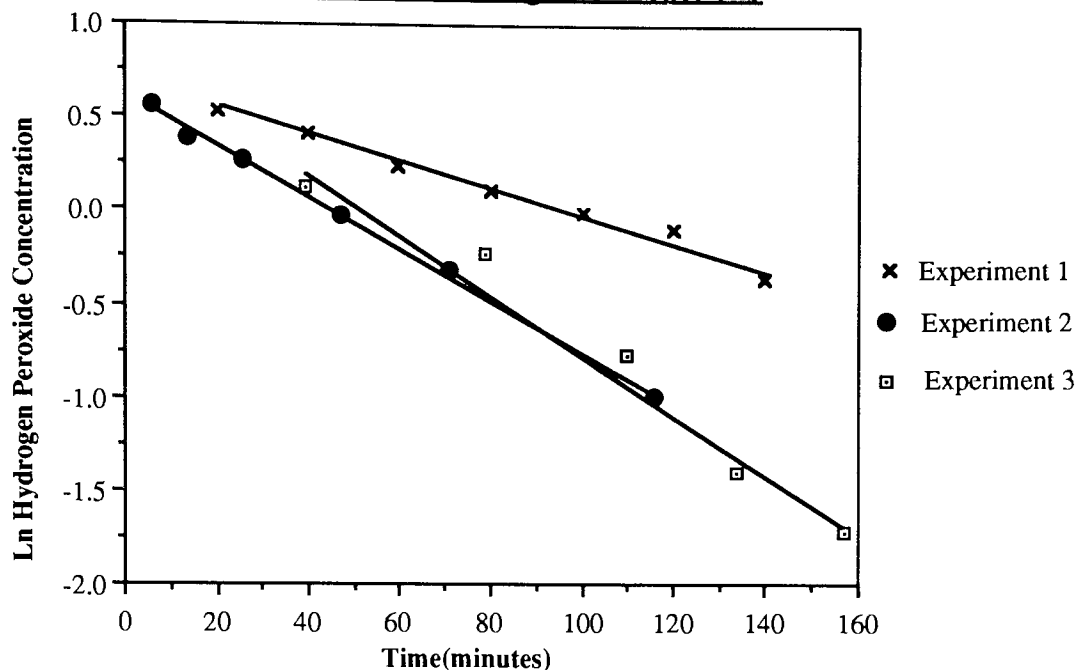
TABLE 7.2

GRADIENTS AND INTERCEPTS ON THE Y AXIS FOR A PLOT OF THE LOGARITHM OF THE CHANGE IN HYDROGEN PEROXIDE CONCENTRATION IN 3 SEPARATE EXPERIMENTS

Experiment Number	Gradient of Line min^{-1}	Extrapolated Intercept on y axis
1	7.08×10^{-3}	0.68
2	1.37×10^{-2}	0.62
3	1.73×10^{-2}	0.98

This information indicates that the rate of loss of H_2O_2 from solution, after the resin has dissolved, is 1st order with respect to concentration, i.e,

$$-\frac{d[H_2O_2]}{dt} = k\,[H_2O_2]^1$$

The variation in the gradients of the lines must be due to experimental error, as the conditions of the 3 experiments were supposed to be identical.

A simple reaction scheme was devised to account for the H_2O_2 and TOC level changes.

FIGURE 7.19

A SIMPLE SCHEME FOR RESIN DISOLUTION

$$Fe^{2+} + H_2O_2 \xrightarrow{k_1} Fe^{3+} + \cdot OH$$

$$\cdot OH + Organic \xrightarrow{k_{2i}} Oxidised\ Organic \quad (Many\ such\ equations)$$

$$\cdot OH \xrightarrow{k_3} Side\ Reaction \quad (Several\ such\ equations)\ fre$$
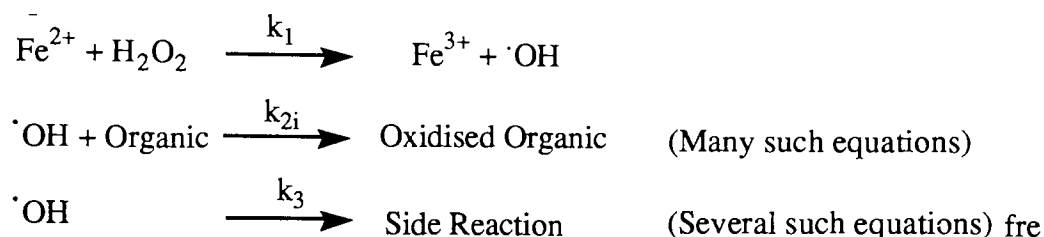
If the $[Fe^{2+}]$ remains essentially the same, then a first order reaction would be seen i.e.,

$$Instantaneous\ Efficiency = \frac{\sum_{i=1}^{\infty} k_{2i}\ [Organic]}{\sum_{i=1}^{\infty} k_{2i}\ [Organic] + k_3}$$

$$-\frac{d\ (TOC)}{dt} = \frac{k_1 \sum_{i=1}^{\infty} k_{2i}\ [Organic]}{\sum_{i=1}^{\infty} k_{2i}\ [Organic] + k_3}$$

7.1.5 Monitoring the Changes in Sulphate Concentration During the Fenton's Reagent / Resin Reaction

It was decided to monitor the changes in sulphate level because it was hoped that these changes would provide information about the loss of sulphonic acid groups from the Lewatit resin structure.

SO_4^{2-} concentration was measured by adding a solution of $BaCl_2$ to samples of resin reaction solution taken during the reaction, which created a precipitate composed of $BaSO_4$ and organic material. The precipitate was removed from the resin solution, dried; weighed; then heated strongly on a bunsen for 15 minutes, and reweighed.

FIGURE 7.20

Graph showing the comparison between the mass of dried precipitate before and after heating strongly in a crucible
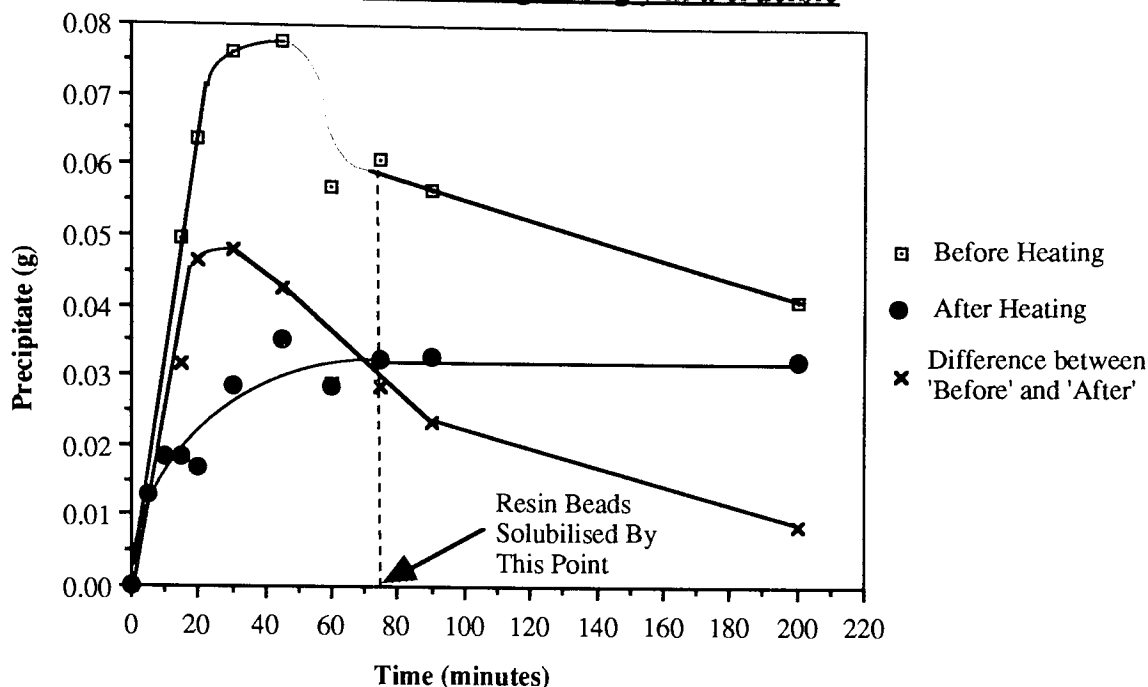
In Figure 7.20 the 'Before' trace shows the total amount of material precipitated when the $BaCl_2$ was added to the resin digestion solution. This material will consist of $BaSO_4$, along with organic acids such as barium oxalate (it would be expected that some organic acids would co-precipitate along with the $BaSO_4$). The 'After' trace represents inorganic material not burnt off when heated by a bunsen burner. This will consist of $BaSO_4$ and BaO (the BaO coming from decomposition of barium organic acids). The 'Difference' trace will represent the amount of organic acids precipitated from solution at any one time.

It was decided to calculate the maximum amount of $BaSO_4$ that would be expected in the precipitate, based on the elemental analysis of Lewatit resin.

7.1.5.1 Experimental Details

5 g of resin was reacted with 70 cm³ of H_2O_2 in 200 cm³ of water, with 0.065 g of $FeSO_4.7H_2O$ (the catalyst). 10 cm³ samples of the resin solution then had $BaCl_2$ added dropwise until no further precipitate was seen. The precipitate was then removed by filtration, dried, weighed, and heated by a bunsen burner for 15 minutes and reweighed. The weight of the remaining

precipitate was then found.

7.1.5.2 Calculation of Sulphur Concentration in Solution

S content of the dry resin (from elemental analysis) = 4.64%

Mass of S in the resin = 0.232 g

Assuming all S in solution is in the form of SO_4^{2-} then the mass of SO_4^{2-} in the resin reaction solution after resin dissolution = 0.696 g

Plus contribution of SO_4^{2-} from catalyst = 0.718 g

Mass of SO_4^{2-} in each sample of resin reaction solution after resin dissolution (0.718 / 27) = 0.0265 g

Ba and SO_4^{2-} comprise 58.84% and 41.16% respectively of the $BaSO_4$ molecule.

Expected mass of $BaSO_4$ precipitated per sample = 0.0646 g

Actual mass of $BaSO_4$ precipitated in post-resin dissolution samples = 0.0325 g

i.e., 50% of the expected maximum yield.

There are two possible explanations why a lower amount of $BaSO_4$ than expected is detected.

a) Agar-agar was not used, by an oversight, to coagulate the precipitate produced on the addition of $BaCl_2$ to the sample (as suggested in Vogel's Textbook of Quantitative Chemical Analysis) [106]. This would have resulted in a decrease in material collected when the resin solution was filtered.

b) The resin beads used in the reaction may have been slightly damp, resulting in a lowering of the mass of bead available for dissolution.

7.1.5.3 Discussion of the Results

7.1.5.3.1 The Variation in the Amount of Organic Material Precipitated

It would be expected that the maximum of organic material would be precipitated at a point near the highest TOC level, and this is seen. The amount of material precipitated then falls rapidly until the resin has dissolved, whereupon the rate of fall of mass of organic material precipitated slows. Since the organic material consists of organic acids, this result shows that these organic

212

acids are at their maximum concentration in the reaction solution during resin dissolution.

TABLE 7.3

SOLUBILITIES IN WATER OF SOME ORGANIC BARIUM COMPOUNDS [102]

Compound	Formula	Solubility (g) in 100 cm^3 cold water
Barium oxalate	BaC_2O_4	0.0093
Barium tartrate	$BaC_4H_4O_3.H_2O$	0.026
Barium citrate	$Ba_3(C_6H_5O_7)_2.7H_2O$	0.0406
Barium malonate	$BaC_3H_2O_4.H_2O$	0.143
Barium formate	$Ba(CHO_2)_2$	27.26
Barium acetate	$Ba(C_2H_3O_2)_2$	58.8

7.1.5.3.2 The Variation in the Amount of Barium Sulphate Precipitated

The results shown in Figure 7.20 suggest the following processes occur during resin dissolution. As the resin bead is dissolved, more and more sulphonic acid groups will be exposed to oxidation by ·OH radicals. On oxidation by ·OH, each sulphonic acid group is cleaved from the benzene backbone of the resin, and forms a SO_4^{2-} group in solution which is detected by the addition of $BaCl_2$ solution. As the resin beads are dissolved, the rate of SO_4^{2-} release decreases, until there are no undissolved resin beads left, and no more SO_4^{2-} is released into the resin reaction solution. The plateau reached for SO_4^{2-} in solution indicates that all the S released by the dissolution of the resin beads is in the form of SO_4^{2-}, and not as part of the organic molecules in solution. If some S had been incorporated into the organic molecules present in the reaction solution, it would be expected that as these molecules were degraded by Fenton's reagent attack, more SO_4^{2-} would be seen in solution. Therefore, by the time that all solids have been dissolved, all sulphonic acid groups have been converted to sulphate.

FIGURE 7.21

**Graph showing the relationship between pH and
time in the standard resin digestion reaction**
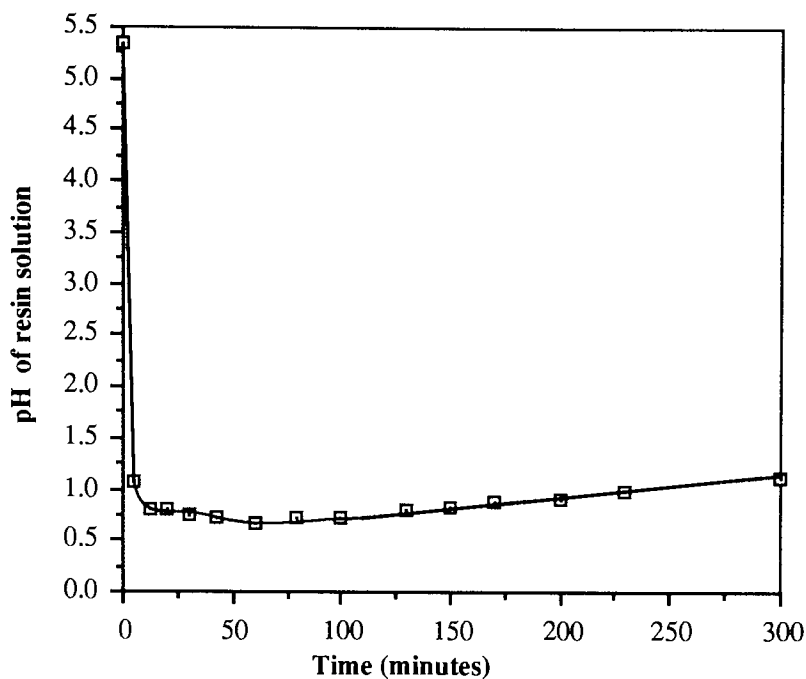
FIGURE 7.22

**Graph showing the relationship between pH and time in
the standard resin digestion reaction (pH scale expanded)**

Gradient of Dashed Line =
$y = 0.54 + 1.91\text{e-}3x$ $R^{\wedge}2 = 0.999$

214
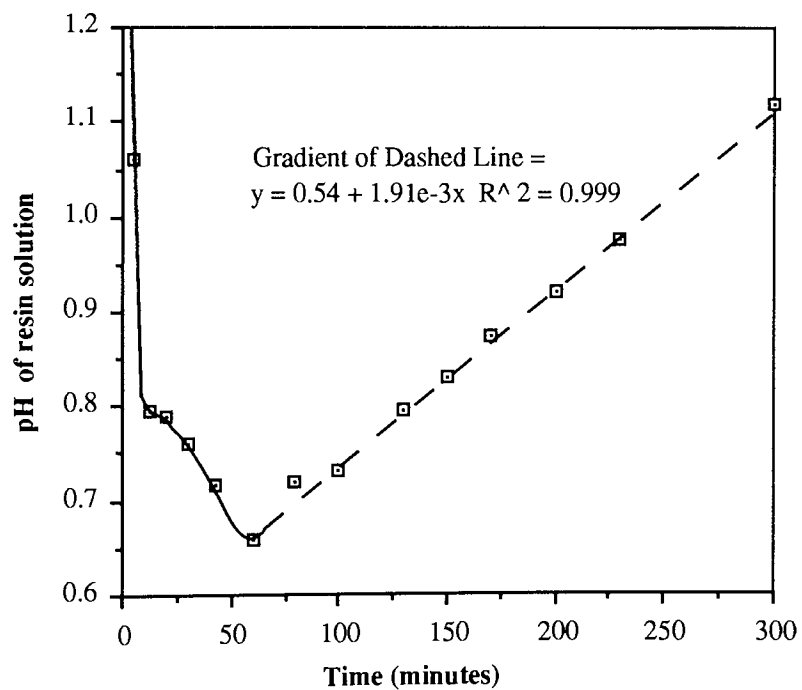
The initial rapid fall in pH, seen in Figures 7.21 and 7.22, is presumably related to the formation of H_2SO_4, created by the release of SO_4^{2-} into solution (see Section 7.1.5). This rapid fall is probably then slowed by three effects:-

a) The reduction in the rate of SO_4^{2-} release from the bead, as the surface area of the bead falls.

b) Organic acids formed by the degradation of the resin acting as buffering agents.

c) The fact that pH is a logarithmic scale related to the activity of $[H^+]$.

After 60 minutes the rate of SO_4^{2-} release into solution has slowed sufficiently for the buffering effect of the organic acids to become the dominant factor determining the change of the pH of the resin destruction solution. Soon after this point the pH rises linearly until the end of the observed stages of the process, as more and more buffering agents are produced. If the activity coefficient of H^+ does not vary markedly over this period, then the rate of loss of H^+ is first order (remembering that pH is a logarithmic scale).

7.1.6.1 Calculation of the Expected Minimum pH in the Resin Destruction Reaction

The theoretical minimum pH was calculated, based on the amount of S in the resin. It was assumed that all S was in the form of SO_4^{2-}, and there was a negligible buffering effect of organic acids at the point of minimum pH.

7.1.6.1.1 Experimental Details

10 g of resin was reacted with 140 cm^3 of H_2O_2 in 400 cm^3 of water, with 0.13 g of $FeSO_4.7H_2O$ (the catalyst).

7.1.6.1.2 Calculations

S content of the resin (from elemental analysis) = 4.64%

Mass of S in the resin = 0.464 g

Assuming all S in the solution is in the form of SO_4^{2-}, the mass of SO_4^{2-} in the resin reaction solution after resin dissolution = 1.392 g

Mass of H_2SO_4 in the resin reaction solution after resin dissolution = 1.421 g

1.421 g of H_2SO_4 in 540 cm^3 of water = 0.0268 M solution of H_2SO_4

H_2SO_4 dissociates producing two protons, so the $[H^+]$ in solution = <u>0.0536 M</u>.
Assuming an activity coefficient of 1,

$$pH = - \log_{10} [H^+]$$

<u>Calculated pH = 1.27</u>

<u>Measured pH = 0.66</u>

This calculated pH value is much higher than the measured minimum pH value, a fourfold discrepancy in $[H^+]$. No explanation could be devised for this discrepancy.

7.1.7 Monitoring the Changes in Number and Quantity of Various Organic Components During the Fenton's Reagent / Resin Reaction

Samples of the resin digestion solution taken from different points in the resin destruction process were injected into a gas chromatograph. The column type was 10% Carbowax 20 m on Unisorb, with the column being heated to 150°C. Nitrogen was used as the carrier gas, with sample injections of 1 µl. Upon analysis of the results it became clear that for most of the samples all the peaks were occurring at the same position, with the relative areas of the peaks altering with time. Each of these peaks may represent either a single compound or a closely related group of compounds. In the following graph, Figure 7.23 (see overleaf), the data are classified according to peak position, which was measured as the time elapsed between sample injection and peak detection.

FIGURE 7.23

Graph showing the variation in area of eluted peak for samples taken from various stages of the resin digestion reaction and injected into a GC

Position of peaks observed on GC trace (seconds from initial injection of sample)
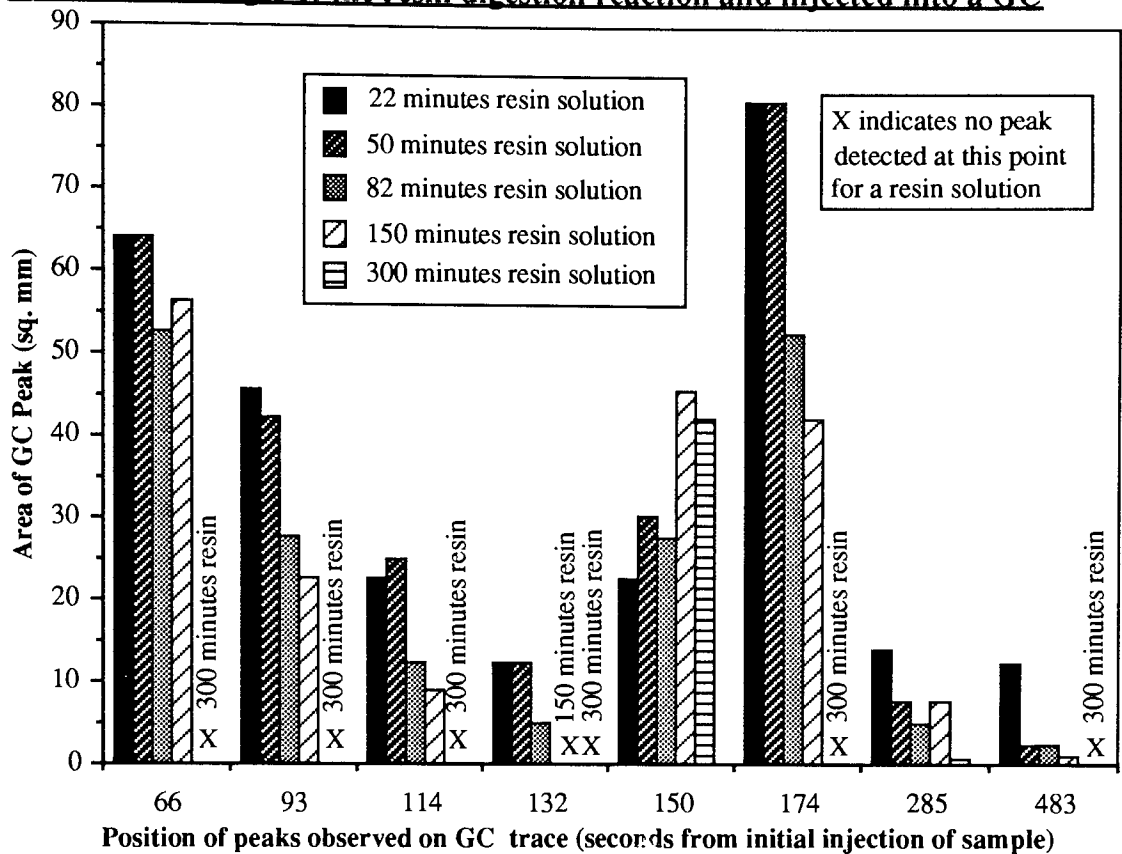
Figure 7.23 shows that 8 components were detected in 22, 50, and 82 minutes resin solution, 7 in 150 minutes resin solution, and 2 components in 300 minutes resin solution. The observed general trend of reduction of the number of components detected would be expected, as the TOC level of the resin solution falls with time and the number of components in the resin falls.

The way the area of each peak changes with each sample of the resin reaction solution (and therefore time) can be used to suggest a general reaction mechanism for the formation and destruction of the organic component associated with each peak position.

Taking the peak at **174 seconds** as an example, it can be seen that there is a large amount of the component (called, for example, "A") responsible for the peak, early on in the reaction. After 50 minutes the amount of "A" in solution falls rapidly as it is destroyed by the Fenton's reagent. This pattern of change can be related to the conversion of A into one or more different components. The peaks at **93, 114, and 132 seconds** exhibit similar behaviour to the peak at 174 seconds.

The way in which the areas of the peaks measured at **66 seconds** vary with time differs to that of the areas registered at 174 seconds. In this case the concentration of the component responsible for the peak (say, "component B"), stays more or less stable until at least 150 minutes after the start of the reaction, after which it falls rapidly to zero by the end of the reaction. This behaviour can be explained by invoking the existence of a precursor molecule, such as "A". If the component "B" is formed from "A", and "B" is destroyed at the same rate as it is formed then a stable concentration of "B" can be anticipated. After all the precursor "A" has been destroyed, the remaining "B" will be destroyed. This pattern is seen for the **66 seconds** peak and also for the **285 seconds** peak.

The variation of peak area with time for the peak at **150 seconds** is again different from that of the previously described peak positions. It can be seen that the amount of the component (say, component "C") present in the reaction mixture increases with the passing of time, until 150 minutes is reached. After this point the concentration of the component "C" appears to fall slightly when the end of the reaction is reached. It seems likely that these changes in the concentration of "C" are the result of the formation of a component relatively resistant to further attack by Fenton's reagent. Thus, assuming that the rate of degradation of C is significantly slower than its rate of formation, an increase in concentration with time would be expected, at least until the precursor of C has been completely consumed. The final disappearance of this precursor may account for the small dip in concentration of C noted between 150 minutes and 300 minutes into the reaction.

In summary, these observations can be rationalised as follows

General Reaction Pathways for Various Components, A, B, and C, of the Resin Reaction Solution
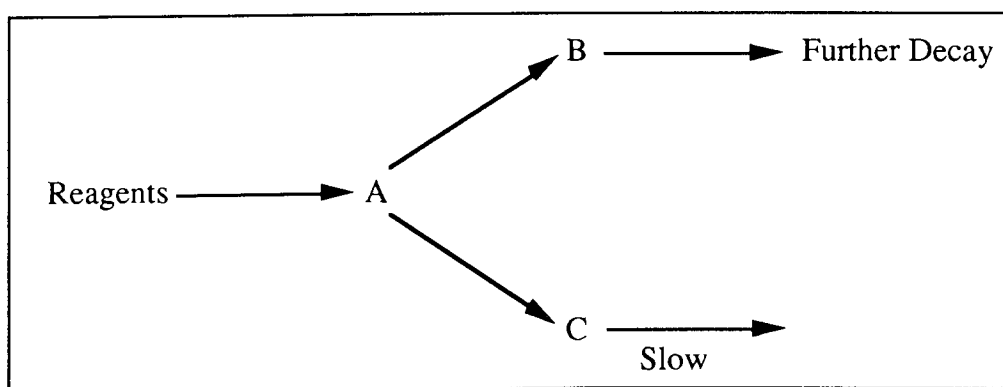
FIGURE 7.24

Graphs showing typical changes in absorbance at four different wavelengths during the standard resin digestion reaction
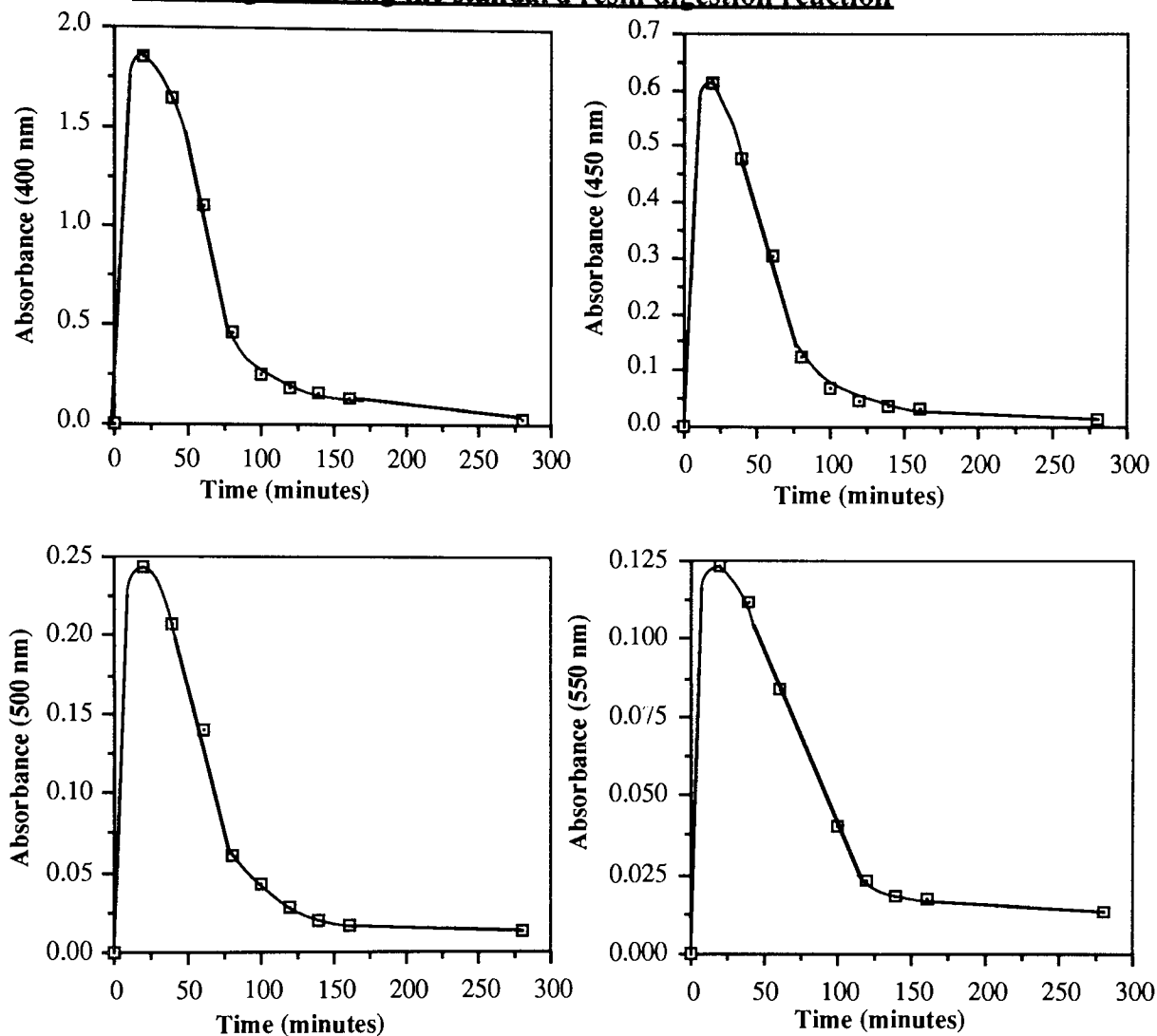
FIGURE 7.25

Graph showing the relationship between the logarithm of the absorbance (after the initial rise), and time for 4 wavelengths during the same standard resin digestion reaction
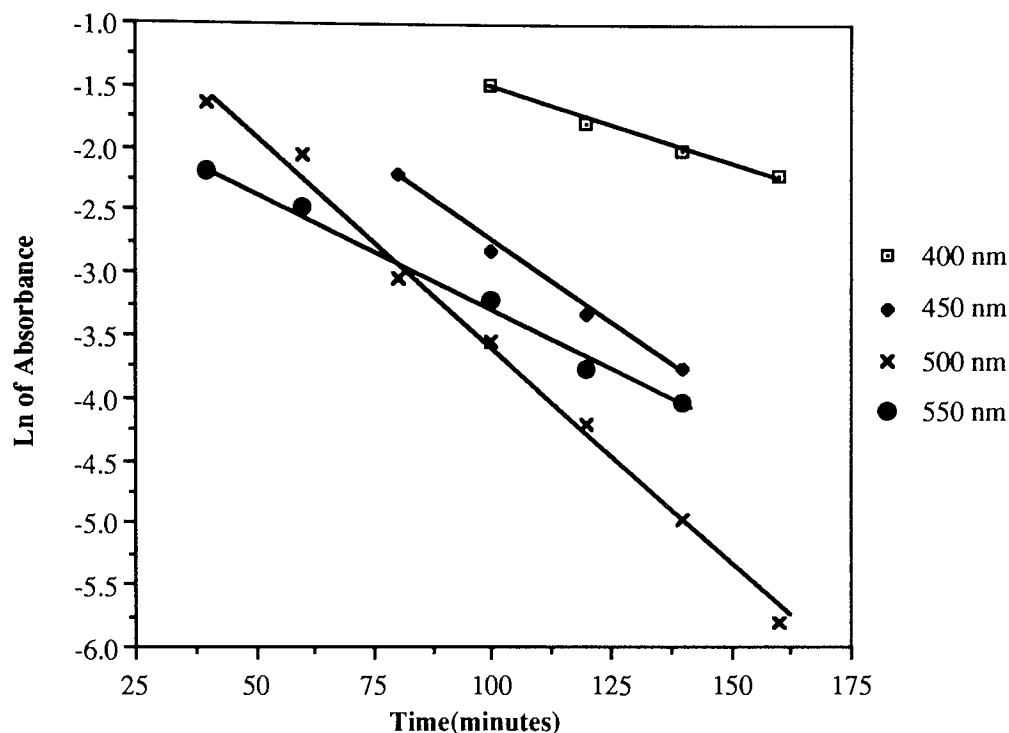
TABLE 7.4

GRADIENTS AND INTERCEPTS ON THE Y AXIS FOR A PLOT OF THE LOGARITHM OF THE CHANGE IN ABSORBANCE, AFTER INITIAL RISE HAS BEEN COMPLETED, AT VARIOUS WAVELENGTHS

Absorbance (nm)	Gradient of Line min^{-1}	Extrapolated Intercept on y axis
400	1.19×10^{-2}	-0.32
450	2.6×10^{-2}	-0.16
500	3.48×10^{-2}	-0.13
550	1.91×10^{-2}	-1.38

Figure 7.24 shows that, at all the wavelengths measured, absorbance rapidly reaches a peak at 20 minutes after the start of the reaction and then falls until the end of the reaction. Figure 7.25 indicates that the rates of absorbance fall are first order, which is in contrast to the rate of fall

220

of TOC level, which is found to be zero order (see Section 7.1.3). The changes in absorbance seen at all wavelengths are due to the creation and destruction of strongly UV / visible light absorbing organic molecules. Thus, the diference in the rate of absorbance change for each wavelength presumably indicates differential rates of destruction for different coloured organic molecules.

The absorbance rise and fall seen in all graphs is much faster than the changes in TOC level, indicating that the strongly absorbing molecules are predominantly produced in the earliest stages of the reaction, before being rapidly destroyed, as shown in Figure 7.26. Phenols and analines turn dark brown when oxidised, which is the colour of the resin digestion solution, so it seems likely that these oxidised aromatics are amongst the first molecules seen in solution after Fenton's reagent has been added to the resin beads [59]. After the concentration of these molecules has reached a peak at 20 minutes, they are rapidly oxidised, resulting in the fall in the absorbance of the resin solution.

FIGURE 7.26

Graph showing the comparison between TOC Level and absorbance for the standard resin digestion reaction
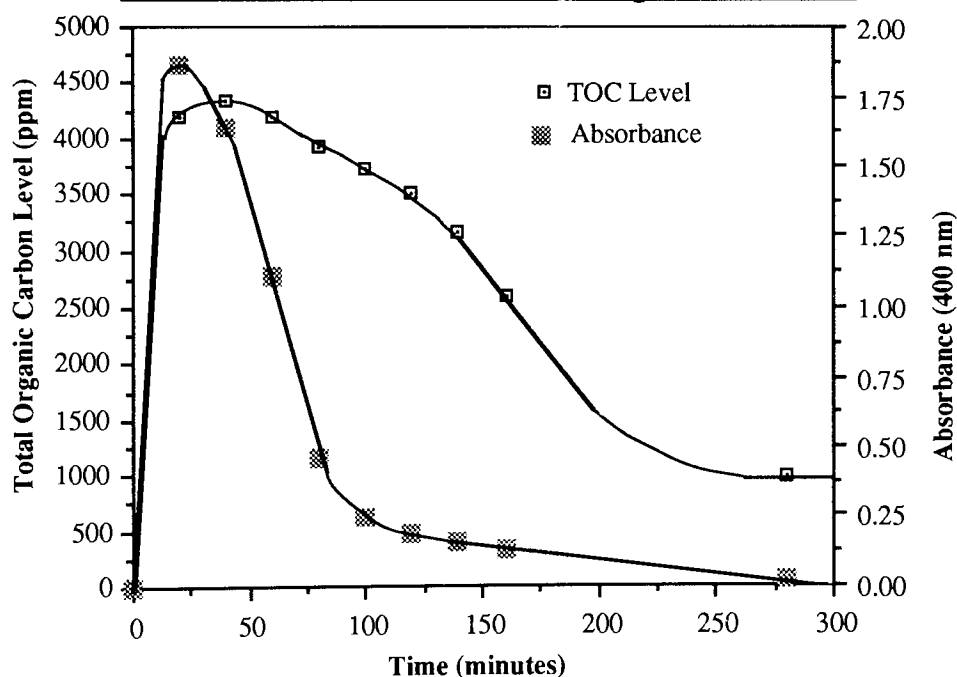
7.1.9 The Use of Spectroscopy and GC-MS to Suggest the Identity of Organic Molecules in the Resin Digestion Solution

Various approaches were used in the spectroscopic analysis of the resin digestion solution. Different approaches were necessary because of two problems with spectroscopic analysis of the resin solution. The first problem is that there is a large variety of components in the resin solution. This makes it hard to decide which molecules are present. The second problem is that the organic molecules to be analysed are in aqueous solution, which makes standard analytical techniques such as IR spectroscopy and GC-MS very difficult to use.

The first approach taken was to attempt to separate out various components of the resin digestion solution, followed by analysis of these components. By using this method a reduction in the number of components to be analysed at any one time occurs, and also analysis of the components could be carried out in a non-aqueous environment The second approach taken was to remove the water from the resin solution by evaporation, leaving behind only the non-volatile organic portion of the resin solution. This organic matter could then be analysed by techniques such as IR, which cannot be used in the direct analysis of the aqueous solution. Finally, two reaction solutions were analysed directly by NMR and GC-MS at different times during the reaction. The first reaction analysed was that between Fenton's reagent and Lewatit ion-exchange resin, whilst the second reaction analysed was that between Fenton's reagent and CALIX.

7.1.10 The Extraction of an Organic Component from the Resin Solution by Use of an Immiscible Organic Solvent

It was decided to try to extract some organic components of the resin solution by shaking the aqueous resin solution with various immiscible organic solvents (the solvents were then dried over anhydrous $MgSO_4$.

Carbon tetrachloride, benzene, toluene, dichloromethane, chlorobenzene, and nitrobenzene were each separately shaken for half an hour with each of the resin solution samples. After this had been done samples of each solvent were injected into a GC to see if any organic solute was present. Upon analysis of the GC traces it was found that no components of any of the various resin samples could be detected in the organic solvents. However, it was noted that when

nitrobenzene or chlorobenzene was shaken with some of the resin solutions a large amount of an orange / yellow precipitate (called "X" from this point onwards) was formed at the junction between the resin solution and the organic solvent. Since the organic solvent was pure (HPLC grade) it was decided that X must represent material originating in the aqueous resin solution. The largest amounts of X were seen in the 33 and 75 minute resin samples, with very little X being observed in 123 minutes resin sample, and no X at all in samples from later in the resin reaction. X was separated from the resin solution / organic solvent mixture by centrifugation and use of an eyedropper.

7.1.10.1 Possible Explanations for the Formation of X

1) X may be produced by very slightly soluble organic molecules being forced out of a saturated organic / aqueous solution by the dissolution of a small amount of chloro / nitrobenzene in the aqueous layer (although these solvents are 'immiscible' in water, a small fraction of the solvent will always mix with the water). A similar effect is seen when NaCl is added to a saturated solution of an organic compound in aqueous solution (the use of NaCl in this manner is known as "salting out").

2) The chloro / nitrobenzene may have extracted a component that is undetectable when the solvent is analysed by GC. The absence of this component in aqueous solution may result in X becoming less soluble in water, causing it to precipitate out.

3) Particular properties of the organic solvent / water interface may encourage nucleation of X around solvent droplets in the aqueous layer, resulting in the precipitation of X.

Insufficient information was available to decide which of these explanations was the most probable.

7.1.10.2 Physical Properties of X

X is a yellow / orange sticky substance that was found to dissolve in ethanol, acetone, THF and DMF. It did not appear to dissolve to any significant extent in nitrobenzene, chlorobenzene, or water.

7.1.10.3 Spectral Analysis of X

X was analysed by IR, NMR, and GC-MS. NMR spectra were also obtained of a sample of the resin solution before and after it had been shaken with the nitrobenzene or chlorobenzene, to try to identify any extracted material by observing changes in the spectra.

It can be assumed that the only elements present in a compound are C, H, and O. Evidence from Section 7.1.5 indicates that S is not present in any organic molecule in solution after 75 minutes from the start of the reaction. X could be extracted from resin samples taken after this time, indicating there was no S in the substance X.

7.1.10.4 NMR Analysis

FIGURE 7.27

PROTON AND CARBON-13 NMR SPECTRA OF 'X'
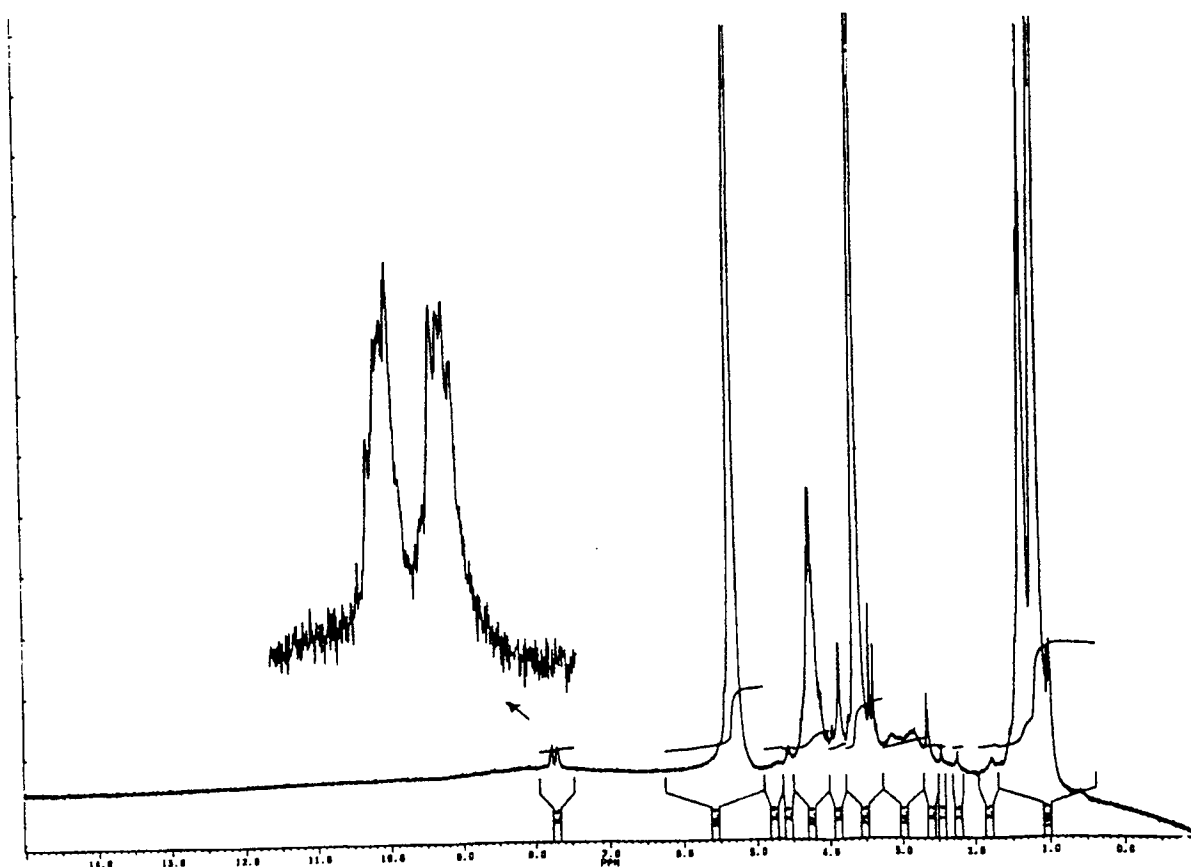
Proton NMR
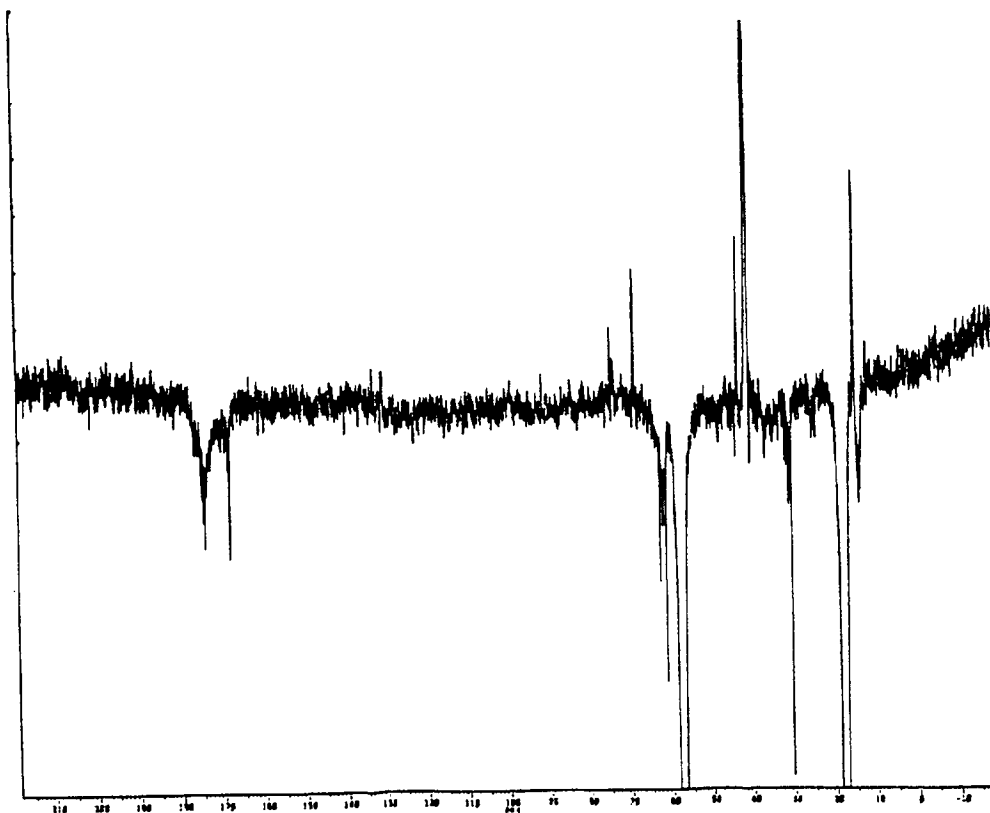
Carbon-13 NMR

The first observation made when the ^{1}H NMR spectrum is studied is that there is only a very small aromatic peak present. Thus, X consists mainly of an aliphatic compound/s containing C,H, and O. Tables 7.5 and 7.6 (see overleaf) detail the functional groups which NMR analysis suggests may be present in X.

TABLE 7.5
ATTRIBUTION OF PROTON NMR PEAKS TO
FUNCTIONAL GROUPS OF 'X'[107]
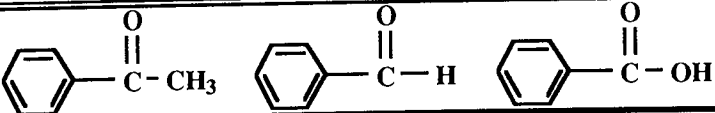
PPM (^{1}H), δ	Possible Identity of Group
1	$CH_3\text{-}CH_2\text{-}R$
1.1	$\text{-}CH_2\text{-}CH_2\text{-}R$
1.3	$\text{-}CH_2\text{-}CH_2\text{-}R$
1.8	$\text{-}CH_3\text{-}C\text{=}C$
2.25	$\text{-}CH_2\text{-}C(\text{=}O)H,\ \text{-}CH_2\text{-}C(\text{=}O)R,\ \text{-}CH_2\text{-}C(\text{=}O)OH$
2.45	$\text{-}CH\text{-}C(\text{=}O)H,\ \text{-}CH\text{-}C(\text{=}O)R,\ \text{-}CH\text{-}C(\text{=}O)OH$
2.7, 3.0	May be primary alcohol
3.4	$\text{-}CH_2\text{-}OH$
3.6	$\text{-}CH\text{-}OH$
3.9	$\text{-}CH\text{-}OH$
4.3	$\text{-}C\text{-}OH$
1 to 5.2 [108]	The primary alcohol signal may appear anywhere from 1 to 5.2 ppm
5.4	$\text{-}C\text{=}CH_2$ [108]
7.7	

TABLE 7.6
ATTRIBUTION OF CARBON-13 NMR PEAKS TO
FUNCTIONAL GROUPS OF 'X' [107]

PPM (^{13}C), δ	Possible Identity of Group
15	-CH$_2$-
17	CH$_3$-
18	-CH$_2$-
30	-CH$_2$-
31	-CH$_2$-
40	-CH-
44	-CH-
57	-CH$_2$-, Alcohols
61	Alcohols
63	Alcohols
68	Alcohols
74	Alcohols
168	RCOOH, R-C=C-COOH
174	RCOOH, R-C=C-COOH

Summarising the results displayed in Tables 7.5 and 7.6, NMR indicates that X consists of several components that include alkane, alkene, alcohol, and carboxylic acid groups in their structure. Other groups that may also be present are aldehydes and ketones.

FIGURE 7.28

PROTON NMR SPECTRA OF A RESIN DIGESTION SOLUTION BEFORE AND

AFTER EXTRACTION OF 'X'
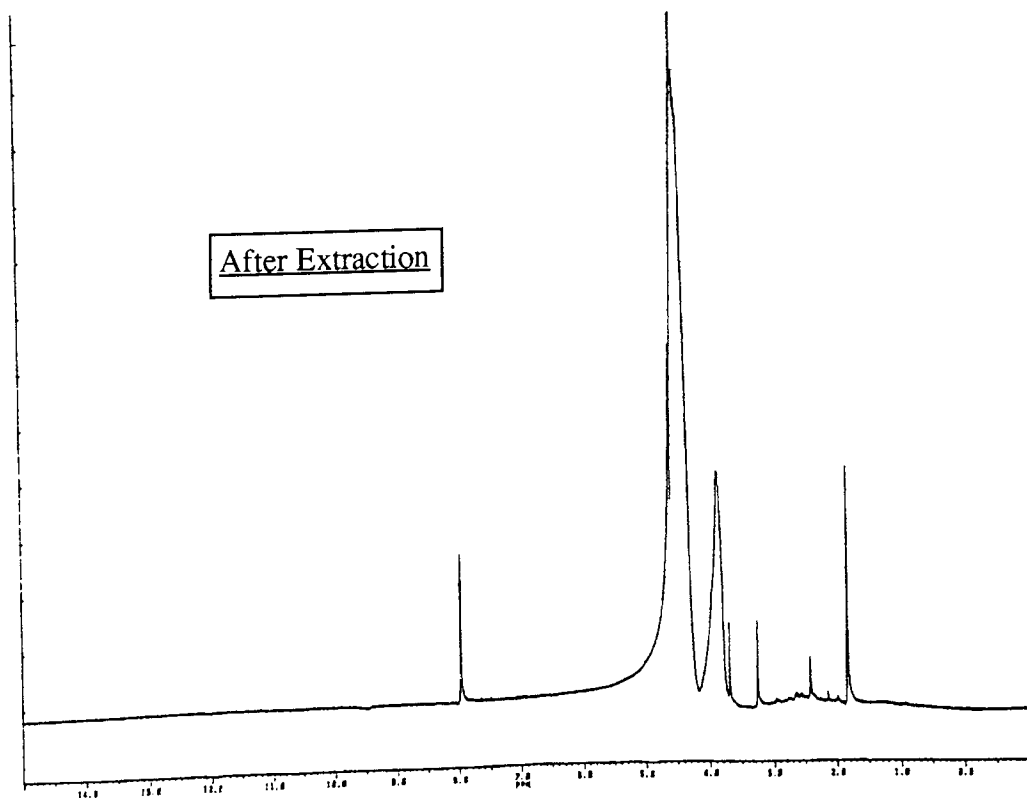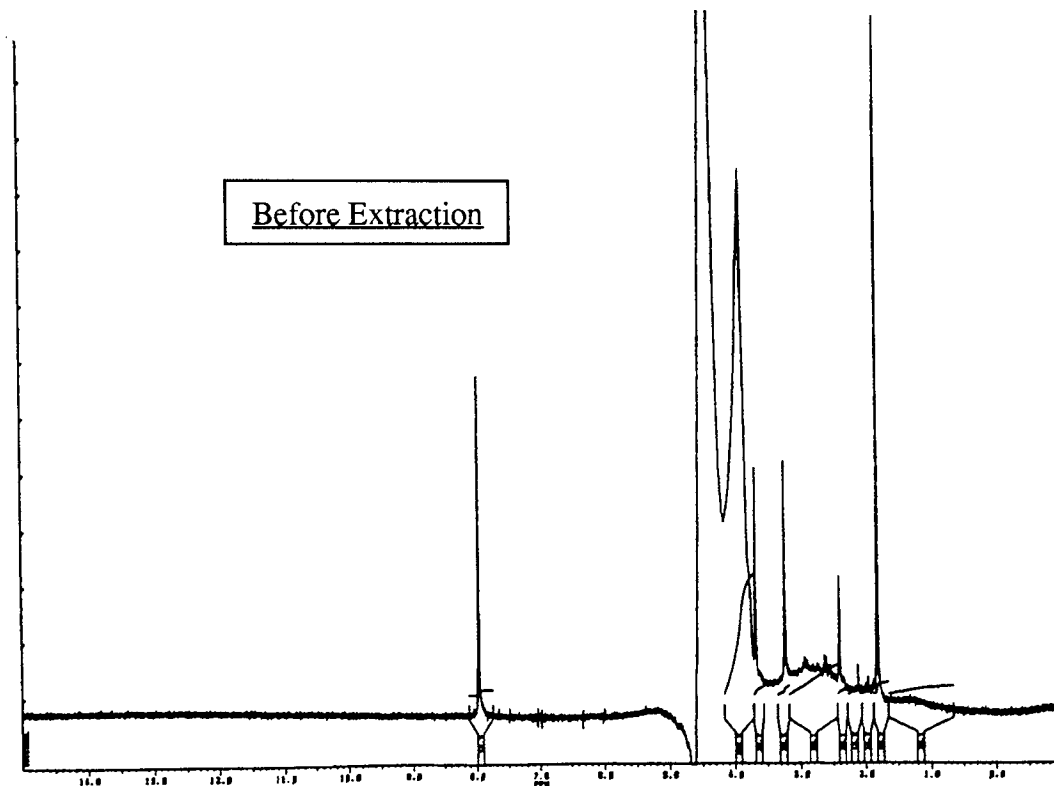
FIGURE 7.29

CARBON-13 NMR SPECTRA OF A RESIN DIGESTION SOLUTION BEFORE

AND AFTER EXTRACTION OF 'X'
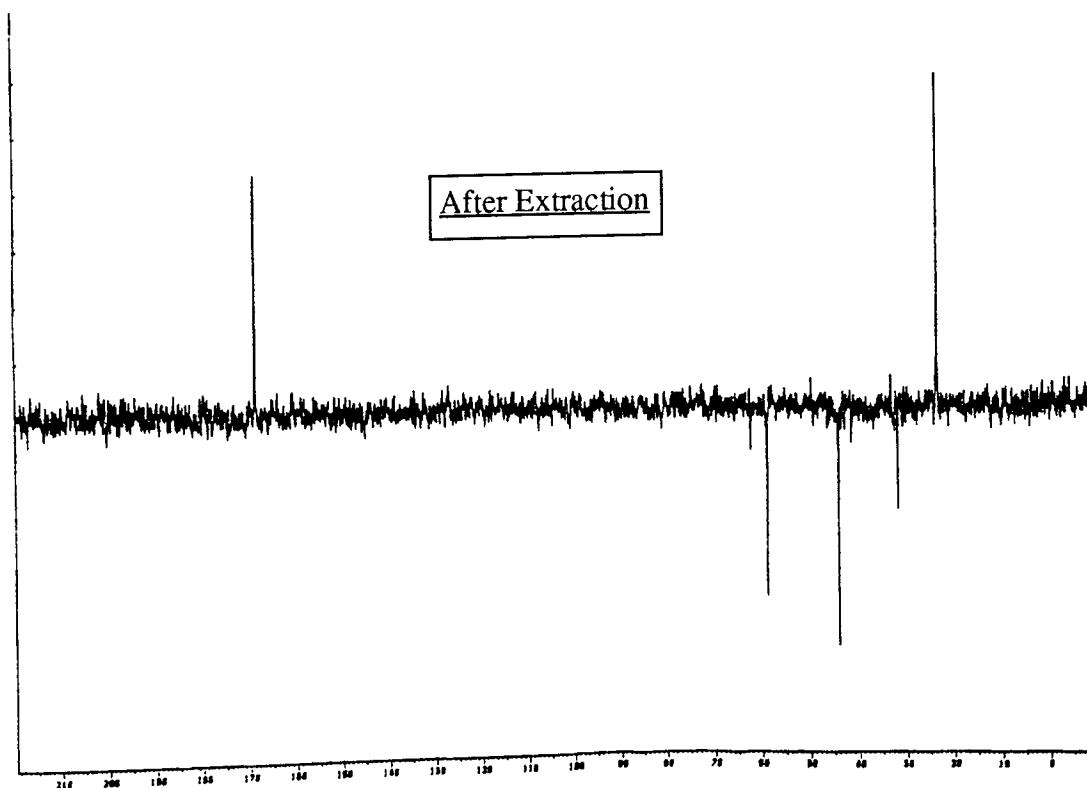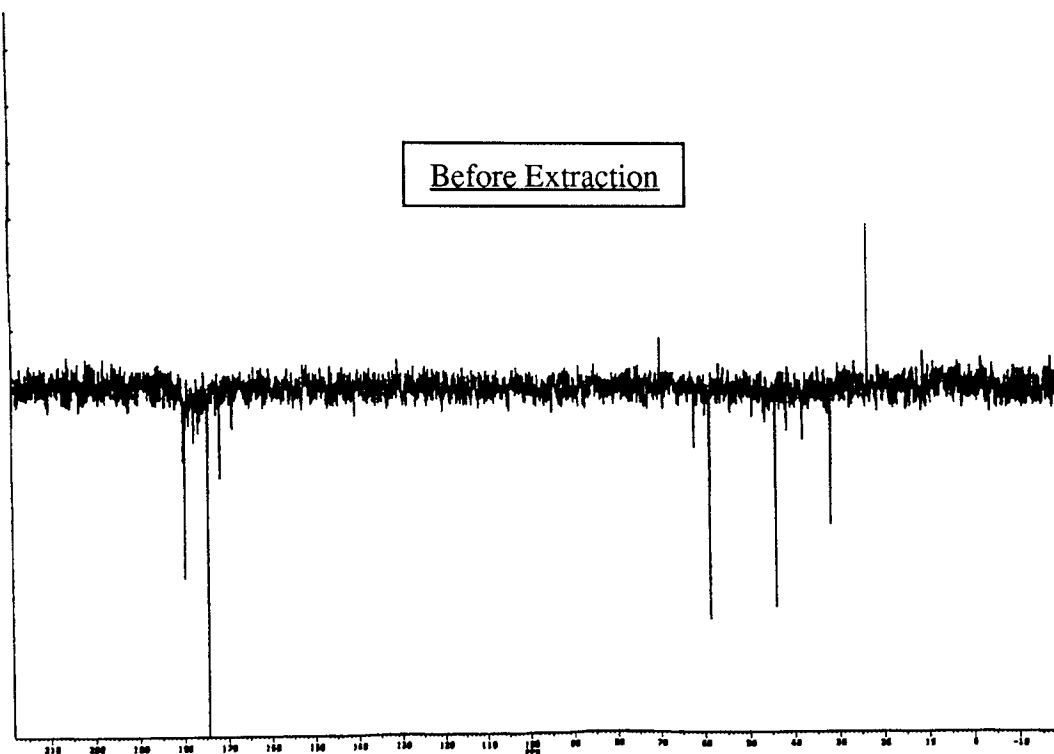
The ^{1}H NMR of the "after" spectrum appears to be identical to that of the "before" spectrum except for the large reduction in the relative size of the peak seen at $\delta = 1.92$ ppm. This suggests that X largely consists of the material responsible for the peak at this point. The peak of 1.92 ppm probably represents $-CH_2-C=C$ i.e., compounds with an alkene group have been extracted from the resin solution, forming X.

The ^{13}C NMR of the "after" spectrum is again rather similar to that of the "before" spectrum. It can be seen that the peak at 25 ppm has grown smaller in the "after" spectrum. In my spectra, 25 ppm represents the groups CH_3 or CH, so the reduction in the peak size may indicate that material with a C-C backbone has been removed. However, unlike in ^{1}H NMR, the size of the peaks in ^{13}C NMR are not necessarily an indication of the concentration of the species represented by the peak (due to the nuclear Overhauser effect). This means that the observations of peak size change in ^{13}C NMR must only be tentatively related to changes of concentration of species in solution.

Four peaks ranging from 169 to 179 ppm are absent from the [13]C "after" spectrum. The absence of these peaks may represent the extraction of saturated or unsaturated carboxylic acids from the resin sample.

7.1.10.6 IR Analysis

FIGURE 7.30

THE IR SPECTRUM OF 'X'
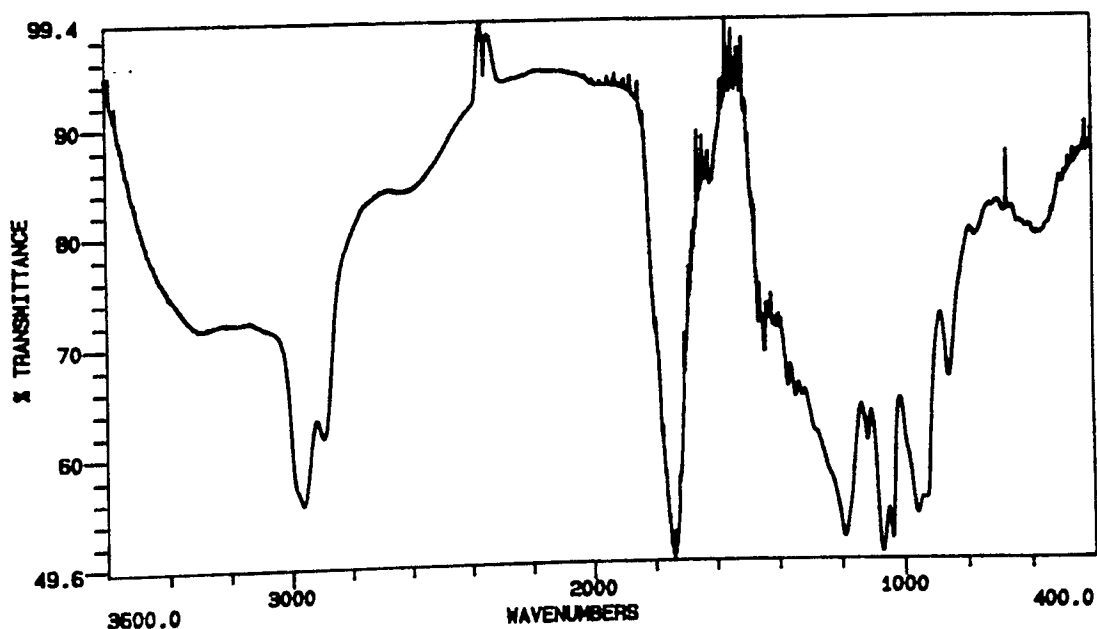
Wavenumbers (cm^{-1})	Possible Identity of Group	Notes
3500	Alcohol, alkane, alkene	Intermolecular bonded alcohol
2950	Aldehyde, carboxylic acid, alkane	Carboxylic acid is a dimer
2850	Aldehyde, alkane, carboxylic acid	Carboxylic acid is a dimer
2600	Carboxylic acid	Carboxylic acid is a dimer
1750	Aldehyde, ketone, carboxylic acid	
1450	Carboxylic acid, sulphonate	
1200	Alcohol, sulphonate, ketone	Saturated tertiary or highly symmetrical secondary alcohol, dialkyl ketone indicated
1150	Sulphonate, alkane, alcohol, ketone	Secondary or tertiary alcohol indicated, dialkyl ketone
1100	Alcohol, alkane	α-unsaturated secondary
1050	Alcohol, alkane	Unsaturated tertiary alcohol
950, 900, 850	Alkane, alkene, carboxylic acid	Carboxylic acid is a dimer
800	Alkene	Trisubstituted alkene
600	Ketone[102], carboxylic acid[102]	Carboxylic acid, straight chain betwen C_4 and C_{14}

Summarising the results shown in Table 7.7, IR spectroscopy indicates that X may consist of components that include alkanes, alkenes, alcohols, carboxylic acids, aldehydes and ketones (all aliphatic) in their structure.

7.1.10.7 Summary of the Spectrometric Analysis of the Precipitate X

The NMR and IR spectra indicate the presence of several functional groups in the precipitate X. These groups include alkanes, alkenes, alcohols, ketones, aldehydes, and carboxylic acids. The group $-CH_2-C=C-$ appears to be a major component of X. With the aid of the spectroscopic data, it was then possible to suggest specific structural formulae for the separate components of X that were analysed by mass spectroscopy.

7.1.10.8 GC-MS Analysis of 'X'

FIGURE 7.31

THE GC SPECTRUM OF 'X'
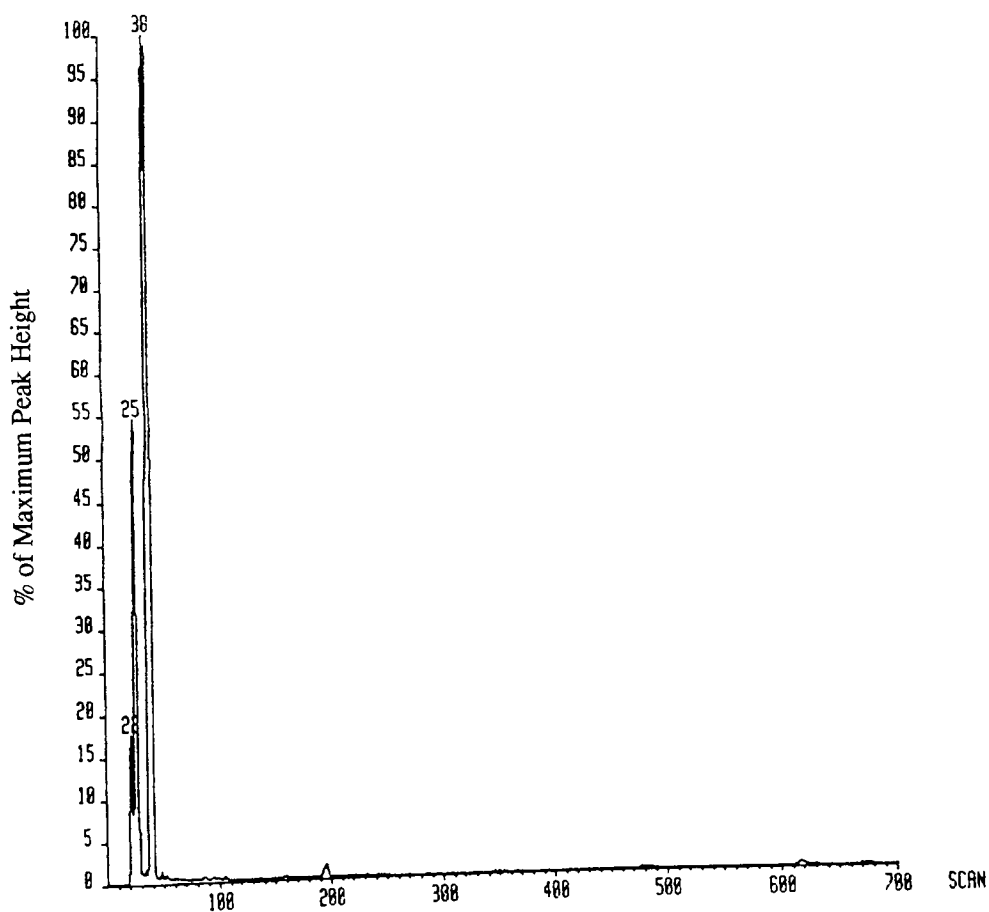
FIGURE 7.32

THE GC SPECTRUM OF X (Y AXIS EXPANDED)
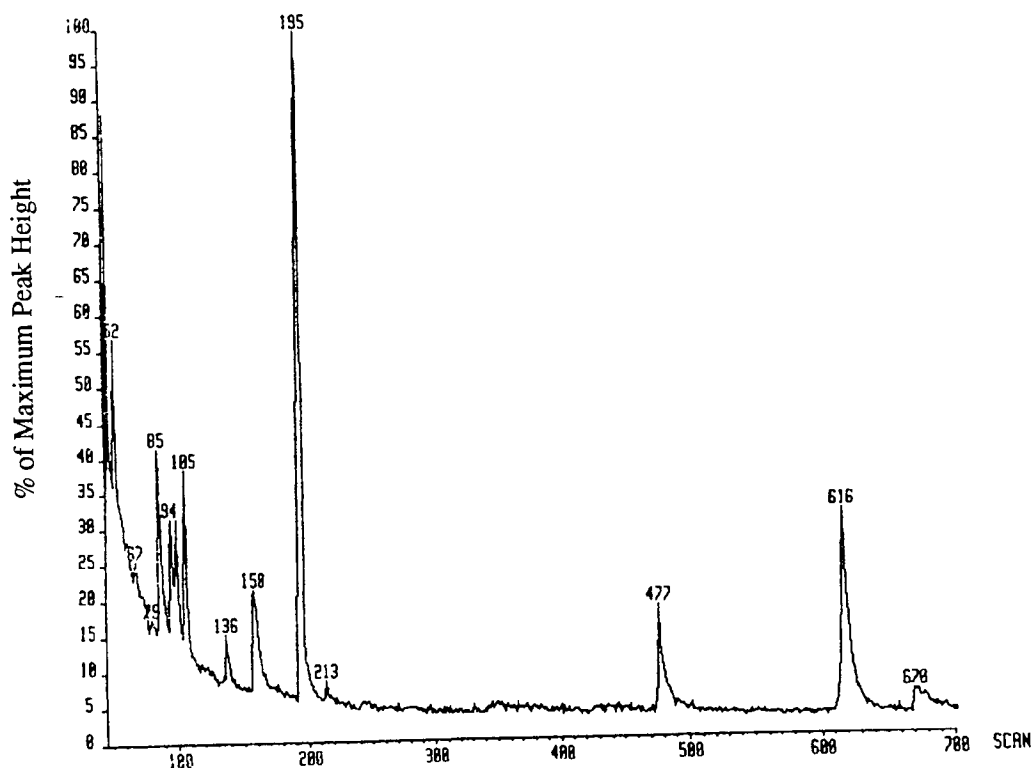
X was sent for GC-MS analysis[34]. Figure 7.31 suggests that X is a mixture of three major

components, whilst Figure 7.32 shows that thirteen more minor components of X were separated

by the GC column of the GC-MS. Five of the components separated by the GC-MS column were

studied further. These components, in order of abundance, were separated at the 38, 25, 22, 195,

and 616 scan positions.

As before, it was assumed that only C, H, and O were present in the components analysed. Since

the NMR results (e.g. Figure 7.27) indicated that only a small amount of aromatic material was

present in X, the components detected at 22, 25 and 38 scans were assumed to be aliphatic in

nature, with the components at 195 and 616 scans being either aliphatic or aromatic in nature.

It was assumed that, since the reaction mixture was heated to 95°C, only organic molecules with

boiling points higher than about 50°C would be present in significant concentration.

Finally, where identifications of compounds present in X are made in later sections, potential

structural isomers of the compound are omitted for the sake of brevity e.g. butan-1-ol would be

mentioned, but not butan-2-ol, butan-3-ol etc.

FIGURE 7.33

THE MASS SPECTRUM OF THE COMPONENT SEEN

AT THE 22 SCAN POSITION
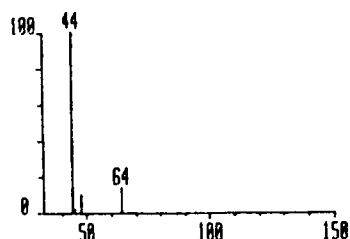
The highest mass peak in the spectrum has a m/e = 64, and it was assumed that this was the molecular ion. The only plausible organic assignments that could be made for this mass, given the C:H:O ratios likely to occur, are $[C_6H_8O_3]^{2+}$, or (less likely) $[C_7H_{12}O_2]^{2+}$.

The largest peak in the spectrum has a m/e = 44. This is the mass of the fragment

m/e = 44
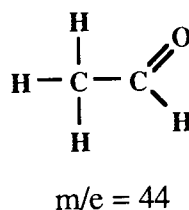
which is commonly produced when straight chain aldehydes fragment [107]. This is tentative evidence that the parent molecule is an aldehyde.

7.1.10.10 Identification of the Component at the 25 Scan Position

FIGURE 7.34

THE MASS SPECTRUM OF THE COMPONENT SEEN

AT THE 25 SCAN POSITION
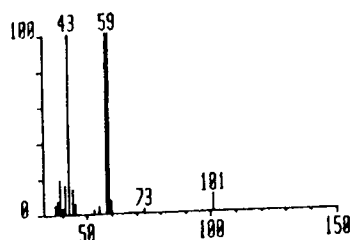
The highest mass peak seen in the mass spectrum, 101, must be a fragment as it has an odd number. Assuming that an H atom has been lost to give the fragment, the component at the 25 scan position can be regarded as a fragment of a molecule of relative molecular mass 102. All possible combinations of C, H, and O were considered for this mass number. Possible molecular formulae are $C_4H_6O_3$, $C_5H_{10}O_2$, and $C_6H_{14}O$, but given the starting material of the reaction (Lewatit ion-exchange resin) and the oxidising reaction environment, it is likely that short chain, highly oxidised molecules will be formed. Therefore compounds with the molecular formula $C_4H_6O_3$ are those which are most likely to be formed.

Several possible constitutional isomers occur for this molecular formula The most likely candidates (based on NMR, IR, boiling point data, and possible reaction mechanisms) are :-

a) 2-Oxo Butanoic acid

b) Butanaloic acid

c) 1-Hydroxy Butenoic acid

d) 3-Hydroxy Butandi-al
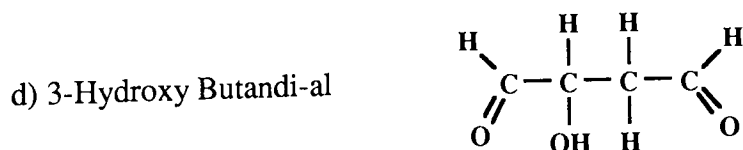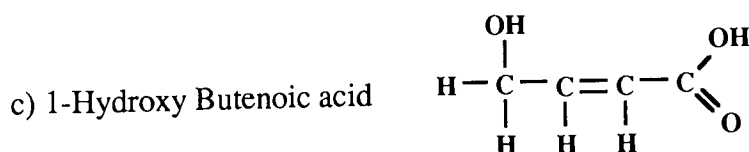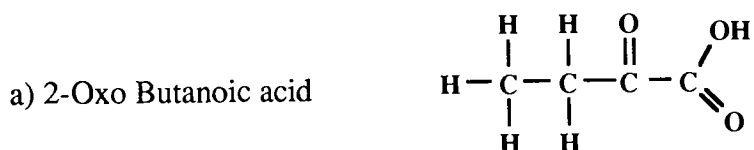
The two largest peaks in the mass spectrum, at 43 and 59 mass units are very probably the fragments

m/e = 43   and   m/e = 59
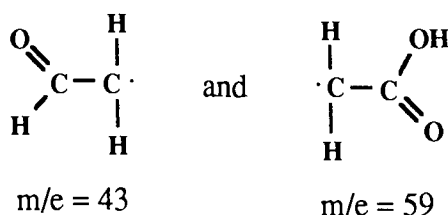
strongly suggesting that the molecule **butanaloic acid,** has split into the two fragments seen above.

7.1.10.11 Identification of the Component at the 38 Scan Position

FIGURE 7.35

THE MASS SPECTRUM OF THE COMPONENT SEEN

AT THE 38 SCAN POSITION
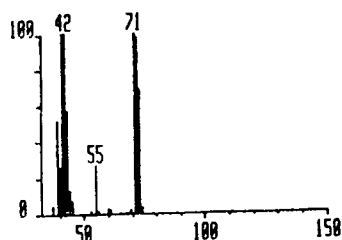
The highest peak seen in the mass spectrum, 71, must be a fragment as it has an odd number. Assuming that an H atom has been lost to give the fragment, the component is a deprotonated fragment of a molecule of relative molecular mass 72. $C_3H_4O_2$ and C_4H_8O are possible molecular formulae, with the former being more likely (due to the reaction conditions, as described previously).

$C_3H_4O_2$ - three possible constitutional isomers with acceptable boiling points were found for this molecular formula :-

a) 2-Oxo Propanal

236

b) Propenoic acid

$$\begin{array}{ccc} H & H & OH \\ | & | & \diagup \\ C = C - & C \\ | & & \diagdown\diagdown \\ H & & O \end{array}$$

c) Propandi-al

$$\begin{array}{ccc} O & H & O \\ \diagdown\diagdown & | & \diagup\diagup \\ C - C - C \\ \diagup & | & \diagdown \\ H & H & H \end{array}$$
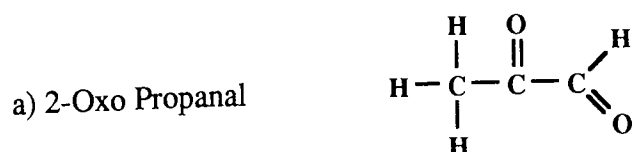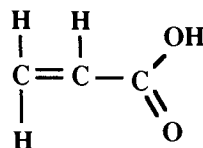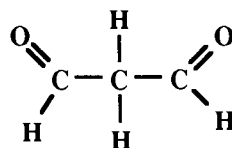
The fragment in the mass spectrum at 55 mass units is 17 mass units less than the molecular ion. This gap commonly represents the loss of OH from a short chain carboxylic acid [107] i.e., the fragment is

$$\begin{array}{ccc} H & H & \\ | & | & \\ C = C - & C\cdot \\ | & & \| \\ H & & O \end{array}$$
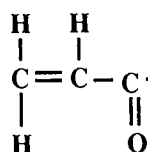
m/e = 55

and the fragment at 42 mass units is probably

$$\begin{array}{c} H \\ | \\ C = C = O \\ | \\ H \end{array}$$
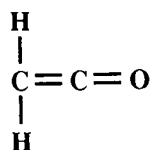
m/e = 42

Combined with data from Section 7.1.10.5, which suggests that the -CH$_2$-C=C group is common in the resin solution, this fragmentation information strongly supports the identification of **propenoic acid** as the source of the peak at 71 mass units. This identification was confirmed when it was found that the fragmentation pattern of pure propenoic acid very closely matched that seen in Figure 7.35.

FIGURE 7.36

THE MASS SPECTRUM OF THE COMPONENT SEEN

AT THE 195 SCAN POSITION
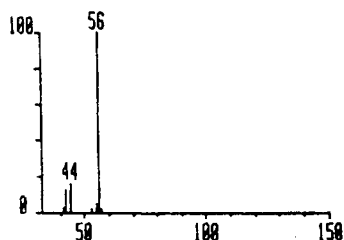
The highest mass peak in the mass spectrum, 56, may be the molecular ion. Only one possible molecular formula, C_3H_4O, and one likely conformational isomer, based on the previous IR and NMR results, could be suggested for this formula :-
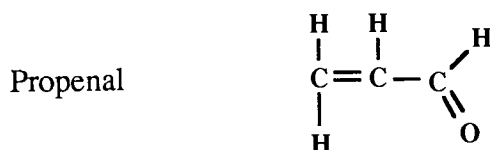
Propenal

The peak seen at 44 mass units will probably be the fragment

m/e = 44
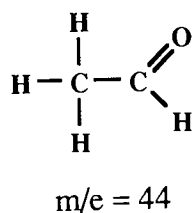
which is frequently produced when straight chain aldehydes fragment, further confirming the attribution of propenal to the peak at 56 mass units. Finally, the fragmentation spectrum of pure propenal was found to be similar to that seen in Figure 7.36.

FIGURE 7.37

THE MASS SPECTRUM OF THE COMPONENT SEEN

AT THE 616 SCAN POSITION
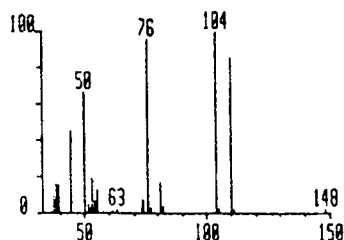
The highest peak in the mass spectrum, 148, may be the molecular ion. Possible molecular formulae are $C_4H_4O_6$, $C_5H_8O_5$, $C_6H_{12}O_4$, $C_7H_{16}O_3$, etc. Three conformational isomers of the formulae $C_4H_4O_6$ and $C_5H_8O_5$ are consistent with available NMR and IR data,

Dihydroxy maleic acid

or for $C_5H_8O_5$

a) 2-Hydroxy Pentanedioic acid
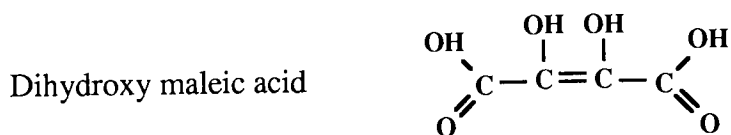
b) 2,3,4 Trihydroxy Pentandi-al
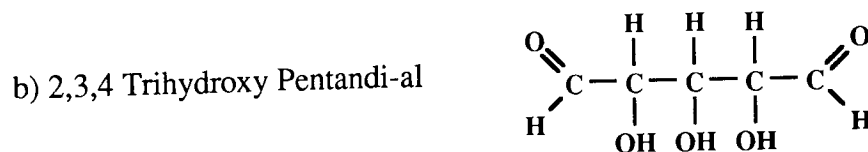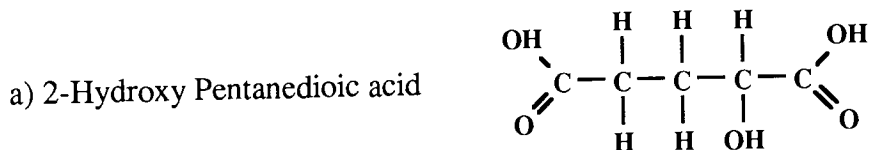
The closest fragment (in mass) to the molecular ion, 104, is 44 mass units away from the molecular ion. This difference is characteristic of the loss of the fragment

m/e = 44
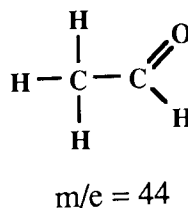
from a straight-chain aldehyde, suggesting that 2,3,4 trihydroxy pentandi-al is the molecule

239

responsible for the molecular ion [107].

The fragment at 76 mass units probably represents the loss of a C_2H_4 unit from the backbone of the 104 mass unit fragment, whilst the fragment at 50 mass units probably represents the loss of a C_2H_2 unit from the 76 mass unit fragment. The 76 and 50 mass unit fragments cannot be directly obtained from the molecular ion because other expected fragments are not seen in the mass spectrum

i.e, $148 - 76 = \underline{72}$, $148 - 50 = \underline{98}$ with no major peaks being seen at 72 or 98 mass units.

7.1.10.14 A Summary of the Results of the Analysis of an Organic Component ('X') of the Resin Solution

The precipitate X represents a major part of the resin reaction mixture. The GC-MS, NMR, and IR results show that X is a mixture. The GC-MS results have strongly indicated the identity of 4 out of the 5 major constituents of X. These are, in order of concentration (highest concentration first),

1) Propenoic acid

2) Butanaloic acid

3) May be a straight chain aldehyde ?

4) Propenal

5) 2,3,4 trihydroxy pentandi-al

7.1.11 Removal of All Water from the Resin Digestion Solution

Due to the high acidity of the resin digestion solution the first step taken before any analysis was undertaken was to adjust the pH of the solution to approximately 7 by adding $CaCO_3$ powder. The $CaSO_4$ formed was then removed from solution by filtration and centrifugation. All the water was then removed from the sample by using a combination of a rotary evaporator and a vacuum desiccator. Since a rotary evaporator operating at 50°C was used to remove the water, only organic compounds with a boiling point higher than 50°C would remain in the sample to be analysed. After all water had been removed from the sample a light brown powder remained. Some of the powder was dissolved in D_2O to obtain ^1H and ^{13}C NMR spectra, and another part of the powder was placed in a KBr disc and analysed using an IR spectrophotometer.

FIGURE 7.38

SUPERIMPOSED IR SPECTRA OF VARIOUS SAMPLES OF RESIN REACTION SOLUTION (WATER REMOVED)
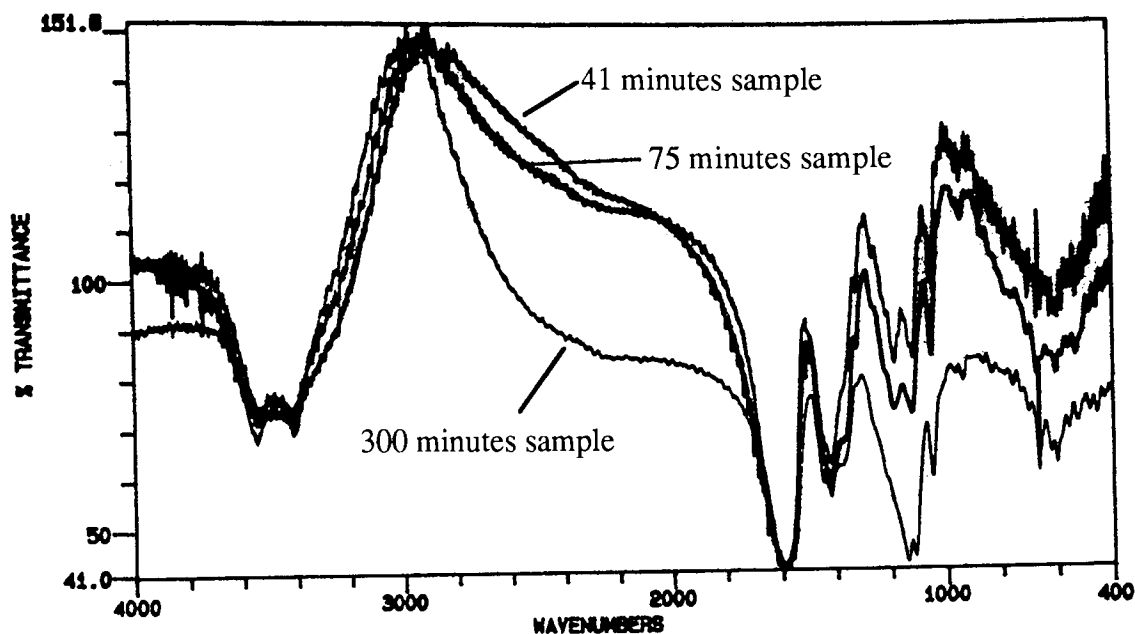
Upon close inspection of the IR spectra it can be seen that the spectra for all three samples are nearly identical. This is surprising since the resin extracts come from very different parts of the resin digestion process. 41 minutes resin solution represents a point 14% into the reaction whilst 75 and 300 minutes represent 25% and 100% into the reaction, respectively (100% represents the point when no H_2O_2 is left in the reaction solution). The similarity of spectra shows that there are similar classes of compounds present in the resin reaction solution during most of the reaction. This could mean that

a) these compounds are being constantly created, or that

b) these compounds have been created by a point 14% into the reaction and are resistant to subsequent degradation.

It would seem to be more likely that condition (a) holds, as it is difficult to imagine an organic material remaining unaltered for the large majority of the resin destruction reaction.

If ^1H NMR spectra (see Appendix 2) are inspected in a similar manner, it can be seen that the positions of the peaks stay the same in all three samples. However the size of nearly all the peaks

241

falls with time, indicatating a reduction in the concentration of the chemical groups responsible for the peaks. The only peak that does not reduce in size is the peak at 1.6 ppm, which presumably represents the aliphatic backbone of various organic molecules. The ^{13}C NMR spectra for the 41 minutes and 75 minutes resin samples are again nearly identical. The 300 minutes resin sample has fewer peaks than the other two samples, but the peaks that are visible are generally in the same location as those of the other samples.

After this initial inspection of the spectra for the resin samples, an attempt was made to assign chemical groups to portions of the spectra. It was assumed that only C, H, and O were present in any material analysed.

TABLE 7.8
ATTRIBUTION OF IR ABSORBANCE MAXIMA TO FUNCTIONAL GROUPS OF RESIN DIGESTION SOLUTION (WATER REMOVED)[107]

Wavenumbers (cm^{-1})	Possible Identity of Group	Notes
3400 to 3600 (broad)	Alcohol	Intermolecular bonded alcohol
1600	Carboxylic acid, aromatic ring	Carboxylate ion
1400	Carboxylic acid	Dimer or carboxylate ion
1200	Alcohol, ketone	Saturated tertiary or highly symmetrical secondary, dialkyl ketone
1100	Alcohol, alkane, aromatic ring	α-unsaturated secondary, aromatic is di-substituted
1000	Alkene, alkane	Vinyl alkene indicated
450	Carboxylic acid[102]	Straight chain between C$_4$ and C$_{14}$

TABLE 7.9
ATTRIBUTION OF PROTON NMR PEAKS TO FUNCTIONAL GROUPS OF RESIN DIGESTION SOLUTION (WATER REMOVED)[107]

PPM (^{1}H), δ	Possible Identity of Group	Notes
1.6	$-CH-CH_2R$, $-CH_2-C=C$	
2.16	$CH_3-C(=O)H$, $CH_3-C(=O)R$, $CH_3-C(=O)OH$	
2.91	May be primary alcohol[108]	The primary alcohol signal appears anywhere between 1 and 5.2 ppm
3.55	$-CH_2-OH$	
3.76	$-CH-OH$	
8.21	May be phenol or derivative[108]	The phenol signal appears anywere between 4 and 10 ppm

TABLE 7.10
ATTRIBUTION OF CARBON-13 NMR PEAKS TO FUNCTIONAL GROUPS OF RESIN DIGESTION SOLUTION (WATER REMOVED)[107]

PPM (^{13}C), δ	Possible Identity of Group	The samples in which peaks are seen
26	CH_3-, $-CH-$	41, 75, 300
35	$-CH_2-$	41, 75
36.5	$-CH_2-$	41, 75
43	$-CH_2-$	41, 75
44	$-CH_2-$	41, 75
49.5	$-CH-$, Alcohols	41, 75
50.5	$-CH_2-$, Alcohols	41, 75
61	Alcohols	41, 75, 300
64	Alcohols	41, 75
73	Alcohols	41, 75
173	$RCOOH$, $R-C=C-COOH$	41, 75, 300

In summary, all available spectroscopic data for the dehydrated resin samples support the hypothesis made that organic molecules with carboxylic and alcohol groups are the main constituents of these samples.

7.1.12 Direct Analysis of the Resin and CALIX Reaction Solutions

The degradation of Lewatit ion-exchange resin and CALIX (calix[8]arene-p-octasulphonic acid) was followed by NMR spectroscopy of samples taken from the respective reaction mixtures. The resin digestion solution was also analysed by injecting a sample taken from the resin reaction mixture at 53 minutes from the start into a GC-MS combination.

7.1.13 NMR Analysis of the Resin Digestion Mixture

Samples from 10, 30, 75, 105, 135, 195, 250, and 300 minutes (3% to 100% of a standard resin reaction) were analysed using ^{1}H and ^{13}C NMR.

FIGURE 7.39
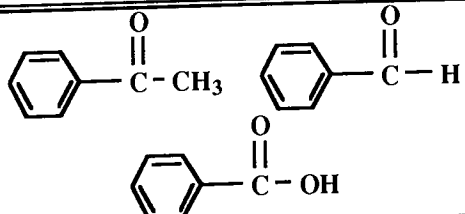
Graph showing the times when resin samples were taken for NMR analysis. (standard resin digestion reaction)
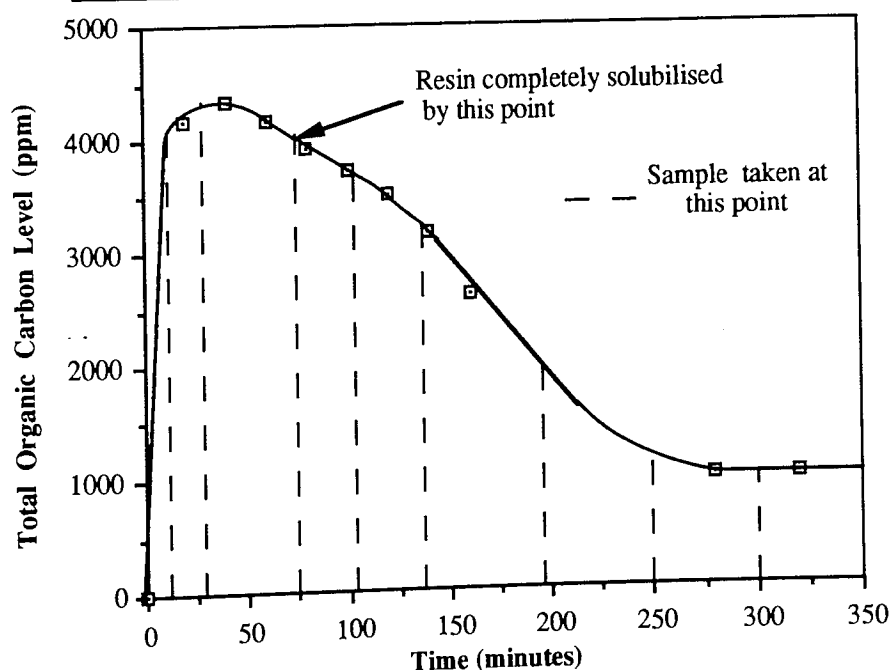
7.1.13.1 Proton NMR

All ^{1}H NMR spectra for the resin digestion reaction can be seen in Appendix 1.

244

TABLE 7.11

ATTRIBUTION OF PROTON NMR PEAKS TO FUNCTIONAL GROUPS OF RESIN DIGESTION SOLUTION[107]

PPM (^{1}H), δ	Possible Identity of Group	Samples in which peaks seen (minutes into reaction)
1.2	CH_3-CH_2R, $-CH_2-CH_2R$	10, 30, 75
1.7	$CH_3-C=C$	195
1.8	$CH_3-C=C$	10, 30, 75, 105, 135, 195, 250, 300
1.9	$-CH_2-C=C$	10, 30, 75, 105, 135, 195, 300
2.1	$-CH_2-C=C$, $CH_3-C(=O)R$, $CH_3-C(=O)OH$	10, 30, 75, 105, 135, 195, 250, 300
2.4	$-CH_2-C(=O)H$, $-CH_2-C(=O)R$, $-CH_2-C(=O)OH$	10, 30, 75, 105, 135, 195, 300
3.2	CH_3-OH	10, 30, 75, 105, 135, 195, 250, 300
3.7	$-CH-OH$	10, 30, 75, 105, 135, 195 250, 300
4.6 - 4.7	Peak due to water	
Broad band, 6 - 7.9	Mixed aromatic molecules, low concentration	30, 75, 105, 135, 195, 250
7.9		10, 30, 75, 105, 135, 195, 250, 300

7.1.13.1.1 The Peak at δ = 1.2 ppm

The peak at 1.2 ppm starts off very large, but rapidly becomes smaller, with only a small peak being left in the 75 minute resin sample. It is not seen in any sample later than 75 minutes. This suggests that the compounds responsible for this peak are produced only during resin dissolution, and are rapidly oxidised once they are free in solution.

The peak at 1.2 ppm probably represents the chemical group 'alkanes'. The only source of these at the start of the reaction would be the resin backbone (made up primarily of CH_2 groups). As the resin backbone breaks up, fragments of the backbone would be released into solution resulting in an 'alkane' NMR peak.

7.1.13.1.2 The Peak at $\delta = 1.7$ ppm

This peak is only seen in the 195 minute resin digestion sample, suggesting it may just be an instrumental artefact. This is particularly likely for this sample, as only poor quality ^1H and ^{13}C spectra were obtained for this sample.

7.1.13.1.3 The Peak at $\delta = 1.8$ ppm

This peak is the largest peak seen, in all the samples, and does not change in size throughout the reaction. This suggests that this peak represents the most important breakdown product in the resin reaction solution, throughout the whole reaction. Since it is seen throughout the reaction, and the peak position is characteristic of the group 'alkenes', the peak probably represents short chain oxidised alkenes.

7.1.13.1.4 The Peak at $\delta = 1.9$ ppm

This peak is very large in the first sample (10 minutes resin solution), rapidly reducing in size until 75 minutes is reached. After this point its size remains more or less stable. The large size of the peak early on in the reaction indicates that the compounds responsible for the peak are being produced in large quantities at the start of the reaction, during the resin dissolution. Once the resin has dissolved, after 75 minutes, the compounds are produced at a rate equal to the rate of their destruction until the end of the reaction, suggesting that they are an important intermediate in the resin destruction process.

As for the peak at $\delta = 1.8$ ppm, this peak probably represents the presence of short chain oxidised alkenes in solution.

7.1.13.1.5 The Peak at $\delta = 2.1$ ppm

This peak can be seen in all samples of resin reaction solution, but is always small. This probably means that the compound responsible for the peak is being formed constantly during the whole reaction, and is being degraded at the same rate at which it is created. The small height of this peak can be explained in one of two ways. The process by which the compound responsible for the peak is formed could be a relatively unimportant side reaction, resulting in only a small concentration of the compound at any one time. Alternatively, it may be that the compound responsible for the peak is an important breakdown product of the resin, but it is very reactive. This would result in there only being a low concentration of the compound in solution at any one time.

The peak position suggests that either alkenes, ketones, or carboxylic acids are present. These molecules could be formed during the degradation of the resin backbone, or during the ring opening of highly oxidised aromatic molecules.

7.1.13.1.6 The Peak at $\delta = 2.4$ ppm

This peak is present in all samples, but is always small. As before, this could mean either that the compound responsible for the peak is relatively unimportant, or that the compound is very reactive.

The peak position suggests that either aldehydes, ketones, or carboxylic acids are present. These would be produced by oxidation of other organic molecules in solution.

7.1.13.1.7 The Peak at $\delta = 3.2$ ppm

This peak is a medium / small sized peak in the 10 minutes resin digestion sample, gradually getting smaller until the 75 minutes sample. Its size is stable in the 105, 135, 195 and 250 minutes samples, with the peak in the 300 minutes resin sample being very small.

The size of the peak early in the reaction indicates that the compounds responsible for the peak are being produced in large quantities at the start of the reaction, as the resin is dissolving. Once the resin has dissolved, after 75 minutes, the compounds are produced at a rate equal to their destruction until 250 minutes into the reaction. After this point the parent compound/s that is/

are being oxidised to produce the compound responsible for the peak at 3.2 ppm appear finally to be depleted, resulting in the very small peak in the 300 minutes sample. The mixed aromatic compounds, seen in the broad peak from 6 to 7.9 ppm may be source of the oxidised compounds responsible for the peak at 3.2 ppm, since they are not seen after 250 minutes.

7.1.13.1.8 The Peak at $\delta = 3.7$ ppm

This peak is present in all samples, but is always small. As before, this could mean either that the compound responsible for the peak is relatively unimportant, or that the compound is very reactive.

7.1.13.1.9 The Peak from $\delta = 6$ to 7.9 ppm

This is a broad, low peak, which starts at about 6 ppm and ends about 7.9 ppm. The peak can be seen in all the samples except for the first and last resin reaction solution sample and its' size remains the same throughout the reaction. As the peak probably represents a mixture of aromatic molecules it seems that various oxidised aromatic molecules are being formed during most of the reaction.

7.1.13.1.10 The Peak at $\delta = 7.9$ ppm

This peak is very large in the 10 minutes sample, gradually reducing in size until at 135 minutes when it is quite small. After this point it stays the same size until the end of the reaction. The large size of the peak early on in the reaction indicates that at this point the compound responsible for the peak is a very important breakdown product of the resin. The subsequent fall in the size of the peak indicates that the compound is being degraded by the Fenton's reagent at this point in the reaction. However, once 135 minutes is reached the peak size appears to stabilise. Since the peak represents an oxidised aromatic compound it is difficult to imagine that the stability of the peak size is due to a constant rate of formation of the compound. Instead the peak must represent the formation of an aromatic compound that is resistant to further oxidation. Such a compound might be a ring compound with many or all its H atoms replaced by oxidised organic groups.

e.g.
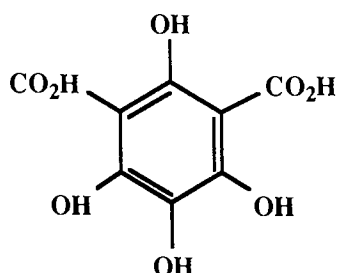
7.1.13.2 Carbon-13 NMR

All ^{13}C NMR spectra for the resin digestion reaction can be seen in Appendix 1.

TABLE 7.12
ATTRIBUTION OF CARBON-13 NMR PEAKS TO FUNCTIONAL GROUPS OF RESIN DIGESTION SOLUTION [107]

PPM (^{13}C), δ	Possible Identity of Group	Samples in which peaks seen (minutes into reaction)
23	CH$_3$, -CH$_2$-	10, 30, 75, 105, 135, 195, 250, 300
32	-CH$_2$-, -CH-	10, 75
44	-CH$_2$-, -CH-	10, 30, 75, 105, 135, 195, 250, 300
59	Alcohols	10, 30, 75, 105, 135, 195, 250, 300
169	RCOOH, R-C=C-COOH	10
172	RCOOH, R-C=C-COOH	30
174	RCOOH, R-C=C-COOH	30, 75, 195, 300
180	RCOOH, R-C=C-CH=O	30, 75, 300

The ^{13}C spectra indicate that there are alkane chains (carbon backbones of molecules) and alcohols present in all samples of the resin. In addition saturated and unsaturated carboxylic acids are seen in many of the samples, and unsaturated aldehydes may be present in 3 of the 8 resin reaction samples. Since NMR spectra show, in the main, differences in functional group in a molecule, and not chain length differences, progressive chain degradation would account

for the presence of carboxylic acids and aldehydes in some spectra but not others.

7.1.14 GC-MS Analysis of the Resin Digestion Mixture

An aqueous sample taken at 53 minutes into the standard resin digestion reaction was injected into the GC column of a GC-MS. The column was an Alltech 30 m x 0.32 mm Heliflex with bonded fused silica type RSL-300, heated to 150°C with nitrogen as the carrier gas.

FIGURE 7.40

THE GC SPECTRUM OF A RESIN DIGESTION SAMPLE
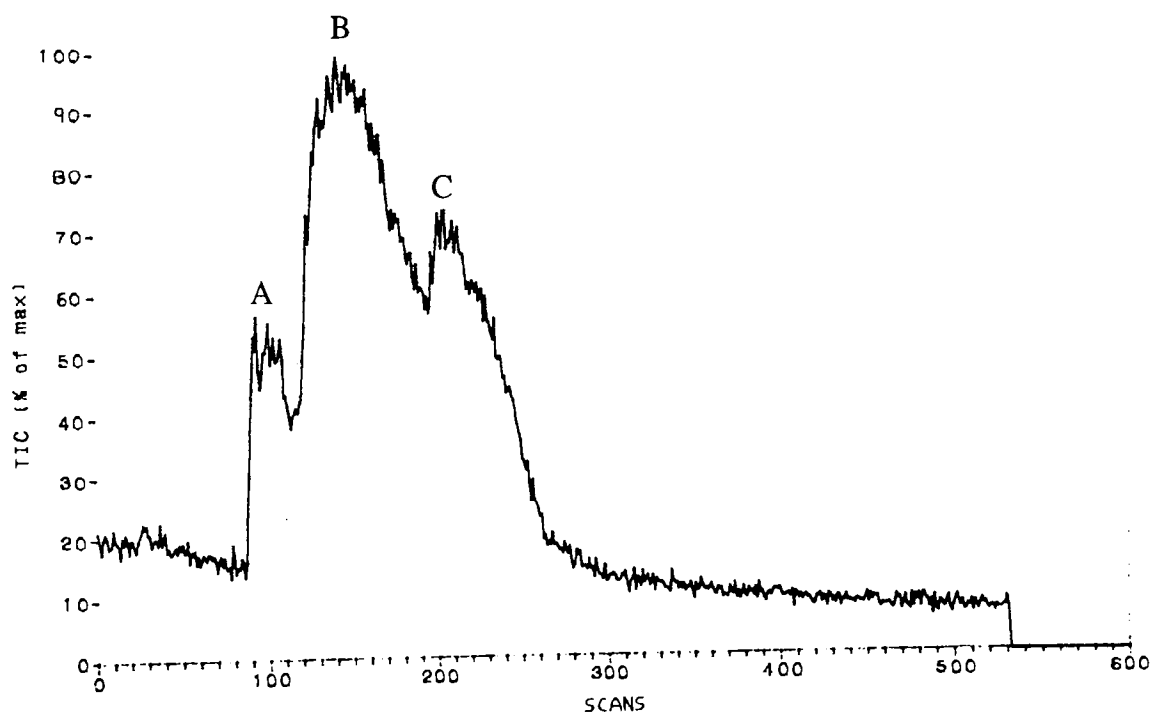
As can be seen from Figure 7.40, the GC column has not resolved the many components of the resin solution very effectively, with only three very broad, non-baseline resolved peaks being seen. Each GC peak must represent a group of components with similar boiling points and properties. Thus, when the mass spectra for each of the 3 GC peaks was analysed the fragmentation pattern were studied in an attempt to suggest the type of compound represented e.g. alcohol, carboxylic acid. It was decided to refer to the first GC peak as "A", the second GC peak as "B", and the third GC peak as "C".

The mass spectra for each of the three GC peaks can be seen to be composed of a large number of individual peaks (up to 211 peaks in one mass spectrum), which presumably reflects the large

250

number of components that were responsible for each GC peak. Fortunately, the very large majority of these peaks were small, and so these peaks were regarded as being background 'noise'.

Analytical work described in this chapter indicates the presence of several functional groups in the resin reaction solution. These groups include alkanes, alkenes, alcohols, ketones, aldehydes, and carboxylic acids. Using this information, it was possible to suggest specific structural formulae for each of the major mass spectrum peaks seen when the GC peaks "A", "B", and "C" were analysed by MS.

As before, it was assumed that only C, H, and O were present in the components analysed. It was also assumed that, since the reaction mixture was heated to 95°C, only organic molecules with boiling points higher than about 50°C should be considered when identifying mass spectrum peaks. Again, where identifications of compounds present in the resin reaction solution are made, potential structural isomers of the compound are omitted for the sake of brevity.

7.1.14.1 The Mass Spectrogram of "A"

FIGURE 7.41

THE MASS SPECTRUM OF THE GC PEAK 'A'

251
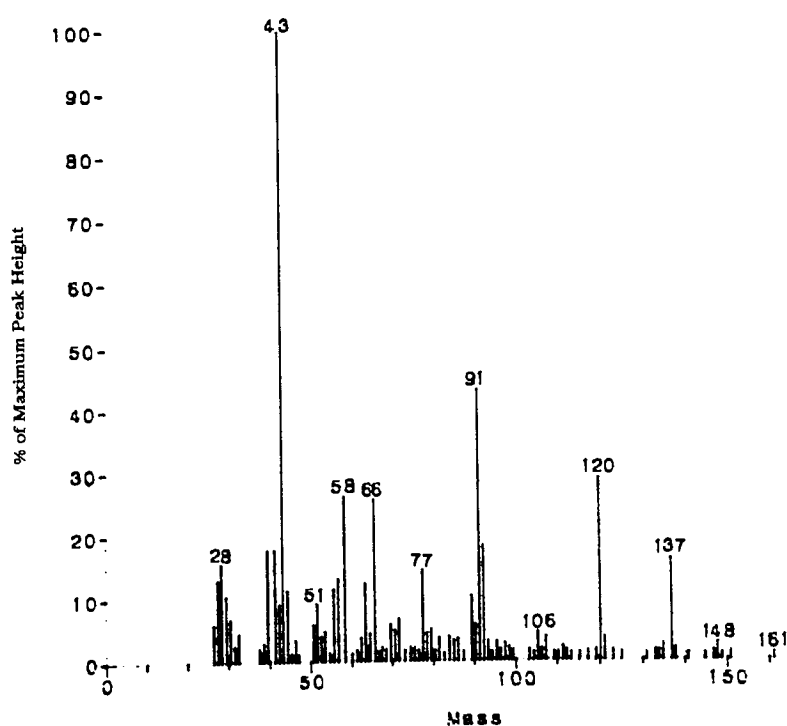
The following peaks were judged to be significantly larger than the background 'noise'.

| | 17 | 29 | 14 | 11 | 8 | 15 | 15 | Spacing between peaks |

137   120   91   77   66   58   43*   28   Larger Peaks

(* = Largest Peak)

No clear pattern was immediately discernible in the mass spectrogram of "A", suggesting that each peak is the result of a separate type of component of "A" e.g. alcohol, ketone, carboxylic acid. All peaks with odd mass numbers will represent fragments of larger molecules. In many cases the fragment will simply be a deprotonated parent molecule, whilst in other cases the fragments will be part of a much larger parent molecule.

7.1.14.1.1 The Identity of the 28 Mass Unit Peak

This peak must be that of a fragment, probably

$$
\begin{array}{cc}
H & H \\
| & | \\
\cdot C - C \cdot \\
| & | \\
H & H
\end{array}
$$
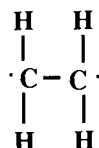
This fragment is commonly seen when a straight chain aldehyde fragments[106].

7.1.14.1.2 The Identity of the 43 and 58 Mass Unit Peaks

Only a very few combinations of C, H, and O are possible for the mass number 43. It was decided that the only fragment that this peak could represent is a deprotonated ethanal molecule i.e.,

$$
\begin{array}{c}
H \\
| \\
\cdot C - C \diagup\!\!\diagup O \\
| \quad \diagdown H \\
H
\end{array}
$$
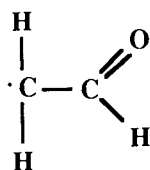
Since the next peak seen in the mass spectrum, at 58 mass units, is 15 units (a CH_3 group) heavier than 43, the 58 unit peak almost certainly represents a propanal molecule.

Propanal (b.p. 48.8°C)

$$m/e = 58 \longrightarrow m/e = 43 \quad + \quad m/e = 15$$
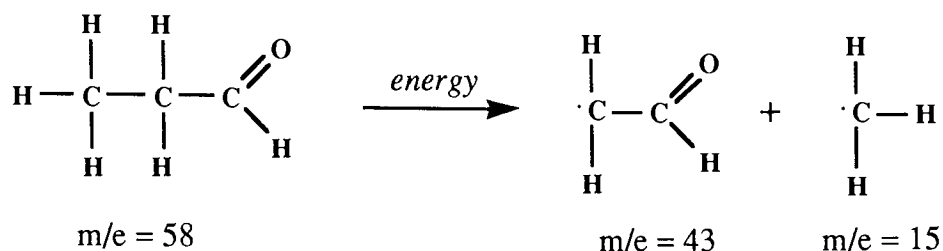
7.1.14.1.3 The Identity of the 66 Mass Units Peak

No reasonable molecular formula could be found for this number of mass units so no identity could be suggested for this mass spectrum peak.

7.1.14.1.4 The Identity of the 77 Mass Unit Peak

It was assumed that this fragment represented a deprotonated molecule of 78 mass units. The most likely molecular formula for this mass was found to be $C_2H_6O_3$ but no plausible constitutional isomer was found for this formula.

7.1.14.1.5 The Identity of the 91 Mass Unit Peak

It was assumed that this fragment represented a deprotonated molecule of 92 mass units. Two molecular formulae and several structural isomers are are possible for this mass number, $C_2H_4O_4$, and $C_3H_8O_3$ but it seemed likely that only the molecule

Glycerol
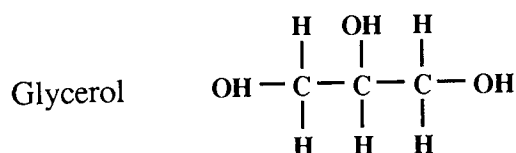
would be present in the resin reaction mixture.

7.1.14.1.6 The Identity of the 120 Mass Units Peak

Two molecular formulae are possible for this mass number, $C_4H_8O_4$ and $C_5H_{12}O$. There is a difference of 2 x CH_2 groups between this mass number and the previous mass number, 92. Therefore this molecule could have a C backbone 2 atoms longer than glycerol, or it could be a tetra-ol derived from butene.

253

7.1.14.1.7 The Identity of the 137 Mass Unit Peak

It was assumed that this fragment represented a deprotonated molecule of 138 mass units. The only molecular formula that is feasible for this mass number is $C_7H_6O_3$ i.e,

2-Hydroxy Benzoic acid
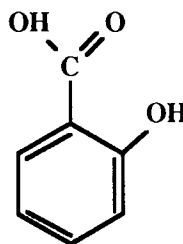
7.1.14.2 The Mass Spectrogram of "B"

FIGURE 7.42

THE MASS SPECTRUM OF THE GC PEAK 'B'
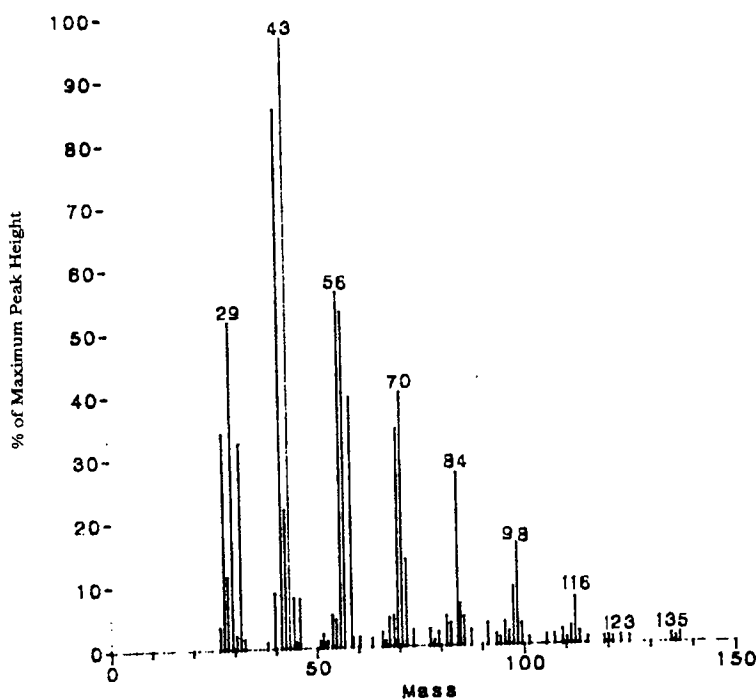
The following peaks are significantly larger than the background 'noise'.

(* = Largest Peak)
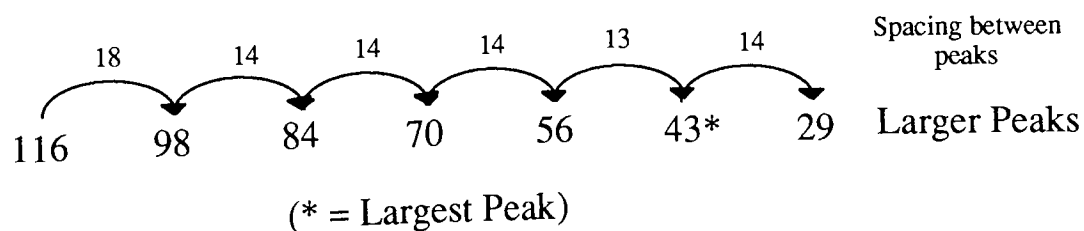
In this case a drop of 14 mass units between fragments in the mass spectrum appears to be common. This can be related to differences of one methylene group in a group of chemically similar organic molecules e.g. $H(CH_2)_nCHO$ i.e., the GC has separated out broadly similar compounds into a single, broad peak.

As before, it is likely that the peak at 43 represents the fragment

$$
\begin{array}{c}
H \\
| \\
\cdot C - C \overset{\displaystyle O}{\underset{\displaystyle H}{\diagup\!\!\diagdown}} \\
| \\
H
\end{array}
$$
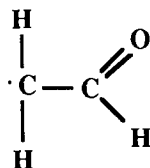
The peak at 29 presumably represents a deprotonated methanal molecule, derived from the heterolytic bond breakage in the ethanal fragment

$$
\begin{array}{ccccc}
H & & & & H \\
| & \diagup O & & \diagup O & | \\
\cdot C - C & \longrightarrow & \cdot C & + & \cdot C \\
| & \diagdown H & & \diagdown H & | \\
H & & & & H \\
m/e = 43 & & m/e = 29 & & m/e = 14
\end{array}
$$
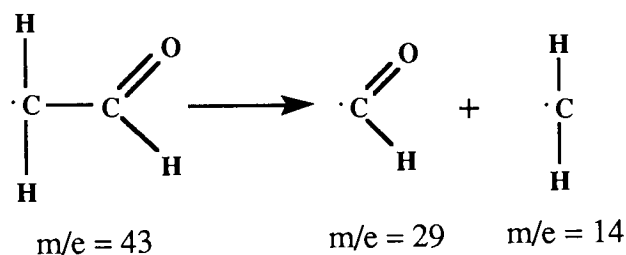
The masses 56, 70, 84, and 98 probably represent the series C_3H_4O, C_4H_6O, C_5H_8O, and $C_6H_{10}O$ with the first member in the series being

Propenal
$$
\begin{array}{ccc}
H & H & H \\
| & | & \diagup \\
C = C - C & \\
| & & \diagdown\!\diagdown O \\
H & &
\end{array}
$$
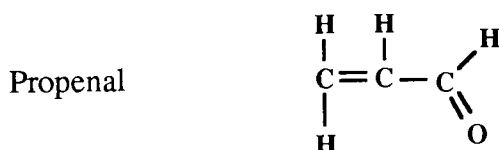
No information on the subject could be found, but it was hypothesised that the fragment at 43 mass units was formed by the breakup of the propenal molecule i.e.,

Propenal

$$
\begin{array}{ccccc}
H & H & H & & H \\
| & | & \diagup & energy & | & \diagup O \\
C = C - C & \longrightarrow & \cdot C - C & \\
| & & \diagdown\!\diagdown O & & | & \diagdown H \\
H & & & & H \\
m/e = 56 & & & m/e = 43
\end{array}
$$

255
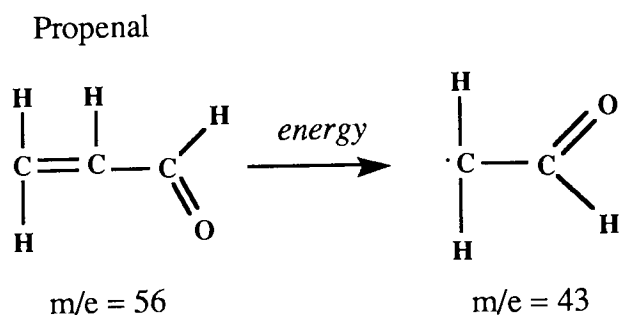
The mass 116 probably represents $C_4H_4O_4$ or $C_5H_8O_3$ i.e., between this mass and the previous mass, 98, a molecule of water has been eliminated.

$C_4H_4O_4$ - could be

Maleic Acid

$$\underset{CO_2H}{\overset{H}{\diagdown}}C=C\underset{HO_2C}{\overset{H}{\diagup}}$$

$C_5H_8O_3$ - could be

4 - Oxo Pentanoic Acid

$$H-\underset{\underset{H}{\mid}}{\overset{\overset{H}{\mid}}{C}}-\overset{\overset{O}{\parallel}}{C}-\underset{\underset{H}{\mid}}{\overset{\overset{H}{\mid}}{C}}-\underset{\underset{H}{\mid}}{\overset{\overset{H}{\mid}}{C}}-C\underset{OH}{\overset{O}{\diagup}}$$
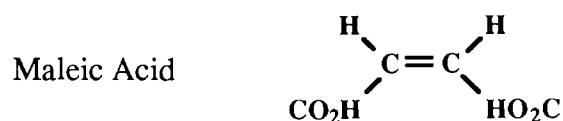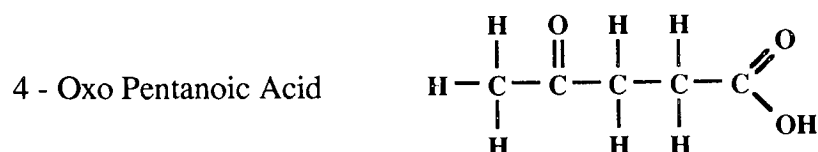
It is most likely that maleic acid is the identity of the molecule responsible for the peak because it has a shorter C-C chain length, and also it is a more highly oxidised molecule.
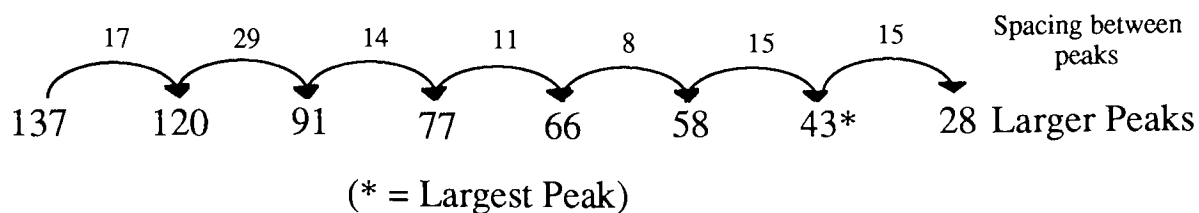
7.1.14.3 The Mass Spectrogram of "C"

FIGURE 7.43

THE MASS SPECTRUM OF THE GC PEAK 'C'
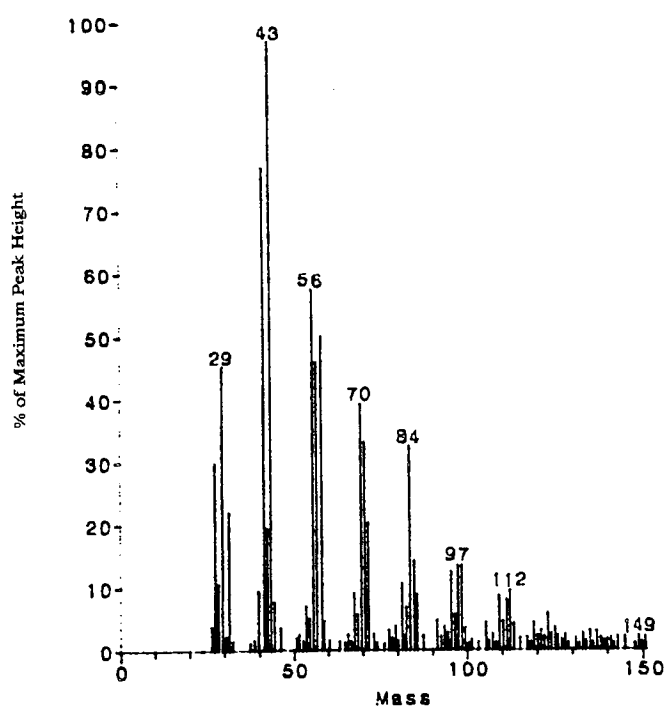
256

The following peaks are significantly larger than the background 'noise'.

Spacing between peaks: 14 14 13 14

Larger Peaks: 84 70 56 43* 29

(* = Largest Peak)
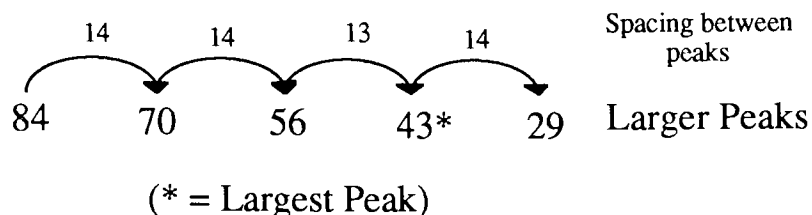
As before, a drop of 14 mass units between fragments in the mass spectrum appears to be common. This can again be related to the consecutive loss of CH_2 groups from a group of chemically similar organic molecules.

The pattern of the major mass spectrum peaks appears to be identical to that for the GC peak 'B' (Section 7.1.14.2), suggesting that the GC peak 'C' may just be the result of a double injection of the sample into the GC.

7.1.14.4 A Summary of the GC-MS Analysis of 53 Minutes Resin Reaction Solution

The two most abundant constituents of the resin reaction solution, propanal and propenal, were identified by the size of their molecular ion peaks and also by the size of their major fragmentation peak, at 43 mass units. The sequence hexenal, pentenal, butenal, and propenal was also seen, suggesting that progressive decarboxylation of this chain is occurring.

Other important molecules in solution are believed to be glycerol, 2-hydroxy benzoic acid, and maleic acid.

7.1.15 NMR Analysis of the CALIX Digestion Mixture

^1H and ^{13}C NMR spectra were obtained of samples taken periodically during the first ~45% of the CALIX / Fenton's reagent reaction (see Appendix 3). Figure 7.44 (overleaf) shows at what point during the reaction each sample was taken for NMR analysis.

FIGURE 7.44

Graph showing the variation in TOC level with time,
in the Fenton's reagent digestion of CALIX
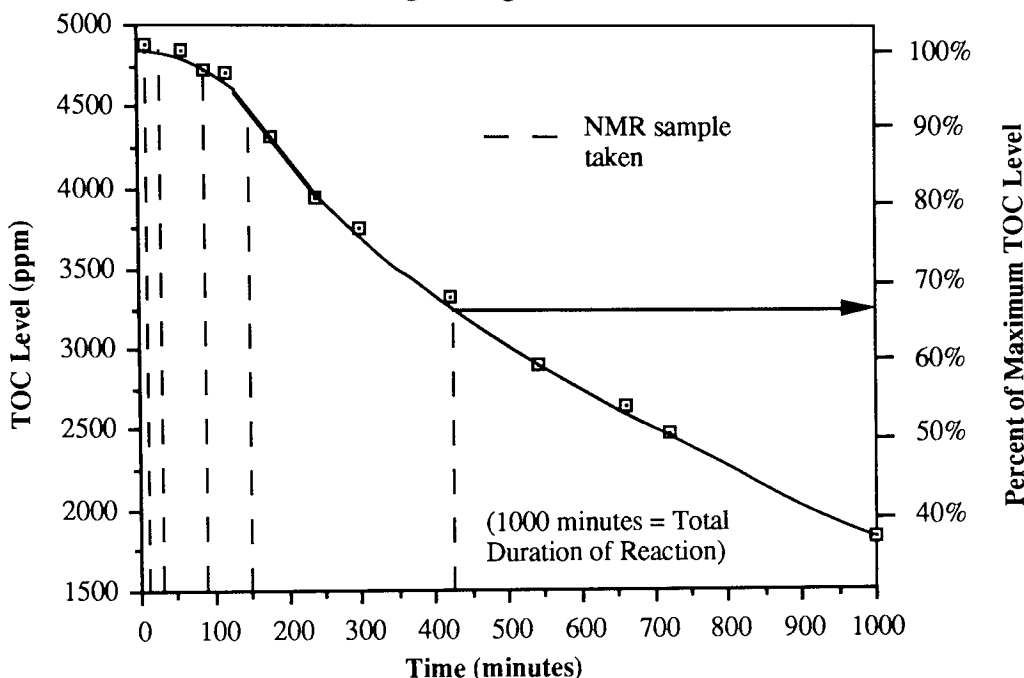
It is to be noted that the data displayed in Figure 7.44 had a sigmoid shape. This presumably reflects the nature of the predominant reactions at the start of the reaction, in which large molecules are broken down into small molecules. It is only after small molecules have been created that relatively rapid TOC loss will be seen, as they are converted to CO_2.

The only elements present in any organic molecule formed in the reaction solution will be C, H, O, and S. Since the S in the starting material, CALIX, is highly oxidised (SO_3) only highly oxidised C-S compounds will be seen.
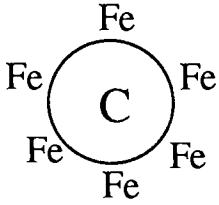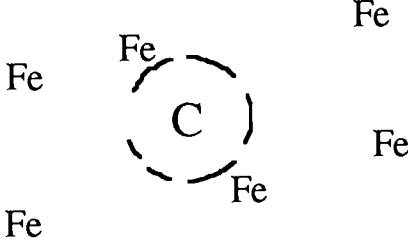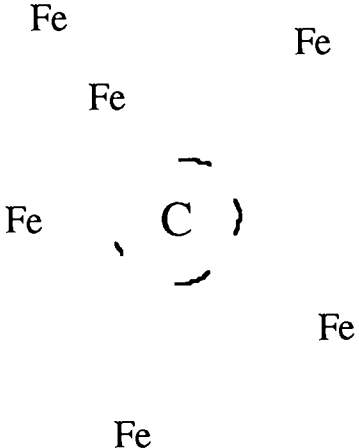
All NMR spectra for the CALIX digestion reaction can be seen in Appendix 3.

7.1.15.1 Proton NMR

The ^1H NMR spectra show massive peak broadening for the first samples taken (at 0 and 20 minutes after the start of the reaction) which renders them useless. The first usable spectrum was found to be that of the spectrum of the sample taken 39 minutes after the start of the reaction, although this also showed extensive peak broadening. Successive samples were less and less affected by this broadening. It is hypothesised that the peak broadening was due to the presence of paramagnetic Fe^{3+} close to the CALIX molecule (See Figure 7.45).

258

FIGURE 7.45
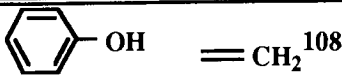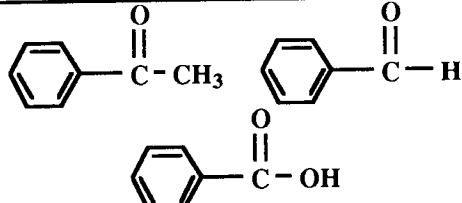
THE EFFECT OF IRON(III) ON THE PROTON NMR ANALYSIS OF THE CALIX

/ FENTONS REAGENT REACTION

Fe Fe (C) Fe Fe Fe Fe	1) At the start of the reaction, the iron catalyst is primarily associated with the sulphonic acid groups of the CALIX molecule, causing massive peak broadening of the organic signal in proton NMR.
Fe Fe Fe (C) Fe Fe Fe	2) The CALIX molecule degrades as Fenton's reagent attacks it. The iron starts going into solution, away from the remains of CALIX molecule. This leads to a reduction in peak broadening.
Fe Fe Fe Fe (C) Fe Fe	3) The CALIX molecule has degraded, with all the sulphonic acid groups having been converted to sulphate ions As a result of this iron is no longer co-ordinated in close proximity to large concentrations of organic molecules Even if the Fe in solution is co-ordinated with an organic molecule/s, most of the organic material will not be near an Fe ion, resulting in the absence of paramagnetic broadening.

(C) = CALIX
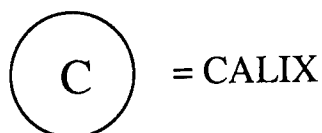
The available spectra were examined, and it was noted that the position and relative sizes of the peaks in each spectrum are very similar (only position information could be obtained for the 39 minutes spectrum, due to band broadening).

TABLE 7.13
ATTRIBUTION OF PROTON NMR PEAKS TO FUNCTIONAL GROUPS IN CALIX DIGESTION SOLUTION [107]

PPM (^{1}H), δ	Possible Identity of Group	Samples in which peaks seen (minutes into reaction)
1.8	-CH-C=C	39, 90, 150, 420
1.9	-CH-C=C	39, 90, 150, 420
2.4	CH_3-C(=O)X where X=H, OH, or R	90, 150, 420
3.2	CH_3-OH	39, 90, 150, 420
3.6	-CH_2-OH	39, 90, 150, 420
4	May be primary alcohol	39, 90, 150, 420
4.2	May be primary alcohol	39
1 to 5.2 [108]	The primary alcohol signal may apprear anywhere between 1 and 5.22 ppm	
6	⬡-OH ═CH_2 [108]	90, 150, 420
8	⬡-C(=O)-CH_3 ⬡-C(=O)-H ⬡-C(=O)-OH	39, 90, 150, 420

As Table 7.13 shows, the positions of the peaks in all the spectra are very similar. The relative sizes of the peaks are also very similar. The only peaks which show a relative size variation with time are the peaks at $\delta = 3.2$ ppm and at 1.9 ppm. The peak at 3.2 ppm gets smaller with time, which may reflect a fall in the concentration of primary alcohols, as they are oxidised to other compounds. The peak at 1.9 ppm increases in size, being at its largest in the sample taken at 150 minutes, then decreasing in size. This may reflect the cleavage of the -CH_2- CALIX backbone group from the benzene repeat units early on in the reaction, resulting in the formation of CH-C=C groups. After reaching a maximum level, the concentration of CH-C=C groups would then fall as oxidation to other groups occurred.

The constancy of the peak at 8 ppm suggests that there is no significant loss of aromaticity during

the time scale of sampling the reaction mixture. This would suggest that the aromatic rings, which are the building blocks of the CALIX molecule, are not significantly degraded during this time. This must mean that only the non-aromatic groups of the CALIX molecule are being oxidised during the first part of the reaction.

7.1.15.2 Carbon-13 NMR

Table 7.14 shows that the ^{13}C NMR spectra varied more than the ^{1}H NMR spectra.

TABLE 7.14
ATTRIBUTION OF CARBON-13 NMR PEAKS TO FUNCTIONAL GROUPS IN CALIX DIGESTION SOLUTION [107]

PPM (^{13}C), δ	Possible Identity of Group	Samples in which peaks seen (minutes into reaction)
18	CH_3	90, 420
25	CH_3, -CH-	39, 150
26	$-CH_2-$	90, 420
28	CH_3, -CH-	90, 420
30	$-CH_2-$	90, 420
33	-CH-	39
33	$-CH_2-$	150
37	$-CH_2-$	39, 90, 150, 420
46	$-CH_2-$, C-OH	39, 150
53	$-CH_2-$, C-OH	90, 420
59	Alcohols	39, 90, 150, 420
65	Alcohols	90, 150, 420
70	Alcohols	39, 150
167	RCOOH, R-C=C-COOH	39, 90, 150, 420

There also appears to be a strong "pairing" effect in the position of the peaks in the samples i.e. the 39 minutes and 150 minutes samples tend to have closely related peaks, and the 90 and 420 minutes samples appear to have closely related peaks. Since NMR spectra show, in the main, differences in functional group in a molecule, and not chain length differences, progressive chain degradation would account for the "pairing" of spectra, as shown by Table 7.14

7.1.15.3 Discussion of the Results

The lack of variation in the ^{1}H NMR spectra is difficult to explain, as it suggests that not much degradation of the CALIX molecule has occurred during the first 45% of the reaction. At this point, approximately 35% of the original C in solution has been oxidised.to CO_2. What the results may be showing is that loss of aromaticity is a relatively slow process, compared to oxidation of the CALIX backbone and sulphonic acid groups.

The ^{13}C results provide experimental evidence for the process of decarboxylation, in which parts of the CALIX molecule are progressively oxidised to CO_2.

7.2 The Chemical Reactions Occurring During the Fenton's Reagent Digestion of Lewatit Ion Exchange Resin

All the analytical data described in the previous results sections were considered, and an attempt is made here to produce a coherent summary of the processes occurring during the Fenton's reagent destruction of Lewatit DN ion exchange resin.

262

FIGURE 7.46

THE SURFACE OF A RESIN BEAD IN THE FIRST SECONDS AFTER

HYDROGEN PEROXIDE ADDITION
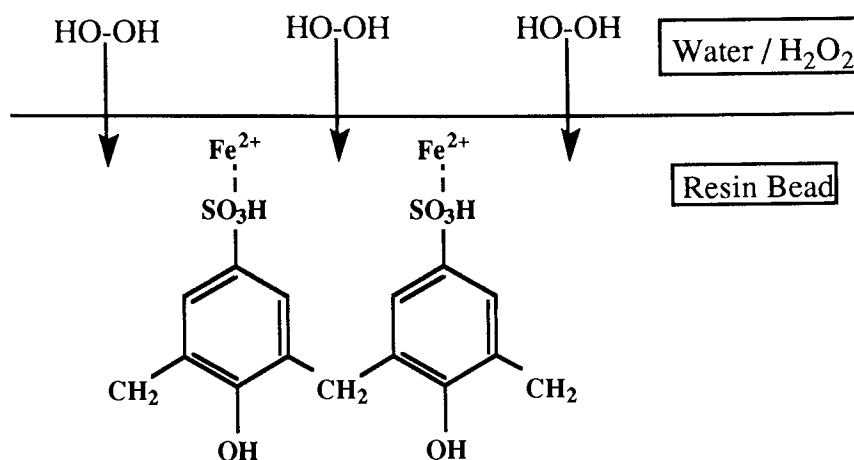
Figure 7.46 shows how, seconds after initial addition of H_2O_2 to the water / resin mixture, the H_2O_2 penetrates the surface of the bead. 20 seconds after the H_2O_2 has been added it can be seen that a brown colour has developed in the reaction solution (see Section 7.1.1). This discolourisation is presumably due to highly oxidised phenol derivatives. This implies:-

a) Rapid oxidation of the resin repeat unit has occurred.

b) Rapid cleavage of the CH_2 resin backbone has occurred, releasing aromatic compounds into solution.

The brown colour continues to deepen until at 10 minutes the mixture is visually opaque. The spectroscopically measured absorbance of the resin mixture (Section 7.18) increases rapidly during the first 10 minutes, confirming the visual observations.

The SO_4^{2-} concentration in the reaction solution above the resin rises quickly, as the sulphonic acid group is cleaved from the benzene ring, leaving behind a hydroxyl group on the ring (Section 7.1.5). The benzene ring, activated by the new OH group, is attacked further by $\cdot$OH radicals, causing the resin bead to become sticky as glue-like molecules are formed at the bead surface (Section 7.1.1). As the sulphonic acid group is oxidised to SO_4^{2-}, forming sulphuric acid, the pH of the reaction solution plummets from 5.3 at the start to about 0.9, 10 minutes later (Section 7.1.6). Fe ions released from the sulphonic acid group are temporarily solvated by H_2O molecules, but as the concentration of organic molecules builds up in solution, the Fe is

increasingly co-ordinated by organic acids (Section 7.1.2).

Small pits on the surface of the resin are preferentially enlarged as the bead solubilises, and a large and rapid TOC rise occurs as the resin bead dissolves (Sections 7.1.1 and 7.13).

At 10 minutes there are many different types of molecule in solution. These molecules are comprised of aliphatic alkyl, alkenyl, ketonic, aldehydic, saturated/unsaturated carboxylic, and alcoholic groups, with the alkyl and alkenyl groups being present in high concentrations. Aromatic molecules, probably mainly carboxylic acids and phenols, are also present in high concentration (Section 7.1.13).

7.2.2 From 10 Until 30 Minutes into the Reaction

The absorbance of the reaction solution peaks at 20 minutes, as the concentration of oxidised phenols released from the resin beads reaches its maximum. After this point the concentration of these types of organic molecule falls, even though the TOC level is still rising, indicating that these molecules are being preferentially destroyed. The concentration of SO_4^{2-} continues to rise, although the rate of formation of SO_4^{2-} falls during this period, due to the reduction of the surface area of the beads. The pH of the resin digestion solution continues to fall, but at a slower rate than in the first 10 minutes, as the increasing concentration of organic acids in solution begins to have a significant buffering effect.

The Fe concentration reaches a maximum, at 20 minutes, as all the iron catalyst from the resin beads is released into solution. As soon as the maximum is reached, AA suggests that the Fe concentration has apparently started to fluctuate, but this is an instrumental effect caused by the changing concentration and type of organic acids produced by the degradation of the resin.

By 30 minutes, the surfaces of all the resin beads have become perfectly smooth, due to ·OH radicals generated in solution attacking the resin (by this point there is no Fe in the resin structure, so no ·OH radicals are created there).

At 30 minutes there are many different types of aliphatic molecules present, containing alkenyl, ketonic, aldehydic, saturated/unsaturated carboxylic, and alcoholic groups. The concentration of alkyl and alcoholic groups has fallen, relative to that at 10 minutes. Highly oxidised phenol

derivatives are still present in low concentration, with aromatic carboxylic acids also being present, at a slightly lower concentration.than that seen at 10 minutes.

7.2.3 From 30 Until 60 Minutes into the Reaction

The absorbance continues to fall rapidly as highly coloured aromatic molecules are degraded. The rate of SO_4^{2-} formation slows still further, as the beads get smaller and by 60 minutes the resin has almost completely dissolved with almost no SO_4^{2-} being produced in solution. The pH of the resin digestion solution continues to fall slowly over this period, until at 60 minutes the minimum pH of 0.66 is reached. The apparent Fe concentration continues to vary under the influence of the changing chemical matrix. During this period the maximum TOC level is reached, 40 minutes after the start of the reaction. After this point the rate of mineralisation of organic molecules in solution is greater than the rate of dissolution of the resin beads, and the TOC level continues to fall until the end of the reaction.

The analysis of the resin reaction mixture, with its water removed (Section 7.1.11) indicates that there are high melting point molecules, containing alkyl, alkenyl, alcoholic, carboxylic (saturated and / or unsaturated), and probably aldehydic / ketonic groups are present during the 30 to 60 minute period of the reaction. The analysis of similar samples taken later during the reaction suggests that all these chemical groups are present throughout the rest of the reaction. The GC-MS analysis of the resin reaction mixture, using a sample taken at 53 minutes after the start of the reaction, suggest that the most common molecules in the solution at this time are propanal and propenal. Hexenal, pentenal, butenal, glycerol, 2-hydroxy benzoic acid, and maleic acid were also detected in this sample.

A precipitate 'X' can be separated from the resin reaction mixture during this period. 'X' is a major part of the resin reaction solution at this point. Spectrometric analysis of this precipitate indicated that the major constituent of this precipitate is

Propenoic acid

$$
\begin{array}{c}
\text{H} \quad\ \text{H} \qquad\ \text{OH} \\
| \qquad | \qquad\ / \\
\text{C} = \text{C} - \text{C} \\
| \qquad\qquad\ \backslash\!\backslash \\
\text{H} \qquad\qquad\ \text{O}
\end{array}
$$
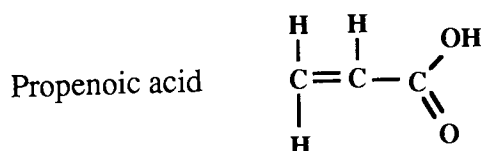
along with lower concentrations of butanaloic acid, propenal, and 2,3,4 trihydroxy pentandi-al.

7.2.4 From 60 to 100 Minutes

It is during this period that the resin beads have finally dissolved, at about 75 minutes after the start of the reaction. At this point major alterations in the shapes of the plots of absorbance, [SO_4^{2-}], and [Fe] against time can be seen, highlighting the change of the reaction system from heterogeneous to homogeneous.

At 75 minutes the SO_4^{2-} concentration reaches its maximum level, indicating that all the S originating in the resin has been converted to SO_4^{2-}. The SO_4^{2-} concentration then stays at the same level for the rest of the reaction. The absorbance graphs at 400 nm, 450 nm, and 500 nm show a sudden slowing of the rate of absorbance fall at 75 minutes. This reflects the fact that highly coloured molecules are no longer being created as the resin beads dissolve. Finally, at 75 minutes, the apparent Fe concentration starts to rise, after having fallen for the previous 55 minutes. This could reflect a major change in the chemical matrix at this point.

After 60 minutes the pH of the solution rises linearly until the end of the reaction, reflecting the 1st. order increase in concentration of buffering agents.

The maximum amount of precipitate 'X' could be extracted from solution at about 75 minutes. 'X' was then seen in decreasing amounts until about 120 minutes after the start of the reaction, when no more 'X' could be removed from solution. This suggests that the constituents of 'X' are mainly produced during the dissolution of the resin beads.

At 75 minutes aqueous NMR results show that alkyl, alkenyl, saturated and unsaturated carboxylic, and alcoholic groups are present. The concentration of alkyl and alcoholic groups has again fallen, relative to the sample taken at 30 minutes.

Highly oxidised phenol derivatives are present in low concentration, with aromatic carboxylic acids also being present, at a slightly lower concentration than that seen at 30 minutes.

7.2.5 From 100 to 150 Minutes

The apparent Fe concentration continues to rise, from its minimum at 75 minutes, as the concentration and / or type of molecules complexed with the $Fe^{2+/3+}$ ions in solution changes. After 100 minutes the absorbance of the resin solution at all wavelengths gradually reduces until the end of the reaction.

Two aqueous resin samples were analysed during this period, from 105 and 135 minutes after the start of the reaction. Alkyl, alkenyl, aldehydic, ketonic, carboxylic (saturated and / or unsaturated), and alcoholic groups are present in approximately the same concentrations in both samples. Highly oxidised phenol derivatives are present in low concentration, with the concentration of aromatic carboxylic acids falling with time.

7.2.6 From 150 Until 250 Minutes

After 160 minutes the apparent Fe concentration falls steadily until just after 250 minutes, upon which there is no further change in the Fe concentration.

The relative concentrations of the various organic groups, as shown by ^{1}H NMR, are identical to those seen in the sample taken at 135 minutes, with only the total concentration of organic material falling, as complete oxidation to CO_2 and water occurs.

7.2.7 From 250 Until 300 Minutes (The End of the Reaction)

At 250 minutes the relative concentrations of the various organic groups are identical to those seen in the samples taken during the previous period of time. At 300 minutes the compound mixture is fundamentally the same, with only the highly oxidised phenol derivatives being absent.

'A'

OH

CH$_2$ — (ring) — CH$_2$

SO$_3$H

$\longrightarrow$

'B'

OH

CH$_2$ — (ring) — CH$_2$

OH   OH

OH

$\longrightarrow$

'C'

OH

CH$_2$OH   (ring)   CH$_2$OH

OH   OH

OH

OH

CH$_2$OH   (ring)   CH$_2$OH

OH   OH

OH

a) Unreactive oxidised aromatic derivatives of 'C'

b) Reactive oxidised aromatic derivatives of 'C'

Aromatic Ring Cleavage

Aromatic Ring Cleavage

Unsaturated aliphatic alcohols and aldehydes e.g. glycerol

Oxidation

Aliphatic carbonyls e.g. propanal, propenal

Oxidation

Carboxylic acids e.g. maleic acid, propenoic acid

Decarboxylation

Alkyl and alkenyl derivatives

Oxidation

Alcohols and carbonyls, etc.

268
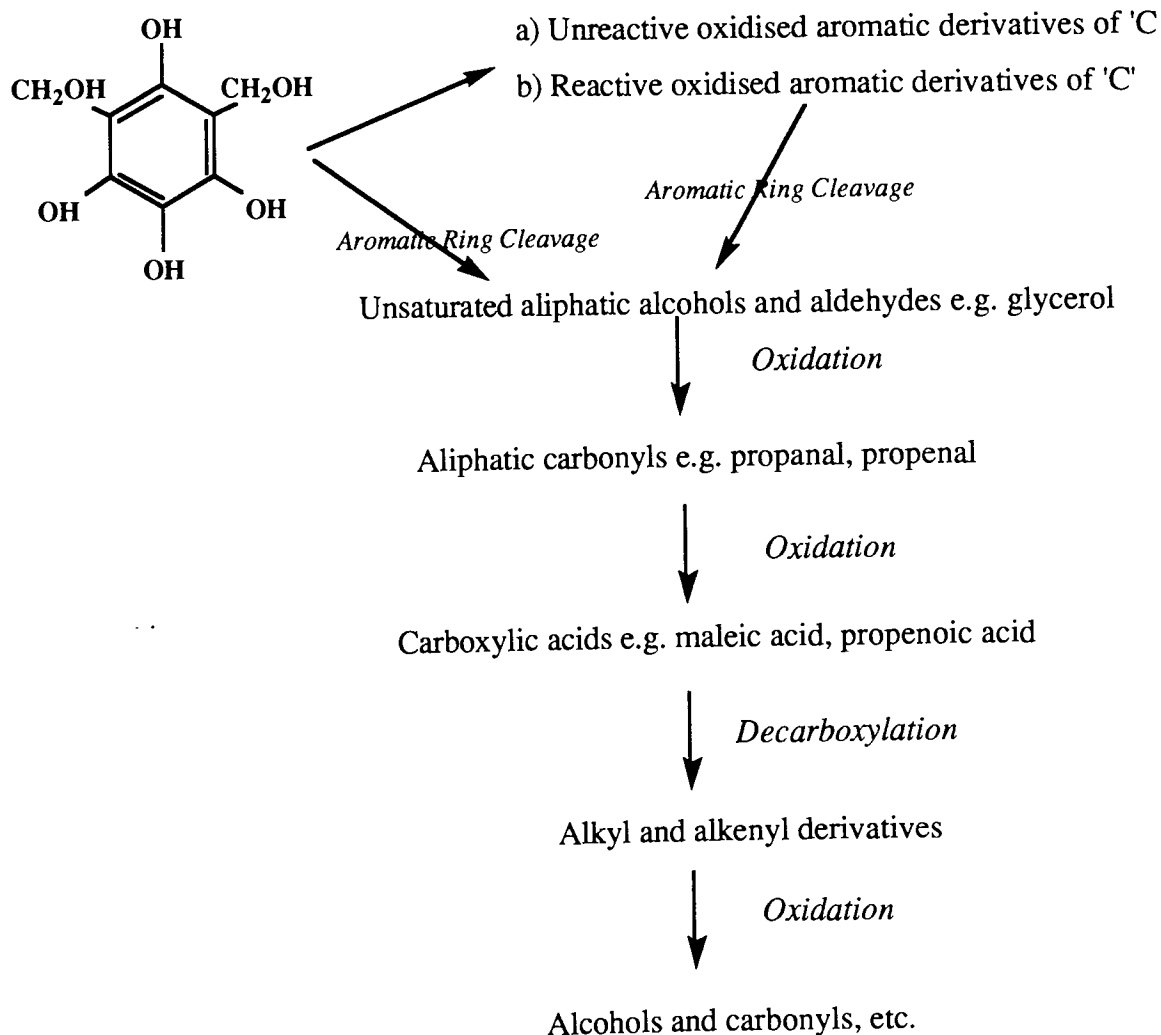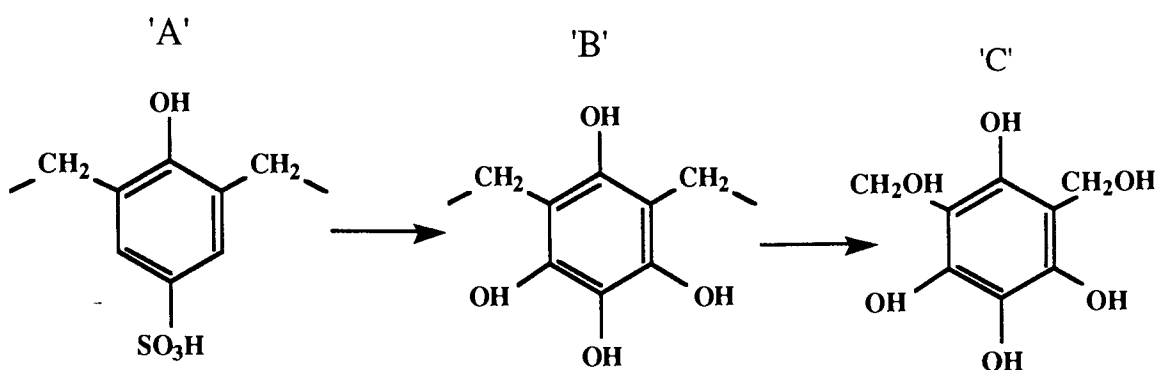
CHAPTER 8

TECHNICAL AND ECONOMIC CONSIDERATIONS OF A RESIN DESTRUCTION PLANT

8.0 INTRODUCTION

This PhD project has been a part of Aston University's 'Interdisciplinary Higher Degree' scheme, which exists to promote research links between industry and academia. It does this by arranging academic research into subjects of special interest to an industrial sponsor. Thus the project I undertook was one that was directly related to a topic of interest to Nuclear Electric. I spent several months of my three year PhD at the laboratories of my sponsors. I also attended 120 teaching hours of Master of Business Administration (MBA) lectures as an integral part of my work. Approximately twice this amount of time was spent on course work and end of module exams, resulting in course credits of one fifth of an MBA.

It was therefore decided to undertake a project to ascertain the general economic and technical considerations that would be involved in a decision to build a full scale plant for the wet oxidation of ion exchange resins. Where relevant the results of my work were integrated with this economic and technical assessment.

8.1 The Market for a Resin Disposal Operation

8.1.1 Britain

At present Nuclear Electric has approximately 300 m³ of radioactive resins stored at many sites around the country (at locations with more than one power station on the same site e.g., Dungeness 'A' and 'B', each station counts as a separate site) [109]. It has also been estimated that approximately 700 m³ more resin will be produced by Nuclear Electric's power stations over the next 40 years [109].

FIGURE 8.0

A MAP SHOWING LOCATIONS WHERE RADIOACTIVE

RESINS ARE STORED IN THE UK

Ownership of Sites

x Scottish Nuclear

● Nuclear Electric
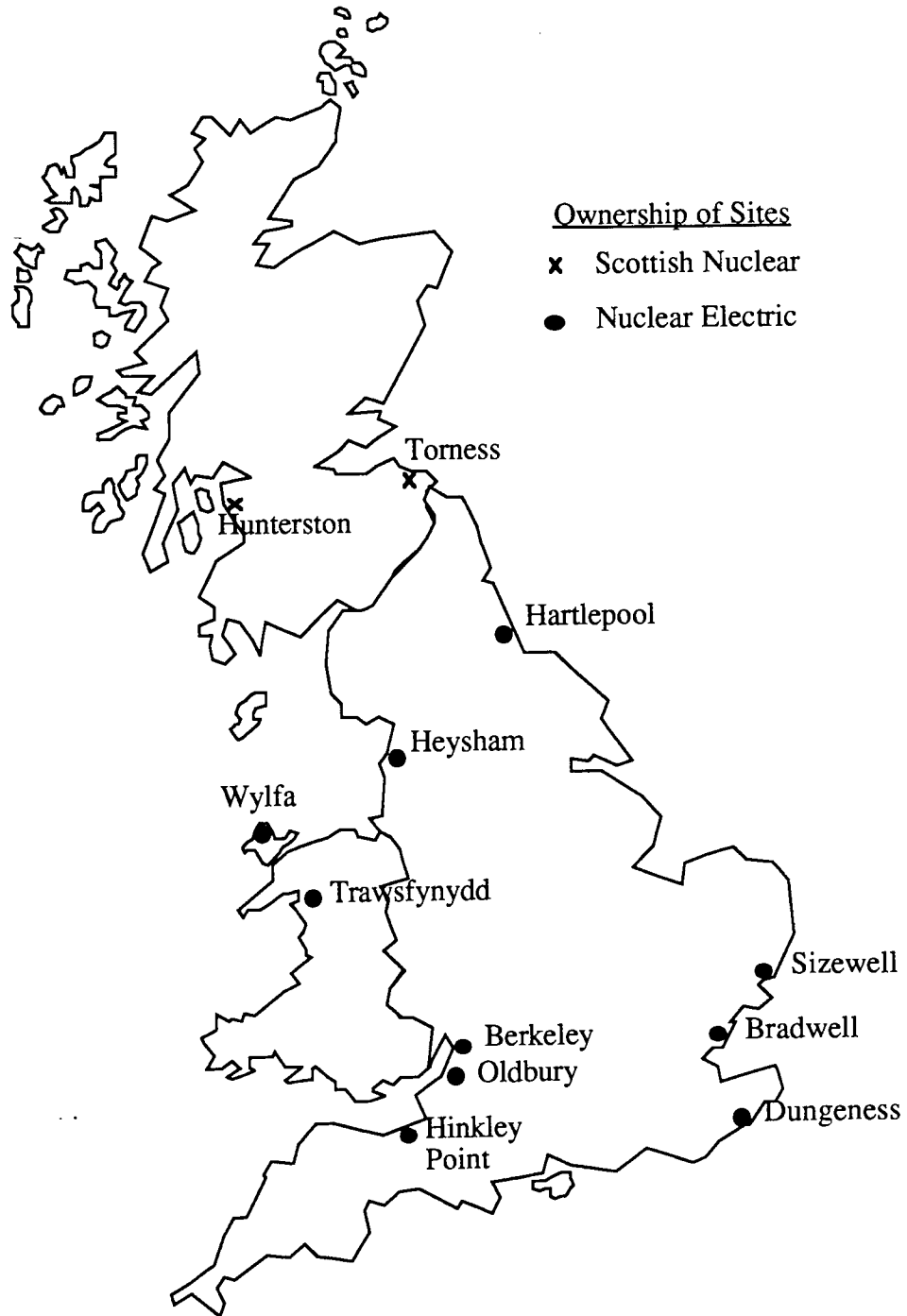
When Sizewell B comes on line in 1994 the total number of resin storage sites will increase to 14. The Atomic Energy Authority has another 300 m³ of resin stored around the country and Scottish Nuclear has between 50 and 100 m³ at 3 sites. Other sources in Britain account for a further 300 m³. It has been estimated that between 300 and 500 m³ more resin will be produced

in the next 40 years [109]. It is not possible to give a more exact figure than this because of uncertainties over how many (if any) nuclear plants will come on stream during this time period and also when existing plants will close.

8.1.2 The Overseas Market

Many thousands of cubic meters of radioactive resins are held at various sites around the world. Abroad, nuclear stations tend to be built at inland sites, in contrast to Britain's predominantly coastal locations for its power plants. Inland power stations generally have tighter standards for the radioactivity level in their waste water discharge flow than coastal stations. This is because they must usually discharge their waste waters into inland waterways, with their restricted water flows, which are be used for drinking water, agriculture and other purposes. As a consequence of these restrictions inland power stations tend to use more ion exchange resins than an equivalent coastal station.

8.2 General Economic Considerations

Section 8.1.2 indicates that there is a potential market for any technology developed for disposal of radioactive resins. This would have the benefit of defraying the R&D costs of developing the system through sale of either

a) the technology (via licensing agreements)

b) the actual resin destruction plant after all the resin stored by Nuclear Electric had been processed.

Furthermore, it should be possible to adapt the equipment design to deal with many other dangerous or environmentally persistent materials. Examples of these could include substances such as pesticides or paper mill residues. Sales of this technology would again help to defray costs involved in the project.

8.3 General Technical Considerations

Nuclear Electric has constructed a pilot plant to test the technology involved in the wet oxidation of ion exchange resins. This plant operates at the $0.1m^3$ volume scale, with up to 10 kg of damp

ion exchange resin being processed at a time. It is envisaged that a full scale plant could treat between 100 kg and 500 kg of resin per reaction run. It was decided to extrapolate information obtained from the pilot plant to design and cost the larger plant, as part of my PhD project.

8.3.1 Factors involved in the design of a full scale resin destruction plant

8.3.1.1 Transportability

The ion-exchange resin to be processed is stored at several sites around the country, and since the resin is radioactive there would be difficulties in transporting it to a central location for processing. Consent from the nuclear industry regulating bodies, would be required, and expensive transportation equipment would be needed to move the radioactive resin. It was decided instead that any resin destruction plant would have to be transportable, being moved from resin storage location to resin storage location by road. This would be done by decontaminating the plant, breaking down the plant into separate sections, loading the sections into containerised lorries, and moving them to the new resin storage site by road. This requirement to transport the plant imposes maximum weight and dimensional constraints on any design. Thus this part of the design must have dimensions of less than 2.45 m by 2.45 m by 12.17 m, and weigh less than 20 tonnes, to fit in a standard ISO container. The design of the whole plant must also be kept simple and modular in nature to allow for easy assembly, disassembly, and post-operation clean up at each site.

8.3.1.2 Safety

Any equipment designed for the handling of radioactive materials must have a high level of safety built in. In my design there are 3 levels of physical containment for the radioactive resin during its reaction.

a) The reactor vessel and associated equipment. Stainless steel would be used for all equipment inside the containment vessel, for strength and corrosion resistance.

b) The ISO container.

c) The ISO container would be placed inside a purpose built building on arrival at each site. This brick building would also contain the control centre and personnel for the resin reaction process.

Real-time monitoring of the progress of the reaction would be carried out by both computer and humans, as a back up for each other. Instruments connected to a central computer can be used to ensure optimum H_2O_2 utilisation by sensing, controlling, recording, and maintaining desired operating conditions.

The equipment would be decontaminated to a level that would meet transportation regulations before being moved to the next site, so that if there were a road crash there would be no major problem with radioactive contamination. All equipment inside the TIR container must be designed to be as maintenance free as possible, to reduce to the minimum the number of times workers have to enter the containment vessel. In my design, apart from remote controlled 2 and 3-way valves, there is only one piece of equipment with moving parts, the pump A (see Figure 8.2). All the other pumps that are necessary for the processing of the resin have been placed outside the containment vessel. The stirring regime has also been designed to be as maintenance free as possible. Conventionally, stirring would normally be performed using an overhead stirrer motor attached to a paddle. However, if instead an air sparging system is used to keep the liquid stirred, the pump can be kept outside the containment vessel, leaving only a pipe inside the containment vessel. Experimental work performed for this PhD project (see Chapter 6, Section 6.2.1.1.1) has shown that blowing air through a reacting resin digestion solution has no effect on the final TOC level of the reaction solution.

Figure 8.1 (overleaf) shows two reactor vessels, one of which is air stirred, and the other which is paddle stirred.

FIGURE 8.1

AIR STIRRED AND PADDLE STIRRED REACTOR VESSELS

Air Stirred Reactor   Paddle Stirred Reactor
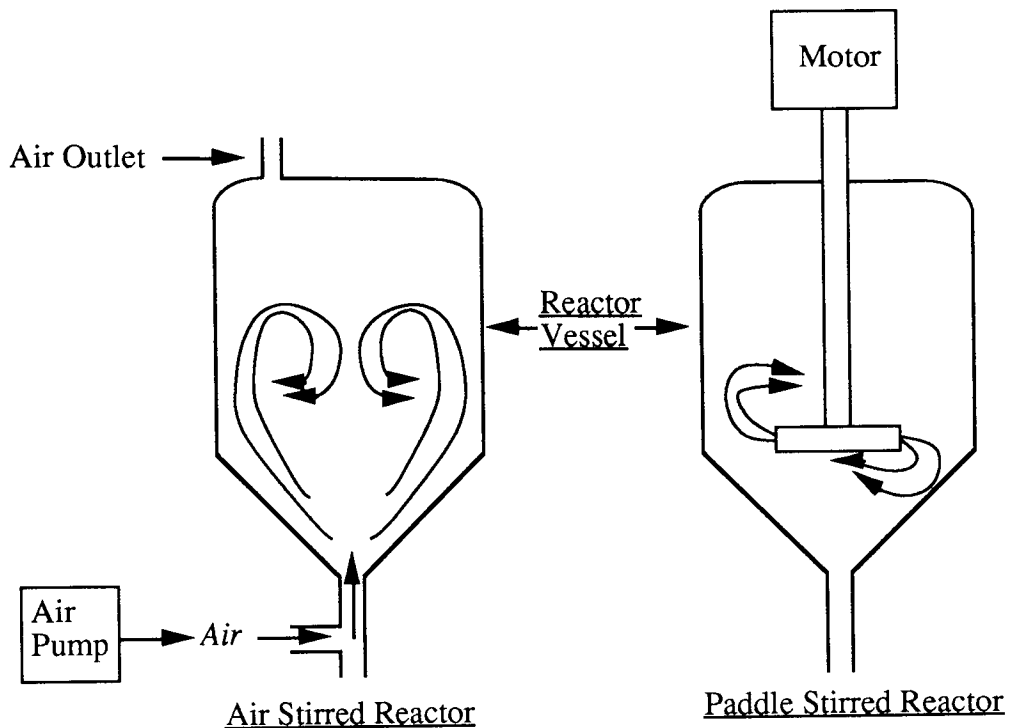
8.3.1.3 Cost of the Equipment

Containment of radioactive materials is involved in this process, and high quality equipment / materials must be used, increasing the cost of plant construction. However, the simplicity of the design, would help to keep costs down. The only item not available "off the shelf" in this design is the stainless steel reaction vessel, which would have to be specially constructed.

8.3.1.4 Automation

All equipment, particularly that inside the TIR container should be designed to operate automatically and under computer control for two main reasons.

a) To reduce the exposure of the workforce to radiation.

b) To reduce the number of staff employed at the site, thus reducing running costs.

Figure 8.2
Full Scale Resin Destruction Plant

Walls of ISO Container

① CO Analyser
② CO_2 Analyser
③ O_2 Analyser
④ pH Meter
⑤ Temperature Probe

Gas Sampling Pump

Analysis Loop

$3m^3$ scrubbing and surge tower

$1.5m^3$ surge tank

$CO_2 + O_2$ Extractor fan $200m^3/hr$

Total Gas Flow (max) $1.2m^3/min$

Water out

Water in

Packed Column Condensor $\left(\begin{array}{c}1m\ high\\30cm\ wide\\40\ tubes\end{array}\right)$

Decontamination Shunt

Tap C

Flange

Liquid Level Sensor

Circuit A

Heat Exchanger $200 - 500kW$

Water out

Water in

Resin/Water

Load Cell

Main Reactor

Heating Mantle $66kW$

$2m^3$ Stainless Steel Reaction Vessel

Valve A

Valve B

Pump A $10m^3/hr$

H_2O_2 $0 - 1\ m^3/hr$

To neutralisation and evaporation

Air/N_2 $0 - 1\ m^3/min$

276

8.4 A Typical Resin Destruction Run

1) Ion exchange resin is pumped as a slurry into the resin reaction vessel.

2) Extra water is added, along with the catalyst and the mixture is heated up to a temperature of 95°C.

3) The mixture is pumped around circuit A, and H_2O_2 addition via valve B is begun.

4) The N_2/air pump is started, and this mixture of gases agitates the resin bead/Fenton's reagent mixture in the reactor. N_2 is added to the air stream as a safety feature as it helps keep the concentration of O_2 in the off-gas at a low level (the O_2 is produced from the decomposition of H_2O_2 to water and oxygen).

5) The temperature is monitored, with a constant temperature of 95°C being maintained by switching the heating mantle on and off, and also by using the heat exchanger on Circuit A. The flow of liquid through Circuit A would be measured by a flowmeter to report the presence of any blockages. An attempt to remove a blockage could be made by temporarily reversing the normal direction of flow of the liquid.

6) As the resin is converted to CO_2 the weight of the mixture in the reaction vessel will change. If the quantities of material entering the system e.g. H_2O_2, are known then a general idea of the progress of the reaction can be obtained by measuring the weight of the {reaction vessel + contents} with the load cells. Direct sampling via valve A can also be used to provide data on TOC level and H_2O_2 concenration.

7) When the resin has all been destroyed, the reaction liquor would be removed via valve A for further treatment.

After all the resin beads at one site had been processed the equipment inside the containment vessel would be decontaminated, and then moved by road to the next processing site.

^{137}Cs, the main radioactive ion in Lewatit resin, could be removed from the equipment by passing water through the apparatus, as ^{137}Cs salts are very soluble in water. Unreacted organic material could be removed from equipment surfaces by use of organic solvents, addition of excess Fenton's reagent, or by passing an abrasive material (suspended in water) through the reactor and associated equipment

The decontaminating agents would be introduced into circuit A via valve B. By use of valve

C it would be possible to decontaminate the packed column condenser circuit as well as circuit A.

8.5 Costing the Construction and Operation of the Resin Destruction Plant

An attempt was made to cost the construction and operation of the plant shown in Figure 8.2. Prices for equipment were obtained from several sources. These sources included information extrapolated from previous equipment purchases, direct contact with manufacturers and utility providers, and estimates of construction costs by qualified members of Aston University staff. All prices have been adjusted to January 1992 levels by the method described by Peters and Timmerhaus [110]. Table 8.0 details the costs of various items required during the construction of a resin destruction plant.

TABLE 8.0

CAPITAL COSTS FOR A RESIN DESTRUCTION PILOT PLANT

Equipment Description	Price, £
H_2O_2 dosing pump, $1 \ m^3 / hr$	15000
Flowmeter for H_2O_2 dosing pump	1400
CO analyser	2700
CO_2 analyser	5000
O_2 analyser	2500
Heating mantle, 66 kW	940
Tubing, stainless steel, per metre	40
Cost for all tubing in design	1800
Welded bend, each	40
Cost for all bends in design	490
Heat exchanger	3600

Level sensor and control unit for reactor vessel	440
pH probe and meter for circuit A	440
6.5 m^3 H$_2$O$_2$ storage vessel	1400
Pump "A", (15 m^3 per hour water pump)	5000
Estimate of cost for 2 m^3 reactor vessel[a]	18000
Resin / water pump (7.2 m^3 per hour slurry pump)	3900
Temperature probe and control unit	400
Pump, Air / N$_2$, 0-1 m^3 per minute	3100
Load cells	700
Extractor fan, 200 m^3 per hour	650
Scrubbing and surge tower	1500
Packed column condenser[a]	3500
TOTAL COST OF MATERIALS	*72,000*
PLUS 30% [b]	*22,000*
PLUS 30% [c]	*28,000*
TOTAL COST OF PLANT	**approx 120,000**

a Estimate from Maurice Santano, Technician, Chemical Engineering Department

b For cost of monitoring equipment, fittings, and unexpected items

c For the costs of initial installation of the equipment

8.5.1 Calculation of Running Costs for a Resin Destruction Plant

All estimates of the running costs will be adjusted to the nearest £5.00.

TABLE 8.1

PRICES OF MAJOR CONSUMABLE ITEMS USED DURING THE

OPERATION OF THE RESIN DESTRUCTION PLANT

Consumables	Price, £
H_2O_2 , 35%, per litre	0.60
Electricity per kWh	0.06
N_2 for purge, per 1 m^3	0.28

8.5.1.1 Staffing

Discussions with Nuclear Electric PLC suggested a permanent staffing level of 3 would be appropriate. Assuming an 8 hour working day, 47 weeks a year, and also that the national average yearly salary of £15,000 would be paid to each person, the cost of employing 3 people would be £24 per working hour. There will also be the cost of staffing overheads, such as pensions, support staff, insurance e.t.c., which are generally regarded as amounting to 2.5 times the salaries of the workers [1]. This brings the cost of employing 3 people to £60 per working hour.

8.5.1.2 Electricity

The heating mantle would be the item of equipment consuming the most electricity. Assuming a 6 hour operating cycle (2 hours initial heating, then 4 hours of resin digestion) the heating mantle would be operational for approximately 5 of these hours. The Fenton's reagent / resin reaction is exothermic for the other hour. A 66kW heating mantle, operating for 5 hours, would consume £20 worth of electricity.

The various pumps and other electrical equipment would consume a further 15 kW per hour, giving a total cost, during the 6 hour operating cycle, of £5.

8.5.1.3 Hydrogen Peroxide

Assuming 50 kg of damp Lewatit resin per run, 1250 litres of H_2O_2 would be required per resin destruction cycle (based on typical figures from previous experimental resin destruction runs). This gives a total cost of £750 per 6 hour operating cycle.

8.5.1.4 Nitrogen

Assuming a requirement for 0.5 m^3 of N$_2$ per minute for the 4 hours of the resin destruction reaction, the total cost of N$_2$ during the operating cycle would be £35.

8.5.1.5 Summary of Running Costs

TABLE 8.2

SUMMARY OF THE RUNNING COSTS OF THE

RESIN DESTRUCTION PLANT

Item	Cost of Item, £, (per operating cycle)
H$_2$O$_2$	750
Labour	360
N$_2$	35
Electricity	25
TOTAL	approx. 1200

8.5.1.6 Factors Not Taken Into Account During the Costing Exercise

Several factors were not taken into account during the calculation of the costs of the resin destruction plant, due to insufficient data being available. These factors were:-

a) The cost of insuring the equipment.

b) The size of contingency funds, for unexpected items of expense.

c) How much decontaminating the equipment would cost, before moving it to each new site.

d) The cost of transporting the equipment from site to site.

e) The cost of the setting up and dismantling of the equipment

f) The final decommissioning costs, once the equipment had reached the end of its' life.

8.6 A Brief Summary of the Processing Carried Out on the Reaction Liquor Remaining After Reaction Completion

Figure 8.3
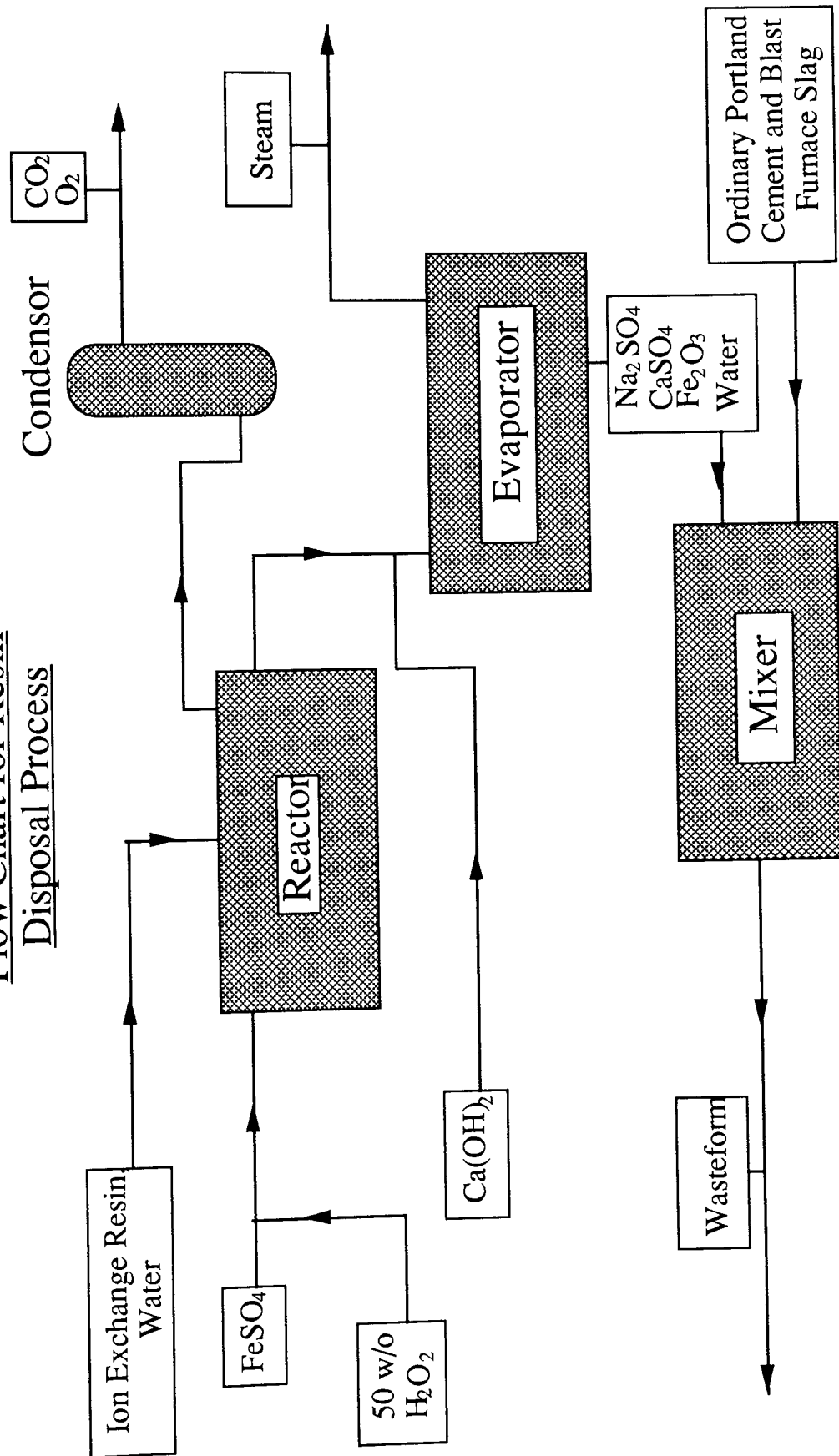Flow Chart for Resin
Disposal Process

Figure 8.3 shows the process that the reaction liquor would undergo once it had been removed from the reactor, via valve A.

The end of reaction liquor would be mixed with calcium hydroxide, to neutralise it, and then pumped to the evaporator, where the water would be evaporated off. The highly radioactive inorganic components of the reaction mixture left behind after evaporation would then be analysed for future reference, mixed with cement, sealed in a steel container and sent for underground disposal.

8.7 UV Heterogeneous Photocatalysis

Research carried out for this PhD project has shown that a combination of UV and TiO_2 is an effective combination for oxidising some organic molecules present in the resin digestion solution (see Chapter 4). The economic and technical benefits/problems of using this technique in combination with H_2O_2 were considered.

8.7.1 Photochemical Reactions in Industrial Manufacturing Processes

Photochemical reactions are common in the industrial manufacture of various types of chemicals. Examples of these reactions include photonitrosylations, photochlorinations, photohydrodimerisations, and photochemical electrocyclic reactions [111]. This means that the photochemical equipment which might be used in a resin destruction plant is likely to be available 'off the shelf", significantly reducing the cost of the modifications to the resin destruction plant. The use of industrial scale UV equipment has also been studied and modelled in detail by various workers, which would help reduce design costs for resin plant modifications [111].

8.7.2 Design Considerations in UV Heterogeneous Photocatalysis

There are several different equipment designs currently used for UV light sources. The simplest and cheapest design, however, is that of the immersion photochemical reactor, and this would probably be the best equipment for use in the resin destruction plant (due to the low maintenance required) [112]. The UV source could be inserted directly into the resin reaction vessel with no

283

major modifications in the overall plant design being necessary.

FIGURE 8.4

AN IMMERSION PHOTO-CHEMICAL REACTOR

Cooling Liquid ⟶

Cooling Liquid

Cooling Liquid

Light Source
Cooling Liquid
Thermal Insulation
Reaction Mixture
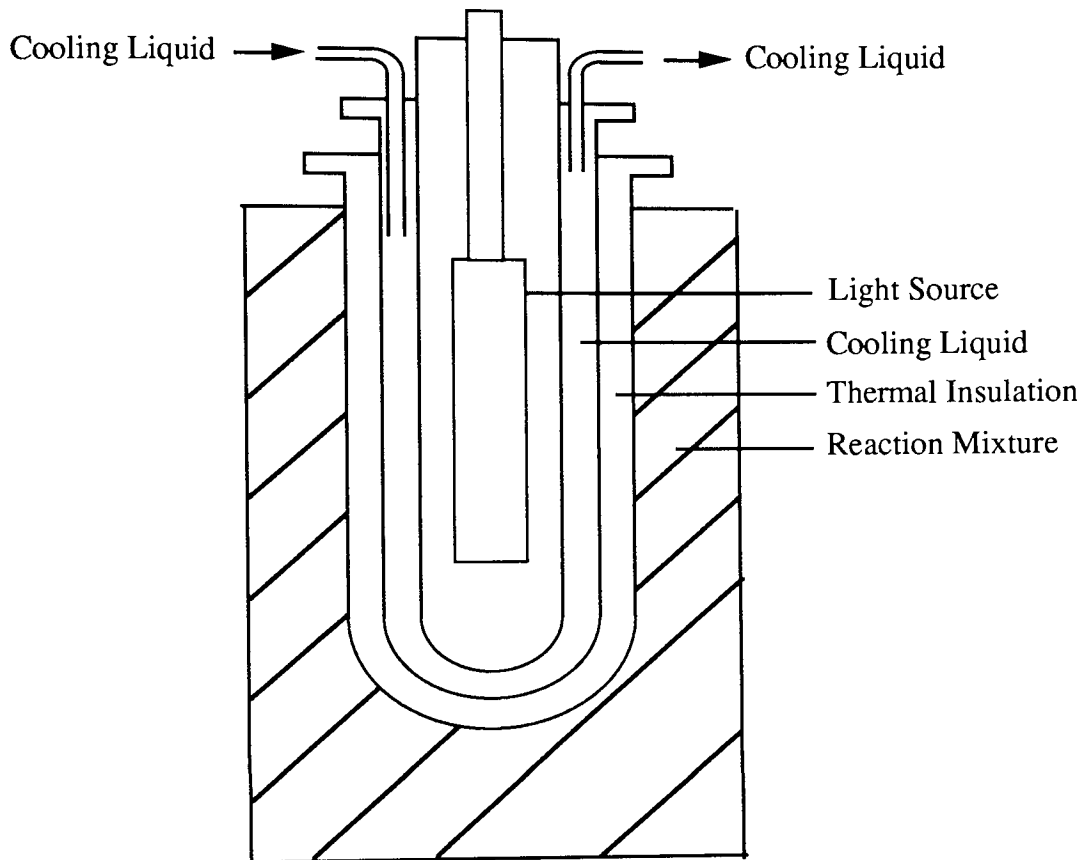
Using the TiO_2 as a powder suspension in the resin solution would be the preferred mode of catalyst use, as it would be circulated by the air stirring system around the reactor, along with the resin digestion solution. The TiO_2 could then be filtered off after the reaction had finished, or sent through to the evaporator, along with the end reaction liquor. This would not significantly increase the amount of waste which has to be incorporated into concrete, since only small amounts of TiO_2 are required in this photocatalytic system (typically 0.1% w/w).

If the TiO_2 were found to affect the setting of the cement at the end of the resin processing treatment cycle, it could either be filtered out or immobilised on a solid structure near the UV source. However the need to filter the TiO_2 or immobilise the TiO_2 on a solid support would complicate the design of the reactor and therefore increase its cost.

8.7.3 An Estimate of the Costs and Benefits of Using UV Photocatalysis to Remove Organic Material from the Resin Destruction Mixture

8.7.3.1 Extra Costs

TABLE 8.3

EXTRA COSTS INVOLVED IN THE USE OF UV IRRADIATION EQUIPMENT

Extra Costs for UV Photochemical Reactor	Price, £
UV photochemical lamp and transformer, for 2 m^3 volume reactor vessel	13900
PLUS 30% [a]	4200
PLUS 30% [b]	5400
TOTAL COST OF EXTRA EQUIPMENT	**approx. 23500**
TiO$_2$ Catalyst, per run	5
Electricity for UV lamp, per hour	5
Labour, per hour	60

a For cost of monitoring equipment, fittings, and unexpected costs

b For the costs of initial installation of the equipment

As described in Section 8.5.1.2, the typical resin destruction cycle would normally last about 6 hours (2 hours initial heating, 4 hours resin digestion reaction). The length of this cycle would be extended if the resin digestion solution was irradiated at the end of the normal Fenton's reagent / resin reaction, resulting in extra labour costs.

FIGURE 8.5

Graph showing the fall in TOC level in a UV irradiated titanium dioxide / 300 minute resin solution
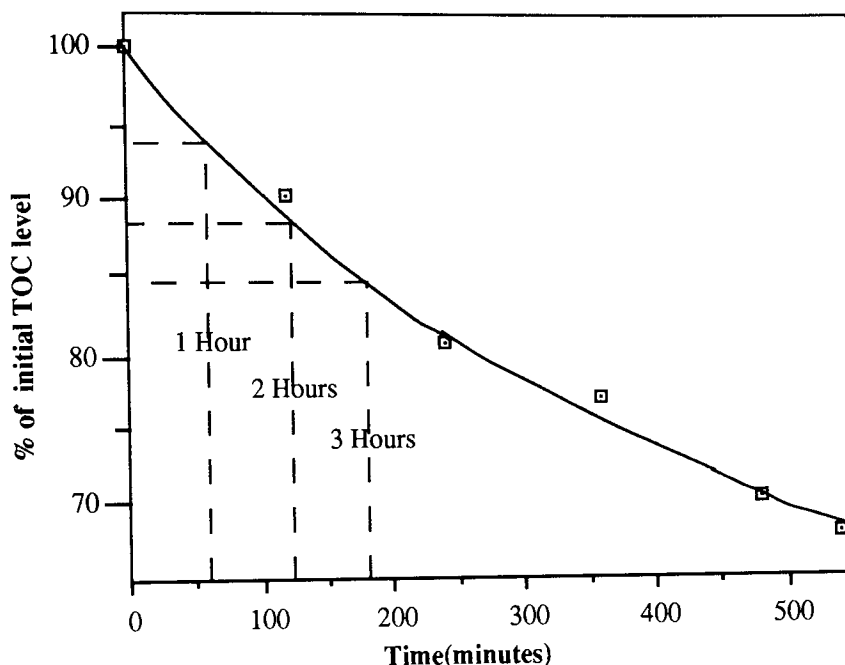
Figure 8.5 shows that the TOC level of the end resin reaction solution falls by 15% (or 195 ppm) in 3 hours of UV irradiation. This information allows a simple calculation of the relative cost benefits and disadvantages of using the UV / TiO_2 system.

Using figures from a typical resin destruction reaction.

TABLE 8.4

TYPICAL TOC AND HYDROGEN PEROXIDE CONCENTRATIONS IN THE STANDARD RESIN DIGESTION REACTION

Time into reaction(mins)	TOC level (ppm)	H_2O_2 Level (M)
0.1	0	2.38
80	3920	1.1
300	980	0

A 1.1 M solution of H_2O_2 (46% of the starting concentration) can be seen to produce a TOC level drop of 2940 ppm in this experiment.

3 hours of UV irradiation of an 980 ppm TOC level resin solution resulted in a TOC level fall

286

of 195 ppm.

Thus 3 hours of UV irradiation produces an equivalent TOC level drop to a H_2O_2 solution of concentration 0.073M. A 0.073 M solution of H_2O_2 is 33 times less concentrated that the starting concentration of H_2O_2.

This means that to be cost effective, the cost of TOC reduction by a UV / TiO_2 combination can be no more than one thirty third part of the cost of the H_2O_2 added at the start of the reaction.

8.8 UV Irradiation of a Resin Reaction Solution

A single experiment was carried out (Chapter 4, Section 4.1.1) in which a 29% reduction in final TOC level was achieved by irradiating a resin solution with UV light for 1 hour.

Using the same calculation method as in the previous section, it was found that this method produced a saving in H_2O_2 equivalent to 0.106M. This means that to be cost effective, this treatment method would have to cost no more than one twenty second part of the H_2O_2 added at the start of the reaction.

8.9 Conclusions

The relative costs and benefits of the UV and UV / TiO_2 systems, when used in combination with Fenton's reagent, depend very strongly on the amount and cost of H_2O_2 added during the reaction. More accurate estimates of the costs and benefits of these techniques, if used in a full-scale resin destruction plant, could only be made when more information about the running conditions of the full-scale plant became available.

REFERENCES

1. Sellers R, private conversation

2. Kirby C, private conversation

3. Cooper M, Hodgkinson D, "The NIREX Safety Assessment Research Program: Annual Report for 1986 / 87", UK Nirex Ltd., Report NSS / R101

4. Means J.L, Alexander C.A, "The Environmental Biogeochemistry of Chelating Agents and Recommendations for the Disposal of Chelated Radioactive Wastes," Nucl. Chem. Waste. Manage., 1981, 2, p183-196

5. Means J, Crerar D, "Migration of Radioactive Wastes: Radionuclide Mobilization by Complexing Agents," Science, 1978, 200, p1477-1481

6. Segal M.G, "Summary of Other Volume Reduction Techniques," STAR Seminar on Volume Reduction of Solid Radioactive Waste, Paper 7

7. Matsuzuru H, Kobayashi Y, Dojiri S, Akatsu J, Morizama N, "A Comparison of the Acid Digestion of Spent Ion Exchange Resins Using H_2SO_4-HNO_3 and H_2SO_4-H_2O_2," Nucl. Chem. Waste. Manage., 1983(4), p307-312

8. Morioka T, Motoyama N, Hoshikawa H, Takahashi T, Suzuki S, Ishikawa T, Uede T, "Method of Treating Radioactive Ion-Exchange Resins by Oxidative Decomposition." European Patent Application EP 0 257 192 A1, published 02/03/88 - Bulletin 88/9

9. Steele D.F, "Electrochemistry and Waste Disposal," Chemistry in Britain, October 1991, p915-918

10. Radioactive Waste Management 2, BNES Conference, 2-5 May 1989, Brighton, paper by Holman D.J, "Process Options for Treatment of Organics,"

11. Fenton H, "Oxidation of Tartaric Acid in Presence of Iron," J. Chem. Soc., 1894, 65, p899-902

12. Evans M.G, "Polymerisation of Monomers in Aqueous Solution," J. Chem. Soc., 1947, p266-269

13. Merz J.H, Waters W.A, "The Oxidation of Aromatic Compounds by Means of the Free Hydroxyl Radical," J. Chem. Soc., 1949, p2427-2433

14. Cotton F.A, Wilkinson G, "Advanced Inorganic Chemistry, 4th Ed.," p483, Wiley Interscience, 1980, London

15. Schumb W, Satterfield C, "Hydrogen Peroxide," ACS Monograph No. 128, 1955

16. Evans D, Upton M, "Studies on Singlet Oxygen in Aqueous Solution. Part 4. The 'Spontaneous' and Catalysed Decomposition of Hydrogen Peroxide," J. Chem. Soc., Dalt. Trans., 1985, p2525-2529

17. Draganic I, Draganic Z, "The Radiation Chemistry of Water," p40, Academic Press, 1971, London

18. Baxter R.A, "Mechanisms of Wet Oxidation by Hydrogen Peroxide," CEGB Report TPRD/B/1009/R87

19. Anbar M, "Induced Oxygen Exchange Between Hydrogen Peroxide and Water," J.Am.Chem.Soc., 1961(9), p2031-2035

20. Kremer M.L, "Evidence for the Catalytic Decomposition of H_2O_2 by Ferric Ions," Int. J. Chem. Kin., 1985, 17, p1299-1314

21. Brown S.B, Jones P, "Recent Developments in the Redox Chemistry of Peroxides," Prog. Inorg. Chem., 13, p159-204

22. Flicstein J.M, Kremer M.L, "Inhibition of the Fe^{3+} - H_2O_2 Reaction by Acetone," J. Catal., 1967(8), p145-150

23. Kremer M.L, "Nature of Intermediates in the Catalytic Decomposition of Hydrogen Peroxide by Ferric Ions," Trans. Farad. Soc., 1962, 58, p702-707

24. Walling C, "Fenton's Reagent Revisited," Acc. Chem. Res., 1975(8), p125-131

25. Walling C, Cleary M, "Oxygen Evolution as a Critical Test of Mechanism in the Ferric-Ion Catalyzed Decomposition of Hydrogen Peroxide," Int. Journ. Chem. Kin., 1977(9), p595-601

26. Walling C, Johnson R.A, "Structure and Reactivity Relations in the Reactions of Hydroxyl Radicals and the Redox Reactions of Radicals," J.Am.Chem.Soc., 1984(1), 96, p133-138

27. Walling C, Amarnath K, "Oxidation of Mandelic Acid by Fenton's Reagent," J.Am.Chem.Soc., 1982, 104, p1185-1189

28. Waters W.A, "Chemical Reactions Involving Free Radicals," Science Progress, 1947, 35, p23-35

29. Walling C, Johnson R.A, "Fenton's Reagent. V. Hydroxylation and Side Chain Cleavage of Aromatics," J.Am.Chem.Soc., 1975, 97, p363-367

30. Wood W, "The Stability of Sulphonated Cross-linked Ion Exchange Resin in Hydrogen Peroxide" J. Phys. Chem., 1957, 61, p832

31. Bibler N.E, Orebaugh E.G, "Iron Catalysed Dissolution of Polystyrenesulfonate Cation-Exchange Resin in Hydrogen Peroxide," Indust. Engineering Chem., Prod. Res. and Devel., 1976, 15, p136-138

32. Segal M.G and Squires R.T 1987, CEGB, unpublished work

33. Perrin D, Armarego W, "Purification of Laboratory Chemicals", 2nd Ed., Pergamon Press Ltd, 1980, London

34. Address: SERC Mass Spectrometry Service Centre, Chemistry Department, University College of Swansea, Singleton Park, Swansea, SA2 8PP

35. Hawkings N, Horton K.D, Snelling K.W, "Dissolution of Organic Ion Exchange Resins Using Iron Catalysed Hydrogen Peroxide," Inis Atomindex, 1981, Abstract No 605735, UKAEA Report No AEEW-R-1390

36. Svemla G, "Vogel's Qualitative Inorganic Analysis," Sixth Ed., Longman Scientific, 1991, London

37. Bailes R.H, Calvin M, "The Oxygen-carrying Synthetic Chelate Compounds. VII. Preparation" J.Am.Chem.Soc., 1947, 69, p1886-1893

38. Richman J.E, Atkins T.J, "Nitrogen Analogs of Crown Ethers," J.Am.Chem.Soc., 1974(7), 96, p2268-2270

39. McAuley A, Whitcome T.W, "Bis(1,4,7 Triazacyclononane)palladium (III): Characterisation and reactions of an unusually stable monomeric Palladium (III) Ion," Inorg. Chem. 1988, 27, p3090-3099

40. Gutsche C.D, Dhawan B, Hyun No K, Muthukrishnan R, "The Synthesis, Characterization, and Properties of the Calixarenes from p-tert-Butylphenol", J.Am.Chem.Soc., 1981, 103, p3782-3792

41. Shinkai S, Kawaguchi H, Manabe O, "Selective Adsorption of UO_2^{2+} to a Polymer Resin Immobilizing Calixarene-Based Uranophiles," J. Polym. Sci. : Part C: Polymer Letters, 1988, 26, p391-396

42. Bambrick D, "The Effect of DTPA on Reducing Peroxide Decomposition," Tappi Journal, 1985, June, p96-100

43. Proceedings of the 7th Meeting of the C.N.R.S, 1980, Paris, paper by Mimoun H, "Activation and Transfer of Molecular Oxygen Catalysed by Transition-Metal Complexes."

44. Nishinaga A, Tomita H, Oda M, Matsurra, "Oxygenation of Nitrophenylhydrazones with Co(II)-Schiff Base Complexes," Tett. Lett, 23, 1982, p339-342

45. Hill C, Schardt B, "Alkane Activation and Functionalization Under Mild Conditions by a Homogeneous Manganese(III)Porphyrin-Iodosylbenzene Oxidizing System," J.Am.Chem.Soc., 1980, 102, p6374-6375

46. Vaska L, "Dioxygen-Metal Complexes: Toward a Unified View," Acc. Chem. Res., 1976, 9, p175-183

47. Dufour M.N, Crumbliss A.L, Johnston G, Gaudemer A, "Reaction of Indoles with Molecular Oxygen Catalyzed by Metalloporphyrins," J. Mol. Catal., 1980(7), p277-287

48. Benedini F, Rindone B, Nali M, Tollari S, Cenini S, Monica G, Porta F, "Bis(salicylaldehyde) ethylenedi-iminecobalt (II) Catalysed Oxidative Carbonylation of Primary and Secondary Amines," J. Mol. Catal., 1986, 34, p155-161

49. Vogt L.H, Wirth J.G, Finkbeiner H.L, "Selective Autoxidation of Some Phenols Using Bis(salicylaldehyde) ethylenediimine cobalt Catalysis," J. Org. Chem., 1969(2), p273-277

50. Martell A.E, "Formation and Stabilities of Cobalt Dioxygen Complexes in Aqueous Solution," Acc. Chem. Res., 1982, 15, p155-162

51. Tsumaki T, "Nebenvalenzringverbindungen. IV. Über einige innerkomplexe Kobaltsalze der Oxaldimine," Bull. Chem. Soc. Jap., 1938, 13, p252-260

52. 170th National Meeting of the American Chemical Society (INOR 048), August 1975, Chicago IL, paper by Adduci A, "Aircraft Oxygen Systems Will Use Metal Chelates,"

53. Vogt A, Kuffelnicki A, "Studies on the Cobalt(II)-Dipeptide-Imidazole System; A New Dioxygen Carrier," Polyhedron, 1990, p2567-2574

54. Henrici-Olivé G, Olivé S "Activation of Molecular Oxygen," Angew. Chem. Int. Ed., 1974(1), p29-38

55. Nishinaga A, Tomita H, "Model Catalytic Oxygenations with Co (II) Schiff Base Complexes in the Oxygenation Process," J. Mol. Catal., 1980(7), p179-199

56. Wieghardt K, Walz W, "Crystal Structure of Bis[bis(1,4,7-triazacyclononane) nickel(III)] Dithionate Heptahydrate and Its Single Crystal EPR Spectrum," Inorg. Chem., 1986, 25, p1650-1654

57. Wieghardt K, Koppen M, "Synthesis and Crystal Structure of Bis(1,4,7-triazacyclononane-NN')-Platinum(II) dibromide dihydrate and its Facile Oxidation by Oxygen: Characterisation of Bis 1,4,7 - triazacyclononane - N N' N'') - Platinum(IV) Tetraperchlorate," J. Chem. Soc., Dalt. Trans., 1983, p1869-1872

58. McAuley A, Hunter G, Whitcombe T.W, "Crystal and Solution Structure of the Palladium (II) Bis(1,4,7 triazacyclononane) Ion: Evidence for Rapid Fluxional Behaviour in a Macrocyclic Complex," Inorg. Chem. 1988, 27, p2634-2639

59. Streitwieser A, Heathcock C, Kosover E, "Introduction to Organic Chemistry, 4th.Ed." p1016, Macmillan, 1992, London

60. Zepp R, Braun A, "Photoproduction of Hydrated Electrons form Natural Organic Solutes in Aquatic Environments," Environ. Sci. Tech., 1987, 21, p485-490

61. Jardim W.F, Kondo M.M, "Photodegradation of Chloroform and Urea Using Ag-Loaded Titanium Dioxide as Catalyst," Wat.Res, 1991(7), 25, p823-827

62. Fox M, "Photocatalytic Oxidation of Organic Substrates," in Photocatalysis and Environment. Trends and Applications ed. by Schiavello M., Kluwer Academic Publishers, 1988, The Netherlands

63. Mopper K, Stahovec W, "Sources and Sinks of Low Molecular Weight Organic Carbonyl Compounds in Seawater," Marine Chem., 1986, 19, p305-321

64. Haag W, Hoigne J, "Singlet Oxygen in Surface Waters. Part 3. Photochemical Formation and Steady State Concentration in Various Types of Waters," Envir. Sci. Tech., 1986, 20, p341-348

65. Oliver B, Cosgrove E, "Effect of Suspended Sediments on the Photolysis of Organics in Water," Envir. Sci. Tech., 1979, 13, p1075-1077

66. Pelizzetti E, Maurino V, "Photocatalytic Degradation of Atrazine and Other S-triazine Herbicides," Envir. Sci. Tech., 24, p1559-1565

67. Okamoto K, Yamamoto Y, Tanaka H, Tanaka M, Itaya A, "Heterogeneous Photocatalytic Decomposition of Phenol over TiO2 Powder," Bull. Chem. Soc. Jap., 1985, 58, p2015-2022

68. Tan C, Wang T, "Reduction of Trihalomethanes in a Water-Photolysis System," Envir. Sci. Tech., 1987, 21, p508-511

69. Matthews R.W, "Photo-oxidation of Organic Materials in Aqueous Suspensions of Titanium Dioxide," Wat. Res., 1986, 20, p569-578

70. Turchi C.S, Ollis D.F, "Mixed Reactant Photocatalysis: Intermediates and Mutual Rate Inhibition," J. Catal., 1989, 119, p483-496

71. Jaeger C.D, Bard A.J, "Spin Trapping and Electron Spin Resonance Detection of Radical Intermediates in the Photodecomposition of Water in TiO_2 Particulate Systems," J. Phys. Chem., 1979, 83, p3146-3152

72. Kalyanasundaram K, Grätzel M, "Interfacial Electron Transfer in Colloidal Metal and Semiconductor Dispersions and Photodecomposition of Water," Coord. Chem. Rev., 1986, 69, p57-125

73. Weiberg K, "Oxidation in Organic Chemistry," Academic Press, 1965, New York

74. Smith D, "Cerate Oxidimetry, 2nd Ed." G. Frederick Smith Chemical Company, 1964, Columbus, Ohio

75. Laitinen H, Harris W, "Chemical Analysis, 2nd Ed." McGraw-Hill, 1975, New York

76. Cotton F, Wilkinson G, "Advanced Inorganic Chemistry - A Comprehensive Text, 3rd Ed." Wiley Interscience, 1972, New York

77. Trahanovsky W, Young L, "Oxidation of Organic Compounds with Cerium (IV). VII. Formation Constants for 1:1 Cerium (IV) - Alcohol Complexes," J.Am.Chem.Soc., 1969, 91, p5060-5068

78. Sengupta K.K, Aditya S, "Kinetics of the Oxidation of Acetaldehyde by Cerium (IV) Salts," J. Indian Chem. Soc., 1968(10), 45, p897-903

79. Hintz H.L, Johnson D.C, "The Mechanism of Oxidation of Cyclic Alcohols by Cerium(IV)," J. Org. Chem., 1967, 32, p556-564

80. Storey R.f, Goff L.J, "Investigation of the Cerium^{IV} Oxidation of Poly(vinyl Alcohol)," J. Polym. Sc.: Part A: Polymer Chemistry, 1989, 27, p3837-3854

81. Kochi J, Sheldon R, "Photochemical and Thermal Reduction of Cerium (IV) Carboxylates. Formation and Oxidation of Alkyl Radicals," J.Am.Chem.Soc., 1968, 90, p6688-6698

82. Dogliotti L, Hayon E, "Transient Species Produced in the Photochemical Decomposition of Ceric Salts in Aqueous Solution. Reactivity of NO_3 and HSO_4 Free Radicals," J. Phys. Chem., 1967(12), 71, p3802-3808

83. Matthews R.W, "Wavelength Controlled Production of SO_4^- Radicals in the Ultraviolet Photolysis of Ceric Sulphate Solutions," Austr. J. Chem., 1984, 37, p475-488

84. Greatorex D, Hill R.J, Kemp T.J, Stone T.J, "Electron Spin Resonance Detection of Radical Intermediates During Photo-oxidation by Metal Ions in Solution," J.Chem.Soc., Farad. Trans. 1, 70, p216-226

85. Dulz G, Sutin N, "Kinetics of the Oxidation of Fe(II) and its Substituted tris-(1,10-phenanthroline) complexes by Ce(IV)," Inorg. Chem., 1963(5), 2, p917-21

86. Confidential Internal CEGB Research Document, 1989, entitled "The Destruction of Ion Exchange Resins Using Fenton's Reagent 3 : Lewatit Cation Exchange Resin"

87. Streitwieser A, Heathcock C, "Introduction to Organic Chemistry, 3rd Ed." Macmillan, 1985, London

88. Lee S.C, "Dissolution of Ion Exchange Resin by Hydrogen Peroxide," En. Res. Abs., 1982, 6, Report DP-1594

89. Baddeley G, Holt G, Kenner J, "Relationship between Sulphonation and Desulphonation," Nature, 1944, 154, p361

90. Morioka T, Motoyama N, "Method of Treating Radioactive Ion-Exchange Resins by Oxidative Decomposition." European Patent Application EP 0 257 192 A1, published 02/03/88 - Bulletin 88/9

91. Bambrick D, "The Effect of DTPA on Reducing Peroxide Decomposition," Tappi Journal, 1985, June, p96-100

92. Fleming I, "Frontier Orbitals and Organic Chemical Reactions," Wiley Interscience, 1973, London

93. Dorfman L, Taub I, "Pulse Radiolysis Studies. 1. Transient Spectra and Reaction Rate Constants in Irradiated Aqueous Solutions of Benzene," J. Chem. Phys., 1962, 36, p3051-3055

94. Christensen H, Sehested K, "Formation of Benzyl Radicals by Pulse Radiolysis of Toluene in Aqueous Solutions," J. Phys. Chem., 1973, 77, p983-987

95. Neta P, Hoffman M, "Electron Spin Resonance and Pulse Radiolysis Studies of the Reactions of OH and O- Radicals with Aromatic and Olefinic Compounds," J. Phys. Chem., 1972, 76, p847-853

96. Solomons T.W.G, "Organic Chemistry, 5th Ed." John Wiley and Sons, Inc., 1992, New York

97. Norman R.O.C, West P.R, "Electron Spin Resonance Studies. Part XIX. Oxidation of Organic Radicals, and the Occurrence of Chain Processes, during the Reactions of Some Organic Compounds with the Hydroxyl Radical Derived from Hydrogen Peroxide and Metal Ions," J. Chem. Soc., Part B, 1969, p389-399

98. Shinkai S, "Molecular Recognition of Calixarene-Based Host Molecules," Journal of Inclusion Phenomena, 1989, 7, p193-201

99. Shinkai S, Mori S, Tsubaki T, Sone T, Manabe O, "New Water-Soluble Host Molecules Derived From Calix[6]arene," Tett. Lett., 1984, 25, p5315-5318

100. Shinkai S, Mori S, Koreishi H, Tsubaki T, Manabe O, "Hexasulphonated Calix[6]arene Derivatives: A New Class of Catalysts, Surfactants, and Host Molecules," J.Am.Chem.Soc., 1986, 108, p2409-2416

101. Gutsche C.D, Gutsche A.E., "Calixarenes 11. Crystal and Molecular Structure of p-tert-Butylcalix[8]arene," Journal of Inclusion Phenomena, 1985, p447-451

102. CRC Handbook of Chemistry and Physics, 58th Ed., 1977-1978, CRC Press, Boca Raton

293

103. Price W, "Spectrochemical Analysis by Atomic Absorption," Heyden and Son Ltd, 1979, London

104. Roos J.T.H, Price W.J "Mechanisms of Interference and Releasing Action," Spectrochim. Acta, 1971, 26 B, p279-284

105. Varma A, "Handbook of Atomic Absorption Analysis," CRC Press, 1985, Boca Raton

106. Vogel A "Vogel's Textbook of Quantitative Chemical Analysis, 5th Ed." Longman Scientific and Technical, 1989, Harlow

107. Silverstein R.M, Bassler G.C, Morrill T.C, "Spectrometric Identification of Organic Compounds, 5th Ed." John Wiley and Sons, 1991, New York

108. Brüker NMR Operators Yearbook, 1991, p80

109. The 1988 United Kingdom Radioactive Waste Inventory. Report No. DOE/RW/89-088

110. Peters M, Timmerhaus K, "Plant Design and Economics for Chemical Engineers," McGraw-Hill, 1991, New York

111. Braun A, "Technical Development and Industrial Prospects of Preparative Photochemistry," in 'Photocatalysis and Environment. Trends and Applications' ed. Schiavello M., Kluwer Academic Publishers, 1988, The Netherlands

112. Clayton R, "UV - Catalysed Oxidation in Water Treatment," The Chemical Engineer, 14th May, 1992, p23-26.

APPENDIX 1

NMR SPECTRA OF AQUEOUS RESIN DIGESTION

REACTION SAMPLES

1 H With Presaturation of Water
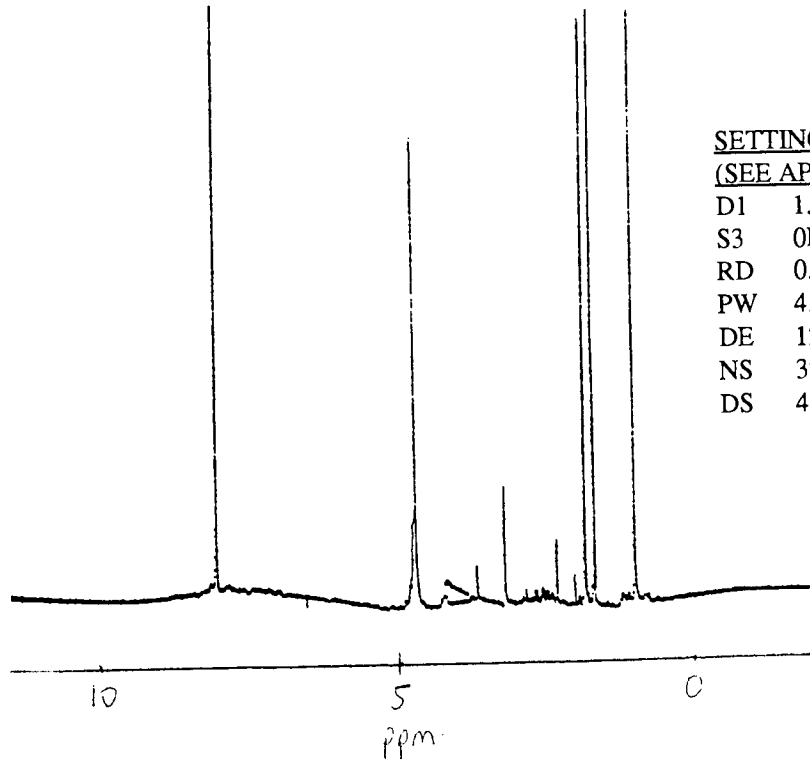
SETTINGS
(SEE APPENDIX 7)

D1	1.0
S3	0L
RD	0.0
PW	4.0
DE	125.0
NS	32
DS	4

13C DEPT
SETTINGS

D1	2.0	S2	14H
S1	0H	RD	0.0
P1	10.0	PW	0.0
D2	.0037	DE	38.8
P2	20.0	NS	18240
P3	4.5	DS	2
P0	14.0	P9	128.0
P4	9.0		

296

1.3.3.1 Jump and Return

SETTINGS

D1	3.0
P3	39.3
DE	127.5
P1	13.1
RD	0.0
NS	296
D2	0.0004
PW	0.0
DS	4

13C APT
SETTINGS

D1	2.0	P2	9.0
S1	16H	RD	0.0
P9	128.0	PW	0.0
D2	.005	DE	37.5
S2	14H	NS	19400
P1	4.5	DS	0
D3	0.007	NE	12
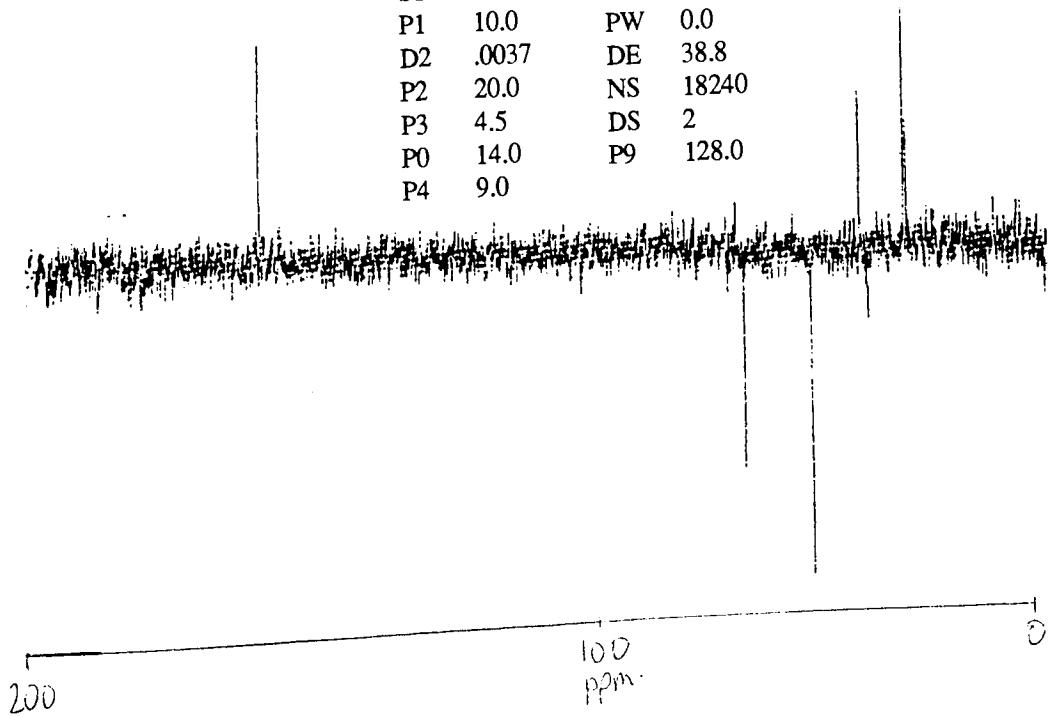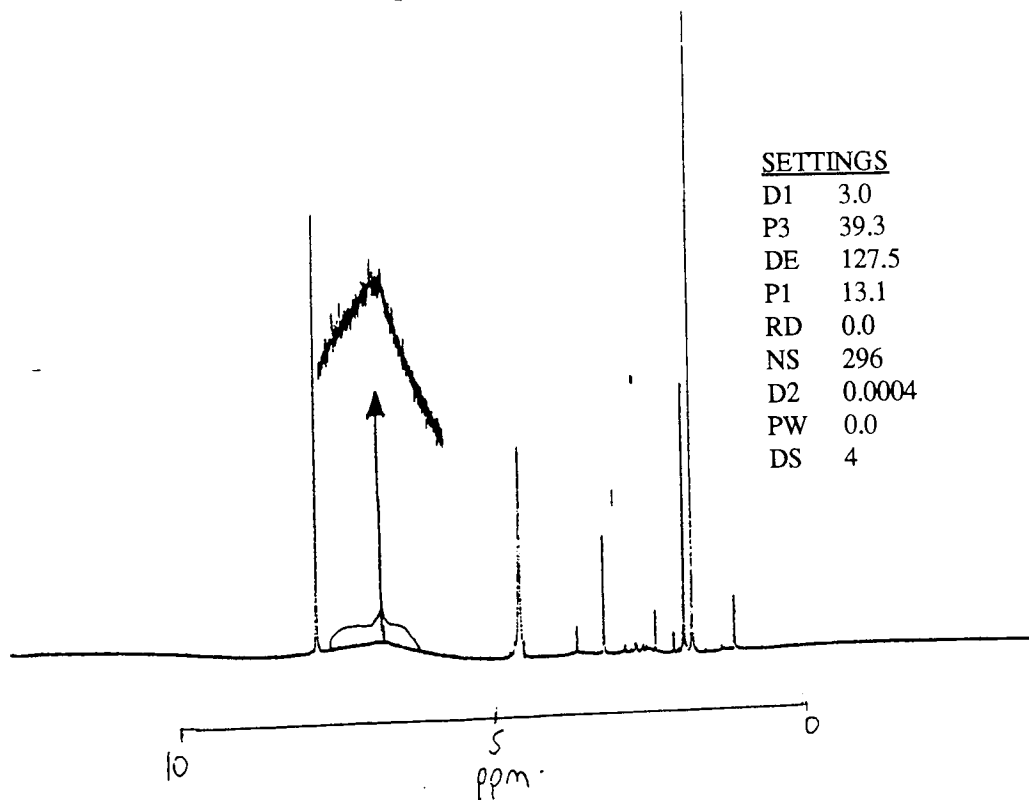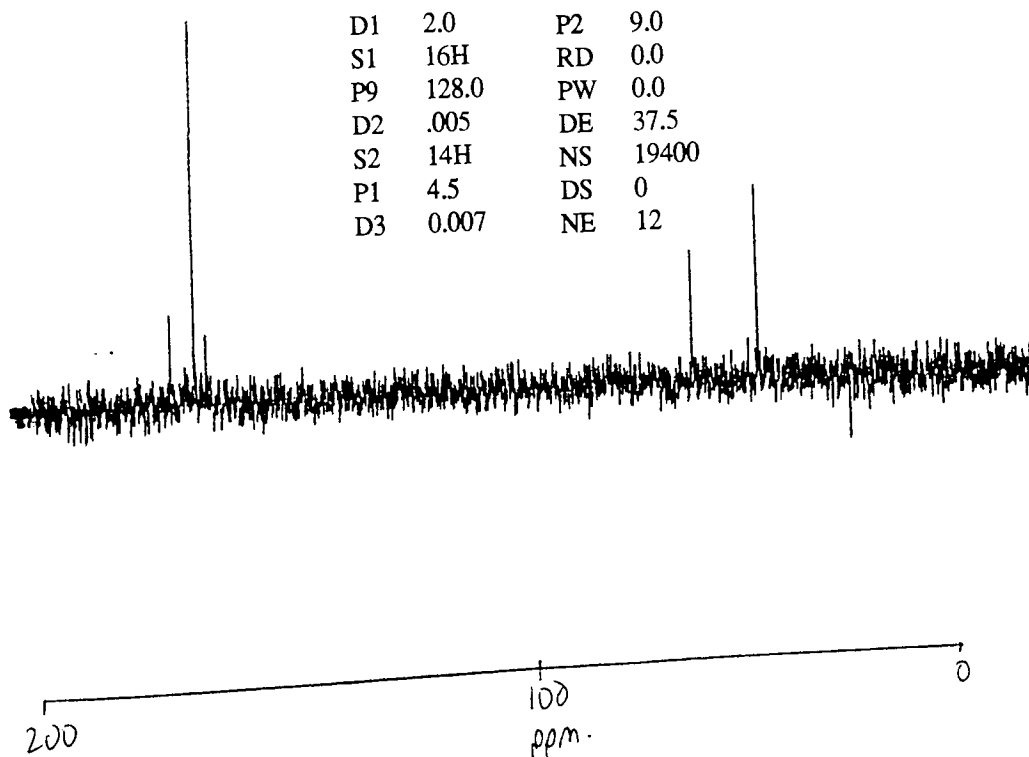
1 H With Presaturation of Water
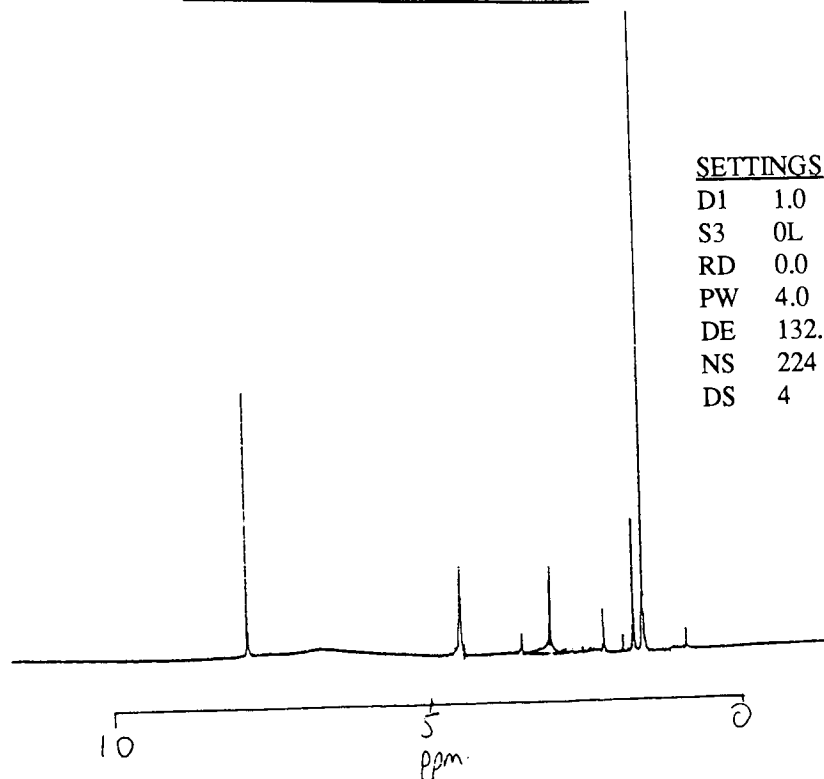
SETTINGS

D1	1.0
S3	0L
RD	0.0
PW	4.0
DE	132.5
NS	224
DS	4

10   5   0

ppm

13C APT

SETTINGS

D1	1.5	P2	9.0
S1	16H	RD	0.0
P9	128.0	PW	0.0
D2	.005	DE	37.5
S2	14H	NS	21996
P1	4.5	DS	0
D3	0.007	NE	14
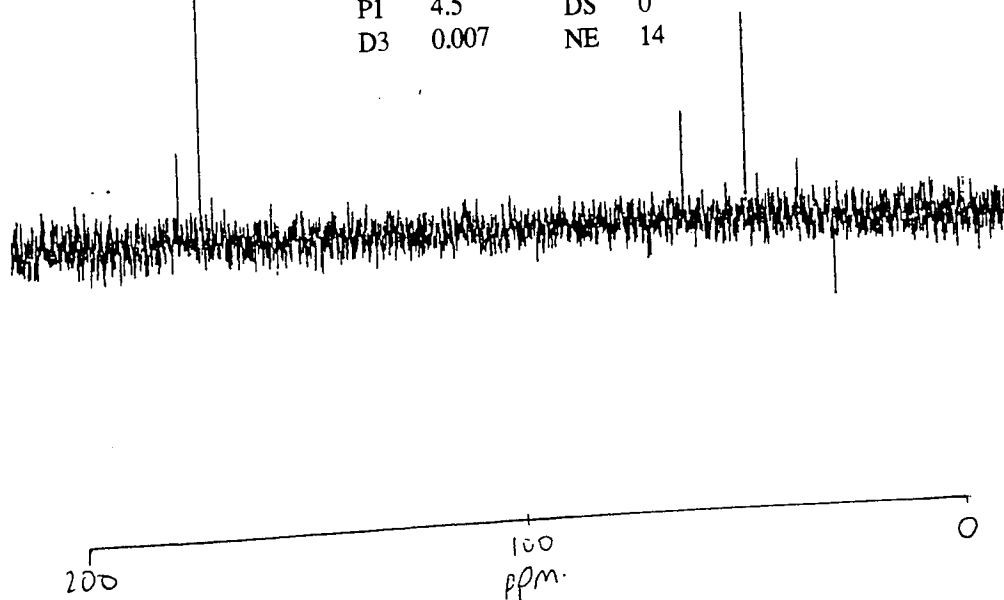
200   100   0

ppm

298

1.3.3.1 Jump and Return

SETTINGS
D1   3.0
P3   39.3
DE   127.5
P1   13.1
RD   0.0
NS   224
D2   0.0004
PW   0.0
DS   4

10   5   0
ppm.
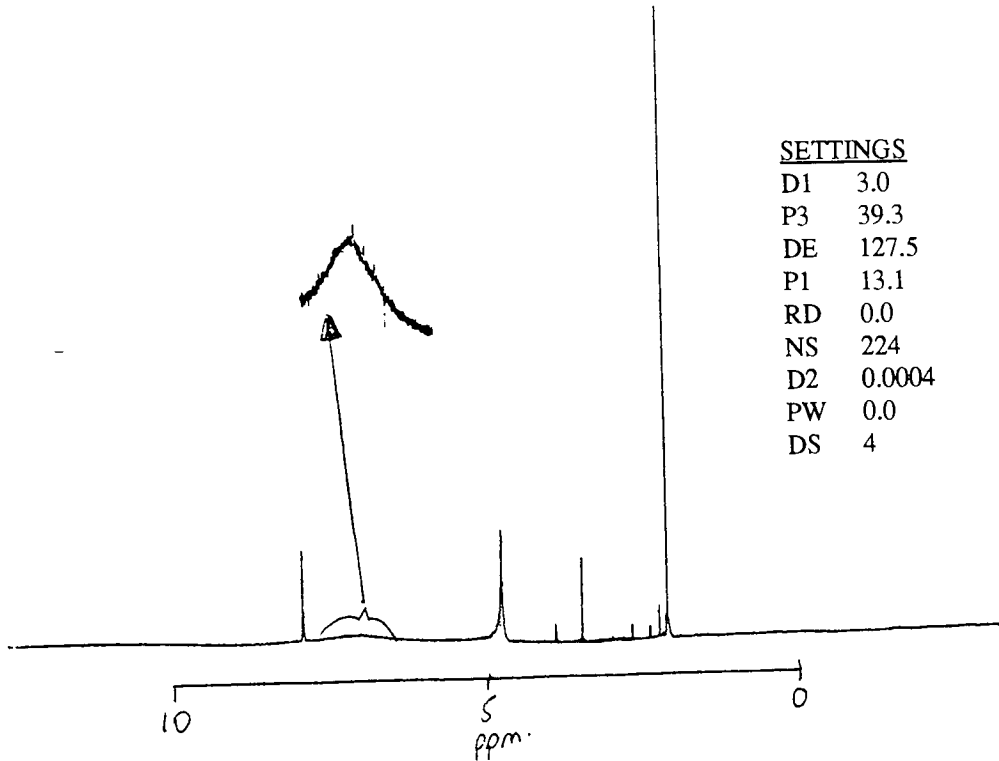
13C DEPT
SETTINGS

D1	2.0	S2	14H
S1	0H	RD	0.0
P1	10.0	PW	0.0
D2	.0037	DE	37.5
P2	20.0	NS	19360
P3	4.5	DS	2
P0	14.0	P9	128.0
P4	9.0		
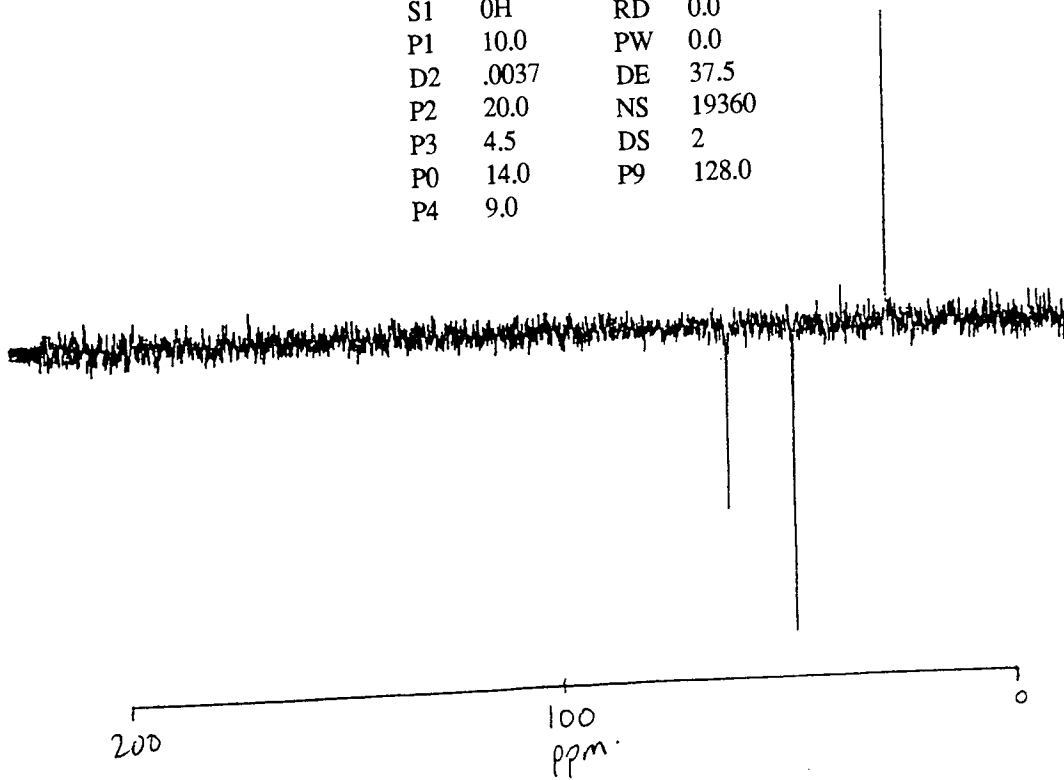
200   100   0
ppm.

1,3,3,1 Jump and Return

SETTINGS

D1	3.0
P3	39.3
DE	127.5
P1	13.1
RD	0.0
NS	80
D2	0.0004
PW	0.0
DS	4

ppm.
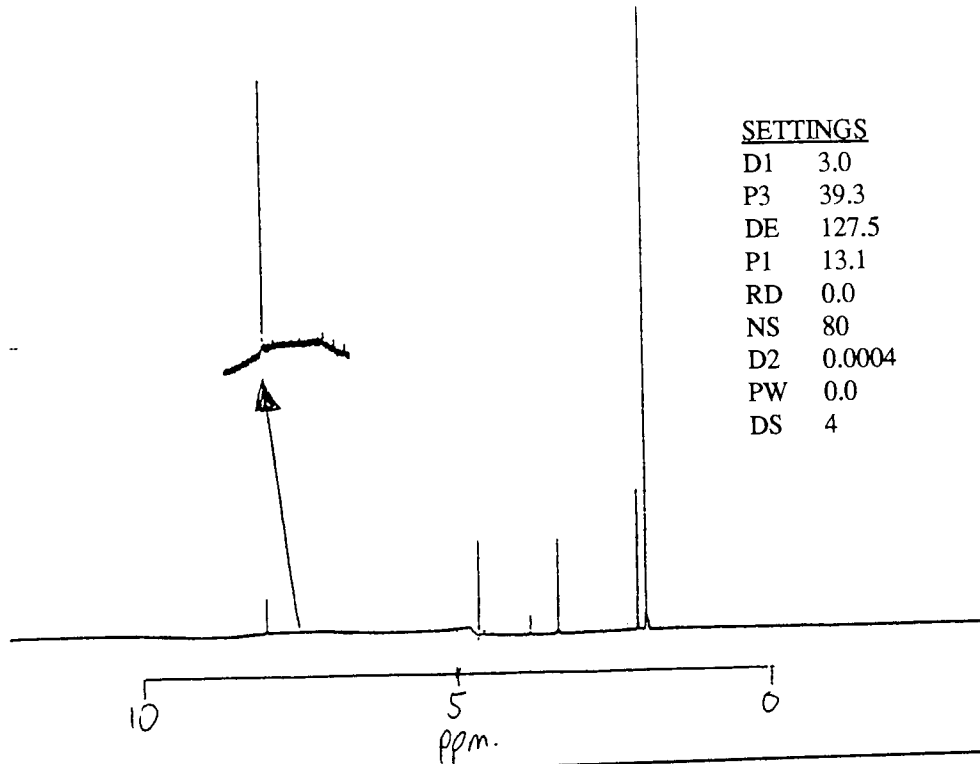
13C APT
SETTINGS

D1	2.0	P2	9.0
S1	16H	RD	0.0
P9	128.0	PW	0.0
D2	.005	DE	37.5
S2	14H	NS	19456
P1	4.5	DS	0
D3	0.007	NE	12
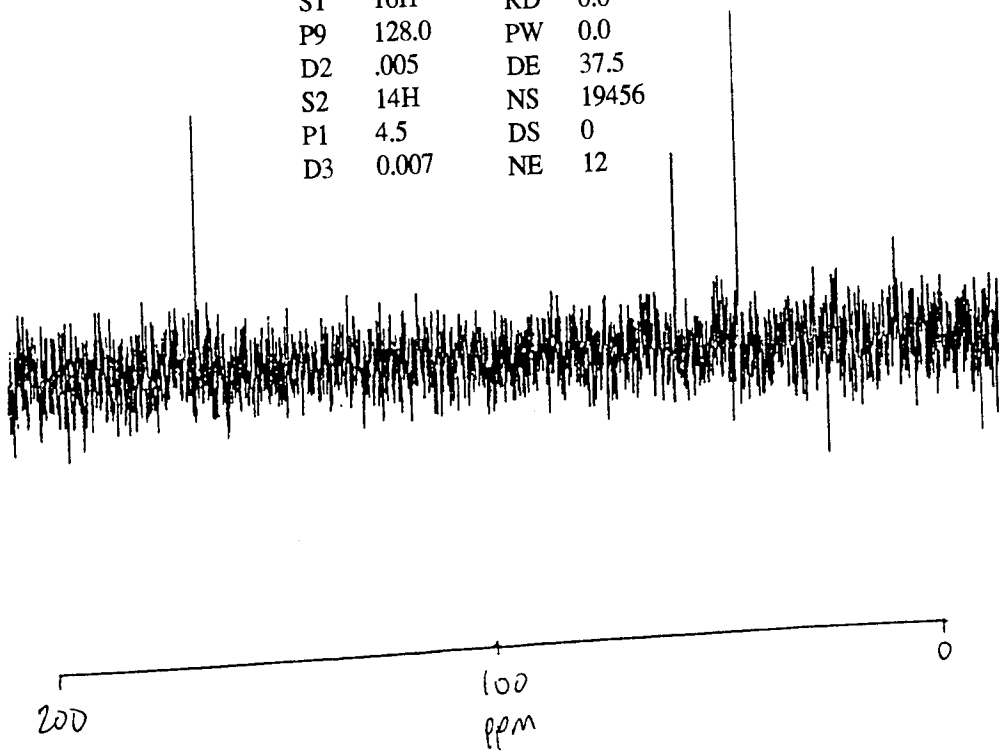
200 100 0

ppm

1 H With Presaturation of Water

SETTINGS

D1	1.0
S3	5L
RD	0.0
PW	4.0
DE	151.25
NS	408
DS	4

10   5   0

ppm.
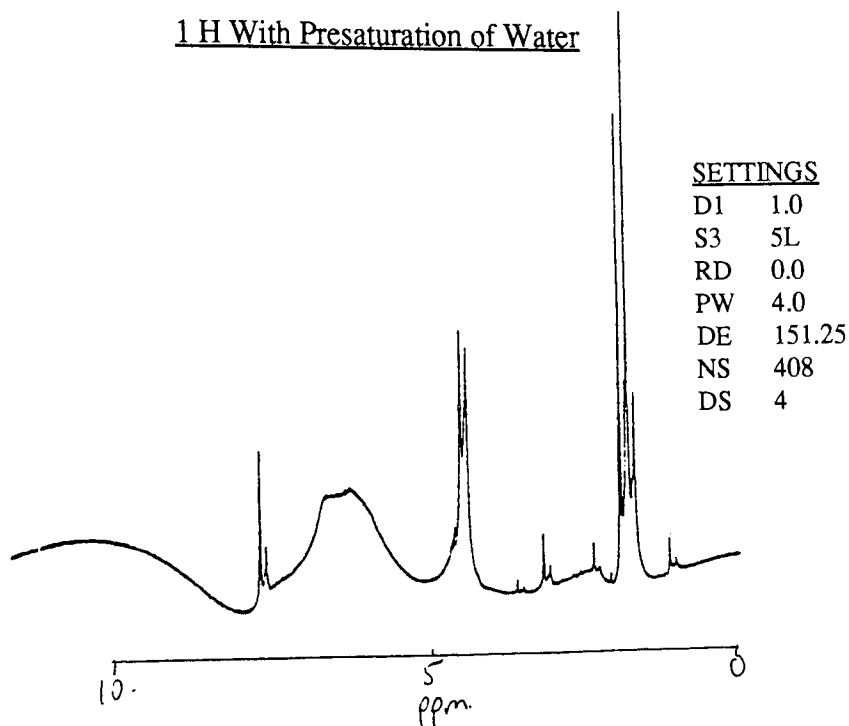
13C APT
SETTINGS

D1	3.0	P2	9.0
S1	16H	RD	0.0
P9	128.0	PW	0.0
D2	.005	DE	40.0
S2	14H	NS	22945
P1	4.5	DS	0
D3	0.007	NE	1
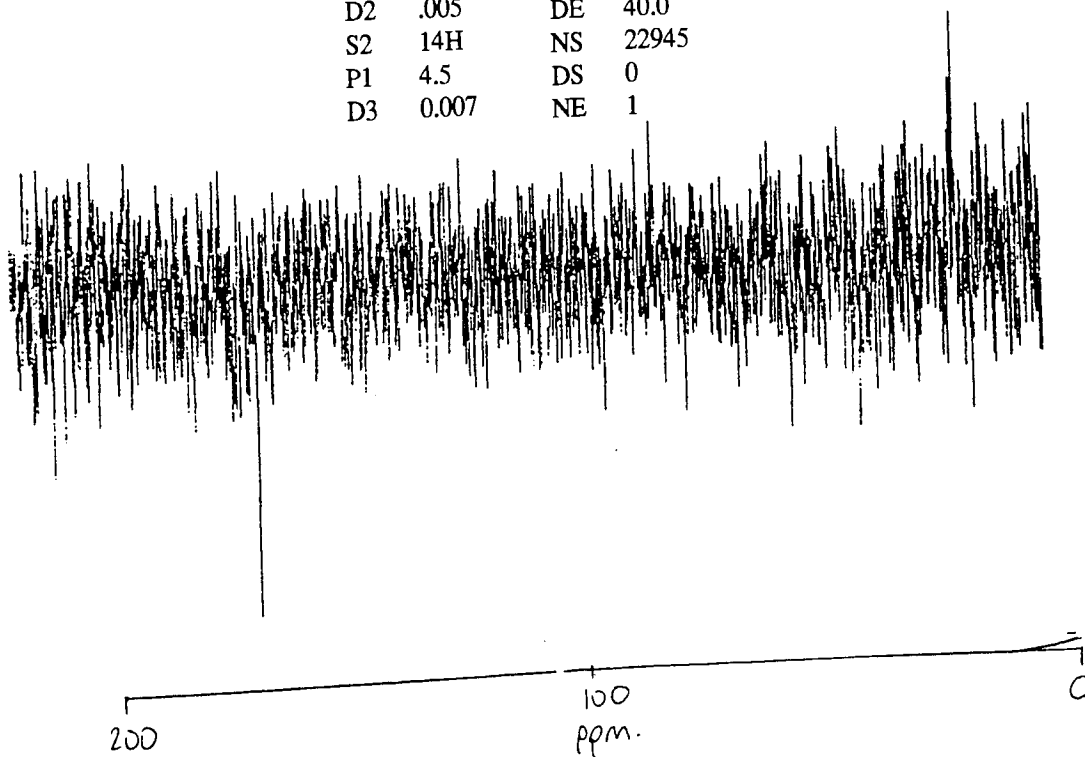
200   100   0

ppm.

301

1 H With Presaturation of Water
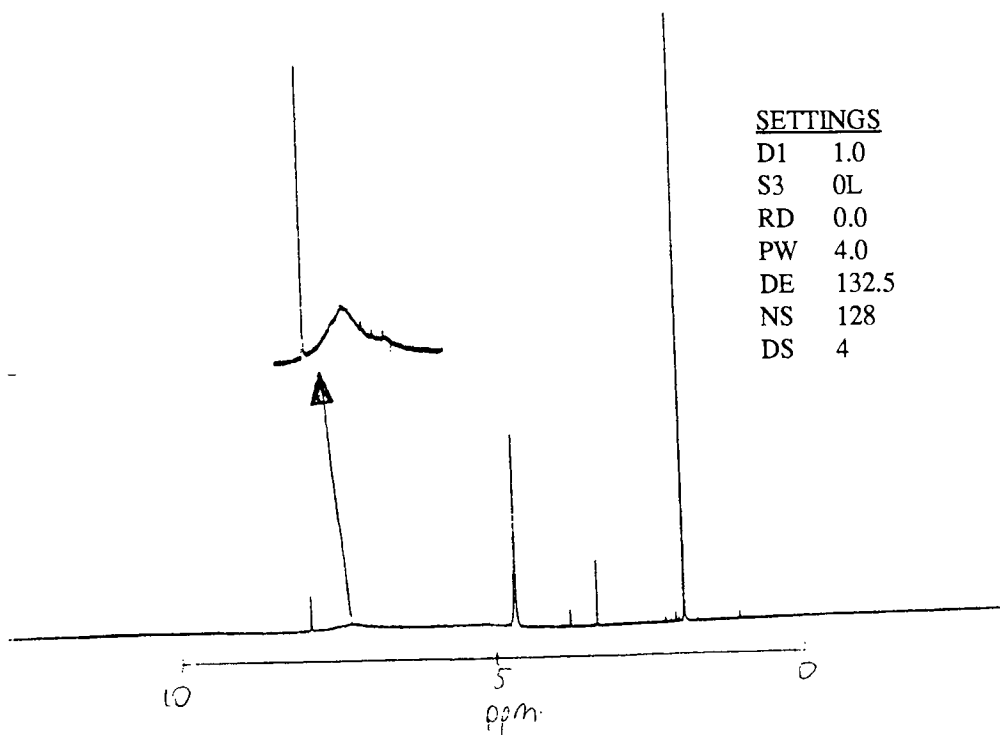
SETTINGS
D1   1.0
S3   0L
RD   0.0
PW   4.0
DE   132.5
NS   128
DS   4

13C DEPT
SETTINGS

D1	1.5	S2	14H
S1	0H	RD	0.0
P1	10.0	PW	0.0
D2	.0037	DE	37.5
P2	20.0	NS	23232
P3	4.5	DS	2
P0	14.0	P9	128.0
P4	9.0		
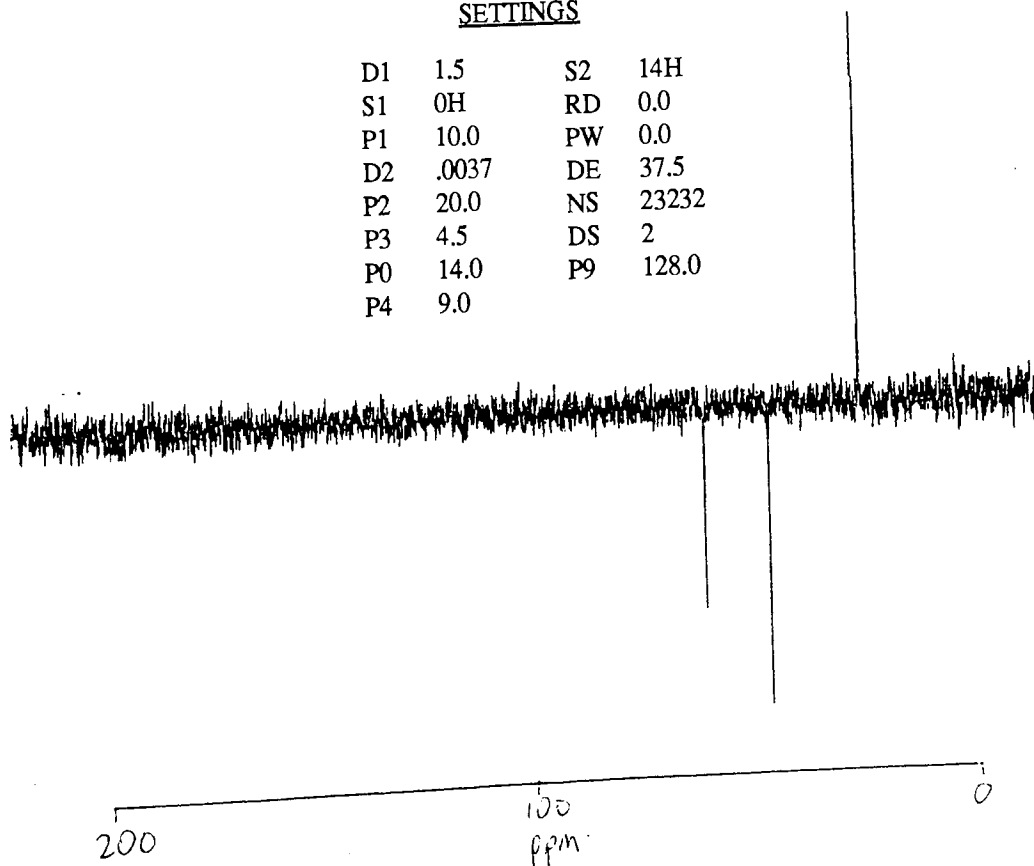
1 H With Presaturation of Water
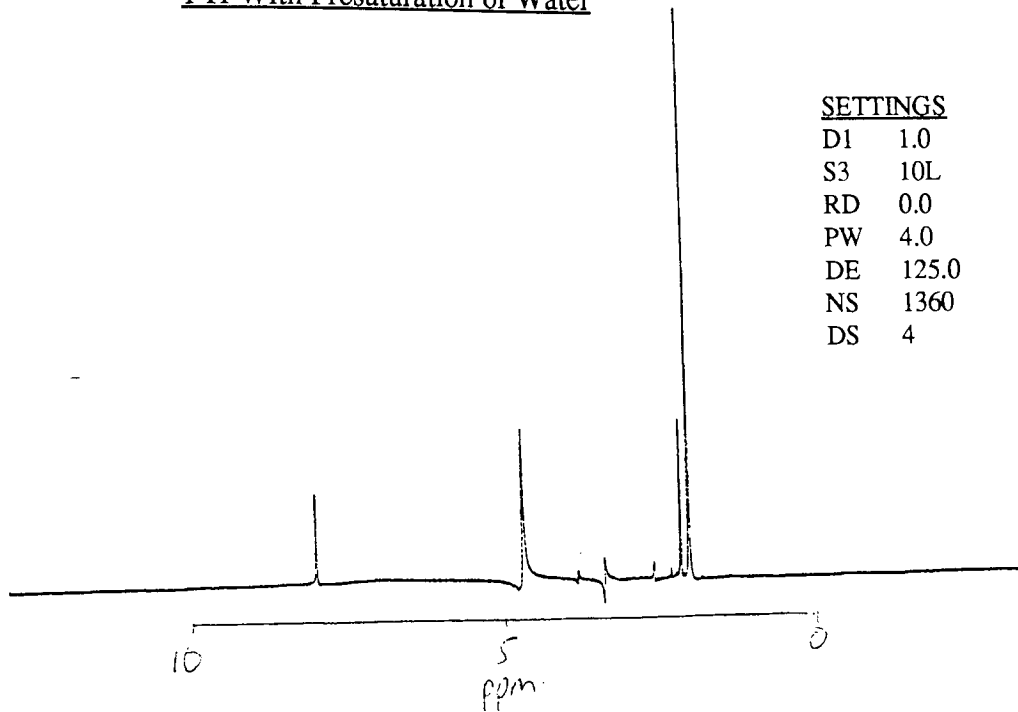
SETTINGS
D1   1.0
S3   10L
RD   0.0
PW   4.0
DE   125.0
NS   1360
DS   4

10   5   0
ppm

13C APT
SETTINGS

D1	3.0	P2	9.0
S1	16H	RD	0.0
P9	128.0	PW	0.0
D2	.005	DE	33.7
S2	14H	NS	20000
P1	4.5	DS	0
D3	0.007	NE	1

200   100   0
ppm

303
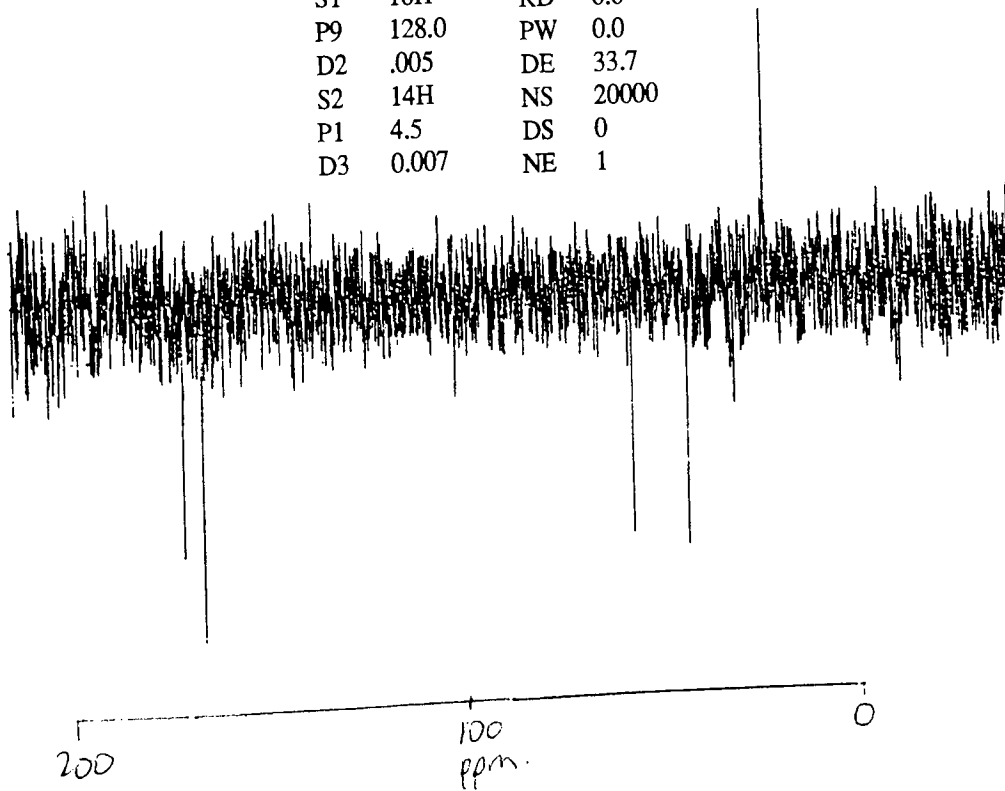
APPENDIX 2

NMR SPECTRA OF RESIN DIGESTION REACTION SAMPLES

WITH THEIR WATER REMOVED
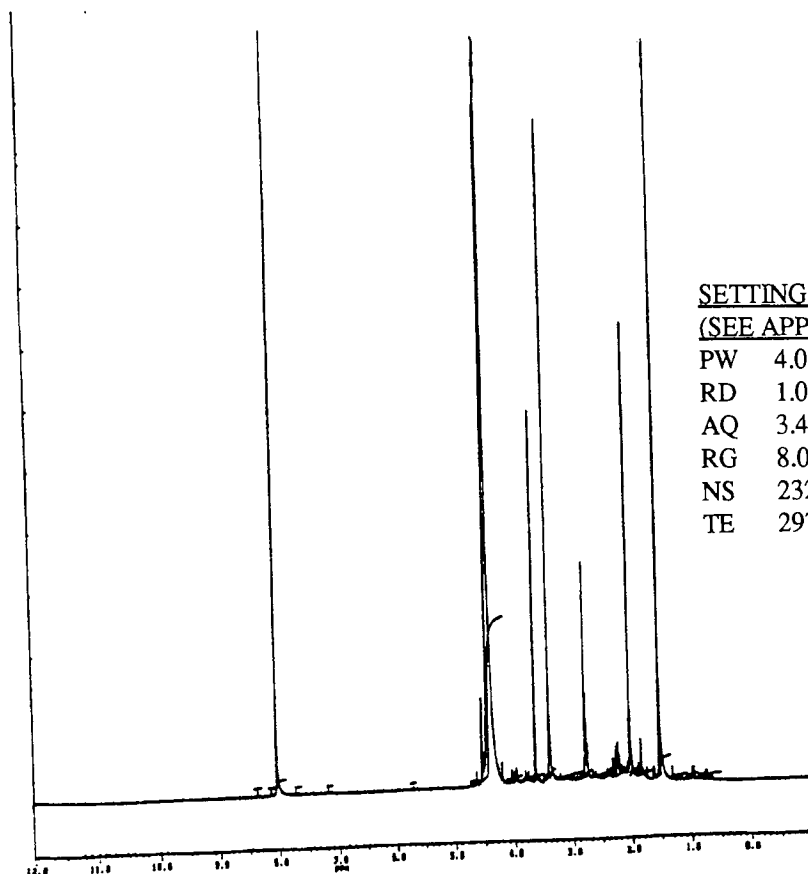
SETTINGS
(SEE APPENDIX 7)

PW	4.0
RD	1.0
AQ	3.4
RG	8.0
NS	232
TE	297
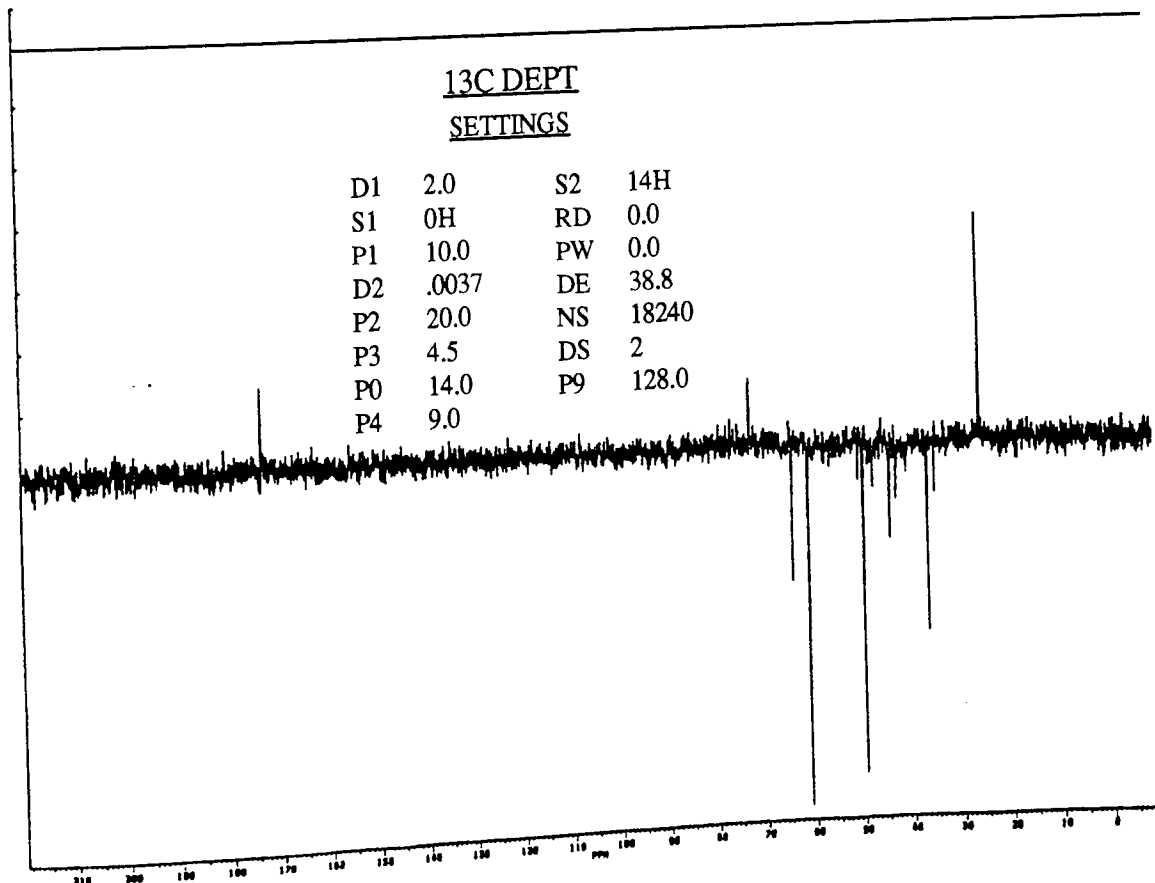
13C DEPT
SETTINGS

D1	2.0	S2	14H
S1	0H	RD	0.0
P1	10.0	PW	0.0
D2	.0037	DE	38.8
P2	20.0	NS	18240
P3	4.5	DS	2
P0	14.0	P9	128.0
P4	9.0		

305

SETTINGS
PW   4.0
RD   1.0
AQ   3.4
RG   8.0
NS   480
TE   297

13C DEPT
SETTINGS

D1	1.0	S2	14H
S1	0H	RD	0.0
P1	10.0	PW	0.0
D2	.0037	DE	38.8
P2	20.0	NS	26193
P3	4.5	DS	4
P0	14.0	P9	128.0
P4	9.0		

306

SETTINGS

PW	4.0
RD	1.0
AQ	4.9
RG	4.0
NS	96
TE	297

13C DEPT
SETTINGS

D1	3.0	S2	14H
S1	0H	RD	0.0
P1	10.0	PW	0.0
D2	.0037	DE	36.6
P2	20.0	NS	79072
P3	4.5	DS	4
PO	14.0	P9	128.0
P4	9.0		

307
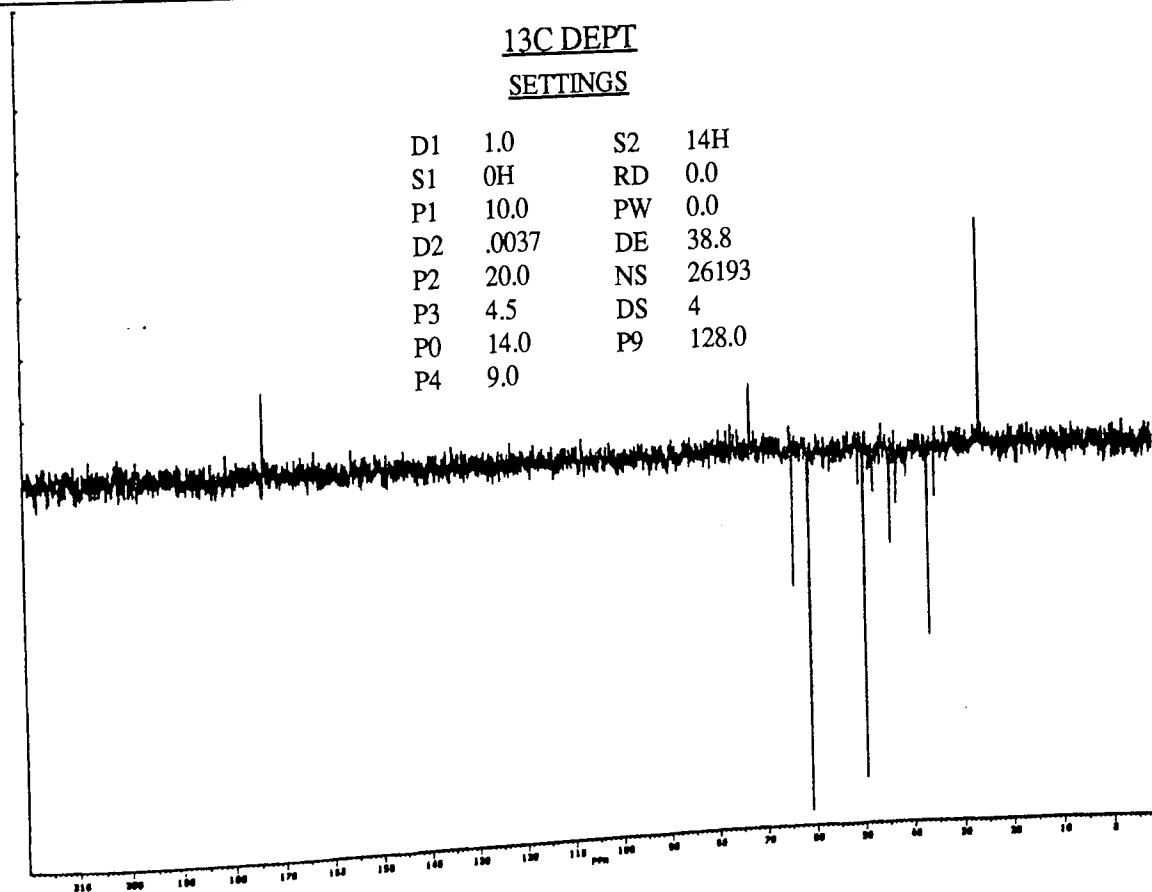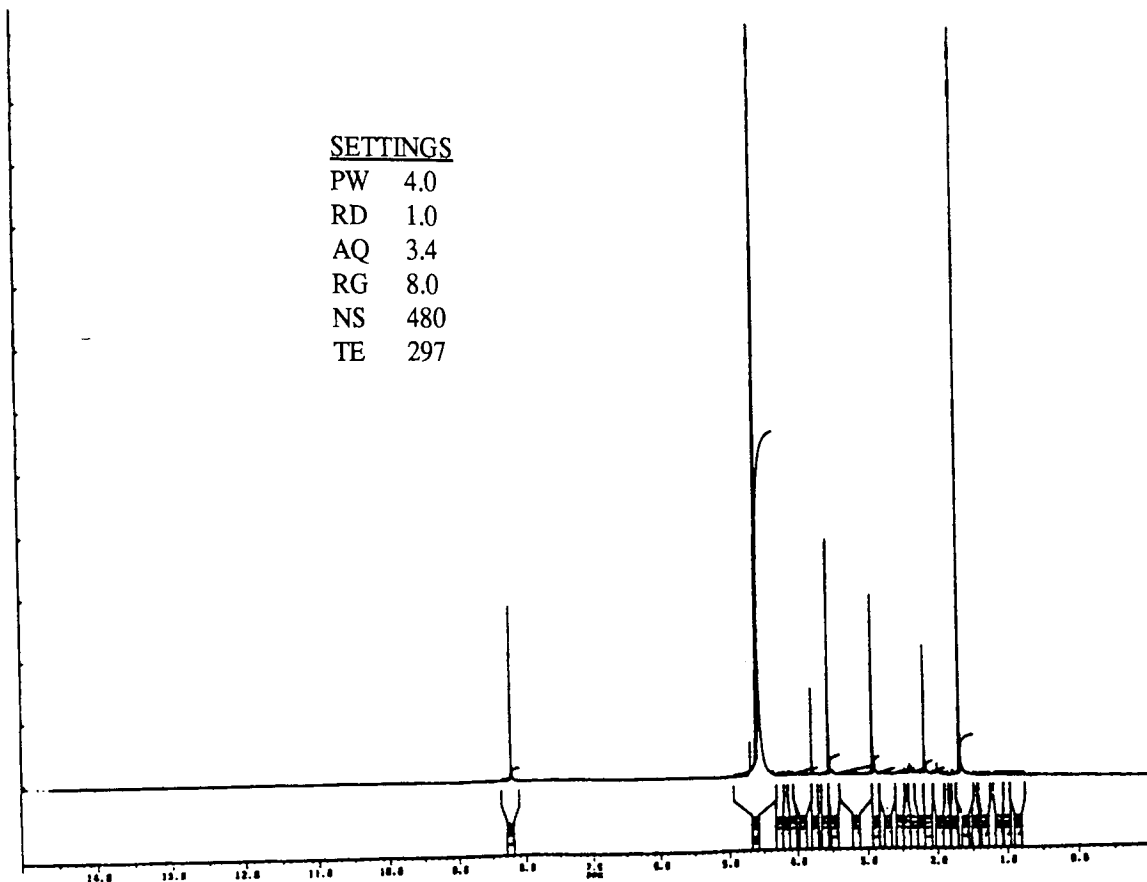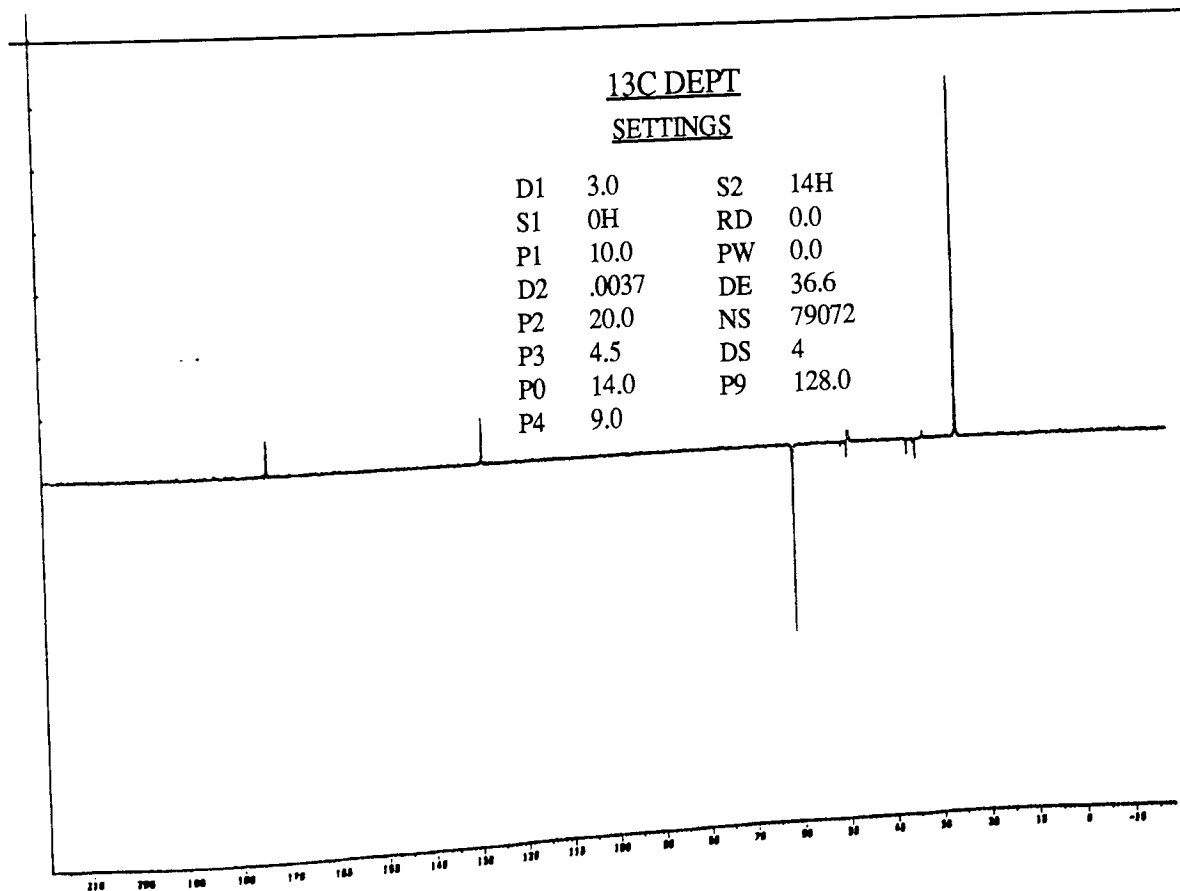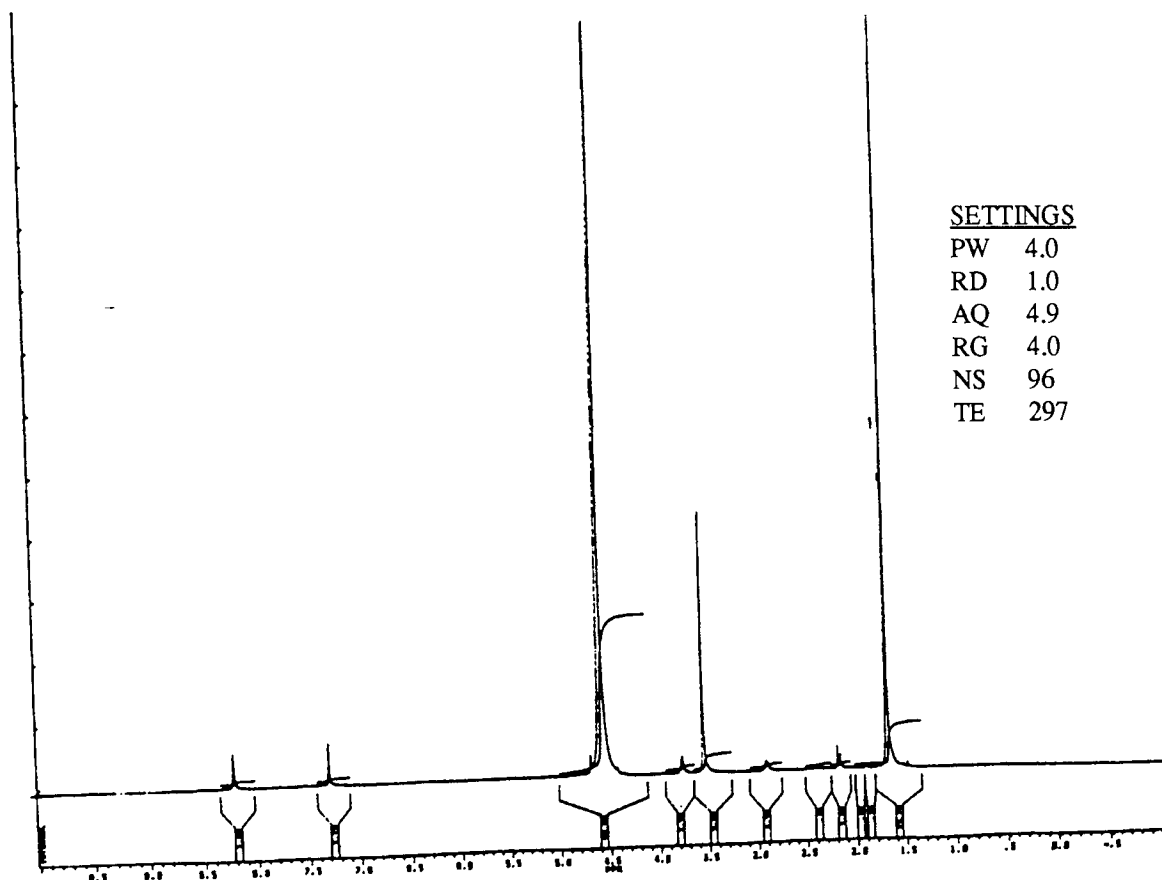
APPENDIX 3

NMR SPECTRA OF CALIX DIGESTION REACTION SAMPLES

1 H With Presaturation of Water
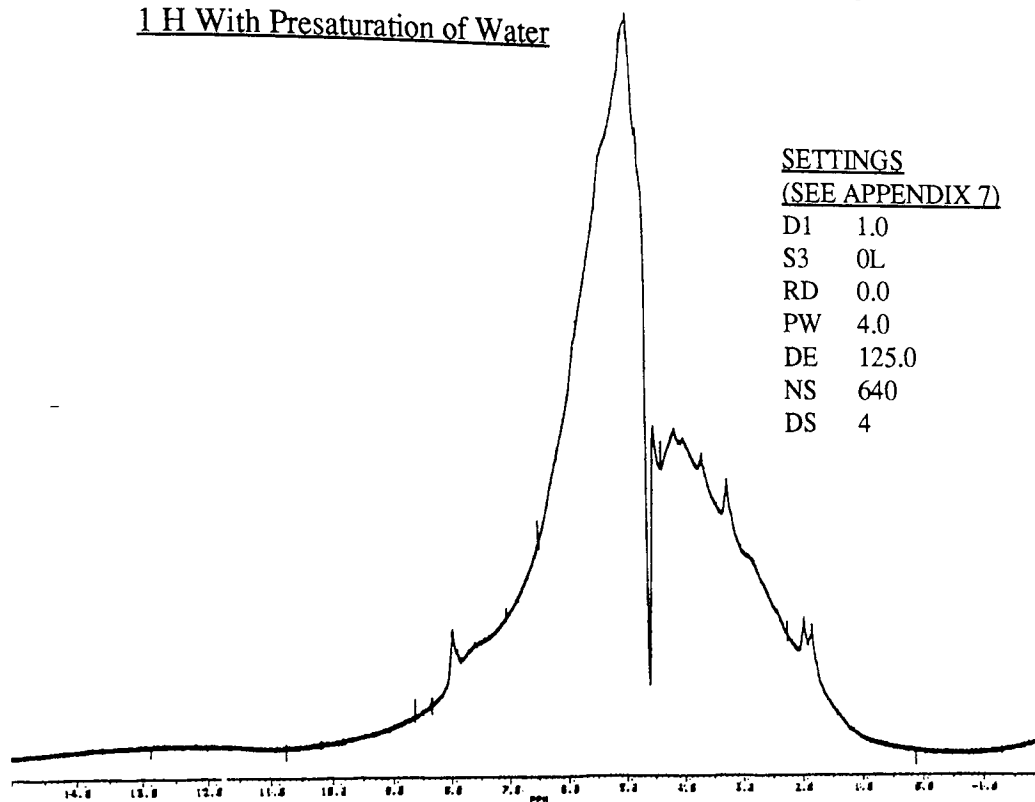
SETTINGS
(SEE APPENDIX 7)
D1	1.0
S3	0L
RD	0.0
PW	4.0
DE	125.0
NS	640
DS	4

13C DEPT

SETTINGS

D1	2.0	S2	14H
S1	0H	RD	0.0
P1	10.0	PW	0.0
D2	.0037	DE	38.8
P2	20.0	NS	17288
P3	4.5	DS	2
P0	14.0	P9	128.0
P4	9.0		
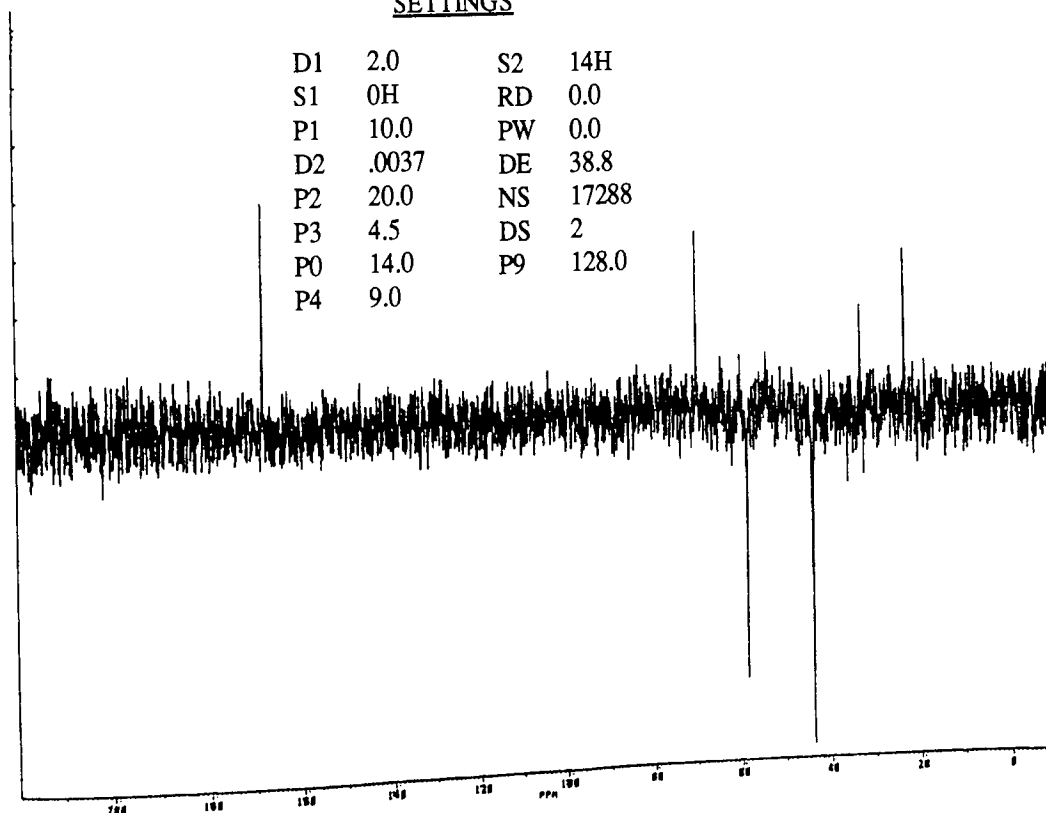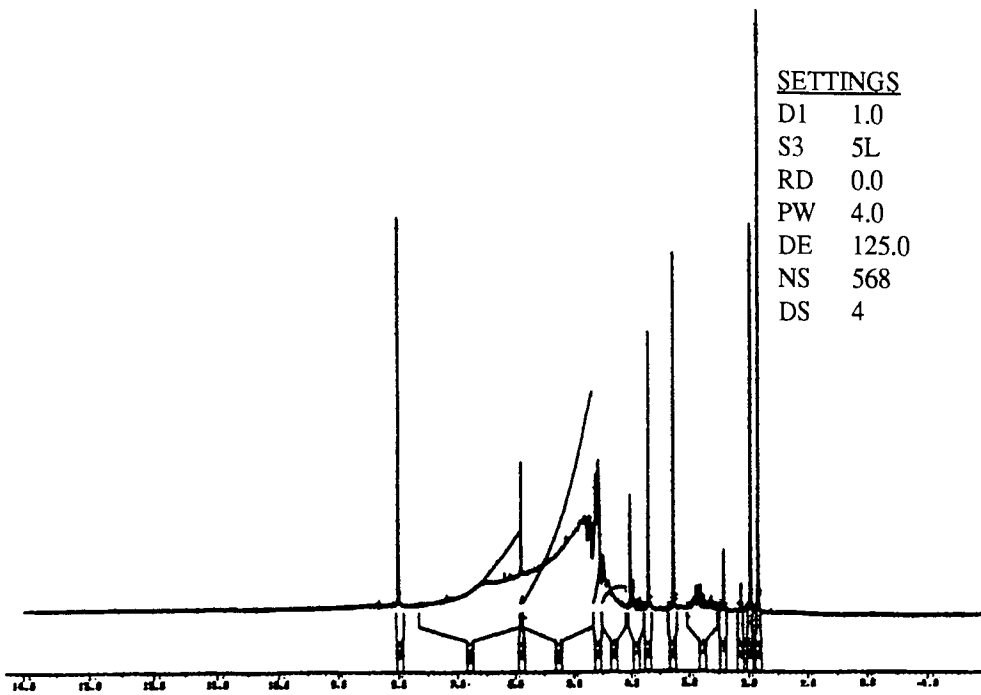
SETTINGS
D1	1.0
S3	5L
RD	0.0
PW	4.0
DE	125.0
NS	568
DS	4

13C DEPT
SETTINGS

D1	2.0	S2	14H
S1	0H	RD	0.0
P1	10.0	PW	0.0
D2	.0037	DE	35.0
P2	20.0	NS	16818
P3	4.5	DS	2
P0	14.0	P9	128.0
P4	9.0		
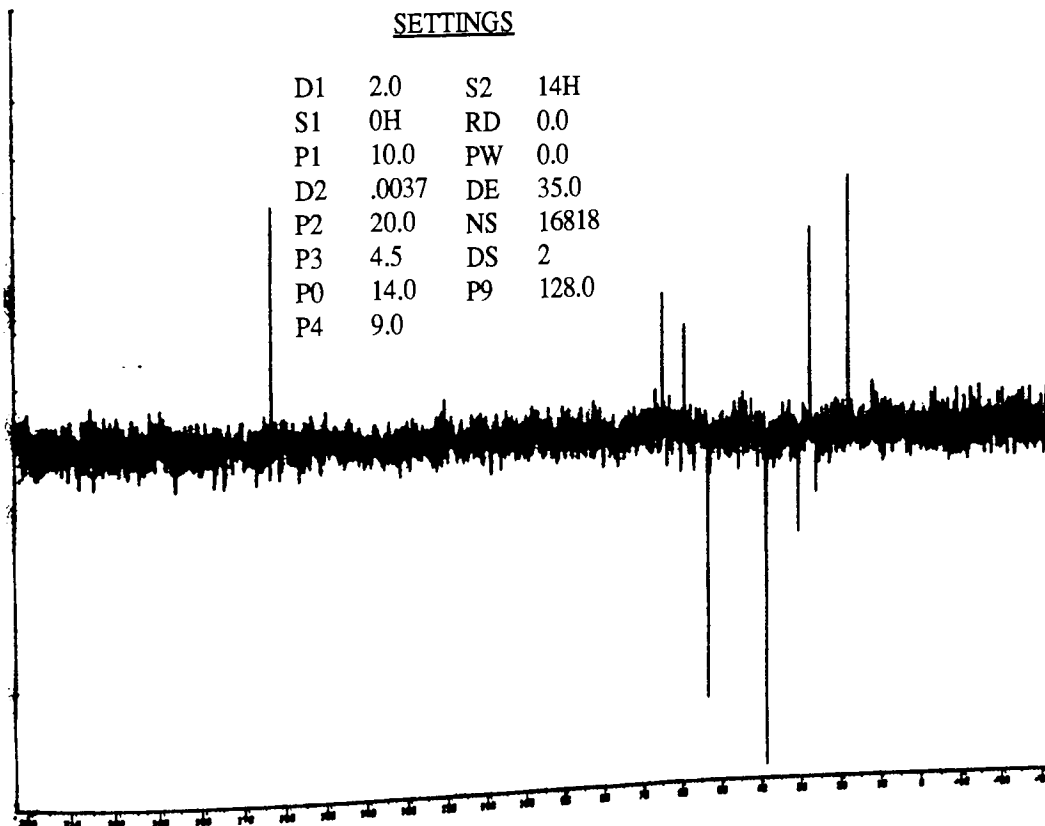
1 H With Presaturation of Water

SETTINGS	
D1	1.0
S3	10L
RD	0.0
PW	4.0
DE	125.0
NS	112
DS	4

13C DEPT

SETTINGS

D1	2.0	S2	14H
S1	0H	RD	0.0
P1	10.0	PW	0.0
D2	.0037	DE	35.0
P2	20.0	NS	43845
P3	4.5	DS	2
P0	14.0	P9	128.0
P4	9.0		

1 H With Presaturation of Water

SETTINGS

D1	1.0
S3	5L
RD	0.0
PW	4.0
DE	125.0
NS	408
DS	4
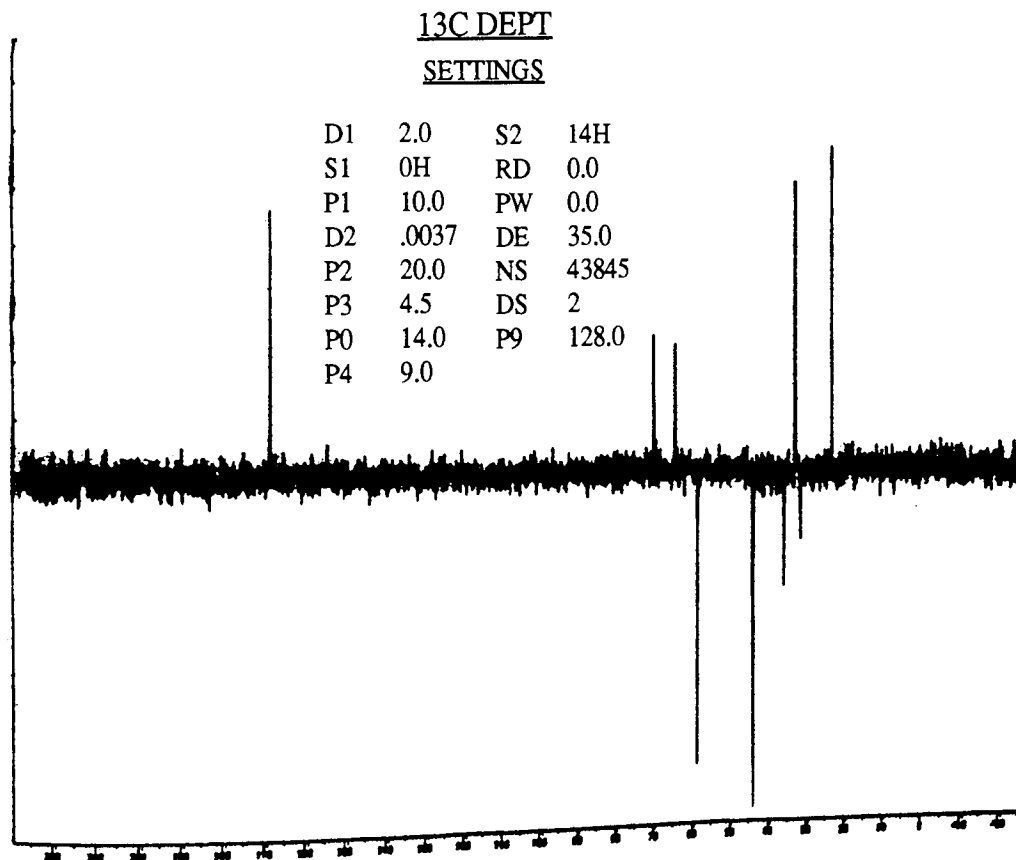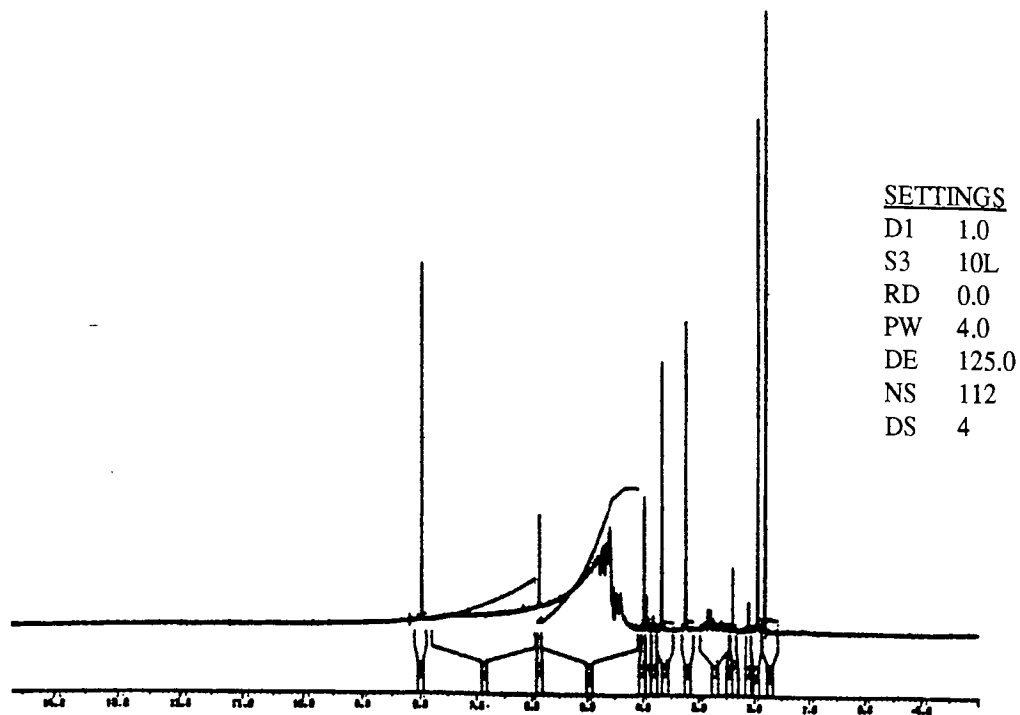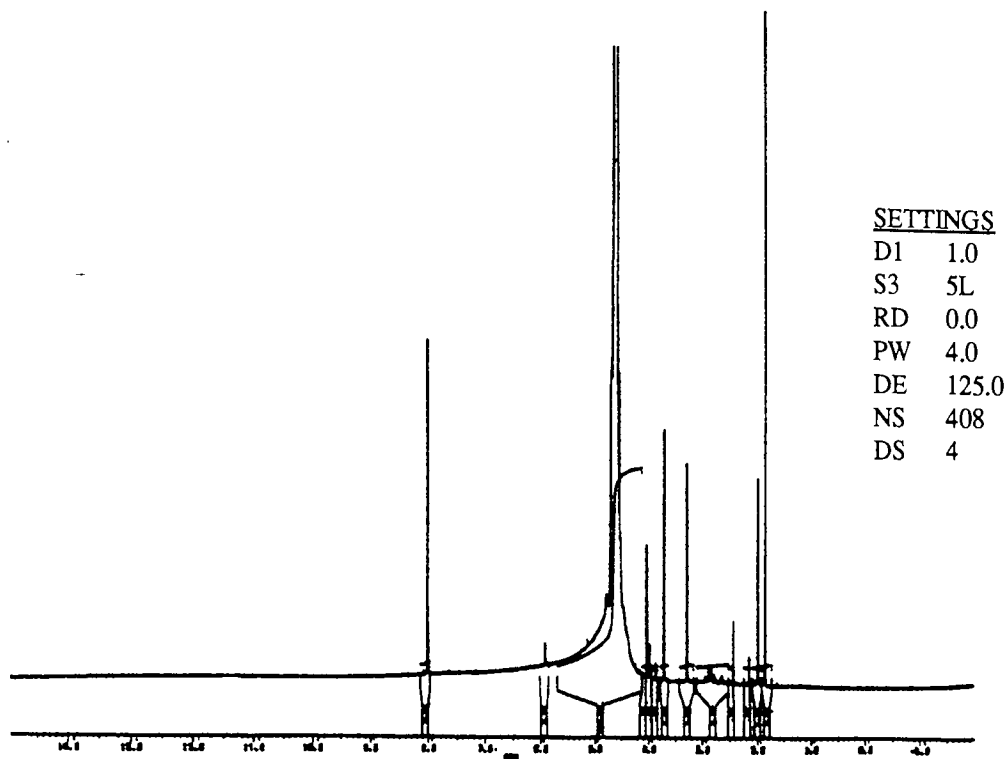
13C DEPT
SETTINGS

|			
D1	2.0	S2	14H
S1	0H	RD	0.0
P1	10.0	PW	0.0
D2	.0037	DE	35.0
P2	20.0	NS	43845
P3	4.5	DS	2
P0	14.0	P9	128.0
P4	9.0		
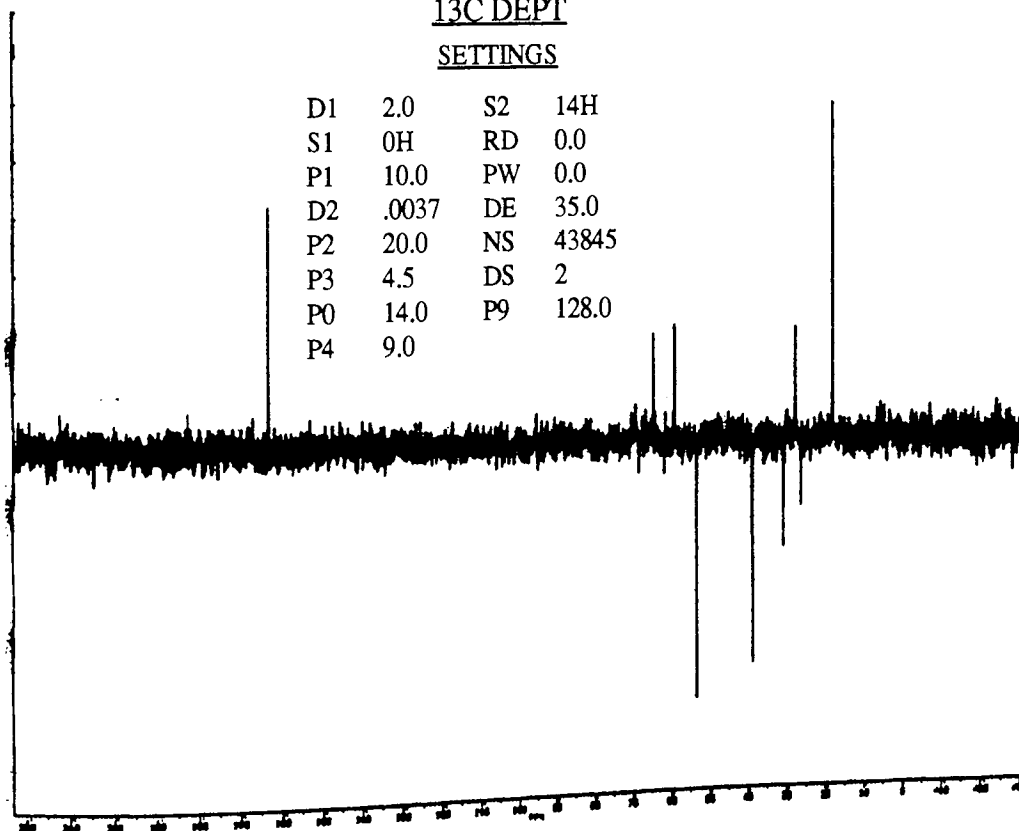
APPENDIX 4

TECHNICAL SPECIFICATIONS OF LEWATIT DN

ION-EXCHANGE RESIN

Lewatit DN is a cation exchanger on a polycondensate resin basis with special anchoring groups.
Lewatit DN is especially selective for Cs and allow its separation from solutions which also contain large quantities of other alkali ions such as lithium and sodium.

A.4.1 Characteristic Data

Form supplied	Na form, (optional H$^+$ form)
Grain shape	Granular and bead
Moisture content	50 to 55% H$_2$O
Total capacity	1.35 mequiv. / ml
Service flowrate	10 to 40 litres / hr per litre of swollen resin
Temperature range	up to 45°C
pH range	
stability	0 to 11
operating range	5 to 11
Elemental Analysis, %	C 45.6, H 4.47, O 45.29, S 4.64

A.4.2 Structural Formula of Resin
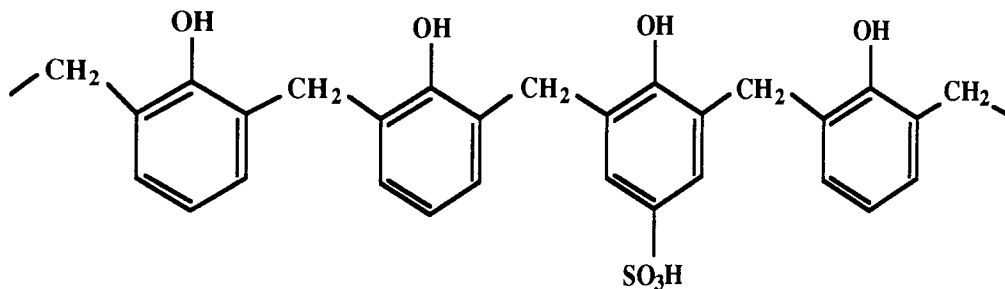
A.4.3 Application Areas

1) Removal of ^{137}Cs from water in fuel element pools adjusted with sodium hydroxide to pH values up to 11.

2) Radioactive effluent or exchanger regenerants from which the long lived caesium activity is to be removed prior to precipitation or evaporation.

APPENDIX 5

THE REACTION OF HYDROXYL RADICALS WITH

SOME SIMPLE MOLECULES

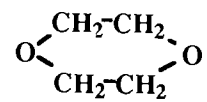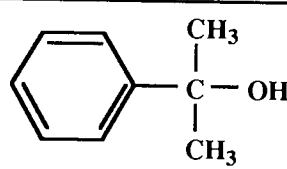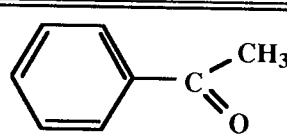## SOME FREE RADICAL OXIDATION PRODUCTS OF SIMPLE MOLECULES [18]

SUBSTRATE	PRODUCT	NOTES
$CH_3 - OH$	$CH_2 = O$	
$C_2H_5 - OH$	$CH_3CH = O$ $HO \cdot CH_2\text{-}CH_2 \cdot OH$	Attack is faster near to oxygen atom
$CH_3 \cdot CH\text{-}CH_2\text{-}CH_2 \cdot OH$ $\quad\;\; \underset{OH}{\mid}$	$CH_3 - \underset{\underset{O}{\parallel}}{C} - CH_2\text{-}CH_2 \cdot OH$ $CH_3 \cdot CH=CH_2 - C\overset{\diagup O}{\underset{\diagdown OH}{}}$	
$C_2H_5 - O - C_2H_5$	$CH_3CH = O$	Cation rearrangement
$O\overset{\diagup CH_2\text{-}CH_2}{\underset{\diagdown CH_2\text{-}CH_2}{}}O$	$CH_2 = O \quad (COOH)_2$ $HCOOH$	
$CH_3CH - COOH$ $\quad\; \underset{OH}{\mid}$	$CH_3 - \underset{\underset{O}{\parallel}}{C} - COOH$	
$(CH_3)_3C - OH$	$CH_3 - \underset{\underset{O}{\parallel}}{C} - CH_3 \quad CH_2 = O$	Radical degradation (spontaneous)
(phenyl)$-\overset{CH_3}{\underset{CH_3}{\overset{\mid}{\underset{\mid}{C}}}}- OH$	(phenyl)$-C\overset{\diagup CH_3}{\underset{\diagdown O}{}}$ $CH_2 = O$	
$HO - CH_2\text{-}CH_2 - OH$	$\overset{H}{\underset{O}{\diagdown}}{=}C - CH_2 \cdot OH$ $\qquad\qquad CH_2 = O$	
$CH_3 - CH \cdot CH - CH_3$ $\qquad \underset{OH}{\mid} \;\; \underset{OH}{\mid}$	$CH_3 - \underset{\underset{O}{\parallel}}{C} - \underset{\underset{O}{\parallel}}{C} - CH_3$	

316

TABLE A 5.1

SOME RATE CONSTANTS FOR THE ADDITION OF HYDROXYL RADICALS TO ORGANIC MOLECULES [17]

Reactant	Rate Constant M^{-1} sec^{-1}	pH
Benzene	7.3×10^9	7
Benzoate ion	6×10^9	6 - 9.4
Ethanol	7.2×10^8	7
Formate ion	2.5×10^9	7
Methanol	4.7×10^8	7
2-Propanol	1.5×10^9	7

APPENDIX 6

TECHNICAL SPECIFICATIONS OF THE UV

PHOTOCHEMICAL REACTOR

1) The' Reading Photochemical Reactor', manufactured by Hanovia Ltd, is used for conducting photo-chemical reactions in a quartz vessel. The lamp contains two medium pressure arc tubes, and a cooling fan in the base.

2) The quartz vessel holds the reagents and this is provided with a water jacket to ensure temperature control when the medium pressure lamps are in operation. The capacity of the vessel is 400 cm^3 and it has a water cooling jacket of 10 mm path length.

3) The reagent vessel is mounted by means of claw clamps fitted to the upright chromium plated tube of the lamp unit.

4) The straight arc tubes are the medium pressure mercury vapour lamps of 500 watts each, with a peak energy emission at 366nm.

5) The control unit is a separate item and consists of a steel case containing four choke units for use with the medium pressure arc tubes.

6) Nominal running characteristics for the medium pressure lamps are 240V +/-10V, 4.4A per lamp (in actual use each lamp used 4.9A).

APPENDIX 7

EXPLANATION OF TERMS USED IN NMR SETTINGS

Description of NMR Settings

1 H With Presaaturation of Water

D1 - Delay for relaxation of X-Nucleus

S3 - Typically 20 - 30L

RD - Relaxation delay

PW - Pulse width

NS - Number of scans

DS - Dummy scans

13C DEPT

S1 - 0H for maximum power pulses

P1, P2 - 90, 180 degree pulses for 1H decoupling

D2 - 0.5 / J(XH) for optimum polarization

P3, P4 - 90, 180 degree pulses for X

P0 - Variable pulse, depending on desired multiplicity selection

S2 -Normal power for CPD decoupling

DE - Dwell time

P9 - Variable pulse related to decoupler power (Waltz decoupling)

1.3.3.1 Jump and Return

As for 1H presaturation.

13C APT

D3 - Evolution period for J modulation

NE - Number of experiments